Role of EFA6B, Exchange Factor of Arf6, in epithelial morphogenesis and collective invasion of human mammary cells

Racha Fayad

UNIVERSITÉ CÔTE D'AZUR

ÉCOLE DOCTORALE
SCIENCES DE LA VIE ET DE LA SANTÉ

THÈSE DE DOCTORAT

Rôle de EFA6B, facteur d'échange d'Arf6, dans la morphogenèse épithéliale et l'invasion collective de cellules mammaires humaines

Racha FAYAD

Institut de Pharmacologie Moléculaire et Cellulaire, CNRS UMR 7275

Présentée en vue de l'obtention du grade de Docteur en Sciences de la Vie de l'Université Côte d'Azur

Mention : Interactions moléculaires et cellulaires

Dirigée par Dr. Frédéric LUTON

Soutenue le 7 Mars 2019, devant le jury, composé de :

Ellen VAN OBBERGHEN-SCHILLING	Directrice de Recherche, INSERM, IBV, Nice	Présidente du jury
Cécile GAUTHIER-ROUVIERE	Directrice de Recherche, INSERM, CRBM, Montpellier	Rapporteure
Andrew EWALD	Professeur, Johns Hopkins University, Baltimore	Rapporteur
Patrick AUBERGER	Directeur de Recherche, INSERM, C3M, Nice	Examinateur
Marc Lopez	Ingénieur de Recherche, INSERM, CRCM, Marseille	Examinateur
Frédéric LUTON	Directeur de Recherche, INSERM, IPMC, Nice	Directeur de thèse

SIGNALIFE

ipmc

cnrs

Summary

Role of EFA6B, Exchange Factor of Arf6, in epithelial morphogenesis and collective invasion of human mammary cells

Epithelial tissue homeostasis is fundamental for the survival and maintenance of a healthy organism. During mammary gland morphogenesis, epithelial cells communicate with their surrounding stroma in order to orchestrate the formation of a functional organ by undergoing multiple cycles of controlled proliferation, epithelial-mesenchymal transition (EMT) and mesenchymal-epithelial transition, migration and invasion. In cancer cells, these processes are dysregulated. Thus, understanding how normal mammary cells preserve their homeostasis during development is crucial to identify the molecular events inducing breast cancer. Homeostasis of epithelia relies on key specific features: apico-basal polarity, cell cohesion and lumen formation. Here stands our protein of interest, EFA6B, exchange factor for Arf6, hence my interest in studying its role in mammary epithelial cells. During my PhD work, I investigated the role of EFA6B on epithelial integrity.

Using CRISPR/Cas9 EFA6B knock-out cells, I showed that the loss of EFA6B deregulates the homeostasis of normal mammary epithelial cells at different levels. First, deleting EFA6B allows the formation of invadopodia rich in integrin ITGB1 and metalloprotease MMP14. My results indicate that EFA6B KO cells invasion is Cdc42-dependent, supported by increased cell contractility and the formation of protrusive branched structures through the Cdc42/MRCK/pMLC and Cdc42/N-WASP/Arp2/3 signaling pathways. Second, we showed that the loss of EFA6B is associated with the engagement of cells into EMT, revealed by a cadherin switch and an upregulation of EMT transcription factors. Third, coherently with EFA6B roles on junction assembly, its depletion prevented cells from polarizing and forming normal acini with central lumens. Collectively, our data are in agreement with previous results showing a correlation between the loss of EFA6B and the breast cancer claudin-low subtype defined by EMT properties, invasion capacities and a decrease in TJ proteins expression.

I also contributed to the characterization of the role of α-actinin1 as an effector of EFA6A in normal epithelial cells (MDCK), and of EFA6B in a tumorigenic mammary cell line (MCF7). I show that EFA6B and α-actinin1 by regulating together the apical cellular contractility coordinate the establishment of apico-basal polarity and luminogenesis, two essential processes for functional epithelia.

Altogether, these results demonstrate that the loss of EFA6B triggers invasive potentials in normal epithelial cells, and modifies their microenvironment (contractility, degradative invadopodia, alteration of the matrisome). We propose the gene *PSD4* encoding for EFA6B as an invasion-suppressor gene that will preserve cells from losing their epithelial features in order to maintain tissue integrity.

Key words: EFA6B, epithelial homeostasis, breast cancer, invasion, invadopodia, Cdc42.

Résumé

Rôle de EFA6B, facteur d'échange d'Arf6, dans la morphogenèse épithéliale et l'invasion collective de cellules mammaires humaines

L'homéostasie des tissus épithéliaux est fondamentale à la survie et au maintien d'un organisme sain. Au cours de la morphogenèse des glandes mammaires, les cellules épithéliales communiquent avec leur stroma environnant afin d'orchestrer la formation d'un organe fonctionnel en passant par de multiples cycles régulés de prolifération, de transitions épithélio-mésenchymateuse (TME) et mésenchymateuse-épithéliale, de migration et d'invasion. Dans les cellules cancéreuses, ces processus sont dérégulés. Il est donc important d'étudier comment les cellules mammaires normales conservent leur homéostasie au cours du développement pour appréhender les événements moléculaires induisant le cancer du sein. L'homéostasie de l'épithélium repose sur le contrôle de propriétés spécifiques : polarité apico-basale, cohésion cellulaire et formation de lumen. Notre protéine d'intérêt EFA6B, facteur d'échange d'Arf6, se trouve au cœur de ces caractéristiques structurelles, d'où mon intérêt à étudier son rôle dans les cellules épithéliales mammaires. Au cours de mes travaux de thèse, j'ai étudié l'impact de la perte d'EFA6B sur l'intégrité épithéliale.

En utilisant des cellules épithéliales normales mammaires invalidées pour EFA6B par la technique de CRISPR/Cas9, j'ai démontré que la perte d'EFA6B dérégule fortement l'homéostasie épithéliale à différents niveaux. Premièrement, sa déplétion entraîne la formation d'invadopodes riches en intégrine ITGB1 et en métalloprotéase MMP14. Mes résultats indiquent que l'invasion des cellules EFA6B knock-out dépend de l'activation de Cdc42. Elle est soutenue par une contractilité accrue des cellules et la formation de structures branchées protrusives contrôlées par les voies de signalisation Cdc42/MRCK/P-MLC et Cdc42/N-WASP/Arp2/3. Deuxièmement, nous avons montré que la perte d'EFA6B est associée à l'engagement des cellules EFA6B knock-out dans une TME, révélée par un échange de cadhérine et une augmentation de l'expression de facteurs de transcription mésenchymateux. Troisièmement, conformément au rôle d'EFA6B dans l'assemblage des jonctions serrées, sa déplétion empêche les cellules de se polariser et de former des acini avec un lumen central. Collectivement, nos données sont en accord avec des résultats précédemment publiés montrant une corrélation entre la perte d'EFA6B et le sous-type de cancer du sein invasif Claudin-low défini par une signature TME et une perte d'expression des protéines des jonctions serrées.

J'ai aussi contribué à la caractérisation du rôle de l'α-actinine 1 comme effecteur d'EFA6A dans des cellules épithéliales normales (MDCK) et d'EFA6B dans une lignée cellulaire mammaire tumorigène (MCF7). Je montre qu'EFA6B et l'α-actinine 1, en régulant la contractilité cellulaire apicale, coordonnent l'établissement de la polarité apico-basale, la formation des jonctions serrées et du lumen.

L'ensemble de ces résultats démontre que la perte d'EFA6B stimule les propriétés invasives de cellules épithéliales normales et impacte leur microenvironnement (contractilité, dégradation de la matrice, altération du matrisome). Nous proposons que le gène *PSD4* codant pour EFA6B est un gène suppresseur d'invasion qui contribue à préserver l'intégrité des tissus épithéliaux.

Mots clés : EFA6B, homéostasie épithéliale, cancer du sein, invasion, invadopodes, Cdc42.

"Prayer indeed is good, but while calling on the gods a man should himself lend a hand."
Hippocrates

"Be realistic, Plan for a miracle."
Osho

"…Another moment of discovery -its antithesis- that is rarely recorded: the discovery of failure. It is a moment that a scientist often encounters alone"
-Dr.S.Mukherjee,
The Emperor of All Maladies

Acknowledgments

I would like to first sincerely thank **Dr. Cécile Gauthier-Rouvière** and **Pr. Andrew Ewald** for agreeing to review my PhD work. Thank you **Dr. Patrick Auberger** for your advices and time as my internal advisor and for accepting to be the examiner of my dissertation. Thank you, Dr. **Marc Lopez**, for your valuable collaboration that definitely helped the progression of my work and for accepting to examine it. And lastly, I would to like to thank Dr. **Ellen Van Obberghen-Schilling** for accepting to be the president of my PhD jury and also for the opportunity she gave me to develop my histology expertise in her lab.

It is a great honor to have you all as the members of my PhD committee.

This PhD work would not have been possible without the guidance of **my supervisor, Dr. Frédéric Luton**. During these three years and a half, you gave me all the support and most importantly the trust I needed to conduct my research project. I learned a lot from you scientifically but also on a personal level. You gave me a great example of how to manage a team and push their members to be at their best. You taught me modesty, generosity, numerous French sayings and a "sioux" way for preparing a "french vinaigrette". I would not have asked for a better mentor, so thank you for this enriching PhD journey!

But these years would not have been so great without the contribution of all **my amazing research group and many great IPMCers:**

Michel, my second mentor, thank you for the great scientific discussions, advices, and for your sympathy.
Maria, la crème de la crème, thank you for carrying your beautiful smile and positive energy every day. My working days would not have been the same without you.
Eric, first "N'oublie pas que tu vas mourir", and second thank you for animating the work days with your artistic talents, your funny lame jokes and most importantly the best start-up ideas.
Monse, thank you for your help, your kindness, and all the moments we shared throughout this PhD.
Manue, Sarah, and Shiraz, for filling the lab with life, fun, lots of dancing sessions, and for the amazing trips we shared.
Tomtom, Mauro and Sophie, thank you for sharing with me your scientific expertise, friendly lunches, and unforgettable IPMC pleasant moments.

We do not always have the chance to thank the people supporting us to be who we are, so I will take this opportunity to show my love and gratitude for their presence in my life:

To my signalife family: **Christelle, Katarina, Georges, Vichnu, Martin, Gaia, Tomas, Ramona, Joanna, Derya, Hala**. Thank you for making the move into a new city smooth and pleasant.

To **Sany,** thank you for being the strong beautiful smart woman you are, for your ambition and relentless hustle to get where you deserve, the top of this world. I am grateful for having you in my life as a friend and a sister, the one and only Hong. And it is only the beginning of a lifetime friendship so "Don't stop us now"!

To "Total eclipse of the heart" crew, **Torsty, Sany, Hereroa, Anthony, and Aidy**, friends who can handle my voice in Karaoke nights are definitely real friends. And as Bonnie Tyler sang, together we took it to the end of the line. So, Cheers to you beautiful friends and to the treasured memories that I will forever keep!

To **Flo**, the perfect flatmate but also a dear bluntly honest friend. Thank you for making me feel at home, for reminding me that being a shopaholic is absolutely normal, and of course for your awaited mean funny comments (I will miss the latter the most).

To **Najla, Nathaly, and Christelle,** it was just perfect to have these dinners à la libanaise and share together the good and bad times.

To **Rudy**, thank you for being my guardian angel.

To **Maryse** and **Roxane**, after emotional letters of separation here comes the 6th year of distance to prove that real friends will always be there for you. Thank you.

To **Zeina** and **Jessica**, childhood friends are a gift from God. Thank you for being this gift and for giving me so much of your time, love and support.

To **Nahida, Rima, Rana, Najwa, Faten, Hiba, Amira,** briefly amazing women and beautiful souls, thank you for the prayers, the food and the care.

To **Ashana, Sabrina, Céline**, and **Meriem**, golden friends sent to make life a next level pleasant trip. Grateful for all that we shared and will keep on sharing.

To the "Dream Team", **Myriam, Sacha, Axel, Annes, Lynda** and **Stéphane**, great minds, and lovable hearts. Thank you "Aging" for bringing us together.

To **Sacha**! sharing with you this French adventure was one of the best things ever. Your presence allowed the worse moments to turn into hilarious memories. So, thank you for your precious friendship.

To **Julien**, thank you for sharing all these after-work long runs, for teaching me how to market a foldable bike, and for sure for the amazing conclusion figure!!

To the two lovable unforgettable souls I lost during this journey, to my grandparents **Hassan and Fadwa Fayad.** I hope I am making you proud of me.
To those who lost their battles against cancer, to the dear **Massoud El-Rayess**.
To those still fighting it, to my precious grandmother **Latifa Bou Nassar**.

To my **large family,** thank you for allowing me to grow by your side where there is no place for judgement or blame but only positive vibes of love, encouragement and blessings (bear with me, families in Lebanon are huge and I am super lucky to have their continuous support): **Alisar and Samer, Sara and Nassib, Nisrine and Wissam, Sawsan and Andrew, Iman and Bassam, Hanan and Raja, Hanaa and Wassim, all my 20 beautiful cousins and their families.**

To **Saad**, you filled my journey with laughter in the toughest times and patience in the craziest moments and above all you gave this precious motto "Sic Parvis Magna", meaning "Thus from small things, great things come". Thank you habubi for always being there for me.

And lastly to my **parents, brother and sister**;
Though far from home, I carried you in my heart so I can walk this journey. Through all the ups and downs, your love and support were as stable as ever. With you by my side, everything seemed possible so thank you for being my best friends, my happy thought and my backbones. I would not have made it without you.

As this PhD comes to an end, I look back and realize that it was an unforgettable lifetime experience, and what made it such a unique journey is all these astonishing people. I want them to know that I was lucky enough to meet them and I will miss having them around, so thank you for being who you are and giving me the time of my life. All the love of the world to you, gorgeous family and friends.

But I cannot leave without a last word for **cancer**;
Even though I am not sure we can become friends, I would like to thank you for the big life lessons you taught me.
So, dear cancer thank you for teaching me that resilience is the only way to survive in any new environment, that evolution and continuous change are needed to become stronger and more performant and that heterogeneity (a more suitable word for it "diversity") provides a better resistance to life threatening events.

Thank you God for this blissful life

To My Family,
To Najwa, Walid, Abir and Ghassan,

All that I am or will be comes from your unconditional love and support.
الحياة جوهرها أنتم، فلولاكم ما قيمة الحياة

List of Abbreviations

AJ: Adherens Junction

ALDH1: Aldehyde Dehydrogenase 1

MCF7: Michigan Cancer Foundation-7

APC: Antigen Presenting Cell

Arf: ADP Ribosylation Factors

ARHGAP: Rho GTPase Accelerating Protein

ARNO: (ARF nucleotide-binding site opener)

Arp: Acidic ribosomal phosphoprotein

BC: Breast Cancer

BM: Basement Membrane

BRCA: Breast Cancer Susceptibility Gene

CAF: Cancer-Associated Fibroblasts

CDH: Cadherin

c-Myc: Avian myelocytomatosis virus oncogene cellular homolog

CRB: Crumbs

CXCL12: C-X-C ligand

DCIS: Ductal Carcinoma in Situ

E-cadh: E-cadherin

EFA6: Exchange Factor for Arf

ECM: Extra-Cellular Matrix

EGF: Epidermal Growth Factor

EGFR: Epidermal Growth Factor Receptor

EMT: Epithelial Mesenchymal Transition

TFs: Transcription Factors

ER: Estrogen Receptor

ERK: Extracellular signal-regulated kinase

FAK: Focal Adhesion Kinase

FGF: Fibroblast Gowth Factor

FOX: Forkhead Box

GAGs: Glycosaminoglycan

GAP: GTPase Activating Protein

GDI: Guanine Nucleotide Dissociation Inhibitor

GDP: Guanine Diphosphatase

GEF: Guanines Nucleotides Exchanges Factor

GH: Growth Hormone

GPCR: G-proteins Coupled Receptor

GTP: Guanine Triphosphate

Her2: receptor tyrosine kinase erbB-2

HGF: Hepatocyte Growth Factor

HIF: Hypoxia-Inducible Factor

IGF: Insulin Growth Hormone

IRSp53: Insulin-receptor Substrate p53

KO: Knock-Out

LCIS: Lobular Carcinoma In Situ

LOX: Lysyl Oxidase

MDA-MB-231: M.D Anderson Metastasis Breast cancer cell line

MDCK: Madin-Darby Canine Kidney

MLC: Myosin-Light Chain

MLCK: Myosin Light-Chain Kinase

MMP: Matrix Metalloproteinases

MRCK: Myotonic dystrophy kinase-related Cdc42-binding kinase

N-WASP: Neural Wiskott-Aldrich Syndrome Protein

Pa: Pascal

PAK: p21-activated Kinase

PAR: Partitioning Defective

PGs: Proteoglycans

PR: Progesterone Receptor

PSD: Plekstrin sec-7 domain

PTEN: Tumor Suppressor Phosphatase and Tensin Homolog

Rb: Retinoblastoma

RhoA: Ras Homolog Family Member A

Rho GAP: RHO GTPase-activating proteins

ROCK: Rho-associated protein kinase

ROS: Reactive Oxygen Species

SCRIB: Scribble

TEB: Terminal End Buds

TGF-β-R: Transforming Growth Factor Receptor

TIMP: Metallopeptidase Inhibitor

TJ: Tight Junction

TKs: Tyrosine Kinase Substrate

TNC: Triple Negative Cancers

TME: Tumor Microenvironment

uPa: Urokinase Plasminogen Activator

VAC: Vacuolar Apical Compartment

VEGF: vascular endothelial growth factor

WASP: Wiskott–Aldrich syndrome protein

WAVE: WASP-family verprolin-homologous protein

ZO1: Zonula Occludens

List of Figures

Table of Contents

Preface

A brief walk with cancer: History and actuality

"thus for 3000 years and more, this disease has been known to the medical profession. And for 3000 years and more, humanity has been knocking at the door of the medical profession for a cure".

-Fortune, March 1937

This disease is cancer and what else could it be! Described for the first time in 1600 BC, in an ancient Egyptian papyrus (the oldest medical report), a breast cancer case was stated among 47 cases of injuries and trauma, and was the only one to be considered untreatable at the time. Here we are in the 21st century and cancer is still a major threat to our societies. Global cancer estimations have risen to 18.1 million new cases and 9.6 million deaths in 2018. In other words, one in 5 men and one in 6 women worldwide will develop cancer during their lifetime, and one in 8 men and one in 11 women will die because of it. Cancer is also an economic disease where about 170 billion dollars are spent for the management of cancer patients.

From radical surgeries and mastectomy to the discovery of chemotherapy and radiotherapy, cancer has witnessed some improvement at the treatment level but not enough to considerably reduce cancer mortality rate. The aggressiveness and heterogeneity of this disease makes it hard to target or control. Thus, more research is needed to better understand the process of cancer initiation and progression, and thus, propose more personalized and effective treatments.

Who is behind this giant?!

"It's a bad bile. It's bad habits. It's bad bosses. It's bad genes"

-Mel Greaves,
Cancer: The Evolutionary Legacy, 2000

After Hippocrates suggestion that all illness have humoral causes, Galen proposed that cancer is caused by stagnating black bile. Then with the trend of viruses' discovery, researchers claimed that all cancers are induced by viruses; this theory is still true for some cancers. Nowadays, we know that behind cancer initiation and progression stands an accumulation of gene alterations that will disrupt the homeostasis of normal cells. Some key mutations are capable of giving cells the capacity to proliferate and escape cell death and therefore to form a primary tumor. Additional mutations will allow hyperproliferative cells to become aggressive and invasive in order to colonize new organs and form tumors at distant sites. Heterogeneous, complex and resistant to treatment, it would be interesting to identify genes important for protecting normal cells from losing their integrity and becoming cancerous.

My PhD thesis: A step towards better understanding Cancer

My PhD objective was to study the role of EFA6B, our protein of interest, on normal mammary epithelial cell homeostasis. Interestingly, the loss of EFA6B solely disrupted normal epithelial cell behavior (polarity and luminogenesis) and provided cells with powerful invasive capacities. This thesis allowed the identification of EFA6B as a new guardian of epithelial cells characteristics, and an important gene for preserving cells from becoming invasive.

In the hope that the results I present in this PhD thesis will open up new horizons for cancer research and bring us a step closer to conquering the so-called “Emperor of All Maladies”, Cancer

INTRODUCTION

Introduction

This is not an exhaustive summary of the literature. In my introduction, I will try to set a context for my PhD work and to highlight research studies and knowledge relevant to it.

I. Mammary Gland: Physiology and Pathology

1. Physiology

1. 1. Mammary gland morphogenesis: key developmental steps

Mammary gland is one of the main differential organs characterizing mammals; it evolved over 300 million years most probably from sweat glands. This apocrine gland is responsible for producing milk during lactation required to support newborns' survival and development.

For developmental biologists, the mammary gland has always been an interesting model of study; unlike other exocrine organs, its development starts during embryogenesis but continues after birth through different stages of life: embryonic, pubertal and reproductive stages (Macias and Hinck, 2012). Our knowledge of the mammary gland morphogenesis is provided primarily from studies conceived in mouse models and extrapolated to human (**Figure 1**).

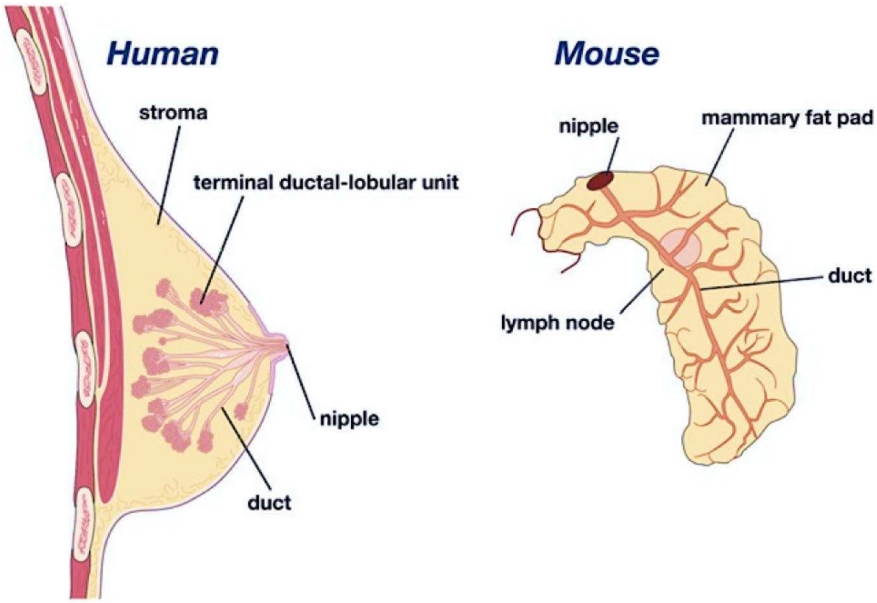

Figure 1: Schematic representation of human and mouse mammary gland.

Some structural differences exist: Rodents develop five pairs of mammary glands at reproducible locations with a fatty stroma rich in adipocytes while human' only pair contains more fibrous connective tissue. Adapted from Visvader, 2009.

Overall, at the cellular level, the mammary gland is similar in human and rodents, and therefore data presented hereafter mostly from rodent models are relevant to the understanding of human breast development and disease.

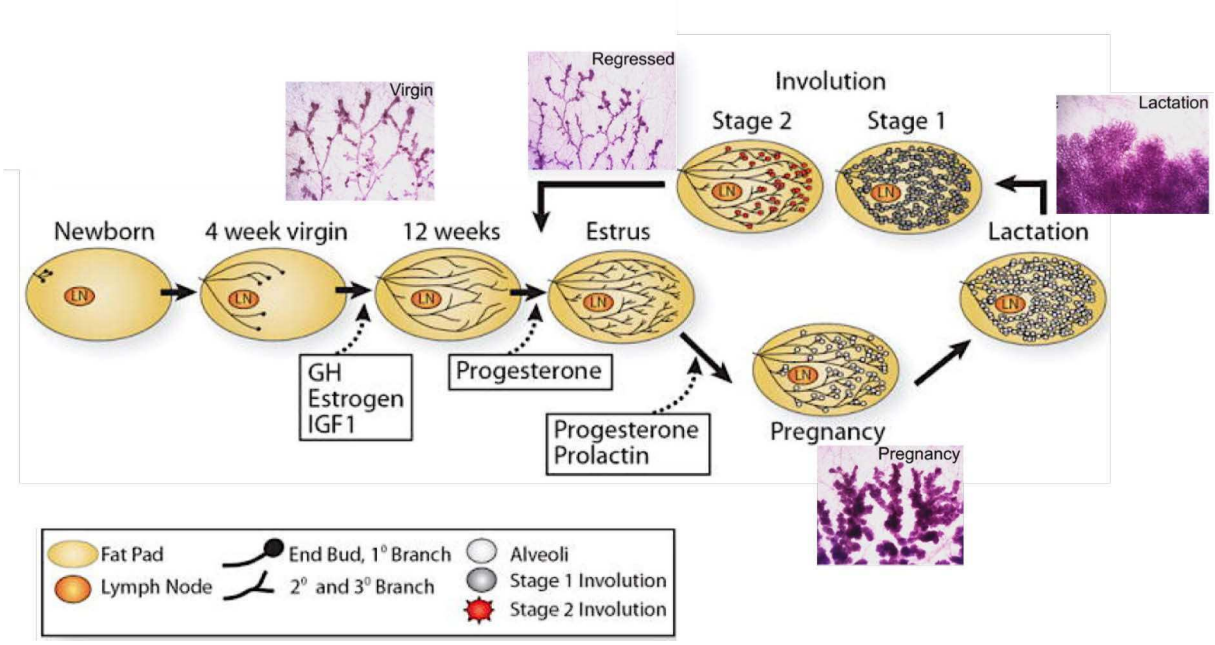

Figure 2: Morphological changes associated with the post-natal stages of mammary gland development.

At birth, mice have few small branches that will grow slowly until hormone-stimulation at puberty. Then, a tremendous growth of the ductal tree occurs. Upon pregnancy alveologenesis is observed with the stimulation of prolactin. Involution is triggered by milk stagnation and consists of two stages. Stage 1 consists of a reversible step where cells start engaging into apoptosis accompanied by alveolar cell detachment. At 48h, cells transition to stage 2 of the involution and alveoli breakdown by a second wave of apoptosis stimulated by the ECM and the proteolytic enzymes. At this stage, milk is definitely lost. The mammary gland is remodeled to its original architecture, and gain a new transcriptional signature. Adapted from Macias and Hinck, 2012 and Schedin et al., 2007.

1. 1. 1. Embryonic development of the mammary gland

Mammary gland derives from the ectoderm germ layer that later differentiates into the epithelial compartment and forms the rudimentary mammary bud present at birth.

First, **mammary placodes** emerge defining the position of future mammary glands. Placodes are defined by ectoderm thickenings consisting of several shaped layers of ectoderm cells and are formed by physiological cell migration and aggregation, but not proliferation.

Interestingly, already at this stage, the mammary gland is surrounded by a stromal compartment composed of cells deriving from the mesoderm. This embryonic mesenchyme plays a crucial role in orienting the differentiation of the epithelial layer into mammary precursors. This information has been proven by combining epithelial mammary cells with different types of mesenchyme. For example, combining salivary mesenchyme with embryonic mammary line produced an epithelium morphologically close to salivary gland (Kratochwil, 1969; Sakakura et al., 1976). In parallel, the

mammary epithelial line releases inductive signals stimulating the differentiation of the close mesenchyme layer into fibroblasts while more distant mesenchyme differentiates into fat pad precursors and adipocytes.

At the end of the fetal development, the mammary gland precursor consists of a small network of polarized bilayered epithelia organized in simple ducts.

1. 1. 2. Puberty & branching morphogenesis

Until puberty, the mammary bud with its few rudimentary branches will remain in a quiescent state and grows proportionally to the body. With hormones and growth factors (growth hormone, Estrogen, insulin-like growth factor…) release, epithelial cells will fill the fat pad with extensive proliferation and will present growing ducts characterized by elongated tubes with multilayered cells forming at the tip the so-called **terminal end buds (TEBs)***. TEBs are round shaped structures that will penetrate the stroma by dividing their outer cell layer (later differentiated in myoepithelial cells) as well as the underlying multilayer of luminal precursor cells (Ewald et al., 2008, 2012; Williams and Daniel, 1983). From these primary ducts, secondary branches sprout laterally to form a more complex tubular network.

****Together with biochemical signals (growth factors, hormones, morphogens, etc.), mechanical cues (cellular contractility, matrix stiffness, intercellular cohesion, etc.) may trigger the activation of several signaling pathways in cells and seem to play an important role in branching morphogenesis, especially in defining the branching sites (Gjorevski and Nelson, 2010; Nerger and Nelson, 2018). In addition, mechanical forces have been shown to stimulate the expression of mesenchymal transcription factors (e.g. Twist1, Snail…) and therefore induce an epithelial-mesenchymal transition of leader cells important for mammary morphogenesis (Gjorevski and Nelson, 2010). It has as well been implicated in increasing extracellular matrix remodeling and the thinning of the basement membrane (physical barriers) by activating metalloproteases that will allow normal epithelial cells to invade the adjacent extracellular matrix, ECM (Mori et al., 2013; Wiseman et al., 2003). For more in-depth information, the following reviews present extensively the roles of mechanical forces in mammary morphogenesis : (Fata et al., 2003; Spurlin and Nelson, 2017; Varner and Nelson, 2014; Xu et al., 2009).****

The final pubertal tree pattern will increase tremendously the area of lobular structures to fill up to 60% of the fat pad and therefore prepare it for lactation when pregnancy occurs. Of note, the quiescent mammary gland of rodents contains ramified ducts only, comprising small lateral or tertiary branches that give rise to alveoli at pregnancy, whereas adult human mammary gland, even in the absence of pregnancy, consists of variable amounts of lobulo-alveoli (Anbazhagan et al., 1998; Naccarato et al., 2000).

1. 1. 3. Pregnancy, lactation and involution: a more complex ductal network

Pregnancy hormones (mainly progesterone and prolactin) will prepare the mammary gland for another round of morphogenesis, and an increase in secondary and tertiary branching. These hormones will stimulate epithelial cell proliferation, angiogenesis and a decrease in the mammary adipose tissue. At this stage, terminal lobular structures will give rise to alveolar buds composed of into differentiated bilayered **alveoli**. During lactation, these alveoli will become milk secreting lobules, characterized by a central lumen and a single layer of secretory luminal cells enclosed in a layer of myoepithelial contractile cells.

When weaning occurs and milk stagnate in the lobules, involution begins bringing back the quiescent ductal mammary architecture and a modified gene expression profile. Apoptosis, stimulated in part by the breakdown of ECM, will play a major part in reducing the excess of branching and replacing it with adipocytes. Besides apoptosis, the crosstalk between ECM and epithelial mammary cells have its role in the involution; as the important remodeling of the stroma by the metalloproteases (**Figure 2**) (Macias and Hinck, 2012).

Conclusion

Mammary gland morphogenesis is a finely tuned complicated process in which different cell types have to integrate external and internal signals to multiple different cycles of proliferation, migration and invasion. The different cellular components of the mammary tissue interact with their surrounding stroma or mesenchyme in order to orchestrate the formation of a functional organ. Identifying the molecular control and the spatiotemporal regulation of these events is key to further understand the cellular homeostasis of this tissue but also for a better interpretation of molecular events inducing and promoting breast cancer.

1. 2. Mammary gland architecture: key components

As presented in paragraph I-a, the mammary gland is composed of stromal tissue in which mammary epithelium develops. Along with external signals (hormones, growth factors…), these two compartments interact and exchange information continuously to ensure a normal and functional gland development.

In this section, we will delve into cell types and constituents of the epithelium and the mesenchyme of mammary gland: characteristics, origin, and interaction.

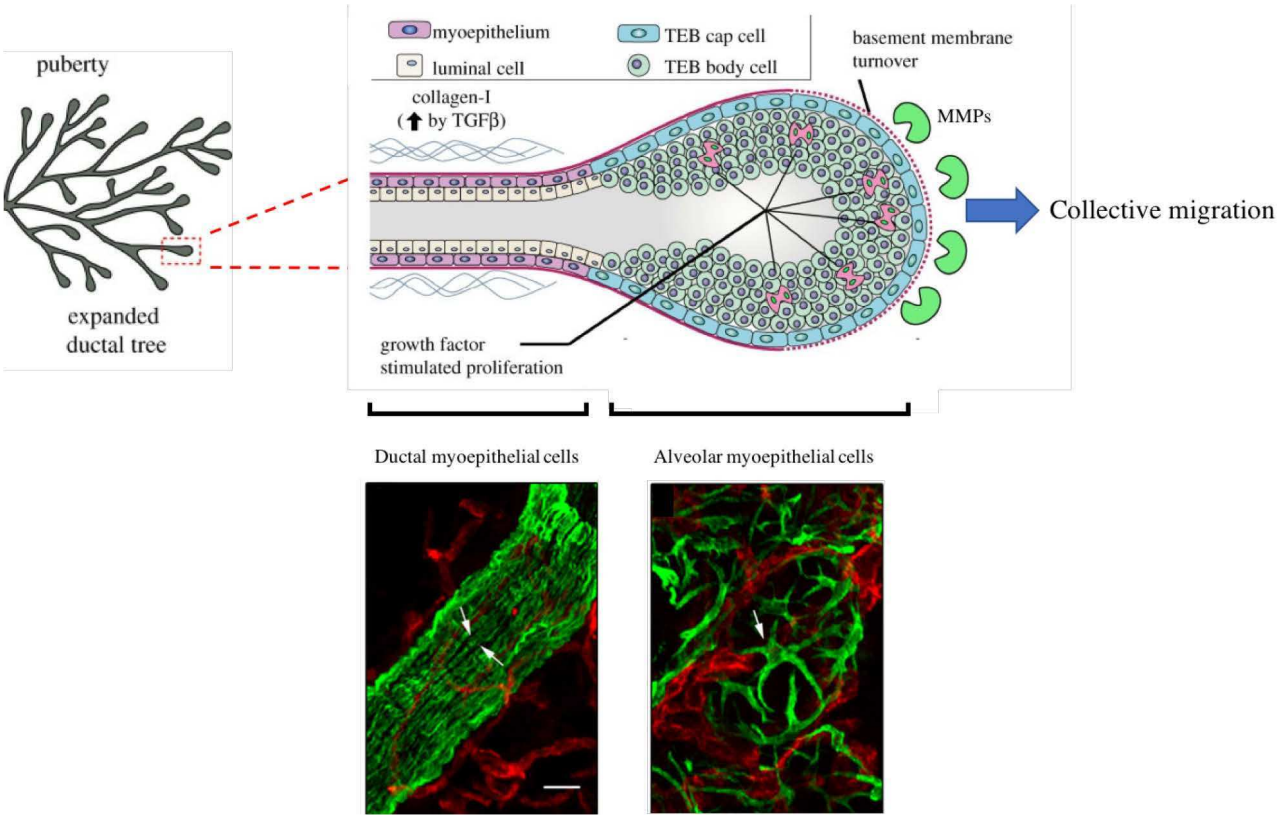

Figure 3: Ductal and TEB cellular composition and branching regulation at the TEBs.

Branching is ensured by TEB collective migration facilitated by MMPs dependent degradation of the ECM. In addition, ECM remodeling by MMPs generates functional peptides which stimulate the proliferation of cells at the TEBs essential for sustaining the ductal elongation. Myoepithelial cells with the turn-over of basal membrane allow the migration of TEB cells but restrain any formation of cellular protrusion. In the lower panel, green indicates the immunostaining of keratin 5 in myoepithelial cells of mice mammary gland. The ductal myoepithelial cells of a 10 weeks old virgin mouse show a continuous monolayer while alveolar myoepithelial cells (2-day lactating mouse mammary gland) show a stellate architecture. Adapted from Moumen et al., 2011; Spurlin and Nelson, 2017.

1. 2. 1. Epithelium compartment

The mammary epithelium is composed of two main epithelial cell types: luminal and basal cells. Luminal cells are Keratin 8 & 18 positive cells facing the lumen and secreting milk during lactation, surrounded by basal/myoepithelial cells (Keratin 5 & 14 positive) characterized by their contractile capacity (smooth muscle α positive) and are in direct contact with the stroma (basement membrane and extracellular matrix).

Luminal and basal epithelial cells are connected within the same layer or between each other through adhesion complexes and will adopt different architectural and functional characteristics depending on the stage of morphogenesis of the mammary gland as well as the functional unit they are composing (ducts, TEB/alveoli).

Luminal cells:

Within the ductal unit (Figure 3), luminal cells are in direct contact with myoepithelial cells and form a **monolayer** of cuboidal polarized cells connected through strongly expressed adhesion complexes: tight junctions, adhesion junctions, gap junctions and desmosomes. In particularly, luminal cells express two specific desmosomal cadherins (desmocollin 2 & desmoglein 2), and one of the most studied adherens junction proteins, E-cadherin (Daniel et al., 1995; Deugnier et al., 2002; Faraldo et al., 2005; Kendrick et al., 2008; Muschler and Streuli, 2010; Pitelka et al., 2009; Runswick et al., 2001; Shamir and Ewald, 2015).

In the TEB (Figure 3), cell proliferation drives the ductal elongation and establishment of **multi-layered** luminal cells (Lu et al., 2008). At this dynamic level, in 3D culture and in mice, stratification occurs when luminal cells of the duct give rise to less polarized daughter cells, expressing fewer adhesion molecules (Huebner and Ewald, 2014). This asymmetric cellular division takes place in an apical vertical manner, placing new cells between the polarized luminal cells and the myoepithelial layer.

Besides proliferation, ductal elongation uses collective migration to drive mammary branching (Ewald et al., 2008, 2012). Collective migration requires cells to stay connected and hence the importance of adhesion proteins. Consistent with these findings, in an *in vitro* model of dissemination, mammary cells expressing Twist1 (a mesenchymal transcription factor) can migrate through a 3D matrix while preserving their adhesive properties (E-cadherin*** expression required) and proliferation capacities (Shamir et al., 2014, 2016). In addition, some studies have revealed the importance of E-cadherin expression at different stages of mammary morphogenesis. Shamir et al, *in vivo*, showed that E-cadherin expression is important for ducts formation and homeostasis; noting that cells negative for E-cadherin have been extruded from the elongating ducts (Shamir et al., 2014). E-cadherin is as well crucial for normal milk secretion during lactation; a reduced amount of milk proteins have been reported in alveoli structures deleted for E-cadherin (Boussadia et al., 2002).

I mentioned that ductal elongation occurs through a collective migration combined to an invasion of the extracellular matrix without sending cellular or membrane protrusions (Ewald et al., 2008, 2012; Huebner et al., 2016). In 1983, Williams & Daniel noticed, using phase real-time phase contrast images, that luminal cells of the TEB are in a dynamic state of extension and retraction (Williams and Daniel, 1983). More recently, *in silico*, these extensions have been seen as attempts to prepare luminal cells for intercalating into the basal layer, and therefore elongating the pubertal ducts (Neumann et al., 2018). One major difference with invading carcinomas that duct elongation of normal mammary adopts collective cell migration with no cellular dissemination. It is interesting to understand in normal mammary models *in vitro* and *in vivo* the mechanisms and signals ruling epithelial homeostasis not only

to understand epithelial tissue development but to also have more insights on which mechanisms might be disrupting the epithelial homeostasis and causing tumor initiation and progression.

Cadherins are transmembrane proteins that develop calcium-dependent intercellular homophilic interactions via their extracellular domain. E-cadherin is the main cadherin expressed by epithelial cells. Its cytoplasmic domain is associated with β-catenin and p120-catenin. The α-catenin binds to β-catenin and other actin-binding proteins such as vinculin and α-actinin, thus allowing the anchoring of adherens junctions to the actin cytoskeleton. Many additional proteins can then be recruited such as Arp2/3, cortactin, and small Rho-GTPases (Rac1, Cdc42 and RhoA) responsible for organizing the actin cytoskeleton associated to E-cadherin

Basal cells:

The **basal layer** consists of myoepithelial cells forming a continuous monolayer around **ducts** and a loose layer (stellate shaped) around **alveoli** enclosing luminal cells that are rarely in direct contact with the basement membrane (**Figure 3**) (Moumen et al., 2011). Structurally, myoepithelial cells are connected to ECM through hemidesmosomes (the integrins) and some non-integrin receptors such as dystroglycan, syndecan, galactosyl transferase and to luminal cells through desmosomes. They are characterized by the expression of P-cadherin and alpha smooth muscle actin, a marker of their contractility function (Daniel et al., 1995; Moumen et al., 2011).

During development, myoepithelial cells play an essential role regulating the overall homeostasis as well as ductal morphogenesis of the developing mammary gland and in establishing luminal cell polarity (Adriance et al., 2005).

Homeostasis of developing mammary gland:

The communication of myoepithelial cells with their luminal neighbor cells is in part ensured by differential expression of ligand-receptor. For example, the exclusive expression of Ephrin receptor EphB4 by myoepithelial cells whereas its ligand Ephrin 2 expression is restricted to luminal cells (Andres and Ziemiecki, 2003). An imbalance of this distribution alters the survival and proliferation of mammary epithelium. Other examples are reviewed by Moumen et al., 2011.

Another crucial function is that myoepithelial cells participate to ECM production by expressing components of the basal membrane (as laminin-1, laminin-5, collagen IV and fibronectin) (Warburton et al., 1982) and remodeling of the latter by secreting matrix metalloproteases (Dickson and Warburton, 1992).

The integrity of myoepithelial layer is a major criterion for maintaining a normal tissue as well as preventing cancer cells of disseminating. In patients, a damaged basal layer correlats with poor prognosis and helps distinguish Invasive Ductal Carcinoma from Ductal Carcinoma In Situ (Man and Sang, 2004; Man et al., 2003; Sternlicht and Barsky, 1997). In mice, P-cadherin (mainly expressed by myoepithelial cells) deficient mammary glands develop late in life hyperplasia lesions in the epithelium (Radice et al., 1997).

Ductal morphogenesis:

Myoepithelial cells are partially responsible for restricting the protrusive potential of TEBs cells during their collective migration. They form a barrier retaining luminal cells from dissemination during TEB progression (**Figure 3**) (Hu et al., 2008; Sirka et al., 2018). Recently, Sirka et al showed that normal myoepithelial cells restrain Twist1+ disseminating luminal cells and prevent them from invading the collagen of 3D organotypic culture (Sirka et al., 2018). On the other hand, myoepithelial cells take part in producing laminins (especially laminin-1), main components of the basal lamina that have been strongly correlated with the inhibition of epithelial cell invasion, especially in malignant contexts (Nguyen-Ngoc et al., 2012).

Luminal cell polarity:

This capacity of secreting laminin-1 stands behind the role of myoepithelial cells in maintaining the apico-basal polarity of luminal cells (Bissell and Bilder, 2003; Gudjonsson et al., 2002). Indeed, luminal cells cultured in 3D collagen matrix have reverted polarity and lack a central lumen, a main characteristic of normal acini. However, when co-cultured with myoepithelial cells in the same matrix, luminal cells display a normal polarity with the apical side of the cells facing the lumen (Gudjonsson et al., 2002).

During lactation, under the stimulation of oxytocin hormone, myoepithelial cells contract and expulse milk from acini into collector ducts, and to the nipple (Reversi et al., 2005). Here, gap junctions and cadherin interaction function as mechanical regulators of the smooth milk ejection.

1) Stem cells

Mammary gland undergoes an extensive remodeling during its development. This characteristic suggests an important regenerative capacity of a stem cell subpopulation. This hypothesis has been demonstrated especially by stem cell enrichment followed by transplantation assays. Epithelial mammary cells, sorted on the basis of various cell surface markers and transplanted into cleared fat pads were capable of generating normal branching epithelia (Daniel, 1975; Faulkin and Deome, 1960; Kordon and Smith, 1998; Plaks et al., 2013; Shackleton et al., 2006; Spike et al., 2012; Stingl et al., 2006; Zeng and Nusse, 2010).

These different studies (reviewed in detail by Inman et al., 2015) used variable markers which generated inconsistencies in the definition of the stem cell or progenitor sub-populations residing in the epithelial compartment of the mammary gland. For instance, whether this sub-population is present in the basal or in both luminal and basal layers is still a subject of controversy. A limiting experimental factor is the fact that manipulating cells *in vitro* and removing them from their environment before injections can affect their behavior and stimulate some stem cell characteristics.

As of today, several markers are used to define mammary stem cells and progenitors. In human breast tumors, a high CD44 and low CD24 expression is believed to mark a sub-population of cells bearing stem cell characteristics (Al-Hajj et al., 2003). However, in 2007, C. Ginestier et al have challenged this notion. In fact, $CD44^{high}/CD24^{low}$ normal and cancer cells were not able of generating a mammary gland when implanted in mice mammary fat pad. They suggested instead the use of aldehyde dehydrogenase 1 (ALDH1) as a more specific marker for stem and progenitor cells (Ginestier et al., 2007).]

In the last decade, lineage tracing techniques allowed researchers to follow cells's origin, segregation, and differentiation*, in situ*, in their physiological contexts. A recent study by C.Blanpain's lab have shown that multipotent stem cells exist only during embryonic mammary development unlike other epithelial tissues. They have also demonstrated that postnatal mammary development is supported by distinct unipotent progenitors of basal and luminal cells (Wuidart et al., 2018).

Nevertheless, limitations and variability related to this new technique exist as well: choice of the right promoters, as well as specific markers to trace and confirm these lineages at different developmental stages of the mammary gland. Therefore, other studies have demonstrated the presence of bipotent mammary epithelial cells in the basal layer (Shackleton et al., 2006; Stingl et al., 2006; Visvader and Stingl, 2014). They suggest that these bipotent cells are capable of generating both luminal and basal cells in the post-natal development (Rios et al., 2014; Wang et al., 2015). An interesting discussion related to these controversies was addressed in the review of L.Seldin, A.Le Guelte and I.Macara, (Seldin et al., 2017).

1. 2. 2. Microenvironment compartment

The microenvironment surrounding cells establishes a part of the tissue architecture and has been implicated in diverse developmental processes as well as diseases. It is mainly composed of: 1) a basement membrane delineating the epithelium compartment and 2) a stroma called extracellular matrix (ECM) adjacent to the latter, homing different cells important for the homeostasis of the mammary gland (as fibroblasts, adipocytes, immune cells, etc.). This pleiotropic aspect comes from the rich diversity of microenvironment components (proteins and their isoforms) and their 3D pattern organization.

The basement membrane (BM) is a highly organized structure lying directly underneath the epithelia. It adopts different morphologies depending on the structural unit of the mammary gland: basement membrane surrounding the ducts is thicker than the layer outlining TEBs which can be a functional consequence supporting growing ducts (measured first by (Williams and Daniel, 1983)). It is mainly constituted of laminins, collagen IV, nidogen and proteoglycans like perlecan (Maller et al., 2010). Laminins, the major BM proteins, are a family of multidomain heterodimers (α, β and δ chains) with the most expressed in developing mammary gland being: Laminin-111, Laminin-332, Laminin-511, Laminin-521 (Aumailley et al., 2005; Prince et al., 2002).

Different integrin receptors will recognize these laminins and play a major role in sensing extracellular composition, density and architecture and translate it into intracellular signals required for epithelial morphogenesis, mainly cell polarity and cell migration. They can also perceive growth factors and cytokine signaling and control morphogenesis (Eyckmans et al., 2011, 2011; Glukhova and Streuli, 2013; Katz and Streuli, 2007). In both rodents and human, various integrin dimers were revealed by immunohistochemistry: collagen receptors (α1β1, α2β1 integrin), fibronectin receptor (α5β1, αvβ3 integrin) and high levels of laminin receptors (α3β1, α6β1 and α6β4 integrins binding respectively laminins 511/521/332, laminins 511/521/332/111 and laminins 332, 511, 521) (Moumen et al., 2011; Ramovs et al., 2017; Raymond et al., 2012).

A great number of studies aimed at understanding the role of these different isoforms and dimers of integrins and their substrates. For instance, the major laminin of the BM, Laminin 111, helps polarizing luminal cells in the alveolar structures (Alcaraz et al., 2008; Gudjonsson et al., 2002). To investigate the role of integrins, KO mice have been established, and revealed that the mammary gland requires the α2 subunit for branching morphogenesis but not the α3, α4 or α6 subunits (Chen et al., 2002; Kass et al., 2007; Klinowska et al., 2001). Homozygous KO of integrin β1 was shown to be lethal for mouse embryos (Fässler and Meyer, 1995), which reflects its importance in early developmental processes. For mammary gland development, integrin β1 has an interesting role in regulating the branching morphogenesis by binding to the metalloprotease MMP14 and remodeling the ECM (Mori et al., 2013). It also acts during lactation on relaxing the focal adhesion tensions in response to myoepithelial contractility (Raymond et al., 2011) and on stimulating mammary epithelial differentiation and milk synthesis (Li et al., 2005; Naylor et al., 2005).

Further information on the role of integrins in mammary gland development can be found in these two reviews : (Glukhova and Streuli, 2013; Kass et al., 2007).

2) Adjacent to the BM lies the stroma, a fibro and fatty collagen I-rich structure, harboring different cell types indispensable for the homeostasis, development, and immunological protection of a normal mammary gland.

The **stroma** or **extracellular matrix** (ECM)*** is composed of fibroblasts, adipocytes, vascular and immune cells embedded in a matrix of collagen I, fibronectins, tenascins, SPARC (secreted protein acidic and rich in cysteine), decorins, proteoglycans, among other proteins such as ECM-remodeling enzymes and their regulators (Inman et al., 2015; Maller et al., 2010).

***ECM protein families:*

Collagens a family of 27 distinct members is grouped into two large subfamily fibrillar collagens and non-fibrillar collagens (Myllyharju and Kivirikko, 2004).

Proteoglycans (PGs) superfamily contains more than 30 large protein chains often linked to one or more glycosaminoglycan (GAGs) chains, such as heparin sulphate (Casu et al., 2010; Iozzo, 1998, 2005).

Elastin fibers are essential ECM macromolecules comprising an elastin core surrounded by a mantle of fibrillin-rich microfibrils and fibulin (structural glycoproteins) (Kielty et al., 2002).

*Glycoproteins are proteins comprising short chains of carbohydrates covalently attached to amino acid side chains (Chothia and Jones, 1997). Some of the members of glycoprotein family are fibronectin, laminin, tenasin-C, etc.****

It has unique biophysical and biomechanical characteristics essential to support a wide variety of cell behaviors such as migration, mechanosensing and signaling. Depending on the developmental stage of mammary gland, the ECM will be modified to stimulate and enable a normal morphogenesis including epithelial branching and differentiation.

The matrix density as well as 3D macromolecules arrangement will dictate the biophysical features of the stroma that recently emerged as a key player in affecting morphogenesis. For instance, during ductal branching, several ECM remodeling enzymes are expressed by both epithelial and stromal cells (like fibroblasts) and play an important role in epithelial branching. Among these enzymes, the most dominant are metalloproteases represented by two major families MMPs and ADAMs (reviewed by (Lu et al., 2011)). To further investigate their role in mammary branching, several mouse models were established with dysregulated MMP expression. An overexpression of MMP3 or MMP14 has shown an increase in lateral branching suggesting that a partial degradation of the ECM is sufficient to increase or facilitate mammary gland branching (Gomes et al., 2015; Mori et al., 2013; Wiseman et al., 2003).

Other interesting enzymes are lysyl oxidases (LOX) responsible for collagen cross-linking which can increase the stiffness of the stroma and thus alveolar morphogenesis (Bonnans et al., 2014). The stiffness reflects the rigidity of the ECM, a biophysical feature that depends on the size and length of fibrillary collagen bundles. The degree of rigidity of the ECM dictates in part the differentiation of mammary epithelial cells (Engler et al., 2006; Schedin and Keely, 2011).

ECM proteins were as well found essential to regulate branching. In a KO mouse model of fibronectin, ductal outgrowth was delayed in virgin mice and alveologenesis was absent in pregnant mice suggesting an interesting role of fibronectin in proliferation and differentiation of mammary epithelial cells (Liu et al., 2010). Similarly, loss of collagens and laminins, in other developing glands (as salivary gland) disrupted branching morphogenesis (Fukuda et al., 1988; Rebustini et al., 2007).

Finally, ECM cellular components play a role in regulating various functions indispensable for mammary gland morphogenesis. For example, fibroblasts, main actors of ECM, will synthesize stromal proteins such as collagens, fibronectins, proteoglycans and many enzymes and communicate with the epithelium through growth factor and proteases (Howard and Lu, 2014; Inman et al., 2015). In turn, adipocytes exhibit an endocrine function; they release hormones regulating the mammary gland function (such as VEGF important for angiogenesis). They also consist of the energy stock needed for milk production, a metabolically demanding process (Gregor et al., 2013; Hovey and Aimo, 2010). Immune cells like macrophages and eosinophils were as well implicated in mammary epithelial branching; they were localized to branching sites where invasion into the fat pad occurs (Gouon-Evans et al., 2000).

A full description of the numerous roles of the stroma and its components is beyond the scope of this thesis, but further information are covered in details in the following reviews: (Howard and Lu, 2014; Huebner and Ewald, 2014; Inman et al., 2015; Kass et al., 2007; Maller et al., 2010; Schedin and Keely, 2011; Shamir and Ewald, 2015).

Conclusion:

ECM is a highly dynamic structure modulated constantly by enzymes secreted by both the epithelial and the stromal cells and is crucial to ensure a normal mammary gland morphogenesis.

However, besides the fibronectin KO mouse model (Liu et al., 2010), studies investigating the functions of other stromal components are held *in vitro* in cell lines. Therefore, research on animal models is needed to further understand the role of stroma in normal morphogenesis in an attempt to have a better understanding of its pathological implication.

2. Breast Cancer

2. 1. Epidemiology, Evolution and Causes

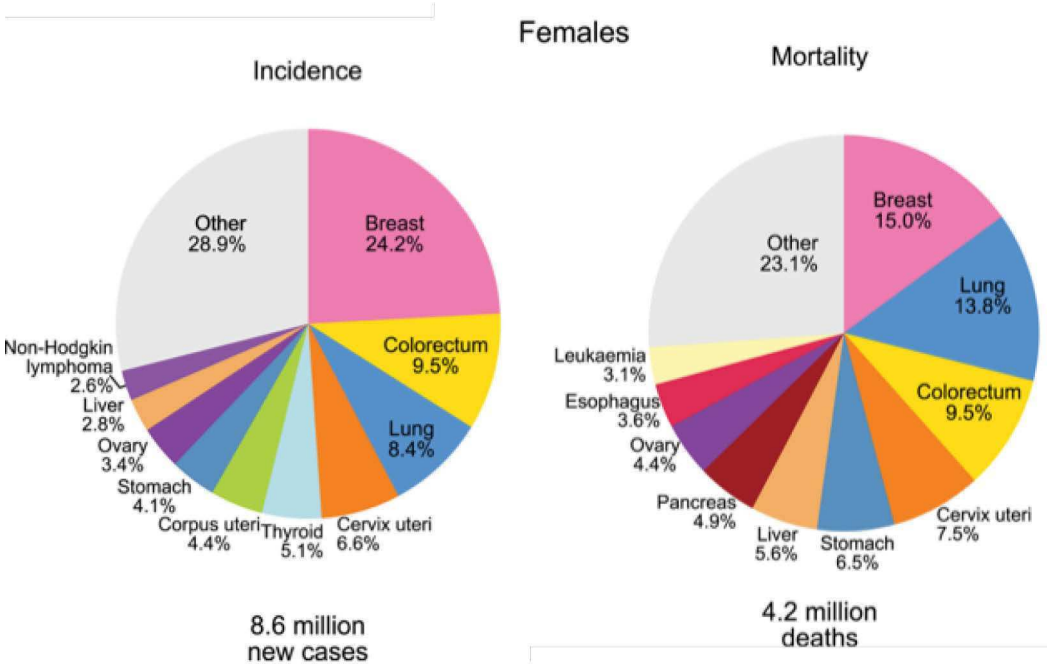

Figure 4: GLOBOCAN estimates of incidence and mortality worldwide for 36 cancers in 185 countries (2018).

Breast cancer shows the highest rates of new cases emergence and death cases in women worldwide. Adapted from Bray et al., 2018.

Breast cancer, the first cancer to be described in history, is still the most frequent cancer among women (**Figure 4**). In 2018, it is accountable for around 25% of all cancers with 2.1 million newly diagnosed cases worldwide. Breast cancer is considered the leading cause of death of women, with a majority (60%) occurring in economically developed countries (Bray et al., 2018).

In France, more than 49 000 new cases and 12 000 death cases are estimated in 2018. This high incidence rate is attributed in majority to *de novo* breast cancer form, characterized by sporadic mutations. Several risk factors can increase the prevalence of these mutations: age (aging population especially in developed countries), reproduction (having a late pregnancy at first birth, or nulliparity), hormone treatment after menopause, early menstruation, nutrition (alcohol, obesity…) (Bray et al., 2018; Britt et al., 2007). To note, only 5 to 10% of breast cancer are linked to hereditary factors with germinal mutations of genes involved in DNA and cell cycle control (like BRCA1, BRCA2 genes or other cancer susceptibility genes).

2. 2. Heterogeneity and Treatments

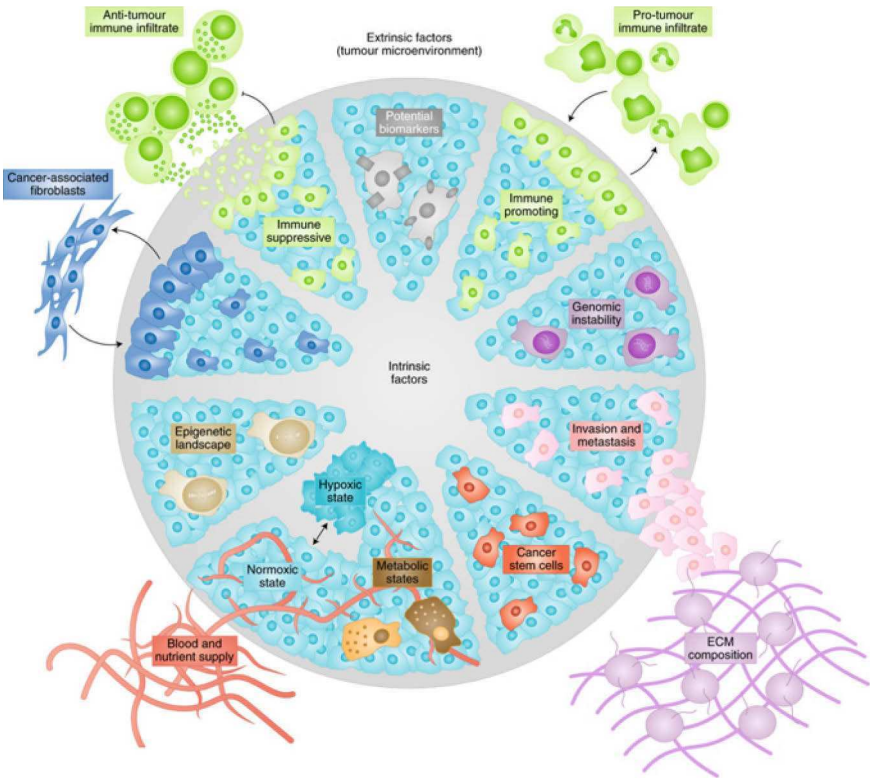

Figure 5: Intrinsic and extrinsic factors causing tumor heterogeneity.

Various factors can contribute to the heterogeneity observed even within the same tumor. The ECM has been largely associated with tumor progression and it can vary depending on the molecular components and their architecture (stiffness, density, etc.) and in its cellular components with cancer-associated fibroblasts, immune cells, and endothelial cells. Hypoxia, cell metabolism, angiogenesis and epigenetics can play a major part in influencing the state of cancer cells (Lawson et al., 2018).

Over the last few years, European countries have seen a notable decrease in breast cancer death incidence. The mammography screening has improved the survival rates by allowing to take in charge patients at earlier stages of the disease. Besides early detection, breast cancer is one of the most treatment-responsive solid tumors. Numerous treatments exist and can vary depending on the subtype and stage of cancer at diagnosis, one can cite: hormone therapy, chemotherapy, radiation therapy, immunotherapy, and surgery. Nevertheless, the total death number of breast cancer patients is still considerable.

This reality lies behind the highly heterogeneous aspect of this disease, more specifically breast cancer (**Figure 5**). Mostly induced by sporadic mutations, breast tumors arise from an endless possible combination of altered genes and pathways. This plethora of causes is reflected by a variability of clinical outcomes and by the different evolution of the tumor in response to treatment. From resistance to relapses, the existing therapies have proven not sufficient to target all breast cancers.

In fact, for early-stage cancer, clinicians usually proceed by removing the tumor surgically. This early management of the tumor has, in parallel, increased the prescription of chemotherapy. Around 60% of patients undergo combine surgery with an adjuvant chemotherapy in order to eradicate disseminated micrometastasis (Andre and Delaloge, 2009; Schmidt et al., 2009; Weigelt and Reis-Filho, 2010).

Even with more effective therapies, up to 25 % of patients develop distant metastasis recurrence and no improvement in survival rates over the last 30 years (Tevaarwerk et al., 2013). It may be that the primary tumor and the metastatic sites do not require the same treatments. Indeed, gene profiling of primary tumors and distant metastasis have demonstrated that secondary tumors acquire new somatic mutations while progressing (Yates et al., 2017). Thus, it might be interesting to sequence tumors at all sites in order to suggest more adapted treatments. Besides the cellular heterogeneity of cancer, the stromal compartment plays an important role in dictating the tumor subtype and its aggressiveness. The exchange of extracellular matrix with epithelial cells has been demonstrated crucial for the development and progression of cancer (Place et al., 2011). Analysis of stroma components by matrisome profiling analysis can give correlations between clinical outcomes and specific treatments. Having this information will help to further stratify the classification of cancer and push towards more personalized treatments. I can refer to the interesting initiative launched by MIT university "The Matrisome Project" aiming to create a data base related to proteins constituting the Extracellular Matrix which can help cumulate data about the tumors' matrisome as well.

For now, therapeutic decisions and prediction of tumor progression are mainly based on breast cancer subtypes which are determined by different prognostic markers (tumor size, hormone receptors' expression, histological grade, invasion, etc.), and more recently by large scale genomic profiling of primary tumors. Therefore, refining the classification of tumors will result in better predictions of the efficiency of a specific therapy, and optimize treatment decisions (Colombo et al., 2011).

2. 3. Breast Cancer Classification

Although pathologists and genomic data analysts have all agreed on breast cancer heterogeneity, they managed to establish common traits in order to classify tumors into clinically meaningful subgroups. For breast cancer, two main methods among others are used to categorize patients' tumors: histological and molecular classifications.

2. 3. 1. Histological Method:

Histological grade

The grading of tumors is based on a semi quantitative evaluation of three morphological criteria: percentage of tubule formation, degree of nuclear pleomorphism and mitotic index (Elston and Ellis, 1991; Weigelt and Reis-Filho, 2010). These features give an estimation of the differentiation state and the proliferative activity of a tumor. The different grades have been strongly correlated with prognosis: better survival rate is attributed to patients with grade I tumors than grade II or III. This grading method combined with an assessment of tumor size and the number of involved lymph nodes form the Nottingham prognostic index, a prognostic tool for breast cancer.

Histological type

The histological classification separates tumors according to their anatomo-pathological nature and is used by the World Health Organization (WHO). Most of breast lesions are initiated in mammary lobules or ducts, and are known as carcinomas. Depending on their location, they will be qualified as ductal (70 to 80% of cases) or lobular (10 to 15%) carcinomas (Weigelt et al., 2010).

Two main carcinomas exist:

a) The non-invasive carcinomas, mainly ductal carcinoma (DCIS) and lobular carcinoma (LCIS) in situ: They form cellular masses that will proliferate without overcoming the basement membrane or invading the stromal conjunctive tissue.

b) The invasive carcinomas: They breach the endogenous physical barrier and are usually associated with poor prognosis. Unequal prognosis exists for the different types of infiltrating cancers indicating that they require different therapeutic management. They are classified according to their morphological aspects. Under the invasive carcinomas, we find different types with variable frequencies: invasive ductal carcinomas (80%), invasive lobular carcinomas (10%), and other rarer types including tubular (2%), medullary (1-3%), mucinous (3%), papillary (2%) carcinomas.

2. 3. 2. Molecular subtypes

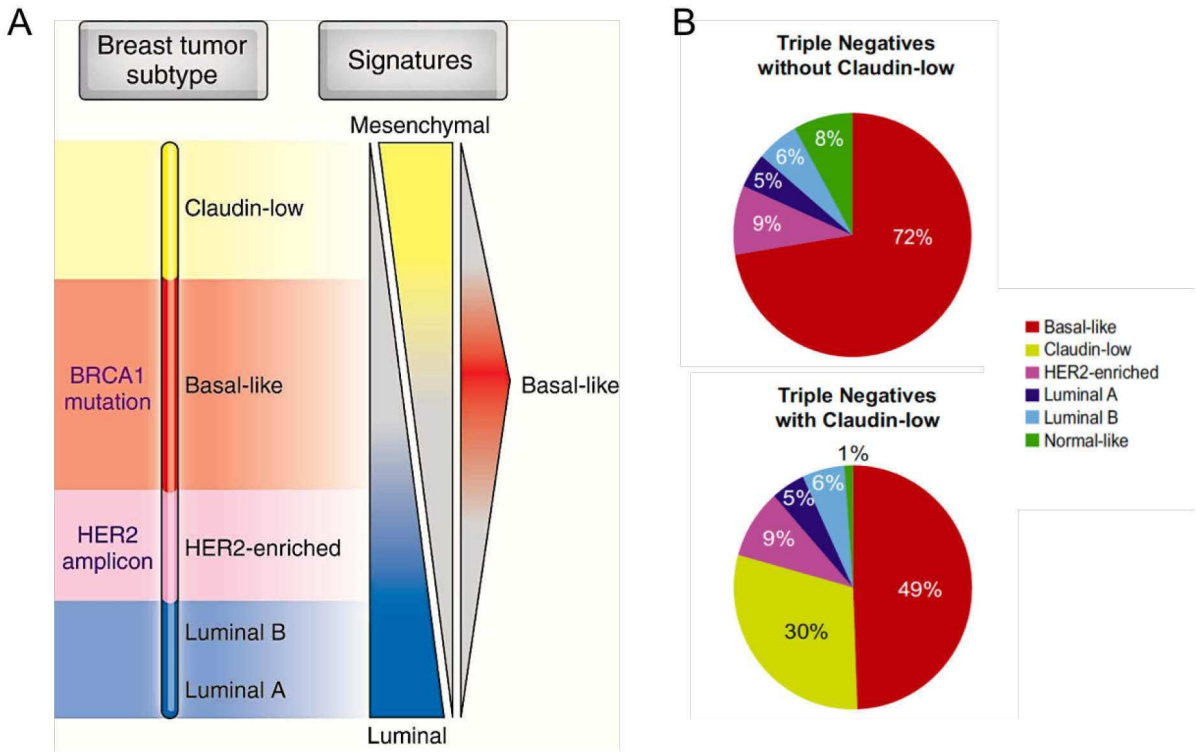

Figure 6: Breast cancer molecular subtypes.

A. Breast cancers are classified into six subtypes: normal-like, Luminal A, Luminal B, HER2-enriched, Basal-like and claudin-low, showing different epithelial status. B. TNBCs are a heterogeneous group primarily composed of Basal-like breast tumors. Claudin-low tumors constitute a significant proportion of TNBCs. Adaptef from Prat and Perou, 2009, 2011.

Classical classification: Receptor status

Up to date, classic clinical tumor classification is based mainly the expression of three hormone-receptors: estrogen, progesterone and Her2 receptors, established by immunohistochemistry on patients biopsies (Torregrosa et al., 1997; Vollenweider-Zerargui et al., 1986). Combined with the histological methods, breast cancer has been classified into the five classical subtypes described below: Luminal A, Luminal B, normal-like, Her2 and basal-like subtypes. This classification is currently used by clinicians to give a diagnosis and decide on the treatment.

Modern classification: Genomic signature

In the beginning of the 21st century, genomic analysis came to refine the classification of this heterogeneous disease by proposing a new molecular classification (**Figure 6**) (Perou et al., 2000; Sorlie et al., 2001). Based on patient tumor samples, six subtypes were defined: two belonging to the positive estrogen receptors ER+ and three that are negative for ER (ER-). More recently a subtype called Claudin-low was added to ER- group (Hennessy et al., 2009; Herschkowitz et al.,

2007; Prat and Perou, 2011b). Surprisingly, this more complex and modern classification did not really differ from the classical classification except for the Claudin-low subtype.

In the positive estrogen receptors branch, two luminal subtypes are distinguished according to the activation of the estrogen pathway and some luminal epithelial characteristics**: Luminal A** expressing high levels of ER and PR receptors with a low proliferation index and **Luminal B** expressing a lower level of PR with a strong Ki67 and have worse prognosis when compared to luminal A. Both Luminal A and B are negative for HER2 receptors (Weigelt and Reis-Filho, 2010). For subtypes negative for ER, four have been separated: normal-like, HER2, basal-like and Claudin-low.

The **normal-like** tumors are still poorly characterized: they share close signature with normal breast tissue and fibroadenoma but they need to be studied further to have their prognosis state and clinical relevance. **HER2 subtype** encloses tumors overexpressing HER2 receptors. This aggressive cancer is characterized by hyperproliferation and bad prognostics.

The **basal-like** tumors are usually of a high grade and associated with poor prognosis. They comprise invasive ductal carcinomas and a high risk of metastasis. They express basal keratins 5 and 14, and other basal markers such as the transcription factor p63, P-cadherin, integrin beta 4, etc. (Review of (Bertucci et al., 2012)). These tumors are often mutated for TP53 or PTEN (Sorlie et al., 2001). BRCA1 mutated tumors fall as well in this subtype. Up to 80% of basal tumors are classified as Triple Negative Breast Cancers (TNBC), related to the lack of ER, PR, or HER2 receptors expression. However, even though tumors are for now called basal-like tumors, one should not confuse then with triple negative ones (Prat et al., 2013). The proposed stratification shows that 70 to 80 % of TNC are basal-like (**Figure 6**).

Claudin-low, the latest classified subtypes, was discovered in 2007 by Herschkowitz et al (Herschkowitz et al., 2007). It is distinguished by a low expression of tight junction proteins (Claudins 3, 4, 7, occluding, etc.), a mesenchymal signature (increase in vimentin and N-cadherin expression, and a downregulation of E-cadherin) and some stem cell features. It accounts for 7-14% of invasive breast cancers. The majority of Claudin-low tumors is TNC, and correlates with large tumor size, young patients, and immune cells infiltration (Prat and Perou, 2011b)(Prat and Perou, 2011b). However, they did not show an important local recurrence rate but they have worse overall survival than luminal A, the most benign subtype (Dias et al., 2017).

II. The Strategies of Cancer

1. Hallmarks of cancer

As mentioned in paragraph I-A, mammary gland is a highly plastic organ that undergoes intense remodeling during different stages of life, which makes it more susceptible to accumulate errors in their genome and therefore encounter tumorigenesis. Tumorigenesis is basically linked to somatic mutations acquired by cells, and providing them with survival and proliferative advantages to escape regulatory mechanisms (immune system, DNA repair system, apoptosis, etc.) and resist to various stresses.

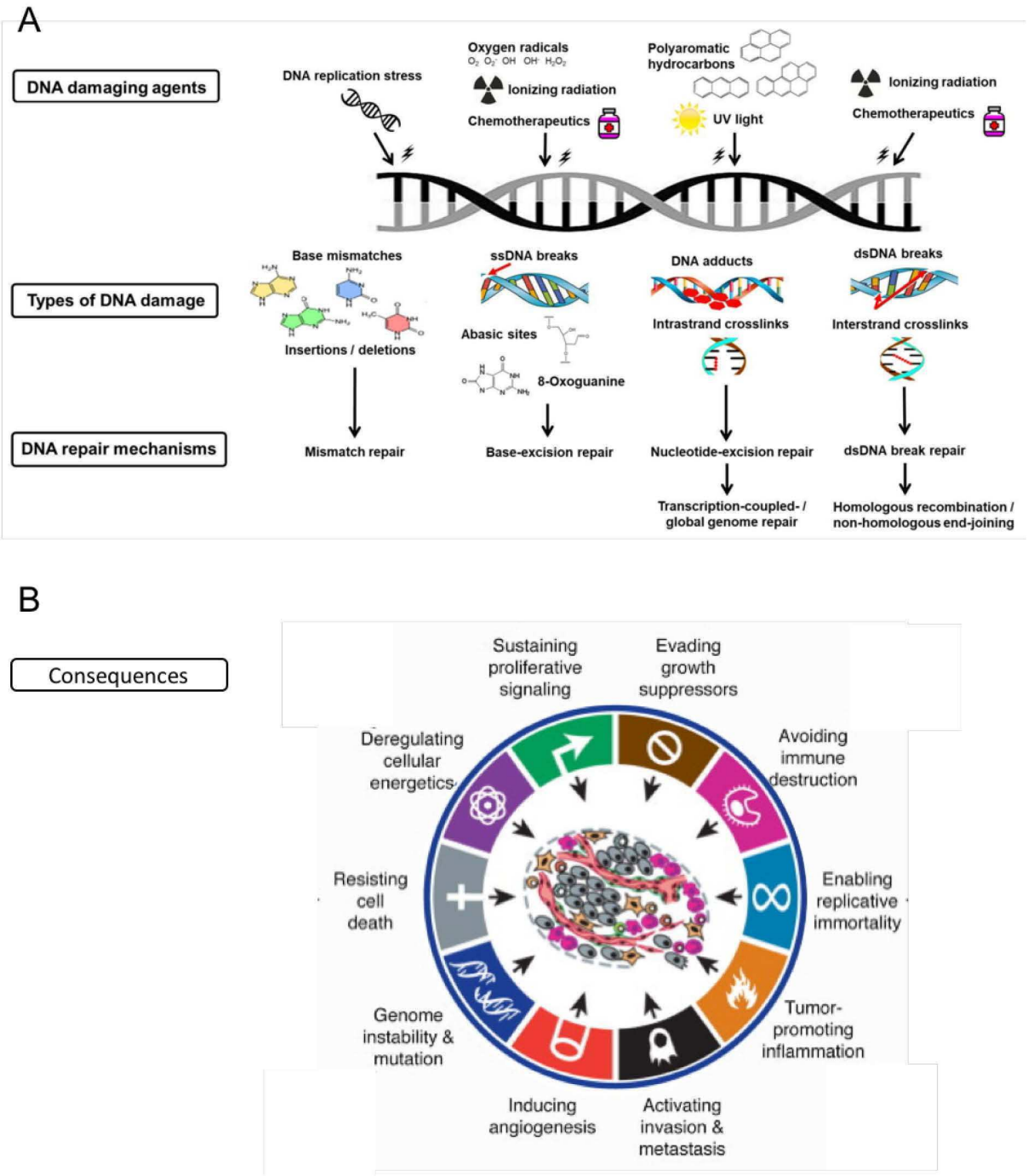

Figure 7: DNA damages and cancer.

A. Various damaging agents (chemical agents, radiations, intrinsic DNA stress) can cause different types of lesions in the genome (base mismatches, DNA breaks, DNA adducts). In normal cells, DNA repair mechanisms are put in place in order to maintain normal genes expression B. Once these mechanisms fail to repair gene alterations, cells will accumulate a number of mutations leading to a deregulation of the homeostatic state of cells (metabolism, balance of proliferation/apoptosis, escaping the immune system…) leading to cancer. Adapted from Hanahan and Weinberg, 2011; Helena et al., 2018.

The last quarter of the 20th century has revealed a set of mutated genes that drastically predispose cells to cancer and drive tumor initiation and progression (**Figure 7**). Mainly, we witnessed the discovery of two major classes of altered genes: oncogenes found up-regulated or over-activated by gain-of-function mutations (such as Ras, myc, cyclin D1, ERBB2 etc.) and tumor suppressor genes that are downregulated or modified by loss-of-function mutations (such as TP53, PTEN, etc.) (Hanahan and Weinberg, 2000). These two gene classes have been identified first in cancer cell models, and later found to be equally altered in patient-derived tumors. In breast cancer, the most frequent oncogenes found altered are HER2 oncogene amplified or overexpressed in 20 to 30% of invasive BC and in majority of high grade DCIS, Cyclin D1 overexpressed in 40 to 50% of invasive BC and amplified in 10-20% of cases, and c-myc amplified or overexpressed in 15 to 25 % of BC cases. Concerning tumor suppressors, *TP53* and *Rb* (retinoblastoma) genes are mutated in 20 to 30% of breast cancers (Osborne et al., 2004). Other mutations were found in the germline and are responsible for increasing the risk of developing breast cancer (such as *BRCA1, BRCA2*, etc.) (Thompson, 1994).

But one is not sufficient! *In vitro*, transforming rodent cells requires at least two mutations in order to acquire tumorigenic capacities, and it is even more complex to transform their human counterparts (Elenbaas et al., 2001; Hahn et al., 1999). In reality, cancer initiation and progression lies behind an accumulation of a multiplicity of impactful mutations. It was suggested that a normal cell turns into a cancer cell after a succession of four to seven genetic changes. It is important to note that only the so-called **driver mutations** targeting genes regulating vital processes for cell homeostasis, but eventually cells will carry numerous silent or **passenger mutations** targeting marginal non-coding sequences or redundant functional genes. After the trend of driver mutations, an increased interest by the research community and pharma companies was given to a set of genes that we will call **secondary driver mutations**. Some gene alterations, even though incapable of transforming a normal cell, are providing important advantages for tumor cells to evolve towards malignancy (Nik-Zainal and Morganella, 2017). For instance, new attempts in curing cancer by targeting secondary driver genes exist such as in Rho GEFs, the activators of Rho GTPases implicated in cancer cells migration (Cardama et al., 2017), or metalloproteases implicated in the degradation of tumor cells extracellular matrix and their invasion (Cathcart et al., 2015).

To add to the complexity of cancer, gene expression can be equally altered by modified epigenetic regulators (e.g. methylation, chromatin state) as well as non-coding RNAs (Flavahan et al., 2017).

Cancer can then be defined by an unlimited number of altered genes combinations. But despite the heterogeneity of this disease, cancer cells seemed to share some acquired common capabilities. *Vogelstein et al* have considered the altered signaling pathways in a cancer cell to regulate three vital functions: genome maintenance, cell fate and cell survival (Vogelstein et al., 2013). Using a more

detailed approach, Hanahan and Weinberg proposed originally six common traits: self-sufficiency in growth signals, insensitivity to growth-inhibitory signals, evasion of programmed cell death, limitless replicative potential, sustained angiogenesis, and tissue invasion and metastasis. With further understanding of the disease, four common features were added: changes in cellular metabolism, genomic instability, escaping the immune system and tumor inflammation (**Figure 7**) (Hanahan and Weinberg, 2011).

***

Compiling the impact of these mutations on cell physiology will lead normal cells through the labyrinth of the metastatic cascade.

1. 1. From tumorigenesis to malignancy: the metastatic cascade

From hyperplasia (defined by an unusual increase in tissue size resulting from cell proliferation), up to invasive metastatic tumors, cells have to climb a ladder of successive genome and cell transformations. Before diving into the molecular regulators, here's a brief walk through cancer sequential progression (**Figure 8**).

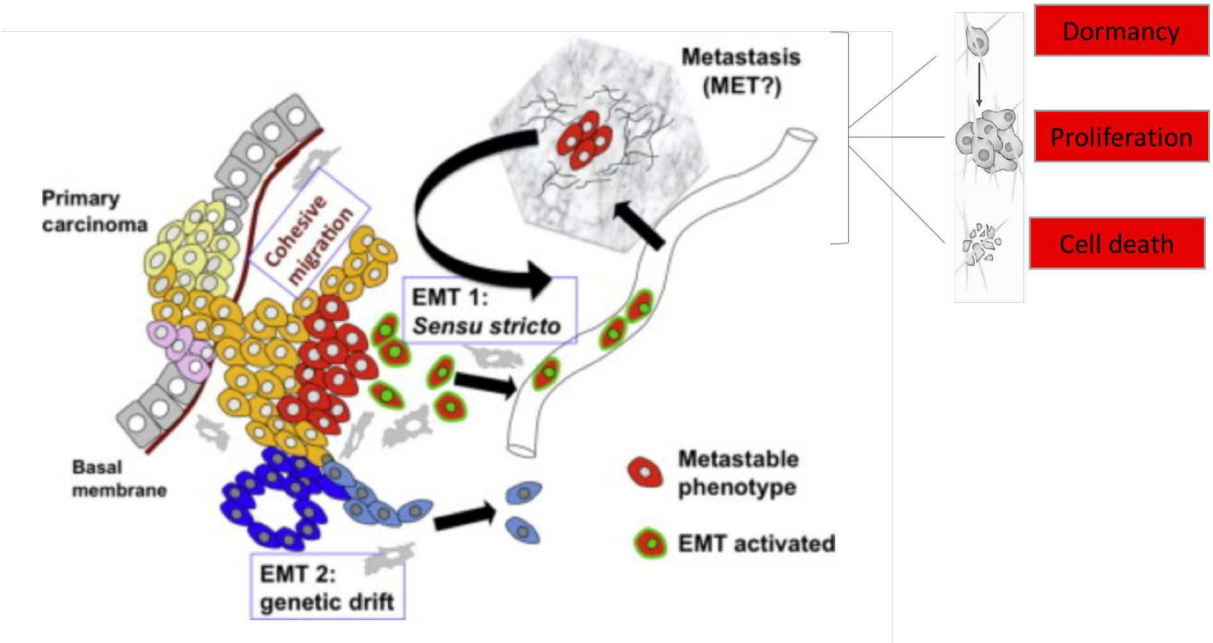

Figure 8: The metastatic cascade.

The metastatic process involves a series of steps that allow a tumor cell to migrate, integrate another tissue and develop a secondary tumor. To this end, invasive cells of the primary tumor degrade the basement membrane, escape into the connective tissue and, penetrate into blood vessels (intravasion). In the circulating system, tumor cells interact with immune system cells and the platelets that protect them during transport. In order to leave the vessels, circulating tumor cells adhere to the inner vascular wall of vessels, and escape through extravasation to the neighboring tissue. Arrived at the secondary site, tumor cells can encounter three different destinies. First, tumor cells can directly adapt to their new microenvironment, proliferate and form a tumor at a distant site, so-called metastasis. Second, they might stay as dormant cells for a certain period of time, a quiescent non-proliferative state requiring a mesenchymal to epithelial transition. Third, tumor cells can fail at this last step to survive the new microenvironment or escape the attacks of the immune system. Adapted from Yap, 2015.

1. 1. 1. Initiation

It is the first phase of tumorigenesis where a normal cell acquires one or several mutations that will be transmitted to daughter cells. These mutations can occur due to an error in DNA duplication during cell division or can be induced by genotoxicity (DNA damage caused by chemical agents) or other toxic factors (such as stress, radiation…). Cells have developed DNA repair mechanisms that will consistently proofread DNA sequence and make sure to either suspend the cellular division in order to fix any possible errors to stop the whole process by initiating apoptotic signals. Since it is a matter of fidelity, it happens that DNA damage will not be accurately repaired leading to genetic alterations (Nikolaev and Yang, 2017; Wood, 2018). Since half a century, a deficiency in DNA repair was linked to disease, in particular cancer.

At each division cycle, more mutations can add up to the existing ones until resulting dysregulated pathways are sufficient to transform the cells carrying them. The transformation is primarily an immortalization, where cells will have the capacity of proliferating at high rates. This will result in a small benign mass, mostly not detectable clinically.

1. 1. 2. Progression

It is an irreversible state where hyper-proliferating cells will gain in autonomy to escape cell death as well as the defense of the immune system. At this stage, cells will undergo mitosis and accumulate a diversification of new mutations. The formation of a tumor can be compared to the theory of species evolution, with the selection of cells benefiting from survival advantages and malignant potentials and resulting in waves of clonal expansion (Merlo et al., 2006).

In support to primary tumor growth, blood vessels and lymphatic systems will be developed by processes called respectively angiogenesis and lymphogenesis in response to signals from stroma and cancer cells. These vessels make it possible to provide nutrients and oxygen necessary for tumors and to remove their metabolic waste (Nishida et al., 2006). Along with the increase of cancer size, tumor cells are likely to go through morphological and functional modifications resumed as the epithelial mesenchymal transition EMT (detailed in 2. Epithelial mesenchymal transition). They will also modify the components of their extracellular matrix and its biomechanical properties, all of which prepare cells to reach the last stage of this cascade by invading and metastasizing.

1. 1. 3. Invasion and Metastasis

The clinical manifestation of metastasis appears when cancer cells successfully initiate detectable tumors at secondary sites of the body. The process of metastasis usually starts by a local invasion of the surrounding tissue, which is followed by some primary cancer cells getting to the blood stream through the endothelial basal membrane (**Figure 8**). Surviving tumor cells have then to adhere to vessels' membrane, exit the periphery and form new metastatic foci. However, how tumor cells succeed to adapt

and proliferate in the new tissue remain ambiguous. This question definitely needs to be further investigated in order to understand and control the metastatic phase, responsible for 90% of cancer patients' death (Ribelles et al., 2014; Wan et al., 2013).

Of note, using available sorting techniques and markers, around 50 circulating tumor cells only are collected per milliliter of cancer patients blood (Yu et al., 2011). Dissemination is therefore considered a rare event, guaranteed only for cells that bypass apoptotic signals and the immune system. In breast cancer, about 25 % of patients develop distant tumors targeting preferentially some organs more than others ***. For instance, bone is the most metastatic site with an occurrence rate of 40 to 60 %, followed by the liver and lungs (occurrence ranging from 19 to 30 %) and finally the brain with 10% occurrence rate (Feng et al., 2018; Weigelt et al., 2005).

The metastatic organotropism is an old theory known as the "seed and soil theory", proposed in 1889 by Stephen Paget (Fidler, 2003; Ribelles et al., 2014). Looking at 900 biopsy records, he noticed that metastasis does not have a random pattern and suggested that this phenomenon can be based on a cross-talk between cancer cells (seed) and the microenvironment of the recipient organ (soil). But the mechanistic by which disseminated cells choose their secondary metastatic sites is still unclear. Recent papers suggest that a communication between cancer cells and their pre-metastatic niche can occur through chemokines and/or exosomes (Borsig et al., 2014; Paolillo and Schinelli, 2017). Notably, in breast cancer, organ-specific homing process was shown to be based on the expression of the chemokine receptor 4 (CXCR4) by tumor cells, while its ligand CXCL12 is predominantly expressed in the lymph nodes, lungs, liver and bone marrow, and weakly expressed in the other organs such as small intestine, kidneys, brain, skin and muscles (Borsig et al., 2014). A recent work by Hoshino et al shows that tumor-derived exosomes can direct cells to specific future metastatic site (Hoshino et al., 2015). For instance, exosomal integrins $\alpha_6\beta_4$ and $\alpha_6\beta_1$ were linked to lung metastasis, while exosomal integrin $\alpha_v\beta_5$ was associated with liver metastasis.

Besides how tumor disseminate, timing is still a notion that we cannot easily approach when dealing with cancer. To answer the question "when do cells leave the primary tumor?", correlations were established between tumor size and metastasis. For instance, patients with large primary tumors are at higher risk of dying from metastasis. But recent studies are challenging this concept of late dissemination and have shown that, in DCIS in women, dissemination takes place as soon as the primary tumor is formed. In murine models of breast cancer, epithelial cells were shown to disseminate in the premalignant phase to the bone marrow (Hosseini et al., 2016; Hüsemann et al., 2008). After dissemination, cancer cells usually stay for a certain time in a quiescent state, called dormancy, defined by a mitotic arrest where cells exit the cell cycle and enter the G0 state.

In the continuity of this work, further investigations are required to determine how and why do early-disseminated cells survive in a dormant state for a considerable time and what factors release them from this dormancy.

These two interesting reviews cover the latest discoveries that have unraveled many signaling pathways and characteristics of the tumorigenic process: (Balani et al., 2017; Wan et al., 2013).

***

In the following sections, we will be focusing on two major biological processes driving this complicated metastatic cascade: the epithelial mesenchymal transition and invasion.

2. Epithelial mesenchymal transition

The epithelial mesenchymal transition (EMT) was first described in the 1980s by Elizabeth Hay during chick embryogenesis as a transformation that accords to epithelial cells a high plasticity crucial for morphogenesis (Hay, 1995). Indeed, the formation of embryonic sheets requires cell migration and therefore, a loss of adhesion proteins and an activation of motility programs, two main characteristics of EMT.

Besides embryogenesis and organ development, EMT has been detected in two other biological contexts: tissue regeneration and fibrosis, and cancer progression (Kalluri and Weinberg, 2009).
We are going to focus on the latter, and try to cover the following questions:

2. 1. What is the role of EMT in cancer progression?

EMT is a dynamic process during which cells will lose major epithelial characteristics and gain mesenchymal properties. This is in response to driver mutations that will cause a change in their transcriptional program and induce complex functional and architectural modifications of the cells providing them with advantages required for cancer development.
It is considered a major first step towards tumorigenesis, but has also been shown to intervene at advanced stages of cancer progression by favoring metastasis and resistance to therapy (Brabletz et al., 2018). However, it is important to keep in mind the plasticity aspect of EMT and the potential cycles of EMT/MET (mesenchymal to epithelial transition***) occurring throughout the process of tumorigenesis. Metastatic cells may recover an epithelial state through MET after encountering the

normal stroma of a dissemination site, a signal suggested to be important to enter dormancy (Bloushtain-Qimron et al., 2008; Chaffer et al., 2007).

***Mesenchymal to epithelial transition-MET:*

*An interesting notion worthy to note is the reversible aspect of the epithelial-mesenchymal transition. Mesenchymal cancer cells are capable of taking a mesenchymal-epithelial transition in order to gain back some epithelial features crucial for succeeding their invasive strategies. Indeed, an Australian research group have used a bladder cancer cell line that can switch between both status to show that, in mice, mesenchymal-type cells were more apt to leave the primary tumor while the epithelial-type cells were better at colonizing new organs (to adapt and proliferate in a new microenvironment) (Garber, 2008).****

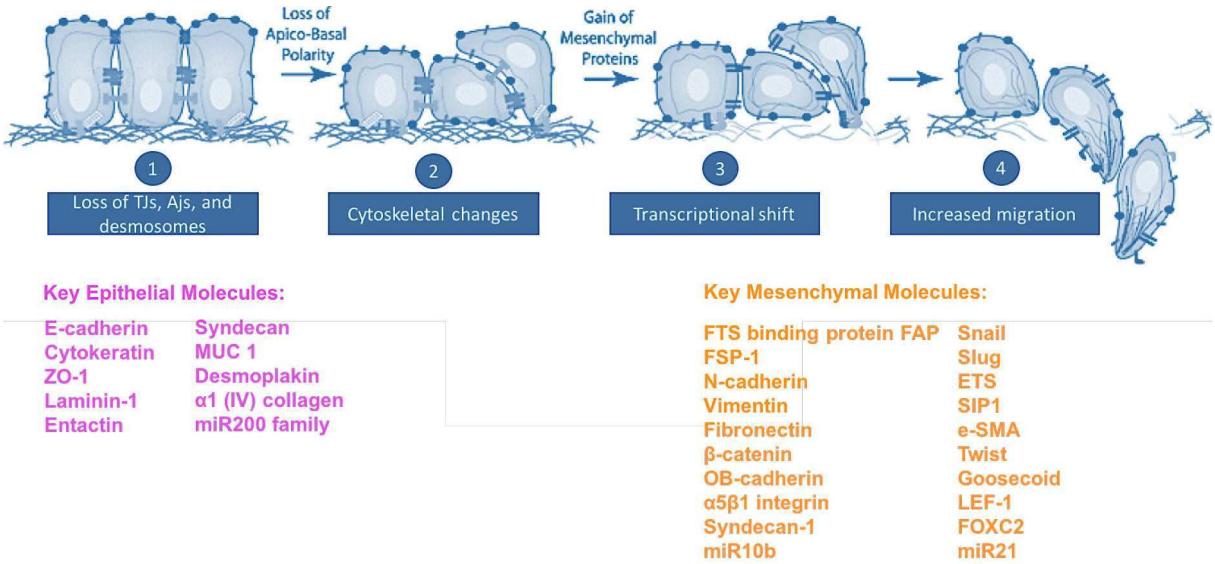

Figure 9: Morphological and gene expression changes of cells undergoing the epithelial-to-mesenchymal transition (EMT).

Epithelial cells are characterized by an apico-basal polarity and express several epithelial markers (E-cadherin, ZO-1). During EMT, cells lose their cuboidal polarized shape and adopt an elongated mesenchymal form. This state is characterized by the expression of mesenchymal transcription factors (EMT-TFs) like Snail, Slug and Twist and other specific markers listed above. This transition is reversible and cells can gain back their epithelial state through MET. Adopted from (Kalluri and Weinberg, 2009; Micalizzi et al., 2010).

Molecular markers associated to EMT have been established in cancer cell models and for the majority validated in animal cancer models (**Figure 9**). The relevance of these biomarkers for human cancer is still under discussion and need thorough research. Yet, some EMT-related markers have shown clinical significance in specific contexts and were summarized by Wu et al. (Wu et al., 2016).

***

The findings presented below are not an extensive summary of EMT, but rather studies relevant for this PhD thesis. I am going to expose the main morphological and functional changes during EMT and the key transcription factors orchestrating the majority of these changes.

2.1.1 There is a first step to everything: loss of polarity and adhesion proteins

Epithelial cells are mainly defined by-two features that are crucial to the function of epithelial tissues: cellular adhesion and apico-basal polarity. Thus, the disruption of these epithelial characteristics during EMT alters the whole tissue integrity and have been shown to boost cancer progression at several levels: increasing tumor growth, facilitating invasion and metastasis, as well as modifying the immune-response of tumor cells.

During early steps of EMT, the disassembly of adhesion complexes such as tight and adherens junctions occurs in epithelial cells. First descriptions of EMT were mainly focused on the loss of E-cadherin, a major epithelial adherens junction protein. E-cadherin function can be regulated through different mechanisms. Transcriptional silencing, gene mutation, or hypermethylation of CDH1 (the gene encoding E-cadherin) promoter have been reported in breast cancer (Conacci-Sorrell et al., 2002). Likewise, the same mechanisms apply to the downregulation of claudins, occludins and ZO1 (Zonula Occludens 1) molecules concordant to tight junctions' disassembly during EMT (Ozdamar et al., 2005; Viloria-Petit and Wrana, 2010).

E-cadherin, is a transmembrane glycoprotein of 120KDa forming homotypic interactions through their extracellular domains and bridging two neighboring epithelial cells. Immunohistochemistry on tumor biopsies has shown that low expression of E-cadherin correlated with cancer metastasis and patients death (Birchmeier and Behrens, 1994). Similarly, in human cell lines, E-cadherin negative cells were characterized by a mesenchymal morphology and the acquisition of migratory and invasive capacities (Frixen et al., 1991). This was followed by an *in vitro* validation; overexpressing E-cadherin in mammary mouse cells resulted in blocking invasion (Vleminckx et al., 1991). Other studies as well classified E-cadherin as an invasion suppressor molecule (reviewed by (Shamir and Ewald, 2015)).

Surprisingly, the loss of E-cadherin that was first attributed to invasive lobular carcinoma, has later been reported in benign lobular carcinoma *in situ* (Vos et al., 1997). As the latter suggests, loss of E-cadherin might not always lead to invasion. Concomitantly, Kowalski shows that often primary breast tumors and their distant metastasis express E-cadherin (Kowalski et al., 2003). In other contexts, its expression has even been considered advantageous for invasion. For instance, *in vitro* knockdown of E-cadherin

inhibited twist1-induced dissemination in primary murine mammary epithelial cells (Shamir et al., 2014, 2016). Thus, in the midst of several studies stating a correlation between E-cadherin levels and metastasis, some did not detect any clear relation linking E-cadherin status with tumor aggressiveness (Shamir and Ewald, 2015).

All these data reveal that E-cadherin is an important protein for maintaining tissue integrity and homeostasis, nevertheless in BC its absence is not a pre-requisite to acquire invasive capacities essential for metastasis. Knowing that cancer cells can take many alternative pathways to reach invasion, variabilities that we just presented can be explained by tumor heterogeneity. It can as well be related to the plasticity aspect of the EMT process with detection bias generated by potential transient modulation of E-cadherin expression levels. This controversy can be linked to the association of E-cadherin with different signaling pathways. Indeed, an additional level of complexity comes from the pleiotropic feature of E-cadherin. Loss of E-cadherin does not only disrupt cell-cell adhesion but it is as well implicated in activating different signaling pathways (contact-inhibition, apoptosis, etc.). In normal cells, E-cadherin is connected to the actin cytoskeleton by their cytoplasmic tail through the catenins adaptor proteins (mainly β-catenin). Once E-cadherin is removed from the membrane, catenins will be released in the cytoplasm, transferred to the nucleus and modify gene transcription. However, catenins are not E-cadherin's only mediators. In cancer cells, E-cadherin-related EMT modifications can be induced by Twist1 mesenchymal transcription factor (Onder et al., 2008) as well as by E-cadherin interactions with transmembrane receptors (EGFR, TGF-β-R, ERBB2), and cytosolic proteins (APC, Rho-GTPases) (Perrais et al., 2007).

During EMT, the strong adhesion ensured by E-cadh is usually replaced by weaker homotypic interactions provided by other cadherins (N-cadherin, P-cadherin), allowing the transition from a pro-adhesive to a pro-migratory state of collective invading cells (Cavallaro and Christofori, 2004; Cavallaro and Dejana, 2011). N-cadherin, the most commonly expressed in cancer cells, has been shown to contribute to invasiveness in human cell lines and metastasis *in vivo* in nude mice (ElMoneim and Zaghloul, 2011; Nakajima, 2004). Yet, in other cellular and animal models, N-cadherin was not sufficient to induce invasion (Shamir and Ewald, 2015). Thus, N-cadherin used extensively as a mesenchymal marker does not always reflect an invasive advantage. It is more appropriate to use it as an indicator of less polarized migratory epithelial cells.
The same applies to P-cadherin. Found in luminal originating breast cancer, it was first correlated with poor clinical outcomes. However, later on, P-cadherin did not really show any major advantages or disruption when expressed in mice mammary gland (Daniel et al., 1995; Radice et al., 2003).

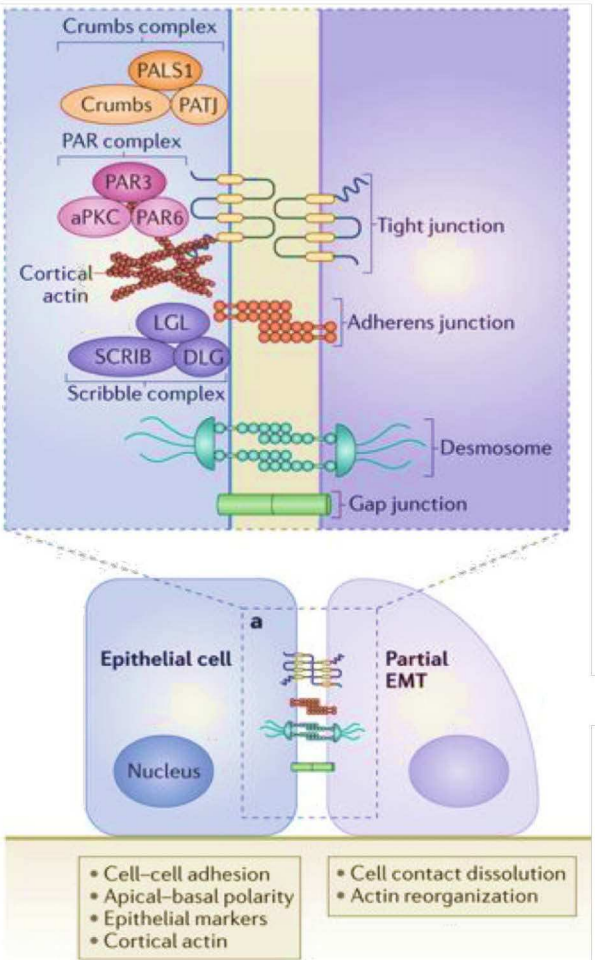

Figure 10: Epithelial polarity complexes.

The epithelial phenotype is characterized by the presence of cell junctions of several types including tight junctions, adherent junctions, desmosomes and GAP junctions. These structures are lost during the first steps of EMT and replaced by structures more adequate for migration and invasion. The actin cytoskeleton rearrangement will form stress fibers facilitating the migration, and different protrusive structures like lamellipods, filopods and invadosomes. In addition, the expression profile integrins is modified, thus regulating cellular adhesion to the ECM. Adapted from Lamouille et al., 2014.

Nevertheless, acquiring a mesenchymal status takes more than disrupting adhesion proteins. Besides their effect on cell-cell-contact, the loss of adhesion proteins disrupts cellular polarity crucial for normal epithelial cell functioning. In fact, epithelial cells establish their polarity after receiving two adhesion cues: the cell-cell contact and cell-extracellular matrix contact. Upon E-cadherin and integrins engagement, cells are polarized along the apico-basal axis through an extensive rearrangement of the cortical actin cytoskeleton and the positioning of three polarity complexes (partitioning defective (PAR3), crumbs (CRB) and scribble (SCRIB)) (**Figure 10**). Each of these polarity complexes determine a plasma membrane domain: PAR3 defining tight junctions, CRB defining the apical domain and SCRIB defining the basolateral domain. During EMT, polarity complexes are downregulated or not found at the

right sites. For example, the loss of E-cadherin blocks the recruitment of SCRIB to the basolateral membrane (Navarro et al., 2005).

In parallel, a switch in the cytoskeleton components from cytokeratin to vimentin filaments can occur and alter membrane proteins trafficking and distribution, such as E-cadh (Hanada et al., 2005; Toivola et al., 2005). It will also affect the cytoskeleton architecture. Epithelial cells transfected with vimentin adopt an elongated morphology and acquire other mesenchymal characteristic like an increase in motility and a high turnover of focal adhesion*** molecules as well as a loss of desmosomes (Mendez et al., 2010).

Focal adhesions are cell-ECM adhesion complexes in which integrins are the core receptors forming mechanical links between actin cytoskeleton and the stroma in many cell types. Focal adhesions are in constant remodeling (dynamic assembly and disassembly) that is important for cell motility during migration. They also act as mechanosensors of extracellular tensions that will be translated into cellular modifications through different signaling proteins like talins (e.g. reinforcing cell adhesion). More than 60 focal adhesion proteins have been described in mammals including catalytic proteins like protein tyrosine kinases such as FAK and Src, protein serine/threonine kinases such as ILK and p21-activated kinase (PAK), and phosphoinositide 3-kinase, as well as other enzymes like proteases and phosphatases. In addition, several adaptor proteins are found associated to focal adhesions like paxillin, vinculin and tensin. In cancer, an increased activity of FAK and Src have been reported and correlated with malignancy; oncogenic focal adhesions can contribute to resistance to apoptosis, increase in proliferation and elevated cell motility and invasion (Wehrle-Haller, 2012; Wu, 2007).

Conclusion:

Normal epithelial cells have a stable polarized architecture and a mobility limited within their monolayers. By disrupting adhesion and polarity, EMT provides cells with motility advantages as well as morphological ones, as elongated cells have less contact with their microenvironment and therefore less retention. The remaining challenge is to overcome inconsistencies related to the existing markers of EMT. We need to better understand the heterogeneity of tumors, in addition to their stochastic gradual evolution, and find targetable common molecules expressed in a transitioning epithelial cell. The emerging techniques of spatial single cell sequencing (Satija et al., 2015; Shapiro et al., 2013; Wang et al., 2018) will help to a certain extent in assessing the variabilities seen intra- and inter-tumors and to discriminate in which contexts specific markers are expressed and which state of the epithelial-mesenchymal transition they reflect. This will give us as well more insights about the temporal expression of mesenchymal transcription factors ruling a major part of EMT as well as other functions detailed in the following section.

2.1.2 Roles of Mesenchymal transcription factors: EMT and beyond

As described above, EMT is mainly detected by the loss of critical epithelial characteristics (polarity, adhesion junctions) and the gain of mesenchymal properties (mobility, migration, invasion). Behind these functional and morphological changes lies a panel of transcriptomic changes led by a group of master regulators of the EMT: the mesenchymal transcription factors (EMT-TFs). Three major families of EMT-activating transcription factors have been the focus of cancer research: SNAIL (containing Snai1 and Snai2/slug), ZEB (with two factors Zeb1 and Zeb2) and basic Helix Loop Helix or TWIST (with Twist1 and Twist2) families (Polyak and Weinberg, 2009; Puisieux et al., 2014a; Yang and Weinberg, 2008). EMT-TFs can modulate the expression of their target genes by directly binding to DNA or by cooperating with other transcriptional regulators. While Twist1 induces the expression of N-cadherin by binding to its promoter, downregulating E-cadherin requires the interaction of TWIST1 with the NURD (Nucleosome Remodeling Deacetylase) complex (Alexander et al., 2006; Cheng et al., 2007)

During the last ten years, several reports have provided evidence that EMT-TFs regulate the expression of core polarity proteins during EMT (Thiery et al., 2009). Zeb1 was shown to bind key polarity genes promoters including the E-cadherin and repress their expression in tumor cells thus reducing epithelial differentiation (Aigner et al., 2007; Graham et al., 2010; Spaderna et al., 2008). Similarly, Snai1 alters cell polarity by repressing the transcription of Crumb3 and modifying the location of Par3 and Crumbs at the junctions (Moreno-Bueno et al., 2008) as well as repressing E-cadherin (Peinado et al., 2005). Even in collective migration where cell clusters express adhesion proteins, leader cells have usually undergone a partial EMT and express EMT-TFs; for instance SNAIL was found at the invasive front of a mammary tumor model (Ye et al., 2015). It was noted that disassembled adhesion complexes can induce EMT-TFs up-regulation. It is hard to tell which stimuli comes first, however feedback loops exist between these two phenomena.

Upregulation of EMT-TFs has been detected in numerous cancers and correlated with poor prognosis of patients. Upregulation of Slug correlated with poor prognosis in human breast cancer patients (Guo et al., 2012). The expression of Snai1 in a transient way was shown necessary for metastatic competence in breast cancer (Tran et al., 2014). ZEB1 is aberrantly present in numerous invasive tumors: breast cancer (Graham et al., 2010; Soini et al., 2011), pancreatic cancer (Kurahara et al., 2012), hepatocellular carcinoma (Zhou et al., 2012), lung cancer (Gemmill et al., 2011), and many others. Zeb2 was found upregulated in the majority of tumors expressing Zeb1. TWIST is overexpressed in breast cancer and correlated with invasion, metastasis and poor survival (Ansieau et al., 2008; Puisieux et al., 2006; Soini et al., 2011; Yang et al., 2004). Likewise, *in vitro*, exogenous expression of EMT-TFs in solid tumors

induced cancer cell motility and invasion (Comijn et al., 2001; Olmeda et al., 2007, 2008; Puisieux et al., 2006; Shamir et al., 2014).

More importantly, tumor suppressor genes act in part by downregulating these EMT-TFs. In breast, pancreatic and hepatocellular carcinoma cancers, TP53 expression inhibits the mesenchymal phenotype acquisition and the invasive capacities of these cancer cells by inducing microRNAs expression (mir-200 and mir-192) that downregulate ZEB transcription factors (Chang et al., 2011; Kim et al., 2011).

According to Thomas Brabletz, in a recent *Nature Reviews Cancer* publication, all tumor cells make use of a program induced by EMT-TFs, but to different extents (Brabletz et al., 2018). EMT is perceived as a reversible coordinated complex cell program and therefore, it is not surprising that EMT-TFs expression and roles will differ according to various cell contexts and conditions. For instance, ZEB1 up-regulation in breast cancer does not promote metastasis while in pancreatic cancer, overexpression of ZEB1 and not SNAIL or TWIST can induce tumor metastasis (Krebs et al., 2017). However, it is interesting to note that its downregulation reduced 70% of metastasis but metastatic lesions were still observed meaning that not all the invasive potential of cancer cells relies on the expression of EMT-TFs and that other factors might be ruling this phenomenon as well (Krebs et al., 2017).
This being said, are EMT-TFs only roles to induce EMT properties? Do they participate to the metastatic cascade by activating other cancer programs?
EMT-TFs' roles have lately been re-evaluated after many studies raveling their various intrinsic activities related to cancer initiation and progression (Garber, 2008). Besides activating common EMT properties, mesenchymal TFs play different roles that have been proven to be tissue specific:

- EMT-TFs have been detected in the premalignant stages of tumors acting as a survival signal against various stresses. EMT-TFs would allow cancer cells to avoid senescence or apoptotic signals induced by oncogenes (Goossens et al., 2017; Puisieux et al., 2014a).
- EMT-TFs activation will support the dedifferentiation of epithelial cells and maintenance of stemness properties usually linked to high proliferative capacity, plasticity as well as resistance to therapy (Morel et al., 2008; Puisieux et al., 2014a). In mammary epithelial cancer cells, Slug acts as the main contributor to cells' stem plasticity features (Scheel and Weinberg, 2012).
- TFs can increase the expression of metalloproteinases important for matrix degradation and invasion (detailed in 4. 3. 3. Proteases & ECM degradation).

- EMT-TFs have been as well detected in non-epithelial tumors which support the statement of Brabletz about the non-EMT programs that can be stimulated by EMT-TFs in tumor cells (Kahlert et al., 2017).

The fact that these TFs are implicated in ensuring other functions adds a layer on the complexity and heterogeneity of this disease.

We have to note that other transcription factors are involved in EMT. We can mention the transcription factors belonging to the families FOX (forkhead box), SOX (SRY box) or GATA (reviewed in (Golson and Kaestner, 2016; Tremblay et al., 2018)).

Conclusion

The aberrant activation of EMT-TFs provides cells with a great plasticity, and the capacity to grow and invade.

2. 2. Which stimuli do activate EMT? One extra level of complexity

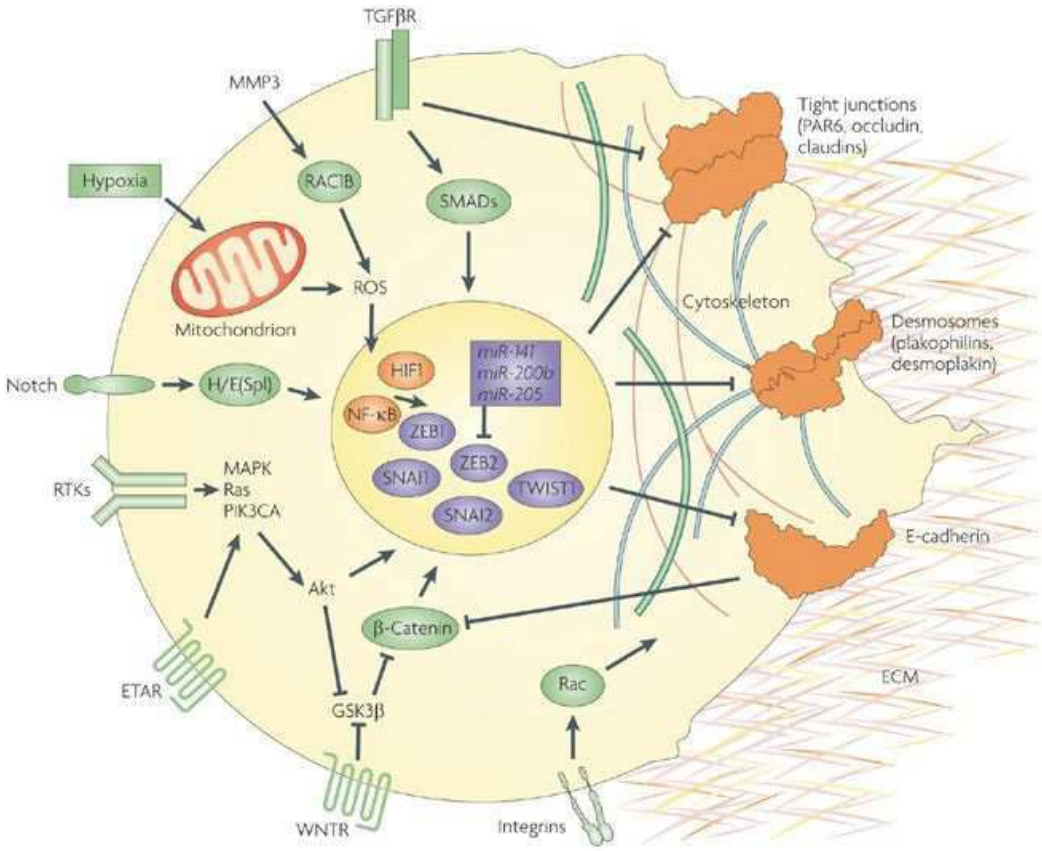

Figure 11: Stimuli and signaling pathways regulating epithelial-mesenchymal transition.

This overview shows the complexity and variety of signaling networks that can participate to the EMT process. Depending on the cell origin and context, several combinations of these pathways can be seen. Some receptors can induce direct effects on adhesion complexes while other will change the transcriptional program of cells and alter protein expression; for instance, the composition of the ECM can be one of the targets. Transcriptional shift is in majority mediated by an upregulation of

mesenchymal transcription factors (Twist, Slug, Snail, Zeb, etc.). RTK: receptor tyrosine kinase, ETAR: endothelin A receptor. Adapted from Polyak and Weinberg, 2009.

EMT-TFs are not the only actors in driving tumor growth and metastasis (**Figure 11**).

EMT is a complex process resulting from the combination of extracellular and intracellular stimuli, translated into various modifications of the cells and their microenvironment. A second level of regulation comes from feedback mechanisms crucial for pushing forward the initial transition from an epithelial state to a more mesenchymal state.

More than 20 signaling pathways have been described to enhance EMT in various cell types during physiological and pathological contexts (Thiery et al., 2009). *Puisieux et al* grouped these pathways under five stresses associated with tumorigenesis (physical constraints, hypoxia, inflammation, metabolic stress, oncogenic stress) (Puisieux et al., 2014b). Stimulating pathways capable of reactivating EMT during tumorigenesis include the TGFβ superfamily, Wnts, Notch, tyrosine kinase receptors ligands (EGF, HGF, FGF), HIF, and many other hypoxia factors.

These pathways have been shown to prompt EMT in major part by inducing new transcriptional programs and more specifically, by upregulating or activating EMT-TFs. For instance, hypoxia, the anaerobic condition that tumor cells can encounter, induces EMT by activating the Notch pathway. Notch activation drives HIF-1a (hypoxia-inducible factor 1a) that will be recruited on the LOX (Lysyl Oxydase) promoter. In turn, increased levels of LOX stabilize EMT-TFs and activate a set of other genes related to EMT. High expression of different Notch receptors was also correlated to Zeb1 and vimentin expression in invasive breast cancer (Han et al., 2011; Lamy et al., 2017). Taking another example, the well characterized transforming growth factor-β (TGFβ) hass been described, among many other EMT-related functions, to induce SNAIL and ZEB genes and alter cell polarity. Further detailed examples can be found in the subsequent reviews (Polyak and Weinberg, 2009; Yang and Weinberg, 2008).

TGFβ and many other EMT inducing factors are in part produced by fibroblasts which can lead us to another level of regulation: the extracellular matrix. Manipulating cells in different conditions *in vitro* has shown that ECM can induce an entry in EMT of normal cells.
Interestingly, as we will see in paragph “4. 3. 3. Proteases & ECM degradationextracellular” proteases can release growth factors and cytokines from the matrix or even increase indirectly EMT-TFs expression.

Having different external stimuli on top of feedback loops and internal signals makes it hard to determine what is leading the cells to EMT. Classifying these triggering events by order of importance or emergence is still not possible and needs further studies *in vivo*.

2.3 Does EMT really occur *in vivo* in cancers? A subject of controversy

The numerous regulatory pathways of EMT add to the complexity of this process and therefore to the overall divergence of scientific opinions. As a matter of fact, EMT was well documented in numerous cancer cell lines, but *in vivo* reporting of EMT showed up very late and did not always validated the *in vitro* observations. Numerous pathologists showed their disagreement on EMT as a cancerous-process. David Tarin published in 2005 an article questioning the existence of EMT and supporting his doubts by mainly lack of relevant markers as well as elongated epithelial cells in cancer tissues (Tarin, 2005).

In patients, claudin-low breast cancer subtype has been characterized by a pronounced EMT signature with high expression of EMT-TFs associated with an increased aggressiveness, a resistance to drugs and high metastatic potential (Feng et al., 2018; Prat and Perou, 2011a). Additionally, L. Chodosh group showed that in breast cancer, upregulation of Snail predicted lower relapse-free survival. Snail was also seen overexpressed in a transgenic mice model for HER/neu-induced mammary tumors, and induced EMT in a primary tumor cell line (Garber, 2008; Moody et al., 2005). A pool of other studies showing EMT *in vitro*, and correlations *in vivo* can be added to the previous examples (Chaffer et al., 2016; Heerboth et al., 2015). However, having different criteria and interpretations for EMT did not make the results very consistent. As we previously seen, EMT was associated with elongated morphological criteria, a downregulation and upregulation of epithelial and mesenchymal markers respectively, but also with an activation of EMT-TFs and some stem cell characteristics. EMT markers soon appeared not applicable to all the different contexts and cancer types. E-cadherin the most used epithelial marker turns out that it is not decreased in every disseminating cell, but rather co-expressed with mesenchymal makers (such as Vimentin) (Yamashita et al., 2018).

Defining EMT general lines by which this process commonly occurs in tumors is a hard task and one of the main subjects of controversy in cancer biology. To add to this complexity, besides the wide panel EMT-TFs that can be stimulated in an epithelial cell, the origin of the epithelial cell in which these programs are triggered is drastically important. TGF-β activation in basal mammary cells induces rapidly and efficiently an EMT phenotype, however luminal epithelial breast cancer were not responsive to TGF-β (Chaffer et al., 2016). The difference here can be set by the chromatin status of different cells. For example, basal cells keep Zeb1 promoter in an open conformation ready (Chaffer et al., 2013).

However, taking into consideration the complexity of cancer, even within the same tumors, different extents of EMT can occur. The radical EMT is now an old concept; today the scientific community talks more about a partial or heterogeneous EMT where cells will be engaged in this transition but not fully and in different ways.

***

About EMT and Invasion

A large amount of work has been done in an attempt to investigate the link between EMT or EMT-TFs and metastasis frequency *in vivo*, migration speed of tumor cells, and invasion capacities.

After all, a partial activation of EMT gives tremendous advantages to cells to invade which makes it hard for now to decide to what extent the engagement in EMT is a pre-requisite for invasion (Heerboth et al., 2015). I consider cancer progression and invasion as a feedback loop process where every signal will be amplified by stimulating other changes that will alter the cell homeostasis, therefore every modification in the cell even in early stages may give some invasive advantages used in further steps of the disease progression.

One of the remaining questions, as defined by Fidler, is : “how many of the steps of the invasion–metastasis cascade can be achieved by an activated EMT program?” (Fidler, 2003)

3. Collective Invasion:

3. 1. Invasion in general

Invasion is the central step of the metastatic cascade comprising several mechanisms adopted by the cells to breach physical barriers (BM, ECM, endothelium) and eventually grow secondary-site tumors. Besides cell-cell interactions, tumor cells will use Cell-ECM interactions and ECM remodeling to complete a successful invasion that will result from a continuum of different interdependent steps.
In vitro, two main types of invasion have been observed: single-cell invasion (including mesenchymal and amoeboid invasion) and collective invasion. The degree of EMT engagement can reflect on the invasion strategy used, thus the least differentiated the more likely cells are going to invade individually.

3. 1. 1. Cellular invasion

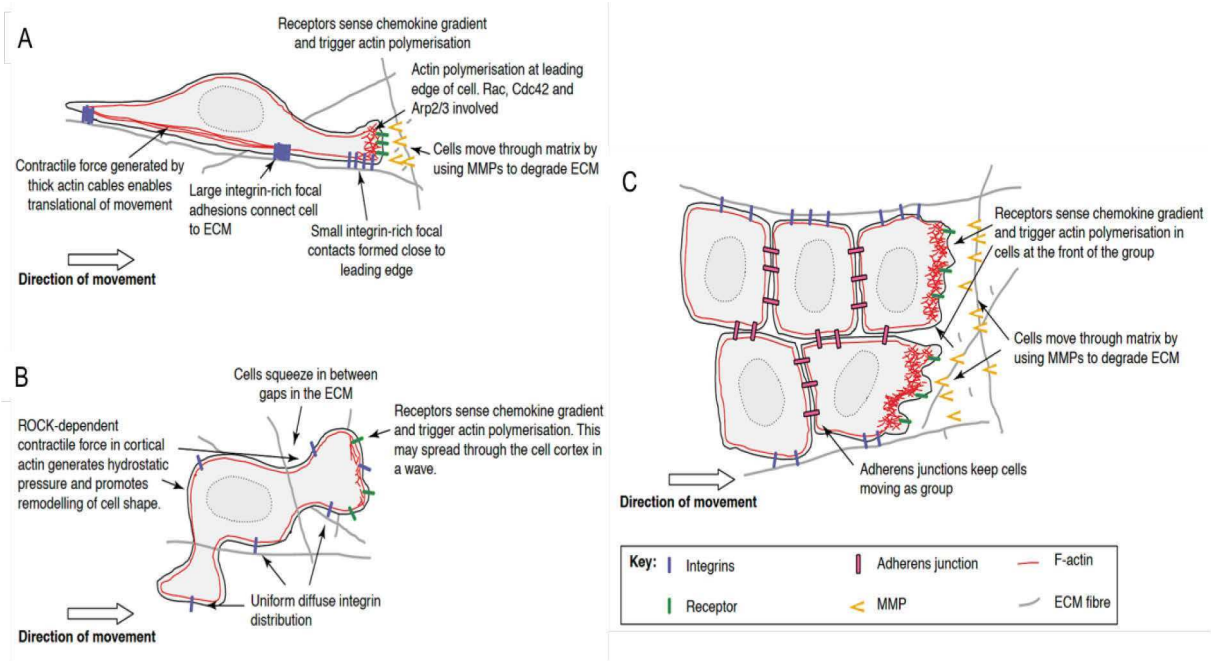

Figure 12: Migration strategies of cancer cells and their molecular programs.

A. Mesenchymal-type migration. B. Amoeboid migration. C. Collective migration. At the invasion front, cells set up membrane protrusions. they interact with the ECM and establish focal adhesion points rich in integrins. The activation of integrins triggers the recruitment of many proteins by their intracellular domain, this allows the anchoring of the cytoskeleton of the cell to the ECM and the transmission of external signals to cells. Surface proteases, such as MMPs, are recruited at the invasion front to degrade the ECM and allow cells to move forward. Contraction of the cellular body generates forces necessary to move the cellular body forward. The disassembly of adhesions sites on the rear of cells allows cells to move forward and start again a new migration cycle. Integrins are then recycled via endoplasmic vesicles to the cells'migration front. Adapted from Sahai, 2005.

- **Single-cell invasion**

Individual cell invasion has been reported *in vitro* and in animal models. Based on cell type, two variants of individual invasion can exist: mesenchymal and amoeboid (Friedl and Wolf, 2003; Sahai, 2005) (**Figure 12**).

Mesenchymal migration: this type of migration consists in having spindle-shape morphology cells mainly ruled by integrin-mediated interactions with ECM, traction forces, and proteases expression to degrade the surrounding matrix. Mesenchymal migration is mostly found in some models of fibrosarcomas and gliomas.

This type of invasion has been associated with increased tumor aggressiveness, increased resistance to apoptosis and an important ECM remodeling (Heerboth et al., 2015; Kalluri and Weinberg, 2009). Disrupting this mechanism is possible by inhibiting RhoGTPases, integrins, MMPs or MLCK (myosin light-chain kinase) (Friedl and Wolf, 2010; Hegerfeldt et al., 2002).

Amoeboid migration: Cells adopting amoeboid migration have a round-shape and low affinity to their ECM. In order to advance within the tissue, they will use high morphological deformability by rapidly juggling cycles of contraction and expansion in order to move between the fibers of the ECM. This migration pattern can be induced by the inhibition of proteolysis in mesenchymal cells, which may explain the failure of anti-cancer therapies blocking metalloproteases (Paňková et al., 2010; Wolf et al., 2003). Used by leucocytes, amoeboid migration is found in some epithelial carcinomas like metastatic rat breast cancer cell line MTLn3 injected in female Fischer 344 rats (Farina et al., 1998).

By reconstructing breast human tissue from cancer patients, a recent study proposes collective migration as the migration strategy of cancer cells and claims an absence of single cell leaving the tumors (Bronsert et al., 2014).

- **Collective invasion**

Collective migration was well described in normal embryonic development during neural tube formation (Davidson and Keller, 1999) as well as different organ morphogenesis especially of the mammary gland (Ewald et al., 2008). In cancer, it consists of a cluster of cells leaving the primary tumor to invade the surrounding tissue or even further organs (**Figure 12**). Main criteria defining this type of invasion are the adhesion complexes preserved between cells during migration, protrusive structures creating the traction forces crucial for movement, and lastly modifications of the ECM by degrading, remodeling or deposing new components (Friedl and Gilmour, 2009). Epithelial tumors commonly migrate in bulks, and it has been shown that circulating tumor cell clusters have 23-50 times increased potential of seeding secondary tumors and therefore are the main precursors of breast cancer metastasis (Aceto et al., 2014).

However, studies have shown a clear heterogeneity within this cellular migrating cohort. As presented in the EMT section, cells at the invasive front leading the migration seems to undergo a partial EMT and to express EMT-TFs while the rest of cells keep a less-mesenchymal phenotype. In the same line of thoughts, *in vivo* and in 3D culture of primary human breast tumors, only leading cells of the cluster have activated a dedifferentiation mechanism and expressed basal epithelial markers (as tumor protein p63, and cytokeratin 14) (Cheung et al., 2013). Leader cells will also have to concentrate proteases, mainly MT1MMP in the case of breast cancer, that will allow matrix degradation, creating galleries for follower cells to be dragged behind passively [proteases families and roles are described in the following sections]. Through a specific reorganization of cortical actin and adhesion complexes, the cell cluster will become a contractile large body. By interacting with the ECM (mainly integrins) and pulling on the collagen fibers, a reorganization of the ECM will occur to optimize their motility. Of note, in some cases, tip cells leading the cluster can be stromal fibroblasts (Gaggioli et al., 2007).

Conclusion

In conclusion, the invasion process is the result of the degrading properties of malignant cells and a "tumor microenvironment" (TME) that will provide a fertile soil for tumor development, progression and metastasis.

***

In the EMT description, I have focused on the importance of cell-cell interaction and adhesion for tumor development. Throughout the following section, I will discuss the inreraction of cells with their microenvironment by focusing on the molecular details of Cell-ECM interactions, ECM remodeling, and ECM degradation.

4. Tumor Microenvironment

A collaborative interaction between cancer cells and their stroma is crucial for tumor cell proliferation, invasion and metastases in most human cancers (Hanahan and Coussens, 2012)(Hanahan and Coussens, 2012). During cancer progression, it is conceived that ECM is continuously reshaped on a molecular and structural level and that it may promote metastatic spread. R. Hynes group showed that the high metastatic potential of primary tumors of human mammary carcinoma xenografts derives from distinct stromal composition when compared to less metastatic tumors (Naba et al., 2014). Furthermore, the clinical outcome of breast cancer patients was shown to be strongly linked to ECM characteristics (Bergamaschi et al., 2008). Moreover, Provenzano et al (2006) defined three Tumor Associated Collagen Signatures (TACS) by using environmental collagen density and collagen fiber organization and corresponded them to stages of mammary carcinoma with correlations on tumor burden, invasion and metastasis (Provenzano et al., 2006). Thus, a deregulation of extracellular matrix (ECM) dynamics is recognized widely as a hallmark of cancer.

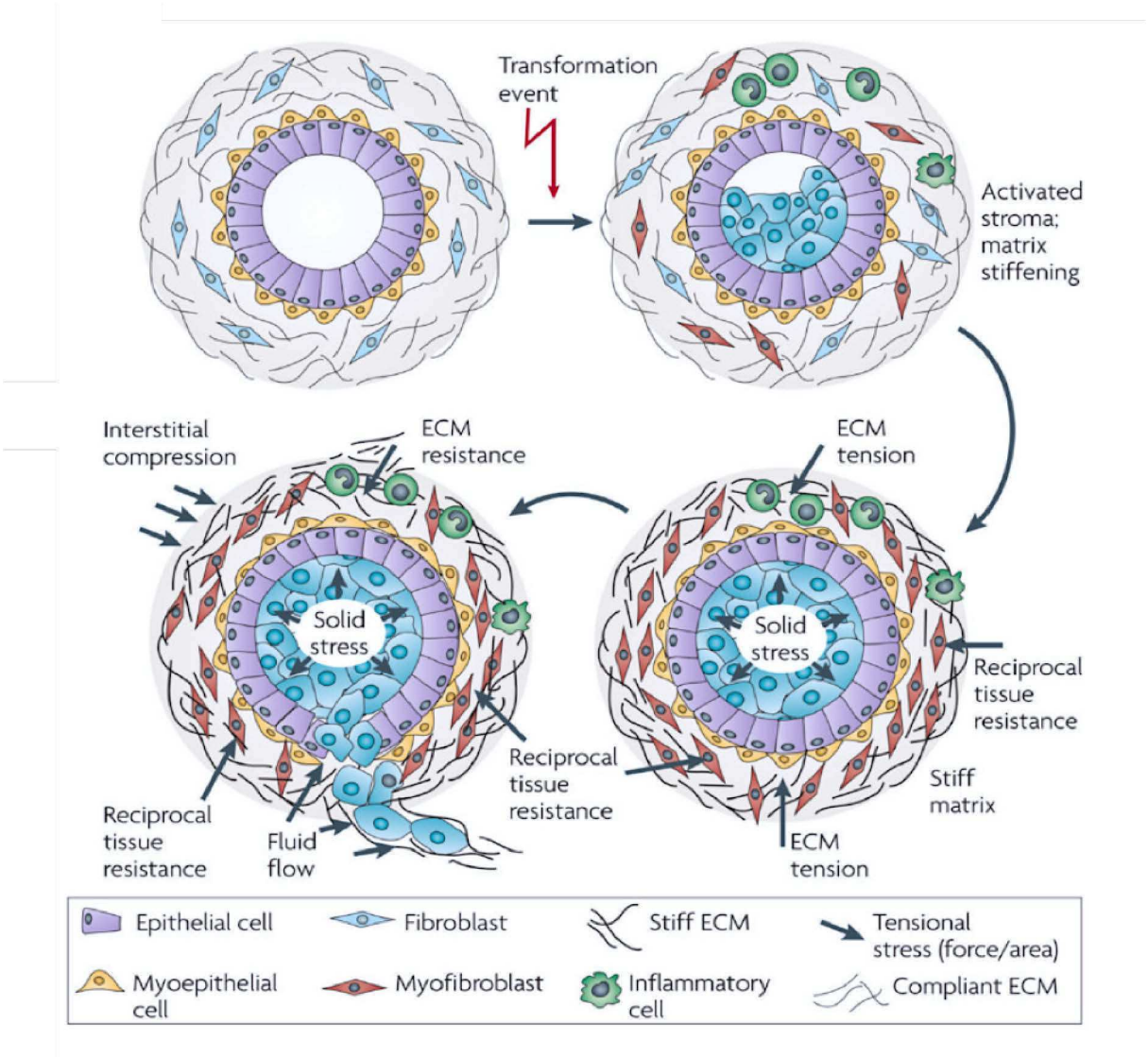

Figure 13: ECM modifications occurring during tumoral progression.

The tumor microenvironment (TME) is connected to every step of tumorigenesis and will undergo various modifications that will affect tumoral progression. It will activate fibroblasts into the so-called cancer associated fibroblasts (main cellular players), recruit immune cells that will increase the inflammation, and increase growth factor and cytokines release. The stroma will also have a different density and assembly of the molecular components like collagen and fibronectin which will provide new physical properties for the ECM enabling tumor migration and invasion (e.g. stiffness). A continuous crosstalk is maintained between cells and TME by reciprocal mechanosensing of the applied tensions. Adapted from Butcher et al., 2009.

4. 1. General composition

TME is composed in majority of the same ECM components of normal mammary gland (presented in "1. 2. 2. Microenvironment compartment"). However, main differences lie behind the variants or isoforms of ECM cells and molecules, the distinct expression ratios, the activity levels of some enzymes

as well as distinct 3D structure assembly of the matrix. And on the basis of these differences, ECM elements will acquire pro-tumorigenic properties (**Figure 13**) (Whiteside, 2008).

Tumor stroma can be divided into two major components: cellular components or stromal cells (e.g. adipocytes, endothelial cells, fibroblasts, immune cells, myofibroblasts, cancer associated fibroblasts) and non-cellular connective extracellular matrix (ECM) composed of proteoglycans, hyaluronic acid, fibrous proteins (e.g. fibronectin, collagen and laminin).

Among the cellular components (**Figure 13**):

- Fibroblasts, the most abundant cell type of connective tissue, regulate in physiological contexts several roles. They secrete and assemble major components of ECM: collagen (notably I, III and V), elastin, fibronectin, fibrillin, proteoglycans, etc., enzymes such as proteases and their regulators (MMPs, ADAMs, TIMPs, etc.) to maintain the balance between ECM degradation and deposition, and cytokines and growth factors that participate to the differentiation of surrounding cells. Activated fibroblasts, called myofibroblasts, will secrete an ECM with altered architecture, as well as different cytokines helping the recruitment of immune cells (Kalluri and Zeisberg, 2006).

- CAFs or cancer associated fibroblasts are activated fibroblasts that display similar roles as myofibroblasts with a main difference that their epigenetic regulation can limit the regression of this activated state .They usually do not undergo apoptosis and support all along the tumorigenesis process (LeBleu and Kalluri, 2018; Tao et al., 2017). CAFs are mainly implicated in architectural modifications of TEM as well as tumors' resistance to therapy. They are also responsible in part of the biophysical characteristics of the matrix such as stiffness discussed in "4. 3. 1. ECM Stiffness".

- Adipocytes, described first as an energy storage, have been described to have a paracrine role by secreting growth factor (such as hepatocyte growth factor) important for the progression of breast cancer (Dirat et al., 2011).

- Immune cells are found infiltrated in the TME indicating a strong inflammation at the tumor site. We can find lymphocytes (T cells, B cells and natural killer cells), macrophages and neutrophils originating from two different lineage of bone marrow. In contrast to their immune role, they have been enrolled in promoting angiogenesis, increasing proliferation, resisting cell death and activating invasion (Condeelis and Pollard, 2006; Hanahan and Coussens, 2012; Murdoch et al., 2008).

The ECM of breast cancer is reviewed in (Insua-Rodríguez and Oskarsson, 2016; Lu et al., 2012).

***

While some authors believe cancer is mainly the result of a complex cancerous microenvironment surrounding cells (Whiteside, 2008), I think that cancer is the resultant of back and forth interactive crosstalk between tumor cells and their TME. Therefore, metastasis occurs only when their cooperation results in cells overcoming the physical barriers as well as resisting to various threats like the immune system.

4. 2. Crosstalk between Cells and their ECM: Role of Integrins

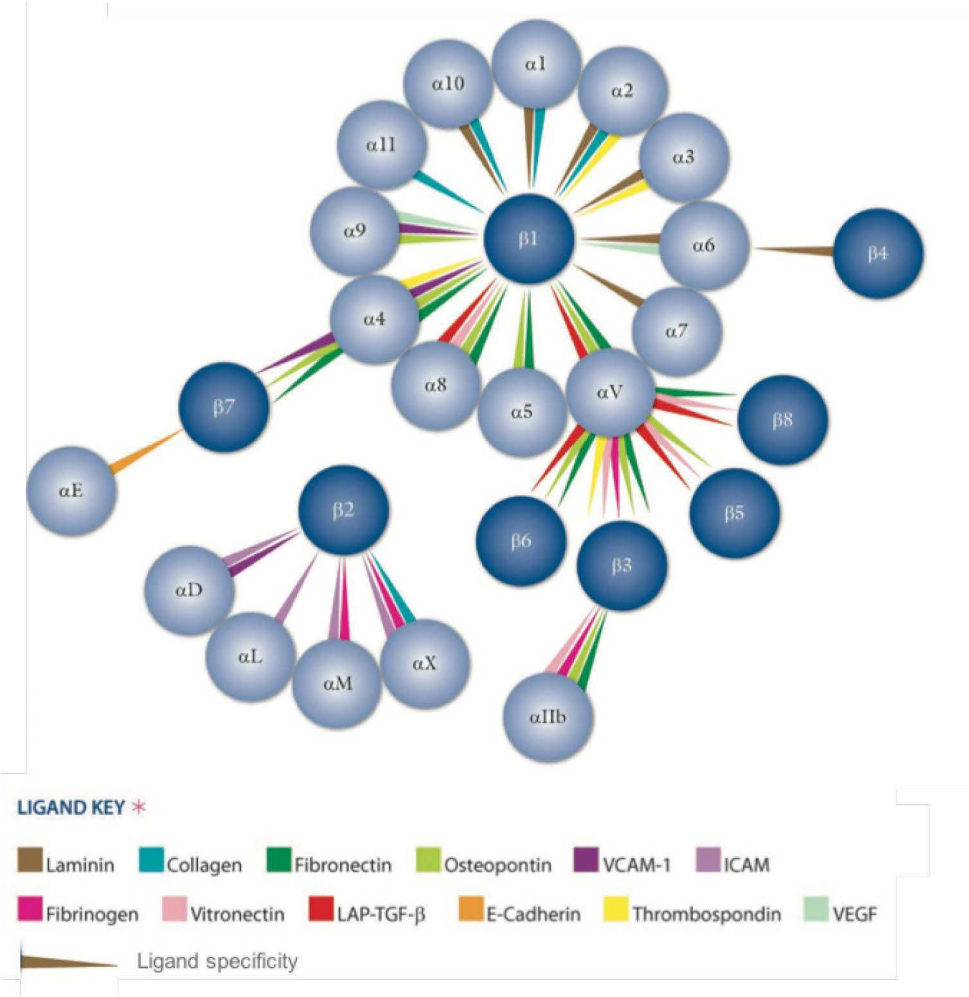

Figure 14: Integrin family and their ligands.

This figure represents the mammalian subunits and their αβ associations. Each heterodimer has a ligand specificity marked here by different arrow colors. In the normal mammary gland, the most expressed integrin receptors are collagen receptors (α1β1, α2β1), fibronectin receptors (α5β1, αvβ3) and laminin receptors (α3β1, α6β1 and α6β4). Some subunits have alternatively spliced cytoplasmic domains like α6, α3, β3 and β4. Adapted from resources.rndsystems.com

ECM-Cell interactions are mainly mediated by specific receptors, such as integrins, DDRs (Discoidin Domain Receptor), and syndecans (Hynes, 2002; Raymond et al., 2012). I will mostly be discussing the role of the major receptors, integrins, tackled in this thesis work.

In mammals, 18 alpha subunits and 8 beta subunits, capable of forming 24 dimers of integrin, have been identified. The association determines the specificity of integrin for its substrate and they can be classified into four main groups according to their ligand (**Figure 14**, **Figure 15**).

In fact, during tumor transformation, cancer cells modify the repertoire of integrins expressed on their surface in order to adapt to their changing tumoral environment and to activate proliferation and pro-invasive signaling pathways (**Figure 15**) (Desgrosellier and Cheresh, 2010; Guo and Giancotti, 2004; Seguin et al., 2015). In breast cancer, integrins β1 and β4 play a key role in breast tumorigenesis. Indeed, the loss of function of β1 or β4 integrins, in different mouse models, inhibited tumor initiation and progression (Huck et al., 2010; Lahlou and Muller, 2011; White et al., 2004). Additionally, integrin α3β1 was involved in tumor progression and metastatic migration in many studies and solely, integrin α3 was detected in aggressive breast cancer cells undergoing EMT (Shirakihara et al., 2013). In contrast, integrin β1combined to integrin α2 was reported to suppress the formation of metastases from primary breast tumors (Ramirez et al., 2011).

Altered integrin expression patterns have been linked to many types of cancer. Correlation between specific integrins expression and patient survival or response to therapy were summarized in the supplementary of Hamidi and Ivaska review (Hamidi and Ivaska, 2018). Different roles of integrins were also seen in breast cancer mouse models (Raymond et al., 2012).

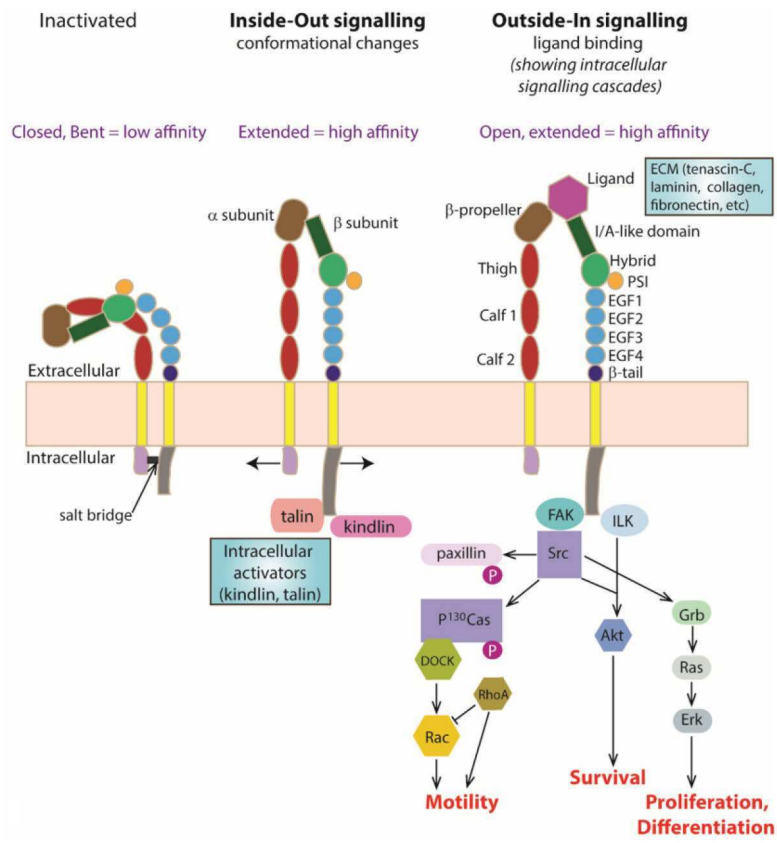

Figure 15: Integrin structure and activation mechanism.

Integrins are on-off switches that allow anchoring cells to ECM and controlling different processes of mammary gland morphogenesis (proliferation, differentiation, migration, survival, etc.). They are also mechanotransducers that can convert tension forces generated by the ECM into intra-cellular signals. Generally, the affinity of integrins to their ligands is controlled by an inside-out signal mediated mainly by talins. Talin activated by PIP2 or FAK (focal adhesion kinase) bind the cytoplasmic tail of integrins and induce conformational changes that can modify integrins' affinity to their ligands (Hynes, 2002). After binding to their ligand, an outside-inside integrin mediated signaling is triggered and can involve the recruitment of Focal Adhesion Kinase (FAK) and its downstream target SRC, or the activation of RAS-MAPK or PI3K-AKT signaling pathways. Less emphasized in the literature is the role of talin in the outside-inside signaling. Some data suggest that once integrins bind to their ligand, talin will change conformation and it will be dissociated so that other effectors can bind the activated C-terminal of integrins (Das et al., 2014). *Adapted from Cheah and Andrews, 2018.*

It is important to stress that, integrins are crucial as well for mechanical sensing, stiffening and remodeling of the ECM, and they intervene at different levels of tumor progression including invasion, metastases and drug resistance (Glukhova and Streuli, 2013; Hamidi and Ivaska, 2018). Furthermore, many studies indicate that signaling molecules activated upon engagement of integrins, such as FAK and ILK, play a key role during tumorigenesis (Lahlou et al., 2012).

4. 3. ECM remodeling

Tumor ECM influences tumor progression when architectural and biochemical features are altered (level of expression of ECM components and/or fiber alignment) (Bissell et al., 1982). Here I would like to clarify on one hand the effect of ECM remodeling, more specifically stiffness, on cancer cells through the process of mechanotransduction and on the other hand the effect of cancer cells contractility in restructuring the collagen matrix to facilitate migration (Simi et al., 2018).

4. 3. 1. ECM Stiffness

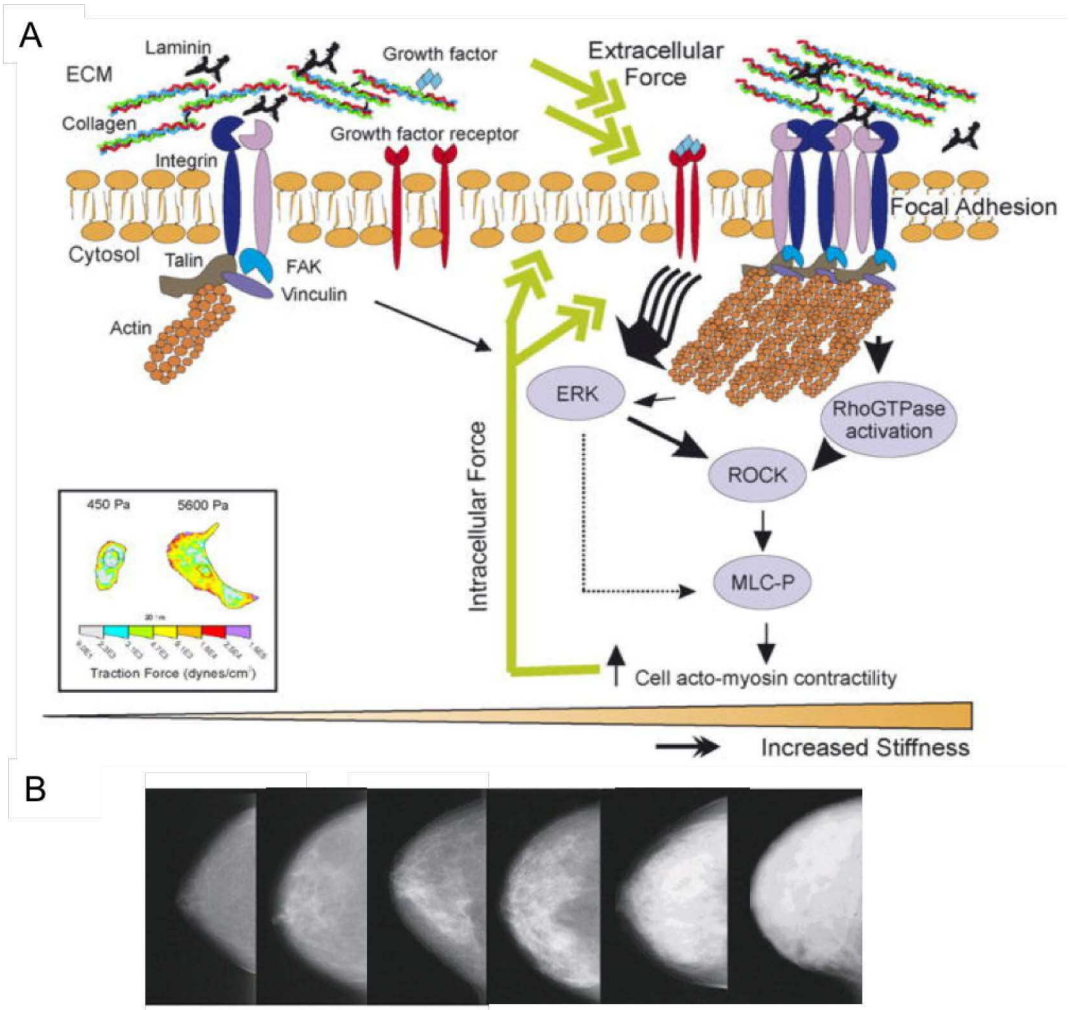

Figure 16: ECM stiffness in patients and associated signaling pathways

A. ECM stiffness and contractility are two related characteristics of the ECM and cells respectively. This panel shows that matrix stiffness applies an external force that stimulates the clustering of integrins. Integrins are mechanotransducers that will in turn increase intracellular signaling and activate Rho associated pathways. As a result, cellular contractility will increase and an inside-outside signaling will allow cells to remodel the ECM (e.g. by aligning collagen fibers) B. Mammographic density of breast showing 0% dense tissue on the first panel on the left and increasing density with more than 75% dense tissue in the last panel on the right. Increased density was associated with higher risk of breast cancer. Adapted from Boyd et al., 2002; Kass et al., 2007.

Somewhat counterintuitive to ECM degradation used by tumor cells to disseminate, dense fibrotic stroma has been correlated with poor prognosis in breast cancer (**Figure 16**) (Wan et al., 2013). In diagnostic, patients with an increased breast density revealed by palpation and measured by mammography have a greater risk for breast cancer (Boyd et al., 2002). Increased deposition of collagen in mouse model of breast cancer significantly increases tumor formation and has been causally linked to tumor metastasis (Provenzano et al., 2008).

Rigid matrix is perceived and translated by cells as mechanical forces measured in Pascal (Pa) and are usually integrate by cells through mechanotransduction. Stiffness has been shown to increase cancer cell proliferation, resistance to apoptosis, and angiogenesis (Pickup et al., 2014). Binding of cells to a tumor matrix inhibits the expression of some tumor suppressors such as BRCA1 or PTEN (tumor suppressor phosphatase and tensin homolog). Moreover, matrix stiffness contributes to the formation of invadopods and focal adhesions required for cell invasion (Menon and Beningo, 2011). Additionally, in recent studies, increased crosslinking of collagen by lysyl oxidase (LOX) family promotes tumor invasion and metastasis by engaging integrin signaling (Kirschmann et al., 2002; Levental et al., 2009; Wan et al., 2013). The LOX prepeptides were capable of inhibiting branching structures formation in Matrigel and to suppress tumor size by more than 60% in xenografts mice model of Her-2 driven breast cancer (Johnston and Lopez, 2018). Lately, preclinical studies involve trials on inhibiting LOX in tumors which shows for now positive results (blocks metastasis, and no toxic side effects reported) (Barker et al., 2012; Bondareva et al., 2009)

In line with the role of integrins, stiffness was linked to tumors aggressiveness by translating the mechanotensions into biochemical cues through integrins (Butcher et al., 2009; Kumar and Weaver, 2009). The group of V. Weaver has suggested a mechanism of action of how matrix stiffness alter epithelial homeostasis. In fact, an increased rigidity of the surrounding stroma will activate integrin clusters in order to enhance ERK signaling, focal adhesion formation in addition to ROCK-mediated contractility (Paszek et al., 2005a). This integrin-dependent mechanotransduction may imply several signaling pathways such as Rho GTPases, FAK/SRC and YAP/TAZ (**Figure 16**) (Dupont et al., 2011; Paszek et al., 2005b; Provenzano et al., 2009).

A recent review covers more details on the impact of altered tumors mechanics (Mohammadi and Sahai, 2018)

4. 3. 2. Contractility

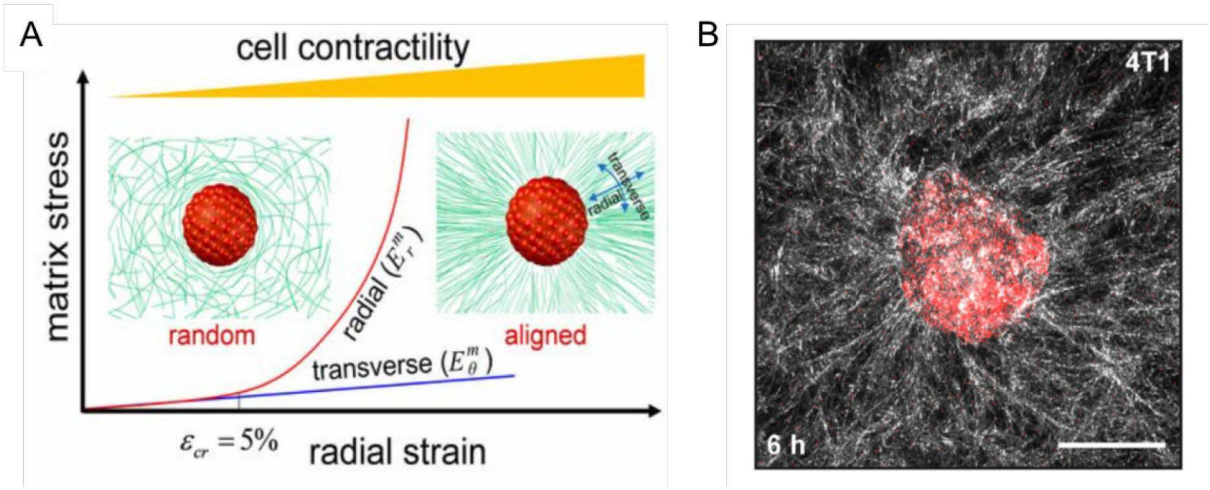

Figure 17: Contractility and collagen fibers alignment.

A. This panel shows that in normal epithelial cells, the collagen fibers adopt a random architecture. When the radial stress increase, cells increase their contractility and in result tend to align their collagen fibers. B. Confocal image of 4T1 mouse mammary tumor cells (in red) presenting a high percentage of aligned collagen fibers (in white) . Adapted from Ahmadzadeh et al., 2017; Piotrowski-Daspit et al., 2017.

Alongside the stiffness of ECM, cancer cells need to use contraction to pull on the extracellular matrix and move forward. This results in aligned collagen fibers organized in parallel structures implicated in determining the migration direction, as well as increase the efficiency and persistence of migrating cells (**Figure 17**) (Piotrowski-Daspit et al., 2017).

Besides migration, contractility of tumor cells has been linked to invasion and metastasis. Two studies have shown that actomyosin-based contractility drives invasion in 3D Matrigel using MDA-MB-231 human breast adenocarcinoma cells by generating forces on β1 integrin adhesion (Mierke et al., 2011; Poincloux et al., 2011).

In mammary cancer cell lines, contractility is mainly mediated by Rho GTPases and enhanced by propagation of tension through intercellular adhesions (Haga and Ridley, 2016; Parri and Chiarugi, 2010; Piotrowski-Daspit et al., 2017). The Rho GTPases signaling pathways will be described in: III. A. RhoGTPases

Conclusion

The biomechanical properties of ECM and their interaction with epithelial cells can drastically affect cancer progression. The evidences aforementioned underscore the importance of ECM dynamic remodeling and ECM-Cell interactions for migration, invasion and metastasis.

4. 3. 3. Proteases & ECM degradation

Besides pulling the ECM fibers and modifying its density, collective migration requires the degradation of ECM by remodeling enzymes, firstly the basal membrane which confine cells in a limited physical space. Different families of matrix modifying proteases have been described: matrix metalloproteinases (MMPs), heparanase, cathepsins, urokinase plasminogen activator (uPa), etc. They are often found aberrantly upregulated in breast cancer and enhance significantly tumoral progression and metastasis (Bonnans et al., 2014; Gomes et al., 2013; Oskarsson, 2013). These enzymes will generate least resistance tracks used by following cells of the migrating cluster. They also serve to release growth factors associated to ECM.

Extracellular Matrix degradation: A focus on MMPs

- **Family of MMPs**

Human have 23 MMPs, with 17 soluble and secreted enzymes and 6 membrane-associated enzymes. They consist of a polypeptide sequence comprising a cysteine residue that contains a Zinc atom (Zn), hence their generic name of metalloproteases. They differ by their tissue specific expression, substrates affinity and their structural architecture (Radisky and Radisky, 2010). Despite the complexity of their regulatory mechanisms, it is possible to identify three major levels: transcriptional regulation, activation of proenzymes and inhibition of their enzymatic activity. The latter is mainly mediated by tissue inhibitor of metalloproteinases (TIMP) family members. They inhibit MMPs in a stoichiometric reversible way through binding to the catalytic site of MMPs and thus mimicking their substrate. A redundancy can be found between different members of this family. Surprisingly, TIMP-1, one of the four natural TIMPs, was shown to be upregulated in breast cancer and in some cases correlated with poor patient prognosis (Nakopoulou et al., 2002; Ree et al., 1997). Besides acting as an endogenous inhibitor of matrix metalloproteinases, TIMP1 has been recognized for its role in promoting proliferation, inhibiting apoptosis in cancer cells and in the accumulation of cancer associated fibroblasts (CAFs) that in turn enhance tumor progression (Gong et al., 2013; Würtz et al., 2005).

MMPs have also their ways to favor tumor progression in different ways in breast cancer. For instance, MMP3 triggers EMT by increasing the cellular levels of reactive oxygen species, which in turn induces Snail1 expression (Radisky and Radisky, 2010). During metastasis, MMP-2 and MMP-9 are the main MMPs activated in order to digest the collagen type IV, major component of the basement membrane (Duffy et al., 2000). In patients, some important MMPs for mammary gland involution are found upregulated during breast cancer such as MMP-2,-3, -9 and -14 (McDaniel et al., 2006; Oskarsson, 2013).

We are going to focus on MMP14 also previously called MT1MMP, the founding member of membrane-associated MMPs, implicated in the core work of this thesis.

- **MT1-MMP/MMP14**

MMP14 has been reported to play several roles (in adhesion and motility, proliferation, activating growth factors, senescence, etc.) with an emphasis on their role in invasion (Feinberg et al., 2016). *In vitro*, in both normal mammary gland branching and breast cancer invasion, MMP14 has been shown to be particularly important for collective migration by degrading the extracellular matrix and favoring motility. MMP14 also participates to pro-migratory positive feedback loop by activating MMP-2 known to induce invasive behaviors. *In vitro*, several studies were able to confirm the degrading capacity of MMP14 in collagenous matrix.

Expressed at tip cells, MMP14 allows cancer cells to sculpt a track facilitating clusters invasion (Friedl and Gilmour, 2009; Poincloux et al., 2009; Wolf et al., 2007). More specifically, MMP14 proteins are concentrated in membrane extensions called invadopodia*** which optimize their action (Poincloux et al., 2009). In mice, KO of MMP14 has shown many bone abnormalities, suggesting a strong involvement of this MMP in normal collagen metabolism and therefore was considered a major collagenase. In addition, mouse models of breast cancer downregulated for MMP14 developed fewer tumors (Andarawewa et al.; Masson et al., 1998).

However, downregulation of MMP14 in mouse epithelial cells did not show any major alteration of normal mammary development *in vivo* (Feinberg et al., 2016). These surprising observations show inconsistency with the *in vitro* experiments carried to examine mammary morphogenesis. A recent study has succeeded to explain these confusing results by showing that during normal mammary branching, the active MMP14 responsible for degrading the matrix is expressed by the cells of the periductal stroma while during cancer invasion, MMP14 expression and activity is expressed on the plasma surface of tumor epithelial cells (**Figure 18**) (Feinberg et al., 2016, 2018).

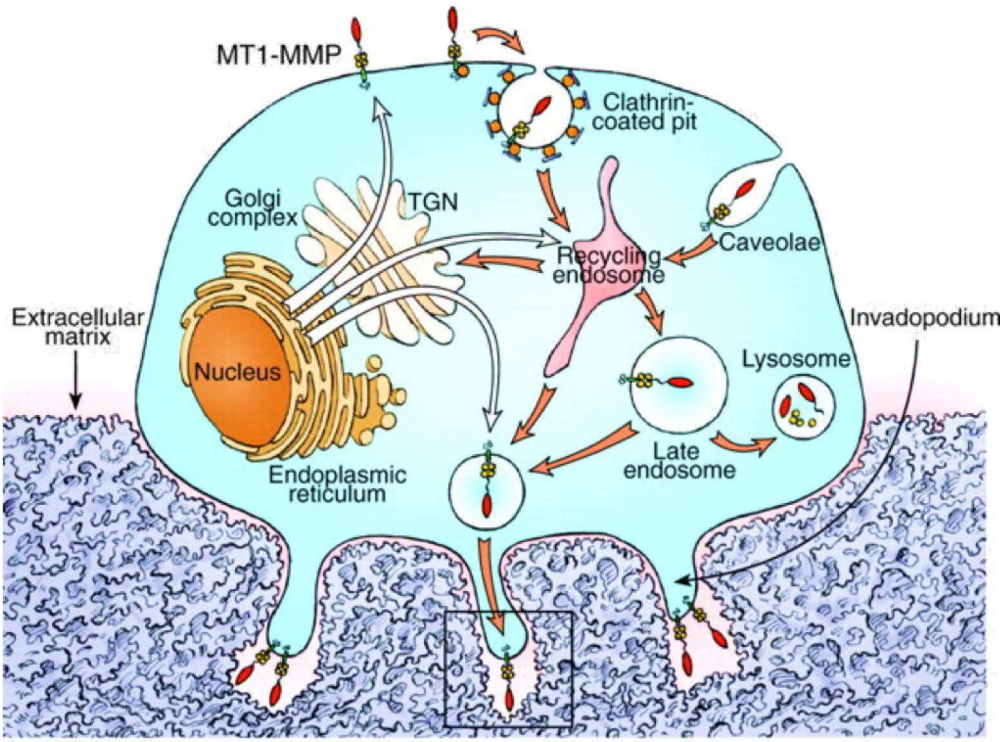

Figure 18: MMP14 intercellular trafficking

MMP14/MT1-MMP is synthetized as a proenzyme and its activation occur in a post-golgi compartment. In normal cells, it is sometimes transported with TIMP2, a metalloprotease inhibitor. It is usually recycled in a clathrin-dependant vesicles and send in part to degradation in the lysosome. In cancer cells, MMP14 is directed from late endosomes to invadopodia (degradative structures enabling invasion) and from the post-golgi compartment. This will allow the concentration of MMP14 in invadopodia and will increase the degradation of the ECM essential for collective migration. Adapted from Poincloux et al., 2009.

***Invasive cells grow membrane extensions in order to migrate and metastasize. There are four types of protrusions including: blebs, filopods, lamellipods, invadopodia (Friedl and Wolf, 2003).*

Invadopodia are actin-dependent structures that function in ECM remodeling and invasion. The formation of these structures was linked to src signaling; different substrates of src have been localized to invadopodia (N-WASP, cortactin, Arp 2/3, etc.). Invadopodia will ensure adhesion and cell signaling roles as well as the secretion of MMPs to promote invasion. Through cytoskeleton organization and Arf6-dependent exocytosis mechanisms, MT1MMP is concentrated and activated in invadopodia (Clark and Weaver, 2008; Marchesin et al., 2015a; Poincloux et al., 2009).***

Conclusion

Invasion, after all, is the resultant of continuous cross-talks between cells and TME. It is a combination of several deregulated signaling pathways, aberrant protein expression as well as biomechanical and structural modifications. What was presented in this part of the introduction is a brief overview of few of the possible mechanisms enhancing invasion and metastasis.

III. Support system of tumorigenesis: the Ras SUPERFAMILY

The Ras superfamily of small guanine triphosphate (GTP)-binding proteins comprises over 160 human member and, according to their similar structure and function, can be divided into five major families: Ras, Rho, Ran, Arf/Sar and Rab families (Takai et al., 2001). Discovered in the 1980s, they belong to a class of protein called small G proteins capable of binding guanylyl nucleotides. These monomeric proteins act as binary molecular switches cycling between a so-called inactive state in GDP form and an active state in GTP form. Although they have intrinsic GTPase activity, with the exception of Arf proteins, they exhibit low GDP/GTP exchange activities. Thus, to pass from one state to the other, their intrinsic activities are catalyzed by by GEFs (Guanines nucleotides Exchanges Factor) and GAPs (GTPase Activating Protein) proteins (Bos et al., 2007). The regulation of Ras superfamily proteins by various GEFs and GAPs besides other post-translational modifications as well as space localization leads to a regulation of a broad range of cell processes (cell differentiation and proliferation, actin cytoskeleton reorganization and vesicular trafficking) (Wennerberg et al., 2005).

III. A. RhoGTPases

1. Generalities & Regulators

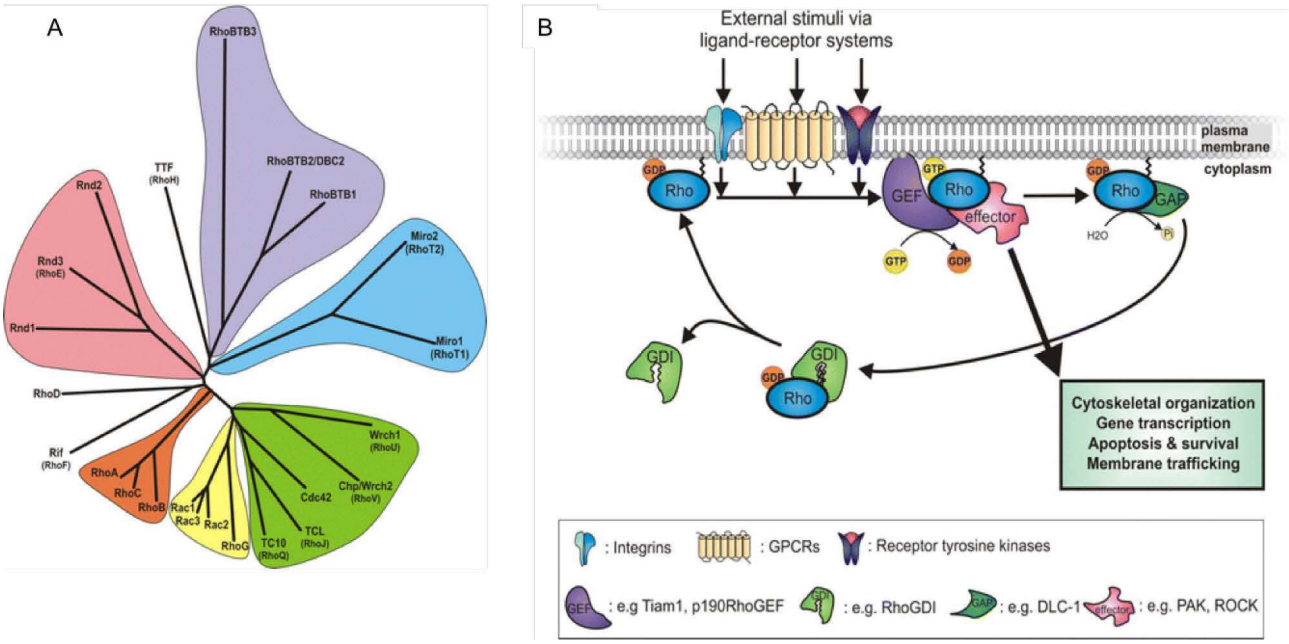

Figure 19: Rho GTPase family and their regulation process

A. Dendogram of the family of Rho GTPases. B. Regulation process of Rho GTPases. Rho GTPases are activated at the membrane level by GEF proteins which will allow the binding and activation of downstream effectors. Their deactivation is mediated by the hydrolysis of GTP by releasing the third phosphate. GAPs and GDIs have shown to mediate the passage of Rho GTPase proteins from a GTP active state to a GDP inactive one. Adapted from Ellenbroek and Collard, 2007.

Rho GTPases belong to the Ras superfamily of GTP binding proteins. They are small binary molecular switches (21KDa) activated by different signaling cascades. These signals are mainly transduced from transmembrane receptors like integrins, growth factor receptors, G-protein coupled receptors etc. The Rho genes were first isolated, in 1985, from the abdominal ganglia of Aplysia, a marine snail (Madaule and Axel, 1985). Subsequently, 23 members of the Rho GTPases family have been identified and were divided into subfamilies, based on their sequence identity, structure, and function (**Figure 19**) (Ellenbroek and Collard, 2007). These 6 subfamilies are Rho BTB, Rnd, Miro proteins and the three classical subfamilies Rho, Rac and Cdc42 proteins that we will be focusing on.

The active GTP form of Rho GTPases can bind more than 70 effector proteins and thus, they regulate a variety of cell functions particularly cytoskeleton reorganization, cell adhesion, proliferation, differentiation and vesicular trafficking (Bishop and Hall, 2000; Bustelo et al., 2007).

This diversity of RhoGTPases roles is related to cell types by which they are expressed, and the subcellular location of their activation (Nalbant, 2004). The spatio-temporal regulation of Rho GTPases can be moderated by three main regulators. First, the guanine nucleotide exchange factor proteins (GEFs) are responsible for catalyzing the exit of GDP to allow the spontaneous binding of a guanosine triphosphate (GTP) from an excess of existing GTP pool and therefore the activation of Rho GTPases (Schmidt, 2002). This GTP bound will modify the conformation of Rho GTPases, thus increasing the affinity to their effectors. Second, though Rho GTPases have an intrinsic GTPase activity, GTPase activating proteins (GAPs) are needed to facilitate the switch to an inactive GDP state (Moon, 2003; Tcherkezian and Lamarche-Vane, 2007). The third regulators are the guanine nucleotide dissociation inhibitors (GDIs). GDIs bind to the inactive GDP conformation of Rho GTPases, and sequester them as soluble complexes in the cytoplasm in order to prevent spontaneous activation and other functions that are not yet well defined (DerMardirossian and Bokoch, 2005; Olofsson)

To date more than 70 GEFs, and 60 GAPs were described; many more than Rho GTPases family members. Therefore, the amount of activated Rho GTPases at a specific site of the cell will strongly depend on the expression, localization and activity of their regulators.

2. General Roles of Rho GTPases

After 5 years of Rho genes discovery, Hall and Ridley's work revealed some functions of Rho GTPases in the regulation of membrane ruffling, assembly of focal adhesions and stress fibers in human fibroblasts (Ridley and Hall, 1992; Ridley et al., 1992). In parallel to this, the role of Cdc42 on cell polarity was established in yeast (Adams, 1990; Johnson, 1990). Rho GTPases are major regulators of actin cytoskeleton organization in mammalian cells (Tapon and Hall, 1997), and it did not take long to discover their roles in a wide range of other cellular functions: proliferation and apoptosis, vesicular traffic, cell adhesion, and gene expression (Hall, 2005; Olson et al., 1995; Ridley, 2001a).

3. Rho GTPases and cancer

These cellular functions mentioned above are often disrupted during cancer, and therefore several studies have found the small G proteins of Rho family playing major roles in cell transformation and cancer progression (Karlsson et al., 2009; Ridley, 2001b; Sahai and Marshall, 2002). It has been clearly shown that Rho-GTPases participate in cell transformation induced by the oncogene Ras (Avraham and Weinberg, 1989). Indeed, the expression of negative dominant mutants of RhoA, Rac1 or Cdc42 inhibits Ras-induced malignant transformation (Khosravi-Far et al., 1995; Qiu et al., 1995a, 1995b, 1997).

Unlike Ras family GTPases, no activating mutations have been detected in genes encoding Rho-GTPases in cancer, with the exception of Rho H, whose gene is rearranged or mutated in B-cell lymphoma cases (Pulgar et al., 2005; Rihet et al., 2001). However, some Rho-GTPases are overexpressed in a number of cancers and this high expression rate is often correlated with tumor progression (Fritz et al., 1999; Sahai and Marshall, 2002).

RhoA is overexpressed in carcinomas of the neck and head, breast cancer, as well as in tumors of the lungs and colon. RhoC expression is increased in pancreatic cancers and melanomas with high metastatic potential. Breast and colon cancers are also associated with overexpression of Rac1 and Cdc42 (Sahai and Marshall, 2002). In addition, Rac1b, a splicing variant of Rac1, and Rac3 were found strongly expressed and overactivated in these two types of cancers (Schnelzer et al., 2000). Besides Rho GTPases, a deregulation of the activity or expression of their regulators has been observed in different cancers (Wennerberg and Der, 2004; Wennerberg et al., 2005). Finally, some of the Rho-GTPase effectors have been identified as inducing cell transformation. For example, the expression and activity of PAK (p21-Activated Kinase), an effector of Rac1 and Cdc42, are increased in breast cancers and correlated with tumor invasiveness (Kumar et al., 2006; Ridley, 2004; Vadlamudi and Kumar, 2003). These multiple roles of Rho GTPases in tumor progression have been validated by some small molecular inhibitors. I can cite the work of Zins et al. where they show that inhibiting Rac1 and Cdc42 reduced tumor growth of prostate tumor xenografts (by blocking cell cycle and migration and increasing apoptosis) (Zins et al., 2013).

3. 1. 1. Rho GTPases and Invasion

Rho GTPases play an important role in the reorganization of the actin cytoskeleton and microtubules allowing the formation of membrane protrusions at the migration front and the contraction of the cell body as well as the turn-over of cell-cell and cell-ECM adhesion, all of which jointly contribute to the efficacy of cell migration (Ridley, 2015). And therefore, aberrant activation of these signaling pathways can promote migration and subsequently act as a major contributor to invasion and metastases formation.

3. 1. 2.Regulation of actin cytoskeleton and Protrusion formation

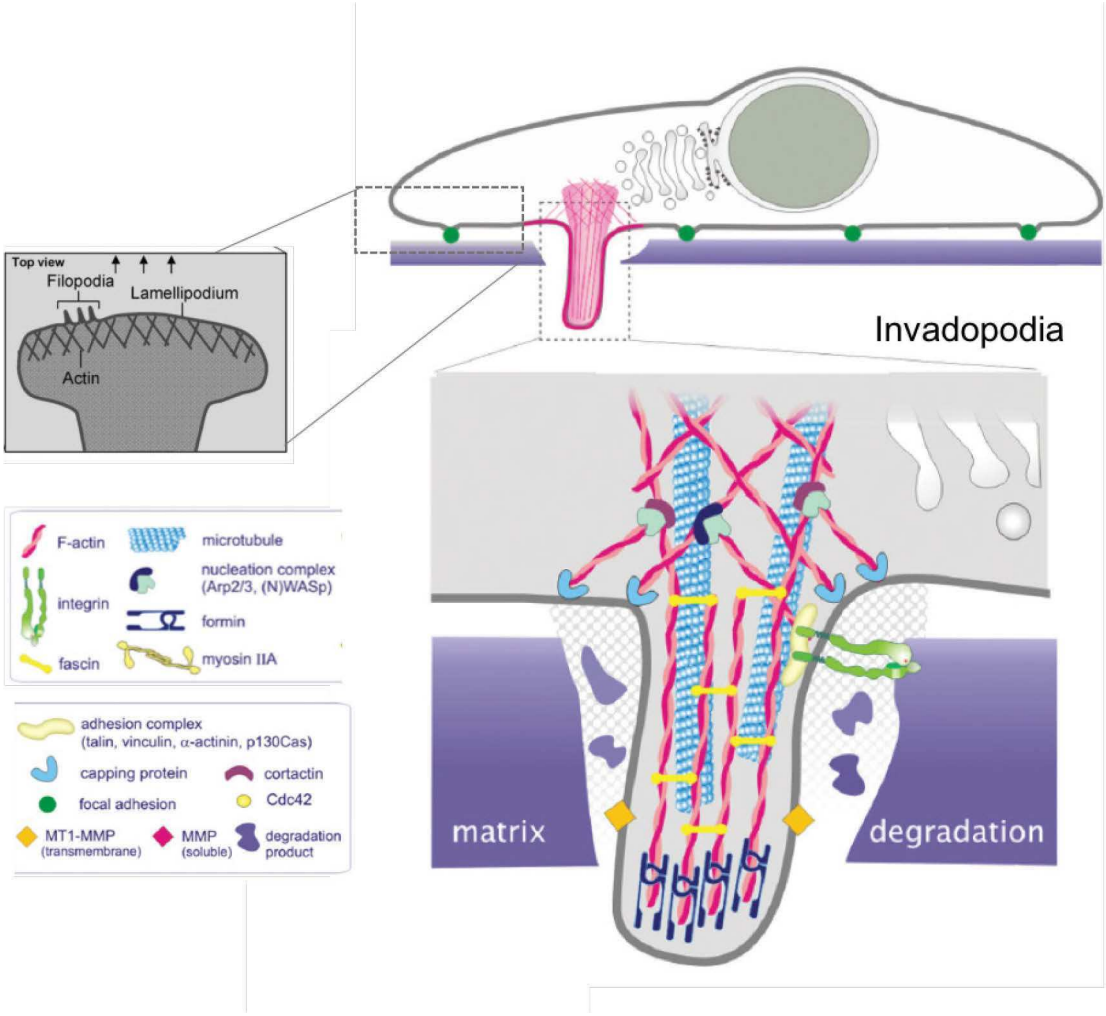

Figure 20: Rho GTPases and protrusion formation.

Taken a single migrating cell, filopodia and lamellipodia will be formed at the leading edge. The polarity in this case implies the activation of Cdc42. Cdc42 contributes to filopodium extension through mDia and formins. Lamellipodium extension recruits Rho and Rac proteins. Contractility of the cell body drives cells forward and is mediated by Rho/ROCK or Cdc42/MRCK. A sustained activation of Cdc42 and Rac allows the formation of invadopodia important for collective migration. Cdc42 maintains the WASP/Arp2/3 complex and promotes invadopodia extension and helps transporting MMP14 to the plasma membrane of these structures. Adapted from Lawson and Ridley, 2018; Spuul et al., 2014.

RhoA, Rac1 and Cdc42 coordinate the dynamics of the cytoskeleton of actin and tubulin and are, therefore, a turning point in cell migration, both under normal physiological conditions as well as pathological context, such as tumor progression (Evers et al., 2000; Ridley, 2001b; Tapon and Hall, 1997).

For instance, inhibiting Cdc42 in swiss 3T3 fibroblasts or neuronal cells decreased migration, abolished microspikes formation and disrupted golgi structure. In tumor cells, Cdc42 inhibition blocked actin-based motility and migration in a metastatic prostate cancer cell line (Friesland et al., 2013). *In vivo*,

Rho and its effector ROCK have been implicated in tumor-cell dissemination (Clark et al., 2000; Itoh et al., 1999; Murata et al., 2001; Somlyo et al., 2000).

Many other examples will be presented while briefly explaining the different membrane extensions that can participate to cell migration.
In migrating cells, four types of protrusions have been reported to be mediated by Rho GTPases (Ridley, 2011).

Lamellipodia are sheet-like protrusions usually observed at the front-rear of collective migrating cells. Activated Rac is required to drive lamellipodia formation (Faroudi et al., 2010; Montell et al., 2012), and will mainly recruit Wiskott-Aldrich syndrome protein-family verpolin-homologous protein (WAVE) that in turn activates Arp 2/3 in charge of actin nucleation and branching. Even though Rac is sufficient for creating these protrusions, Cdc42 and Rho have been found active and contributed to the extension of lamellipodia (Machacek et al., 2009). Other essential actors in this migration type are integrins in part due to their activation of Rac proteins (Lawson and Burridge, 2014). Of note, cells can use other means to migrate, therefore lamellipodia are not considered essential for cell motility however they will provide cells with faster migration when present. For instance, fibroblasts downregulated for Arp2/3 or Rac will use filopodia to migrate (Li et al., 2011; Wu et al., 2012).

Filopodia are implicated in directed cell migration and can be seen in leader cells. They are thin membrane extensions of parallel actin bundles important for mechanosensing the microenvironment, and predominantly organized by Cdc42 (Pichot et al., 2010; Yang et al., 2006). The latter acts through the activation of the Mammalian Diaphanous-related formin (mDia2) that can nucleate and elongate actin filaments (Peng et al., 2003). Cdc42 also targets the insulin-receptor substrate p53 (IRSp53) that will contribute to filopodia formation by curving the membrane and bundling actin filaments (Cory and Cullen, 2007; Lim et al., 2008). Wiskott-Aldrich syndrome protein (WASP) was initially considered one of the main effectors of Cdc42-induced filopodia, but cells lacking both WASP isoforms were able to form filopodia (Snapper et al., 2001).

Blebs, unlike lamellipodia, requires a loss of actin filament interaction with the membrane and therefore they are mostly used in low adhesion situations (Charras and Paluch, 2008). They are formed when plasma membrane detaches from the cortical actin network and cytoplasm flow will push it outwards (Bovellan et al., 2010). The hydrostatic pressure created is supported by Myosin II-induced actomyosin contraction (Tinevez et al., 2009) led in majority by Rho and its target ROCK which phosphorylates the myosin light chain MLC. It is suggested that this is followed by the E-cadherin dependant recruitment of Rac1 to stimulate actin polymerization at the front stabilizing membrane blebbings (Yap and Kovacs, 2003).

Invadopodia are rich actin protrusions important for degrading the extracellular matrix (ECM) specially to allow cells to breach the basal membrane during invasion (Buccione et al., 2009). Cdc42 is the essential Rho GTPases contributing to invadopodia formation through WASP/N-WASP and Arp2/3 complexes. It coordinates the assembly of actin filaments with matrix degradation. Besides Cdc42, tyrosine kinases of Src family appear important for actin bundling with several Src substrates located in invadopodia such as cortactin and WASP/N-WASP (Dovas and Cox, 2010). Reactive oxygen species (ROS) generated by NADPH oxidases (Nox) and Nox organizers, the tyrosine kinase substrate proteins (as Tks5) were shown to be important for invadopodia formation as well as its function by targeting and keeping MMP14 in invadopodia (Diaz et al., 2009; Weaver, 2009). Besides having common actin regulators with other membrane protrusions, the main difference of invadopodia is their capacity to modify and degrade the ECM of tumors by ensuring the trafficking of vesicles containing proteolytic enzymes mainly MMP14 (Poincloux et al., 2009). Microtubules may be important for vesicles delivery and participate with intermediate filaments to the elongation of invadopods (**Figure 20**) (Schoumacher et al., 2010).

3. 2. Polarity and adhesion

In collective migration, leader cells establish a bipolar state where the leading-edge is in contact with the ECM and the rear is connected to neighboring cells by cell-cell adhesion. This new polarity is not a static new state of migrating cells but instead a dynamic cyclic process during which a continuous remodeling of adhesion complexes or the actin network stabilizing them occur.

Some studies argue for a role of Rho-GTPases in the establishment and maintenance of intercellular junctions, in particular by promoting the polymerization of actin at the level of adhesion complexes (Evers et al., 2000; Malliri and Collard, 2003). For example, inhibition of Rac1 or RhoA contributes to the loss of cell polarity and intercellular junctions, and thus to the acquisition of a motile phenotype. Concerning Cdc42, it was first found to be crucial for establishing and maintaining cell polarity in yeast and drosophila models (Drubin, 1991; Etienne-Manneville, 2004; Murphy and Montell, 1996). Later, in mammalian cells, overexpression of Cdc42 and its effector Pak4 was shown to regulate apical junction formation in human bronchial epithelial cells. Similarly in MCF7 cells, a weakly tumorigenic mammary cell line identifying Cdc42/Pak4 importance in establishing epithelial polarity during directed cell migration (Melendez et al., 2011; Selamat et al., 2015; Wallace et al., 2010).

On the contrary, other studies show that the activation of Rho-GTPases contributes directly or indirectly to the loss of adhesion complexes (Lozano et al., 2003; Sahai and Marshall, 2002). Indeed, it has been

shown that an aberrant activation of Rac1 and RhoA resulted in decreased adherence intercellular, thus contributing to tumor progression (Akhtar and Hotchin, 2001; Sahai and Marshall, 2002). In collagen matrix, constitutive activation of Cdc42 or Rac1 has been demonstrated to induce an increased integrin-mediated migration and invasion and suggested to help the disruption of the polarization of T47D mammary epithelial cells in 3D culture (Keely et al., 1997).

Similarly, activated Cdc42 and Rac1 by p120 catenin drive cell migration and invasion of the aggressive metastatic Her2/ErbB2 breast cancer; this was shown *in vitro* as well as *in vivo* in a xenograft mouse model of ErbB2-dependent breast cancer cell line (Johnson et al., 2010). In addition, Cdc42 plays a crucial role in targeting Pak6 to cell-cell adhesions. Pak6 isoform (serine/threonine kinases in the p21-activated) has recently been found to regulate epithelial cell adhesion and to induce Cdc42-mediated epithelial colony escape. Pak6 is often found overexpressed in prostate cancer (Morse et al., 2016).

However, these antagonistic roles may be explained by taking into consideration the fact that Rho-GTPases may have different functions depending on the cell types and stage of the tumor development as well as the effectors implicated.

3. 3. Contractility

Cell body actomyosin contraction was first described regulated by the Rho/ROCK pathway. Activated ROCK can phosphorylate the myosin-light chain (MLC) and/or can desactivate the phosphatase function of myosin binding subunit (Mbs) responsible for the dephosphorylation of MLC which will overall induce cell contraction (Riento and Ridley, 2003). Contractility is important for several physiological functions, and is required to drive focal adhesion and stress fiber formation (Olson, 2004). It was also shown to regulate breast epithelial differentiation in 3D collagen culture (Wozniak et al., 2003). In addition, upregulating Cdc42 activity disrupted mammary gland branching leading to an increase in cell contractility and migration in association with stromal alterations (Bray et al., 2013).

During migration, contractility and tail retraction are essential for cells motility. In 2005, Wilkinson et al have discovered that elongated cell migration is mediated by Cdc42 through the activation of MRCK that in turn phosphorylates MLC, stimulating contraction and subsequently invasion (Wilkinson et al., 2005). Similarly, in fibroblast-led invasion models, follower carcinoma cells require the activation of Cdc42/MRCK in order to migrate (Gaggioli et al., 2007)

3. 4. Collective migration and Spatio-temporal regulation

Collective migration is a complex cyclic process that may require the activation of different Rho GTPases in the same cell at different locations. A fine regulation of these Rho GTPases allows leader cells to invade and degrade the ECM at the leading edge while keeping a connected rear with following cells and pulling them forward (Zegers and Friedl, 2014).

In 2004, a new technique of biosensors allowed the visualization of Cdc42 activity in living cells and the monitoring of its spatiotemporal activity (Nalbant, 2004). This study showed that activity and localization of Cdc42 fluctuated according to the retraction/extension cycles found during migration. A more recent paper monitored the activity and subcellular location of Rho, Rac and Cdc42 with a second generation biosensors and suggested that the different Rho GTPases regulate different cytoskeleton rearrangements in highly plastic edge dynamics (Martin et al., 2016).

The integration of all these modifications (from cell adhesion and polarity to cytoskeleton organization, protrusion formation and contractility) besides the fast dynamics of these events highlight the complex and important roles of Rho GTPases during collective migration and invasion. Further studies *in vitro* and *in vivo* will allow us to better understand the activation cascade of Rho GTPases, the dynamics of their regulators (the GEFs and GAPs), as well as what induces the upstream signaling pathways observed in human tumors.

III. B. Arfs , EFA6 and Cancer

1. Arfs family

1. 1. Generalities

ADP-ribosylation factors (ARFs) are a family of small guanine nucleotide binding proteins, first discovered as co-factors of cholera toxin (Moss and Vaughan, 1995). The mammalian Arf family consists of six related genes divided into three subgroups according to primary sequence homology: class I includes Arf1, Arf2 (not expressed in human) and Arf3, class II Arf4 and Arf5, and class III Arf6 (Tsuchiya et al., 1991). The membrane localization of Arf proteins is ensured by the myristoylated amphipathic N-terminal helix exposed upon GDP to GTP exchange, called N-terminal helix GDP/GTP switch (Antonny et al., 1997; Franco et al., 1993, 1995, 1996).

I am going to highlight the roles of Arf1 and Arf6, the two most studied members, in physiological contexts and in more details in cancer (Donaldson and Jackson, 2011).

1. 2. Roles

Arf1

Arf1 was originally found in the Golgi apparatus where it regulates the formation of protein-coated vesicles important for exocytosis and intracellular vesicular trafficking pathways, comprising the retrograde Golgi-to-endoplasmic reticulum transport and intra-Golgi anterograde transport. Additionally, it has been shown that activated Arf1 may be located at the plasma membrane where it regulates endocytosis by controlling Cdc42 activity through the recruitment of a RhoGAP, ARHGAP10 protein (Kumari and Mayor, 2008). Studies have also shown that Arf1 is able to trigger actin assembly polymerization through the Arp2/3 complex. This mechanism is dependent on the Cdc42 GTPase and its N-WASP effector. Here as well, Arf1 regulated this mechanism through its interaction with the ARHGAP10 (Dubois et al., 2005; Heuvingh et al., 2007; Stamnes, 2002). Of note, ARHGAP10 described here as an effector of the activated form of Arf1 and Arf6 can act as the GAP of Cdc42 and therefore represent a possible link between the activation of Arf6 and the inhibition of Cdc42 activity (Dubois et al., 2005).

Ar6

Arf6 is the least conserved member of Arfs and shares 66% of sequence identity with Arf1. It is ubiquitously expressed and found mostly at the plasma membrane or endosomal compartment. It plays pivotal roles in a wide panel of cellular events including cell surface trafficking, phagocytosis, and cell–

cell adhesion. For example, Arf6 is implicated in the internalization of G-proteins coupled receptors (GPCRs) in both clathrin dependent and independent endocytosis (Houndolo et al., 2005; Hunzicker-Dunn et al., 2002; Montagnac et al., 2011; Naslavsky et al., 2004) and plays important roles in the internalization of some of these GPCRs and the EGF receptor either for recycling or proteolysis (Macia et al., 2012; Montagnac et al., 2011). Additionally, Arf6 participates to the remodeling of actin cytoskeleton, mainly mediated by the activation of Rac1 and lipids-modifying enzymes (as PIP5K type I and phospholipase D) (Béglé et al., 2009; Caumont et al., 1998; Jovanovic et al., 2005), and mostly seen by monitoring membrane extension formation (Franco et al., 1999; Klein et al., 2006).

In epithelial cells, Arf6 uses its different functions (membrane trafficking, cell-cell adhesion, and actin remodeling) to regulate cell polarity. It was initially shown to regulate vesicular trafficking to the apical domain of the cell, and later to mediate the turnover of AJ, the assembly of TJ as well as cyst morphogenesis, and HGF-induced tubulogenesis (Luton et al., 2003; Palacios et al., 2001; Sabe, 2003; Tushir and D'Souza-Schorey, 2007; Tushir et al., 2010).

In vivo, a ubiquitous knock out of Arf6 was carried out in mice to further study its roles but exhibited a lethal phenotype due to liver development abnormalities caused by abnormal cell migration and increased apoptosis (Suzuki et al., 2006).

We should note that these individual functions described above ranging from endocytosis and recycling to actin remodeling and lipid modifications will have, when altered, major effects on a wide range of cellular activities (as cell motility and invasion, cell division, cholesterol homeostasis, etc.). C. D'Souza-Schorey group has an interesting review on Arf6-mediated functions (Schweitzer et al., 2011a).

Of note, a molecular cascade was suggested linking Arf6 activation to Arf1. Once activated by EFA6, Arf6 can stimulate the activity of ARNO which in turn will allow GTP binding to Arf1 (Cohen et al., 2007; Stalder et al., 2011). This notion emphasizes the complexity of Arfs' acitivities, and the importance of keeping in mind the possible crosstalk between different isoforms of Arfs (DiNitto et al., 2007).

1. 3. Arfs in Cancer

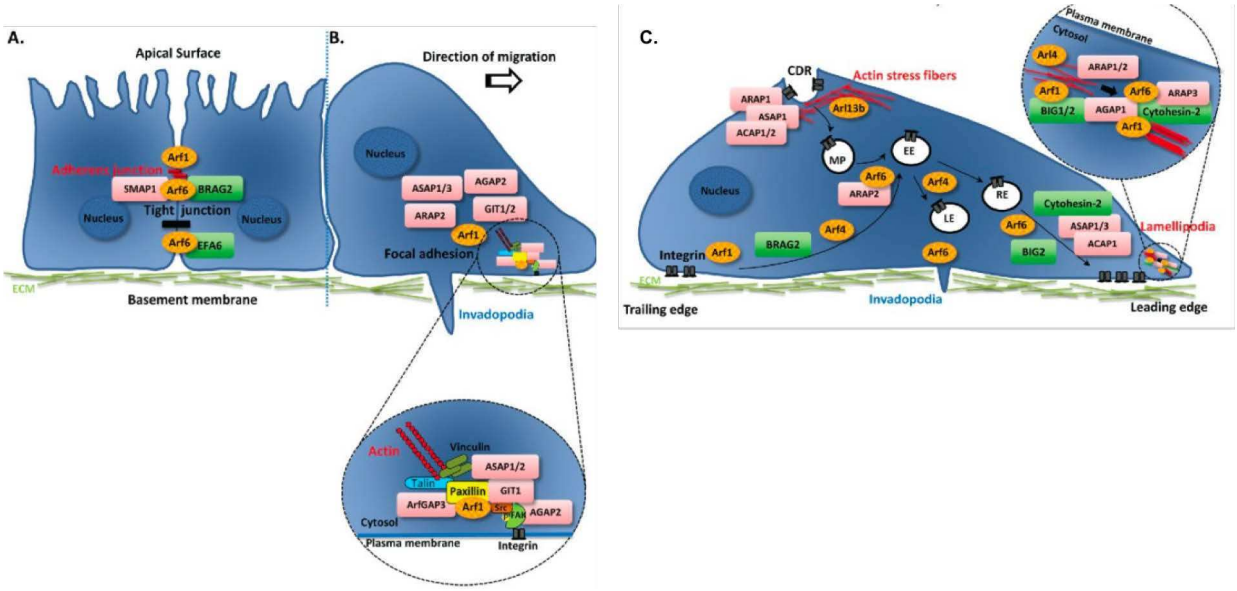

Figure 21: Role of Arf proteins and their regulators in cancer cell migration.

A. Arfs proteins are implicated in the maintenance of adhesion complexes, and the turnover of E-cadherin with different Arf GEFs/GAPs. B. After adhesion complexes disassembly (first step of the EMT process), Arf proteins and their regulators will participate to the formation of new focal adhesions required for cell migration. C. In invasive cells, Arf proteins will be implicated in the recycling of integrins from the trailing edge and they will participate to the formation of different protrusive structures by remodeling the actin cytoskeleton and regulating vesicular trafficking. It is important to note that each step requiring Arf protein's activity is directly bound to the presence of specific Arf regulators. CDR, circular dorsal ruffle; EE, early endosome; LE, late endosome; MP, macropinosome; RE, recycling endosome. .Adapted from (Casalou et al., 2016).

Arf proteins are implicated in key physiological functions of cell homeostasis and therefore it is not surprising to find them dysregulated in cancer.

As we have previously seen, in cancer, EMT will give many advantages to tumor cells, ranging from motility to invasiveness. One of the earliest and main step of this process is the disassembly of adhesion proteins followed by an important remodeling of the cortical actin cytoskeleton. Epithelial cancer cells are strongly affected by any modification of these two components that are direct and indirect targets of Arf proteins (Casalou et al., 2016; Schweitzer et al., 2011b).

1.3.1 Arf1

Arf1 has been shown to act at different levels of tumor progression. In a series of studies of A. Claing group, Arf1 activity was correlated to cell proliferation. In fact, lowering the active levels of Arf1

reduced the proliferation of MDA-MB-231 cells through mechanisms involving the retinoblastoma protein (pRB) hyperphosphorylation limiting gene transcription (Boulay et al., 2011). They have also shown that Arf1 may act upstream Rac1 to control migration (Lewis-Saravalli et al., 2013). In the same line of thoughts, Arf1 was found in complex with ß1-integrin, paxillin, talin and FAK. Its knockdown impaired focal adhesion formation, highlighting its role in migration (Schlienger et al., 2015). Furthermore, Arf1 knockdown impaired invadopodia formation and decreased cell invasion. The suggested mechanism by which Arf1 mediated MDA-MB-231 invasion is through the activation of Rho activity affecting in turn the myosin light-chain (MLC) phosphorylation (Schlienger et al., 2013). The latter constitute the main regulator of contractility often used by cancer cells to pull on the extracellular matrix, reorganize the collagen fibers, and facilitate the migration process (**Figure 21**).

1.3.2 Arf6

Arf6 and polarity

Arf6 has been shown to exhibit important roles in cell-cell adhesion and cell polarity. In breast cancer, it has been described as an important regulator of the assembly and disassembly of adherens junctions by controlling the internalization of E-cadherin in mammary cancer cells (MCF7 and T47D) treated with EGF (Xu et al., 2015). Indeed, E-cadherin is constitutively recycled between the basolateral membrane and the endosomes, and the activation of Arf6 induces a stimulation of its clathrin-dependent endocytosis. Studies conducted on MDCK cells (Madin-Darby Canine Kidney), this time treated with HGF, have shown that Arf6-GTP is able to recruit, at the cellular junctions, the enzyme Nm23-H1 capable of catalyzing endocytosis and to negatively regulate Rac1 protein activity, thus facilitating the disassembly of adherens junctions (**Figure 21**) (Palacios et al., 2001, 2002, 2005).

Arf6 and migration

Endocytosis can play an important role in the migration process as well. In fact, motile cells need to redistribute their integrins at the migrating front. Stimulated by HGF, Arf6 was shown essential for the recycling of integrin β1 in migrating Hela cells (Hongu et al., 2015; Powelka et al., 2003). Similarly, in MDA-MB-231, silencing Arf6 altered the migration of this breast cancer cell line upon stimulation (Hashimoto et al., 2005; Marchesin et al., 2015b).

Arf6 and invasion

The group of H. Sabe in Japan delivered most of the research work presented below describing the involvement of Arf6 in regulating cancer cell invasion using as a model the MDA-MB2311 mammary cell line.

In 2004, they showed for the first time an evidence of the role of Arf6 in breast cancer invasion. In the aggressive mammary tumor cell line MDA-MB231, they demonstrated that Arf6 is localized at invadopodia concordant with the sites of matrix degradation. The knockdown of Arf6 reduced matrix degradation, invadopodia formation and migration through a matrigel barrier. Interestingly, both the expression of dominant-negative (Arf6(T27N)) and the constitutively active (Arf6(Q67L)) blocked invasion. Authors emphasized the importance of Arf6 cycling between active and inactive states, thus regulatory Arfs' GEFs and GAPs can also be possible targets for cancer invasion (Hashimoto et al., 2004). Shortly after, Arf GAPs and GEFs have been investigated. For instance, GEP100 GEF and AMAP GAPs have been implicated in controlling Arf6 mediated invasive activities of breast cancer cells upon EGF stimulation (Hashimoto et al., 2005; Morishige et al., 2008; Onodera et al., 2005). AMAP1 was found overexpressed in invasive breast cancer cells. However, several lines of evidence have demonstrated that AMAP1 binds Arf6 by a non-catalytic domain and acts as an effector of Arf6 rather than as a GAP enzyme. Upon binding to Arf6-GTP, AMAP1 is recruited at the plasma membrane and will bind paxillin and cortactin and modify the actin cytoskeleton, mainly in invadopodia where it was located in MDA-MB231 (Hashimoto et al., 2005; Klein et al., 2006; Morishige et al., 2008; Onodera et al., 2005).

It must be noted that Arf GAPs are the largest group of Arf binding proteins (Randazzo and Hirsch, 2004; Sabe et al., 2006). Having multiple domains, Arf GAPs exhibit enzymatic GAP function but also can bind Arfs as effectors and therefore should be further considered when investigating the pathways by which Arfs mediate their activities.

Moreover, recently a complementary study to the one localizing Arf6 at invadopodia showed that Arf6 together with c-Jun NH_2-terminal kinase–interacting protein 3 and 4 (JIP3 and JIP4) effectors may be controlling the quantity and activity of MT1MMP concentrated in these structures and crucial for degrading the matrix. Arf6 was revealed important for enzymatic recovery of MT1MMP by trafficking it from late endosomes to invadopodia (Marchesin et al., 2015a).

In the same line of studies, in triple negative breast cancer cell models, downregulation of an anti-tumorigenic micro-RNAs resulted in Arf6 upregulation and an increase of invasion. In clinical samples, they found that lymph node metastasis showed higher levels of Arf6 when compared to primary tumors, suggesting an important role for Arf6 in acquiring invasive capacities (Eades et al., 2015).

The pro-tumorigenic role of Arf6 was confirmed in other types of cancer. For instance, *in vitro* and in mouse models, Arf6 was shown to mediate Wnt-induced melanoma invasion and metastasis. Here Arf6 stabilized adherens junctions and thus blocked β-catenin signaling driving cells to malignancy (Grossmann et al., 2013).

Together, these results suggest that Arf6 play an important role in the metastatic process and may be an interesting therapeutic target.

However, we should note that most of the studies aforementioned used mostly one mammary cancer cell line, the MDA-MB-231. Using such highly transformed and aggressive cancer cell line does not allow us to investigate the role of Arf6 in the early stages of the disease where some proteins can have antagonistic roles (such as TGFβ). Besides this, the correlation with human breast cancer done by the group of Hisataka Sabe in Japan who investigated the role of Arf6 in cancer was done on a small number of patients and did not show any clear correlations between Arf6 and breast cancer aggressiveness. Another interesting remark is that studies showing a pro-tumorigenic or pro-invasive capacity of activated Arf6 in breast cancer had to stimulate their cells with EGF or HGF in order to see these effects. It is important to keep in mind that a deregulation of the Arf6 mediated receptor cycling will abrogate the vesicle trafficking and endocytosis mechanisms in which it is implicated. This will have serious effect on the desensitization of pro-oncogenic activated receptors like EGFR which will obviously give tumorigenic advantages to cells.
Interestingly, a recent study shows opposing results to the pro-tumorigenic proclaimed role of Arf6. Indeed, the depletion of NEDD9, a maker of invasive and metastatic cancers, increased the Arf6-dependent MMP14 targeting to late endosomes and thus decreased it at the cell membrane. The downregulation of Arf6 is capable of restoring the MMP14 amount present at the plasma membrane. *In vivo*, blocking NEDD9 has shown less tumor growth and metastasis in xenograft models of breast cancer (Loskutov et al., 2015).
These results suggest that Arf6 may have different roles depending on the cellular context (adhesion status of cells), Arf6 regulators and the stage of cancer studied.

***

2. ARF GEFs: After all it is regulation that matters

One of the fundamental highlights of Arfs activity in most scenarios remains the necessity of cycling between both active and inactive state in order to be functional. Arfs activities are tightly governed by their activators, GEFs, facilitating the binding of GTP and negative regulators, GAPs, enhancing GTP hydrolysis. GEFs and GAPs will also play an important role in spatiotemporal regulation of Arfs and thus the amplitude of Arfs-induced cellular behavior. Besides their role in regulating Arfs, some GEFs and GAPs can directly bind proteins and affect some cellular functions; for instance, Arf GAPs are considered a major group of potential Arfs' effectors. Hence, Arf GEFs and GAPs may seem as attractive therapeutics targets.

The core of my PhD thesis consists of studying the role of EFA6B, a member of EFA6 GEFs family, in cancer progression, and therefore I will present in the following section an overview of Arf GEFs family, with a focus on EFA6 GEFs:

2. 1. The Arfs Exchange Factors

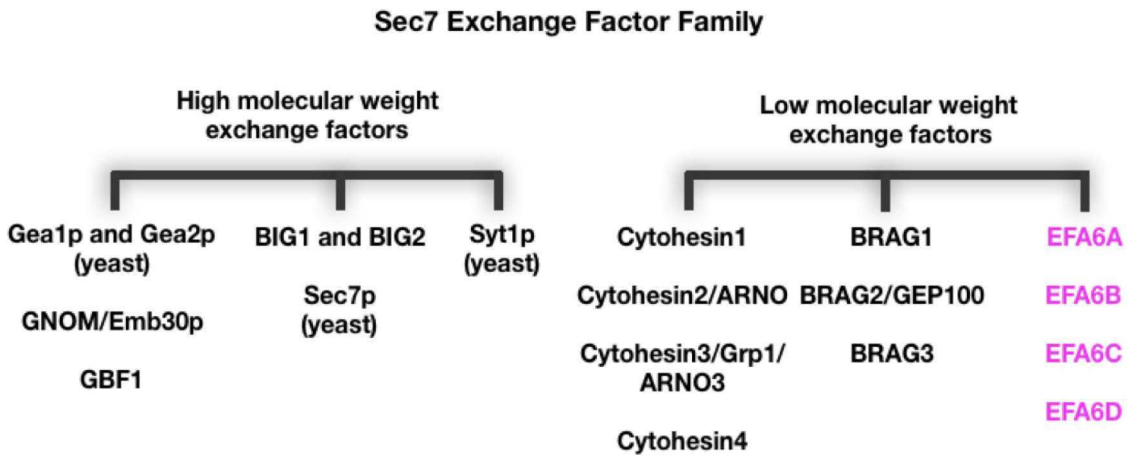

Figure 22: Members of the Sec7 exchange factor families.

The large number of Arf GEFs compared to the number of Arf suggests that Arf functions are under important regulation. Adapted from Casanova, 2007; Jackson and Casanova, 2000.

In human, 15 genes encode members of the family of exchange factors specific to small G Arf proteins, also known as the Sec 7 Domain family, subdivided into two groups according to their sequence homology and molecular weight (**Figure 22**).

The first group is composed of exchange factors of high molecular weight. This sub-family includes Gea1p and Gea2p yeast proteins, GNOM/Emb30p and GBF1, BIG1 and BIG2 proteins, and Syt1p. The majority of these proteins are located in the Golgi apparatus. The second group consists of proteins with

low molecular weight composed of three subfamilies : 1) ARNO and Cytohesins 2) BRAGs and 3) EFA6 proteins, all having a PH domain allowing them to bind to the plasma membranes via phosphoinositides (Casanova, 2007; Jackson and Casanova, 2000).

2. 2. EFA6: genes, distribution and structure

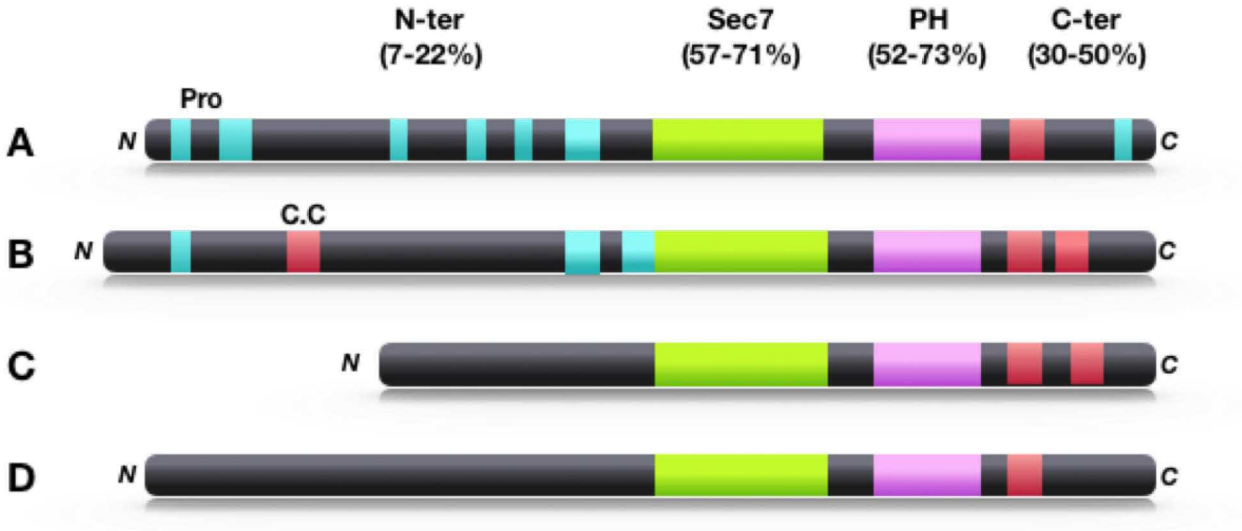

Figure 23: Structures of EFA6 isoforms.

The four isoforms of EFA6 are composed of a variable N-terminal domain, a Sec7 catalytic domain, a PH domain responsible for plasma membrane localization and a C-terminal domain involved in the interaction with different partners.

In 1999, the first member of EFA6 (exchange factor for Arf6) family was cloned by M. Franco and identified as a specific exchange factor for Arf6 (Franco et al., 1999). Since, four isoforms were identified EFA6A, EFA6B, EFA6C and EFA6D encoded by different genes (*PSD*, *PSD4*, *PSD2* and *PSD3,* respectively). Additional isoforms resulting from alternative splicing have been described for EFA6A, EFA6B, and EFA6C (Derrien et al., 2002; Luton et al., 2003; Sakagami, 2008; Sironi et al., 2009).

As determined by *in situ* hybridization, they have various patterns of tissue distribution. EFA6A, EFA6C and EFA6D are widely expressed in neuronal cells showing distinct expression sites with some overlaps in brain regions (Sakagami, 2008). EFA6A was also found in small intestine and colon whereas EFA6D is ubiquitously expressed (Franco et al., 1999; Sakagami et al., 2006). EFA6B was found abundantly expressed in epithelial tissues with high levels in lungs, spleen and thymus (Derrien et al., 2002).

The general structure of EFA6 family comprises a variable N-terminal domain, a Sec7 catalytic domain shown to be sufficient for GDP/GTP nucleotide exchange of Arf proteins (Chardin et al., 1996), a PH domain allowing membrane localization (Macia et al., 2008) and a C-terminal region composed of a

coiled-coil and two proline rich domains mediating the interaction with several partners (such as actin, α-actinin, etc.) (**Figure 23**) (Franco et al., 1999; Milanini et al., 2018).

This GEFs' structure highlights the dual means by which EFA6 proteins can intervene in cellular functions. It suggests that EFA6 could function by coordinating the activation of Arf6 together with the recruitment of effectors through its C-terminal domain.

2. 3. EFA6 Roles:

Since its discovery, 44 articles were published on EFA6 family describing their roles, in majority *in vitro* with the two most studied isoforms being EFA6A and EFA6B.

Consistent with the roles of Arf6, EFA6A was involved in the internalization and recycling mechanisms of different membrane proteins. Thus, the overexpression of EFA6 or an Arf6 mutant blocked in the GTP form leads to a drastic decrease in transferrin internalization (Franco et al., 1999). It was also implicated in the recycling of the β2 adrenergic receptor (Macia et al., 2012). In vesicle trafficking, EFA6A recruits endophilin was also shown to control the activation of Arf6 and clathrin-mediated endocytosis (Boulakirba et al., 2014a).

Besides their activities on remodeling the actin cytoskeleton, some direct roles of EFA6 on microtubule cytoskeleton remodeling were described in *Caenorhabidits elegans*. Independently of Arf6, EFA6 inhibited microtubule growth at the cell cortex of yeast affecting functions like mitosis (O'Rourke et al., 2010). Similarly, EFA6 in *C.elegans* altered axon regeneration by regulating the microtubules dynamics (Tang and Chisholm, 2016).

Being more relevant to my PhD work, the physiological functions of EFA6 proteins like remodeling the actin cytoskeleton and establishment of epithelial cell polarity as well as some recent roles in cancer will be presented in detail below:

2. 3. 1. EFA6 in actin cytoskeleton remodeling

EFA6, like Arf6, is involved in the reorganization and assembly of the actin cytoskeleton (Derrien et al., 2002; Franco et al., 1999). Indeed, Hela cells overexpressing the wild-type form of EFA6A accumulate filamentous actin that co-localize with EFA6A at the level of membrane ruffles. By using different mutants, the C-terminal domain of EFA6A was identified responsible for this remodeling. The overexpression in cells of EFA6A^{E242K} or EFA6A$^{\Delta sec7}$ mutants, which do not possess a catalytic activity,

leads to the formation of actin-rich membrane extensions. Concomitantly, cells overexpressing the mutant that do not have the C-terminal domain had no effect in particular. At least a part of the effect of EFA6A on actin has been suggested to be mediated by the activation of Rac1 (Franco et al., 1999). The localization of EFA6 by the PH domain was shown to be crucial for the C-terminus induced cytoskeleton remodeling. It has been demonstrated that cells overexpressing the C-terminal domain alone which is cytosolic, or the PH domain alone located at the folds of the plasma membrane have a similar morphology to that of control cells. On the other hand, when the C-terminal domain is coupled to the PH domain, it localizes to the plasma membrane and induces changes in the actin cytoskeleton. This means that actin remodeling is mainly mediated by the C-terminal domain of EFA6 only when recruited by the PH domain at the plasma membrane. Another evidence to this role is the capacity of EFA6A to interact directly with actin and α-actinin*** (Macia et al., 2008; Sakagami et al., 2007).

α-actinin is a cross-linking protein capable of binding and maintaining two actin microfilaments parallel to each other in order to form, in collaboration with myosin II, contractile actin filaments. It participates among other to the formation of stress fibers and in the regulation of actomyosin cytoskeleton supporting the TJs.

It is interesting to note that actin cytoskeleton rearrangement can also be seen in the regulation of membrane extensions formation. EFA6A has been shown critical for the development of neuronal protrusions. For instance, in cultured hippocampal neurons, a GEF-defective mutant of EFA6A increased significantly the formation and stability of dendritic spines which are small actin rich extensions important for synapse neuronal signaling (Choi et al., 2006; Sakagami et al., 2004). Interestingly, even though EFA6A is important for neuronal protrusions, a constitutively active Arf6 decreased spine density while its dominant negative increased it. This information proves once again that the regulation of Arf6 by EFA6, which can modulate Arf6 function through its C-terminal domain, is critical to normal cellular functions.

Conclusion

EFA6 coordinates Arf6 activation and recruits effectors to the C-terminal domain that can modulate Arf6 functions.

2. 3. 2. EFA6 in epithelial cell polarity

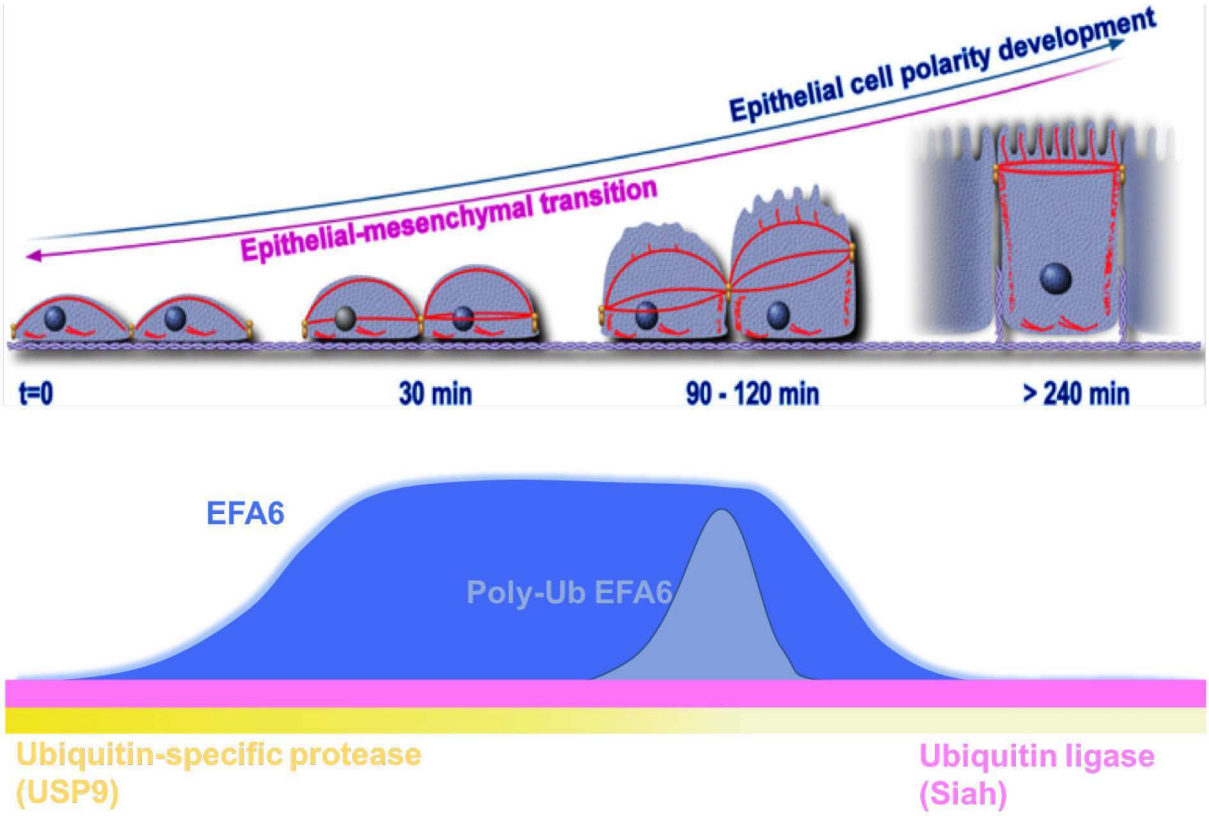

Figure 24: Model for EFA6B regulation by ubiquitinylation/de-ubiquitinylation during epithelial cell polarization.

In non-polarized epithelial cells, EFA6 is submitted to a constitutive ubiquitinylation by the E3 ligase Siah followed by its degradation through the proteasome. As soon as cells engage in the cell polarization program EFA6 is protected from degradation by the de-ubiquitinylase USP9, this leads to a rapid accumulation of EFA6, which will contribute to the reorganization of the actin cytoskeleton and the formation of the TJ. Once the latter is formed, EFA6 is no longer protected from the proteasome and its protein expression level drops down due to the activity of Siah. Since USP9 leaves very rapidly from the contact zone where EFA6 remains concentrated, EFA6 is probably protected from Siah or its degradation by the proteasome, by a USP9- independent mechanism (Théard et al., 2010).

Polarized epithelial cells are defined by two distinct domains at the plasma membrane level: an apical domain facing the lumen and a basolateral domain facing the basal membrane. These two membrane domains are separated by tight junctions (TJs). Our research group has shown the importance of EFA6 in TJs assembly and elucidated by which molecular mechanisms the actin cytoskeleton modulates TJs functions (**Figure 24**) (Klein et al., 2008a; Luton, 2005; Luton et al., 2003). In Madin-Darby canine kidney (MDCK) cells, after E-cadherin engagement, EFA6 is recruited at the cell-cell junctions where it controls the assembly of tight junctions and contribute to the development of epithelial polarity. EFA6 maintains TJs by stabilizing the apical actin ring that supports them and promoting the retention of TJs proteins (Luton et al., 2003). The use of catalytically inactive mutants or mutants without the C-terminal domain demonstrated that Arf6 activation by EFA6 Sec7 domain and regulating this activity by its C-

terminal domain of EFA6 were necessary (Klein et al., 2008a). Here again we show that the cooperation between Arf6 activation and the C-terminal domain activity are important for EFA6-mediated effects.

The levels of EFA6 are critical for TJs biogenesis and are controlled by the deubiquitinating enzyme USP9x. In polarized cells, a low level of EFA6 is maintained by constitutive ubiquitination and turned over by the proteasome. However, while establishing new contacts, epithelial cells require higher levels of EFA6 guaranteed by the USP9x-mediated deubiquitination that protects EFA6 from proteosomal degradation at the nascent cell-cell contact where TJs are assembled (**Figure 24**) (Théard et al., 2010).

Conclusion

EFA6 and its substrate Arf6 favor the development of cell polarity and stabilize the apical actin ring and adhesion complexes. The purpose of the second article presented in this thesis will be to elucidate the role and mechanism of action of EFA6 in lumen formation, a crucial step for having functional normal endocrine glands as the mammary gland.

2. 3. 3. EFA6 in cancer

Even though EFA6 family was shown to be implicated in important physiological roles, it was rarely investigated in pathological contexts. On the basis of transcriptomic data, some papers have suggested correlations between the level of expression of EFA6 and some cancer types in patients. For instance, the mRNA levels of *PSD3* (EFA6D) have been found increased in colon and hepatocellular carcinoma tissues and downregulated in esophageal, breast and ovarian cancer (Hu et al., 2005; Pils et al., 2005; Thomassen et al., 2009; Wang et al., 2002). For ovarian cancer, the downregulation of *PSD3* on the transcriptomic level observed in patient tissues has been linked to poor prognosis and classified among genes worthy of further investigation (Pils et al., 2005; Thomassen et al., 2009). Likewise, a meta-analysis combining eight datasets of 1200 breast tumors has shown that EFA6D mRNA level is reduced in metastasizing breast cancer and therefore suggested as potential metastasis suppressor genes (Thomassen et al., 2009)

However, these studies remain simply correlations that were not further explored or validated at the protein level in cellular or animal models. In 2006, the first study looking into the role of EFA6 on a molecular level in cancer was published. They have suggested that EFA6A overexpression in a human glioblastoma cell line promoted migration and invasion via the activation of an Arf6/ERK signaling cascade (Li et al., 2006).

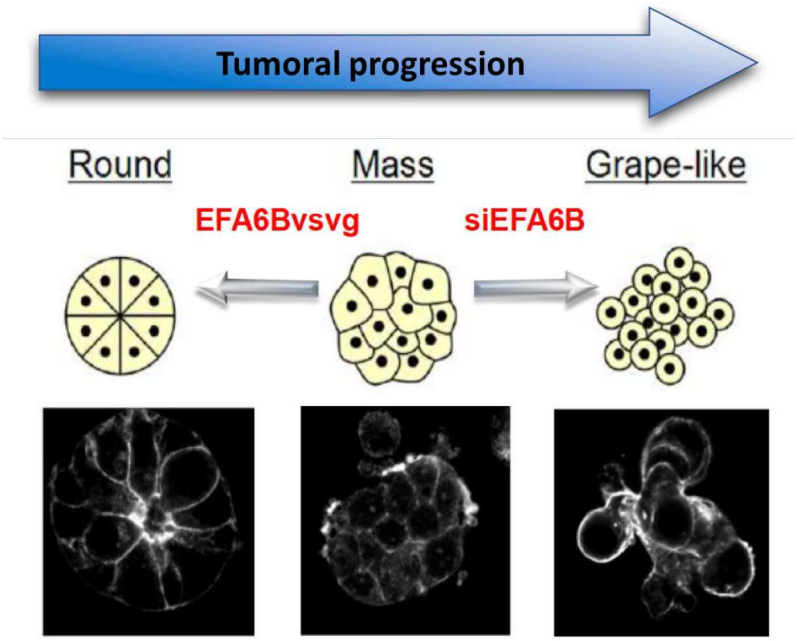

Figure 25: EFA6B regulates the apico-basal polarity of mammary tumorigenic cells.

Exogenous expression of EFA6B promoted the reversion to an epithelial phenotype while its repression leads to unorganized aggregates. Immunofluorescence of MCF7 acini grown in Matrigel™ for 5 to 7 days .Adapted from Zangari et al., 2014.

This study was followed in 2014 by a work led by my research group on the role of EFA6B in breast cancer progression (Zangari et al., 2014). Beforehand, a thorough description of the role of EFA6B in establishing epithelial cell polarity and tight junctions assembly was conducted (Klein et al., 2008a; Luton, 2005; Luton et al., 2003; Théard et al., 2010). Taking in consideration the importance of these characteristics for normal epithelial cells, my research group proceeded to test their hypothesis on a possible role of EFA6B in cancer cells. Using MCF7, a weakly tumorigenic mammary cell line, our previous data showed that EFA6B exogenous expression restored a normal polarized epithelial monolayer of cells grown in 2D on filters, with functional tight junctions. In 3D culture, EFA6B was able to revert the intermediate epithelial-mesenchymal morphology of luminal breast cancer cells MCF7 into a well differentiated apico-basal epithelial phenotype (**Figure 25**). It resulted in cells organizing collectively into normal mammary acini-like structures, with the formation of lumens, and this is by contributing to the fusion of vacuolar apical compartments (VAC) in polarized acini. In addition, *in vivo*, the endogenous downregulation of EFA6B/PSD4 at the transcriptomic and proteomic level was found to be correlated in human breast cancer to poor prognosis associated to the aggressive claudin-low or triple negative subtype (Zangari et al., 2014).

This study clearly showed that the tight junction regulator EFA6B is capable of enhancing the epithelial status of cancer cells and therefore its expression might hamper cancer progression. Of note, the lab

showed that EFA6B mediates these effects in part by the activation of Arf6 (Zangari et al., 2014), suggesting that EFA6B and Arf6 reduced activity/expression are considered pro-tumorigenic.

This conclusion challenges the previous assumptions about the role of Arf6 in cancer. As previously presented in the section of "1. 3. Arfs in Cancer", Arf6 activation or up-regulation has been related to cancer progression. However, it is important to keep a critical eye on the cellular models used and the stimulation required to see some of Arf6 pro-tumorigenic effects. It is not surprising after all to see that such multifunctional proteins like Arf6 and its regulators EFA6 proteins may present opposing roles in different pathological contexts and different stages of tumorigenesis.

In support to our data, a recently published article provided evidence that the loss of NUMB expression, an activator of EFA6B exchange activity, promotes cell migration and invasion. More specifically, NUMB loss allows the formation of membrane protrusions and the acquisition of mesenchymal migratory phenotype due to a reduction of EFA6B/Arf6 activity (Zobel et al., 2018).

We believe that our protein of interest, EFA6B may act as a negative regulator of tumorigenesis at early stages. My PhD subscribes in the continuity of this work, and proposes further results supporting this hypothesis.

THESIS . ARTICLE 1

Article 1

1. Objectives of Article 1

1. 1. General context

“Epithelial integrity and homeostasis are of central importance to survival” (Macara et al., 2014). Indeed, epithelial cells make up a large percentage of our bodies; they form a barrier protecting the internal organs from external stresses (e.g. skin, airways, etc.) as well as composing our glands (e.g. mammary gland, salivary gland, etc.), indispensable for the development and maintenance of a healthy organism. Epithelial cells are structurally characterized by their arrangement into cohesive sheets regulated mostly by adhesion complexes (as adherens junctions, desmosomes, tight junctions, etc.), the apico-basal polarity and the cytoskeleton rearrangement. These properties are essential for epithelial cells to exhibit diverse functions, mainly secretory ones, determined by specific differentiation and activation in response to their microenvironment stimuli (mechanical tensions, growth factors, hormones, etc.).

Epithelia is subject to active modifications: from developmental stages where they have to undergo proliferation, migration and self-organization processes up to adulthood (e.g. tubes, villi, alveoli, etc.). Any deregulation provoking the loss of epithelial identity can induce a range of dysfunctions and diseases (such as eczema, psoriasis, asthma…) or even lead to the most common human cancers in adults, epithelial carcinomas. For instance, in cancer cases, an extreme deregulation of epithelial homeostasis leads to metastasis, the resultant of cells disseminating from the primary tumor. Metastasis is considered the main cause of cancer patients death and therefore, it is of great interest to understand the initiating factors in charge of cancer cells gaining in invasive properties.

While many oncogenic mutations causing growth, proliferation and resistance to apoptosis have been identified ("driver mutations"), epigenetic changes or genes specifically regulating the emergence of metastatic properties are less easily detectable. We will call the alteration of these genes “secondary driver mutations” considering that alone they cannot transform a normal cell however, they will provide newly-transformed cells with functional and phenotypical advantages crucial for malignancy. Of note, this is different from passenger mutations targeting non-coding region or redundant genes that will not contribute to cancer progression.
During carcinogenesis, these mutations may also influence the fate of the neo-tumor and its orientation towards a particular subtype. Thus, identifying such genes alterations and deciphering the associated

signaling pathways would provide a preventive and/or predictive tool for clinicians and help find new therapeutic targets.

The results of this thesis work fall within this pre-cancerous research: we show that our protein of interest, EFA6B, is a non-transforming factor of which loss of expression in normal breast cells promotes Cdc42-dependent invasive properties. Thus, we believe that EFA6B might play an antagonist role in the progression of cells towards aggressive breast cancers.

1. 2. EFA6 Background

Following its cloning in 1999, EFA6A has been demonstrated as an exchange factor for Arf6 and to be involved in actin cytoskeleton rearrangement (Franco et al., 1999). Similar characterization was shown afterward for the other isoforms of EFA6 family. In the scope of this thesis, I have focused on thde EFA6B isoform that has been previously described as a tight junction regulator in normal epithelial cells (Klein et al., 2008b; Luton, 2005; Luton et al., 2003; Théard et al., 2010). EFA6B is recruited upon E-cadherin engagement to help assemble and stabilize tight junctions by strengthening the apical actin cytoskeleton and excluding TJ proteins from endocytosis to retain them at the cell surface. This discovery triggered the curiosity of my research group to investigate the role of EFA6B in a tumorigenic context knowing that the loss of polarity and adhesion complexes represents a major milestone in cancer metastasis (Zangari et al., 2014). In MCF7 cells incapable of assembling tight junctions, the exogenous expression of EFA6B restored a normal apico-basal polarization with the formation of functional tight junctions of cells grown on filters in 2D culture. Interestingly, in 3D Matrigel matrix, the overexpression of EFA6B reverted the mass aggregate phenotype, typical of weakly tumorigenic mammary cell lines, into normal acini with a central lumen, characteristic of a functional mammary epithelial structure.

These results have revealed the capacity of EFA6B to regulate the mesenchymal/epithelial status of cells. Indeed, EFA6B expression blocked the entry in epithelial to mesenchymal transition (EMT) observed normally in MCF7 cells treated with the transforming growth factor beta (TGF-b). This is the first cue indicating a possible role of EFA6B in EMT which opened up new perspectives and areas of investigation for our research group.

Lastly, using transcriptomic and immunohistochemistry analyses, a lower expression of EFA6B in human breast cancer tumors was correlated to the aggressive claudin-low subtype characterized by an EMT signature and a loss of TJ proteins and to poor prognosis of patients (Zangari et al., 2014).

1. 3. Working Hypothesis

To date, EFA6B has shown remarkable functions in epithelial cells ranging from apico-basal polarity, apical actin cytoskeleton organisation, to interfering with the EMT process, all of which contribute largely to epithelial homeostasis. As suggested by the correlation with BC patients and its different roles, disrupting EFA6B expression can lead to dysfunctions during epithelial morphogenesis but also to stimulate cancer progression in tumor cells.

Therefore, during my thesis, I was interested in investigating furthermore the impact of the loss of expression of EFA6B (as observed in claudin-low patients) on mammary epithelial cells.

Thus, we have generated a CRISPR/Cas9 full knock-out model of EFA6B in normal mammary epithelial cells MCF10, considered mainly as basal cells. We also proceeded by establishing a CRISPR/Cas9 KO of EFA6B in HMLE cell line, a normal mammary gland population containing luminal progenitors, mature luminal cells and basal cells. This will allow us to validate our results in a different mammary epithelial cell line but also to investigate any possible differences in EFA6B impacts related to the origin of the cell (mainly between luminal and basal, two major epithelial cells of the mammary gland).

We have decided to work in normal cell lines in order to have a more or less clear genetic background allowing to unravel the consequences of deleting EFA6B. In addition, knowing that EFA6B and Arf6 might have different roles according to the stage of cancer, it was interesting to see if their loss in the early steps of tumorigenesis gives an advantage to cells.

This thesis work consisted on approaching the impact of EFA6B loss by setting three main objectives:

1. **to describe the impact of EFA6B loss on epithelial properties.**
2. **to determine if the loss of EFA6B can endow cells with pro-tumoral features and eventually drive them towards the claudin-low subtype.**
3. **to reveal and decipher the cellular and molecular mechanisms regulated by EFA6B.**

As mentioned before, the existing knowledge focus on few driver mutations, while it is of great importance to identify pre-cancerous factors or the so-called secondary driver mutations. We demonstrate that EFA6B loss can affect the epithelial homeostasis. **Hence, the ultimate goal of this thesis is to describe the tumor-antagonistic and protective advantages of EFA6B expression.**

Thesis . Article 1 . Results

CRISPR/Cas9-mediated knock-out of *PSD4* (EFA6B) promotes collective invasion of human mammary cells

Fayad Racha[1*], Vazquez-Rojas Monserrat[1*], Partisani Mariagrazia[1], Finetti Pascal[2], Virolle Virginie[3], Cabaud Olivier[2], Lopez Marc[2], Birnbaum Daniel[2], Bertucci François[2], Franco Michel[1], Luton Frédéric[1§]

[1] Université Côte d'Azur, CNRS, Institut de Pharmacologie Moléculaire et Cellulaire (IPMC), Valbonne, France

[2] Centre de Recherche en Cancérologie de Marseille, INSERM UMR1068, Institut Paoli-Calmettes, CNRS UMR7258, Aix-Marseille Université, Marseille, F-13009, France

[3] Université Côte D'Azur, CNRS, Inserm, Institut de Biologie Valrose, Nice, France

[*] Both authors contributed equally to this work

[§] Corresponding author: luton@ipmc.cnrs.fr

Abstract

Breast cancer is the second leading cause of cancer death in women worldwide. Primary tumor metastasis is responsible for most of the mortality. Despite the benefits of breast cancer targeted therapies there is still no effective treatments against metastases. Cancer initiation is caused by somatic mutations in oncogenes or tumor suppressor genes, but additional mutations can provide selective advantages to the tumor cells to spread into nearby tissue or distant organs and develop metastatic cancers. The identification of pro-invasive factors and the comprehension of their mechanism of action is therefore of paramount importance. We have recently proposed that EFA6B (Exchange Factor for Arf6, B), a tight junction regulator, acts as an antagonist to breast cancer development. Loss of expression of EFA6B is correlated with the metastatic Claudin-low breast cancer subtype that is characterized by the loss of tight junction and a transcriptomic signature of epithelial-to-mesenchymal transition (EMT). To establish and identify the pro-tumoral impact of the loss of EFA6B we have invalidated the gene *PSD4/EFA6B* in normal human mammary cells using the CRISPR/Cas9 technology. We found that EFA6B depletion is sufficient to induce the formation of cellular branched structures in collagen I by collective invasion. It is accompanied by an up-regulation of EMT transcription factors, alterations of the matrisome, changes in the integrin (ITG) repertoire and increased cell contractility. Consequently, the cells no longer sense the laminin inhibitory signal and form ITGB1-based invadopodia enriched with the metalloprotease MMP14 responsible for the matrix degradation. The invasion depends on Cdc42 activation and two of its effector pathways Cdc42-MRCK-pMLC and Cdc42-N-WASP-Arp2/3. Collectively, our results demonstrate a novel negative regulatory pathway of collective invasion downstream of EFA6B and open up new therapeutic perspectives for breast cancer.

Introduction

Epithelial morphogenesis is essential for embryonic development, organogenesis and tissue repair (Bryant and Mostov, 2008; Lecuit and Le Goff, 2007; Martin and Parkhurst, 2004). It relies on

highly dynamic and conserved processes that help to deform simple epithelial sheets into three-dimensional structures (Lecuit and Le Goff, 2007). Alteration of these mechanisms can cause major developmental defects and diseases such as cancer (Thiery et al., 2009). Most of our knowledge of the molecular and cellular mechanisms comes from the study of simple animal models (e.g. C. Elegans and Drosophila) but there is still much to discover about more complex organisms such as mammals (Fletcher Alexander G. et al., 2017). In this regard, in vitro 3D cell culture models and organoids provide valuable support to the studies of genetically modified animals (Bryant and Mostov, 2008; Cheung and Ewald, 2014; Drost and Clevers, 2018; Martín-Belmonte and Rodríguez-Fraticelli, 2009).

The control of tissue morphogenesis is based on a combination of cellular mechanisms (Ladoux and Mège, 2017; Lecuit and Le Goff, 2007) and on the interaction of the cells with their stromal environment that helps to contain physically and shape through reciprocal communication the epithelial tissue (Bonnans et al., 2014; Howard and Lu, 2014; Sakakura et al., 2013). The mammary gland is an excellent organ model for studying the remodeling of an epithelial tissue because its development takes place after birth, during puberty and undergoes cycles of expansion and involution with each pregnancy (Shamir and Ewald, 2015).

The mature epithelial mammary tissue consists of two layers of distinct cells: the apical luminal cells that rest on a layer of basal cells or myo-epithelial cells, and a small fraction of progenitor cells. The myo-epithelial cells are in direct contact with the basal membrane, composed essentially of laminins and collagen IV, which envelops the epithelial bilayer and separates it from the stroma rich in fibrillary collagen I, fibronectin and proteoglycans in which are found fibroblasts, adipocytes and cells of the immune system. The basic functional unit of breast tissue under development is the terminal end bud (TEB), an alveolar structure formed at the end of a duct. The duct is composed of a double layer of luminal and basal cells, while the TEB is made of multiple layers of luminal cells surrounded by a single layer of basal cells. At puberty, the mammary gland expands by ductal elongation and branching morphogenesis while the TEB penetrates the stroma in a tightly regulated mode of collective invasion. It is believed that this developmental program is co-opted during breast cancer providing mammary tumor cells with metastatic potential (Macias and Hinck, 2012).

Breast cancer is a major public health issue with half a million deaths worldwide each year, the majority of which being due to metastatic dissemination (Bray et al., 2018). Despite the effectiveness of therapies for early detected tumors, the treatment of metastatic cancers remains a largely unresolved problem. There is therefore an urgent need to better understand the molecular mechanisms that regulate invasion in order to develop new treatments. A large number of studies have described the cellular and molecular mechanisms that promote or sustain invasion. Much less is known about intracellular signaling pathways that transmit negative regulatory signals to block the invasive potential of epithelial cells.

We have recently described the anti-tumor potential of the Arf6 exchange factor, EFA6 (Zangari et al., 2014). We initially showed that this molecule, by activating Arf6 and interacting with effectors through its C-terminal domain, regulates the assembly and maintenance of tight junctions (Klein et al., 2008; Luton et al., 2003; Théard et al., 2010). Then, we showed that its level of expression determines the epithelial status of mammary cells grown in 3D culture. In particular, the over-expression of EFA6B in weakly tumoral cells restores a normal epithelial phenotype by stimulating the formation of a central lumen and tight junctions (Milanini et al., 2018; Zangari et al., 2014). Finally, in breast cancer patients, we observe a correlation between the loss of expression of EFA6B (mRNA and protein), the Claudin-Low (Cld-low) cancer sub-type and a reduced survival rate (Zangari et al., 2014).

To identify the molecular mechanisms by which EFA6B acts as an antagonist to the development of breast cancer, we analyzed the consequences of invalidating its gene (*PSD4*) in normal human mammary cells. We have found that EFA6B knock-out mammary cells, of basal or luminal origin, grown in 3D matrices developed branched structures by adopting a collective mode of invasion.

This invasion is dependent on the formation of integrin β1- and MMP14-enriched invadopods. Upstream, the collective invasion is controlled by the activation of an EMT program with a modification of the cell-ECM interaction as judged by alterations in the matrisome, changes in the integrin repertoire and increased contractility leading to remodeling of the ECM by the EFA6B knock-out cells. Downstream of EFA6B, we show that its knock-out activates Cdc42 which in turn elicits two signaling pathways: Cdc42-MRCK-pMLC that regulates contractility, which together with Cdc42-N-WASP-Arp2/3 is required for invasion. Thus, we have identified a new EFA6B-regulated mechanism of collective invasion, which opens up new avenues for the treatment of breast cancer.

Results

Loss of EFA6B in MCF10A stimulates invasive branching in collagen I

To investigate the impact of the loss of expression of EFA6B on breast cancer development, we have inactivated the gene (*PSD4*) encoding for EFA6B in normal human mammary cell line MCF-10A using the CRISPR/Cas9 technology. We have performed two separate rounds of *PSD4* knock-out using two distinct sgRNA targeting the first exon. In total, four out of 250 clones screened by immunoblot for the loss of EFA6B protein expression were isolated. The inactivation of *PSD4* gene was further confirmed by a DNA mismatch endonuclease assay followed by PSD4-targeted genomic and transcript sequencing. **Fig. 1A** shows the characterization of three knock-out clones (clone KO 55, KO 50 and KO 2) for EFA6B and one heterozygous clonal cell line (Het 2.9), with the latter expressing half of the total levels of EFA6B compared to wild-type cells. The expression of EFA6A and EFA6D, the other members of EFA6 family expressed in MCF-10A cells, was unaffected. A slight decrease (20%) of Arf6 expression was observed (see also **Fig. 1C** and **Fig. 2B**) which was also noticed in BC patients whose EFA6B expression was decreased (Zangari et al., 2014). The levels of the other Arf proteins, Arf1 and Arf5, remained unaffected. More noticeable was the severe reduction of Arf6-GTP (80%) levels indicating that EFA6B is a major Arf6-GEF in MCF-10A cells (**Fig. 1C**).

EFA6B has been previously recognized as a tight junction and polarity regulator(Klein et al., 2008; Luton et al., 2003; Théard et al., 2010). To assess the hallmark property of epithelial cells to polarize and self-organize in acini the clones were placed in collagen I gels. Control MCF10A cells formed round aggregates typical of normal epithelial cells. In contrast, all the homozygous EFA6B KO clones outgrow branched structures reminiscent of collective dissemination (**Fig. 1B, upper and middle panels**).

Quantification of cell aggregates displaying at least one branched structure (>2 microns) (**Fig. 1B, bottom panels**) showed that KO clones developed 4 times more membrane and cellular protrusions than WT MCF10A cells (**Fig. 1D**). Re-expression of wild-type EFA6B by lentiviral infection of the KO clone 55 was sufficient to recover the formation of normal round aggregates (**Fig. 1D, clone RESCUE**) indicating that the invasive phenotype was specifically a consequence of the loss of EFA6B. Of note, the heterozygous (het) 2.9 clone expressing 50% of EFA6B, organized identical branched structures and to the same extent than the homozygous KO clones (**Fig. 1D**). Since exogenous expression of EFA6B in EFA6B KO 55 cells rescued the invasive phenotype, we propose that the dominant loss-of-function of EFA6B is likely due to haplo-insufficiency.

Loss of EFA6B stimulates invasive branching in luminal and basal mammary sub-populations

We then set out to determine whether the effect of KO of EFA6B can be generalized to other epithelial mammary cells and whether it has a similar impact on the two major mammary epithelial cell subtypes, luminal and basal. To address these questions, we used the HMLE human epithelial population as it contains luminal progenitors and both mature luminal and basal epithelial cells. Using the EpCAM and CD49f cell surface markers, we sorted luminal progenitors (EpCAM+/CD49f+), mature luminal

(EpCAM+/CD49f-) and mature basal (EpCAM-/CD49f+) cells (**Fig. 2A**) and immediately performed CRISPR/Cas9 mediated invalidation of *PSD4* in each separate population. We obtained one homozygous (KO 3) and one heterozygous clone (Het 25) from the luminal progenitor population and one homozygous clone (KO 1'') from the mature basal population. No clone was obtained from the mature luminal population. Similar to MCF10A clones, EFA6B protein expression was undetectable in the homozygous HMLE KO clones (KO 3 and KO 1'') compared to the wild-type population or clones (WT 23 and WT 2''), while the heterozygous clone (Het 25) expressed 50% of its corresponding wild-type clone (WT 3) (**Fig. 2B**). The expression of the other isoforms, EFA6A and EFA6D, was unaffected. A modest but significant reduction of Arf6 expression was observed in the clones isolated from the luminal progenitor population but not in the basal clone. However, neither Arf1 nor Arf5 levels were altered. In 3D-collagen culture, HMLE WT clones formed cohesive rounded aggregates while the EFA6B homozygous and heterozygous HMLE clones displayed invasive protrusions (**Fig. 2C**). Overall, the HMLE clones displayed a less developed invasive phenotype than the ones isolated from MCF-10A (**Fig. 2D**).
In conclusion, EFA6B is a general negative regulator of the invasive properties of epithelial mammary cells from both luminal and myo-epithelial origins. The dominant-negative phenotype of the HMLE heterozygous clone confirmed our suggestion of classifying EFA6B as an haplo-insufficient tumor antagonist gene. This is in agreement with our previous observations in various cell systems showing that the levels of EFA6 proteins were critical to their functions (see discussion). Also, in BC patients the severity of the histo-clinical data was correlated with the extent of the loss of expression of *PSD4* messengers (Zangari et al., 2014).

EFA6B knock-out cells stimulate an MMP-14 dependent ECM degradation and invasion

The branched structures observed in 3D culture in MCF10A and HMLE cell lines upon the loss of EFA6B expression resemble phenotypically to branching during mammary morphogenesis or collective invasion of cancer cells. Therefore, we next sought to characterize the enzymatic invasive properties found to be crucial for cell dissemination in both normal and cancerous contexts. To demonstrate the capacities of cells to digest their microenvironment, we first seeded them on fluorescent gelatin matrix. In contrast to WT cells, the EFA6B KO 55 clone was capable of degrading the fluorescent gelatin, seen as dark spots underneath the cells (**Fig. 3A and B**). Moreover, we validated their capacity to proteolytically cleave collagen fibers by performing immuno-fluorescence analyses using the Col1-3/4C antibody that recognizes specifically the digested ends of collagen fibers (Monteiro et al., 2013). As shown in **Fig. 3C and D,** the Col1-3/4C staining was virtually absent around the wild-type aggregates while a strong signal was visible along the invasive cellular protrusions extended by the EFA6B KO 55 cell aggregates. In the search of a potential protease responsible for collagen degradation, we screened several candidates using protease inhibitors and found that GM6001, a MMP selective inhibitor, was the most effective (data not shown). We thus focused on the MMP-14 that has been described as the main metalloprotease involved in mammary gland morphogenesis and breast cancer metastasis (Feinberg et al., 2016, 2018; Friedl and Gilmour, 2009; Poincloux et al., 2009). Both, MCCF10WT and EFA6B KO 55 cell lines expressed similar protein levels as assessed by immunoblot (**Fig. 3E**). Using specific siRNA for MMP-14 (**Fig. 3F)**, we found that down-regulation of MMP-14 in the EFA6B KO cells totally inhibited collagen invasion (**Fig. 3G**).
Next, we challenged the invasive capacities of the cells by placing them in a stoichiometric mixture of collagen and Matrigel (1/1 mg/ml). Matrigel is composed of laminin molecules, the main components of the basal membrane that inhibits epithelial cell invasion (Nguyen-Ngoc et al., 2012). Although Matrigel significantly reduced cells invasion, EFA6B KO 55 cells succeeded to form membranous and cellular protrusions (**Fig. 3H**). In 2mg/ml Matrigel, EFA6B KO 55 cells did not present any protrusive aggregates (data not shown). However, unlike WT cells that demonstrated a classic polarized structure

with lumen formation, the EFA6B KO 55 cells remained disorganized and never formed any lumen (**Fig. 3I**).
In conclusion, the EFA6B KO cells are potent invasive cells that have lost the capacity to polarize in response to ECM stimulation.

EFA6B knock-out promotes a change in the ITG repertoire and stimulates the formation of ITGB1-based degradative invadopodia

Maintenance of epithelial cell polarity relies on cues arising from cell-to-cell interaction and cell-to-ECM adhesion. In fact, EFA6B KO cells remain cohesive but have lost the ability to polarize in Matrigel which suggest a deregulation on Cell-ECM signaling level. Transcriptomic profiling of the KO 55 and Het 2.9 clones compared to MCF10 WT cells revealed that the matrisome is the main affected group of genes with up to 10% (48) of the total altered genes (475**) (Supp. Table 1 and Supp. Fig. 1).**
We explored first the protein expression level of the major integrins (ITG) expressed in mammary cells: α2β1, α3β1, α6β1 and α6β4. By combining FACS (**Fig. 4A**), immunoblot analyses (**Fig. 4C**) and confocal immunofluorescence imaging (**Fig. 4E**) we found that the EFA6B KO 55 cells had a good reduction of subunits α6 (50%) and β4 (36%) expression, whilst those of α2, α3 and β1 were unchanged. To determine which integrins were required for EFA6B KO-mediated invasion, we placed spheroids in collagen containing control or integrin blocking antibodies and quantified the number of invasive protrusions (**Fig. 4B**). Antibodies against ITGA6, ITGB4 and ITGB3 had no effect. In contrast, antibodies against ITGB1 and ITGA2 strongly blocked cell invasion (**Fig. 4B**).
The ITGB1-mediated invasion relies on the formation of specialized degradative structures called invadopodia (Eddy et al., 2017). We thus searched for the formation of degradative invadopodia in MCF10WT and EFA6B KO cells. In EFA6B KO 55 cells, staining for cortactin, a marker enriched in invadopodia, revealed the presence of large structures co-stained for F-actin and matching spots of digestion of the gelatin (**Fig. 4F**). In MCF10 WT cells, no degradation of gelatin was visible and the cortactin positive spots, not enriched in F-actin, appeared smaller (**Fig. 4F**). Since the invasion of the EFA6B KO 55 cells is dependent on MMP14, we looked for MMP14 enrichment in invadopodia. Cells were transiently transfected with MMP14-mCherry plasmids and stained for cortactin. In EFA6B KO 55, but not WT, cells expressing low levels of MMP14-mCherry presented extensive co-localization with cortactin (**Fig. 4G**). Next, we determined whether ITGB1 was concentrated into the invadopodia. Again, we found a large co-localization of ITGB1 with MMP14-mCherry in EFA6B KO 55 but not in MCF10 WT cells (**Fig. 4H**). Altogether, these results demonstrated that the loss of EFA6B led to the formation of MMP14-degradative and ITGB1-based invadopodia.

Next, we investigated the expression of fibronectin (FN) and the mammary laminin (LN) proteins LN111, LN332, LN511 and LN521. Immunoblots of whole cell lysate showed no change in the levels of FN, LAMγ2 (LN332) or LAMβ1 (LN111, LN511) (**Fig. 4D**). We thus looked at the LN deposited by cells grown in 3D-collagen. In both MCF10 WT and EFA6B KO 55 cells, the staining intensity for LAMγ2 (LN332) and LAMα5 (LN511, 521) surrounding the cell aggregates were equivalent indicating that the production, secretion and deposition of the major LNs were unaffected (**Fig. 4I**). However, in the KO aggregates, LNs were absent at places where cells invaded the collagen (**Fig. 4I**, arrows).
We conclude that in the absence of EFA6B, there is a modification of the matrisome and integrin repertoire accompanied by the formation of invadopodia, all of which contributes to the collective invasion of the EFA6B KO cells.

EFA6B knock-out induces the expression of EMT transcription factors that promote collective invasion of MCF10A and HMLE cells in collagen I.

The inability of cells to polarize and maintain an epithelial phenotype suggested that they may have engaged to some extent into an epithelial to mesenchymal transition (EMT). EMT is believed to promote invasion by providing cells with migratory and degradative advantages (Heerboth et al., 2015). We observed that the MCF10 EFA6B KO cells had reduced levels of E-cadherin with an increased expression of N-cadherin; a classical EMT cadherin-switch (**Fig. 5A**). In addition, transcriptomic analysis showed alteration of the cell-cell adhesion **(Supp. Fig. 1).** Knowing that EFA6B is a TJ regulator and its expression correlated with the loss of tight junction proteins and the Cld-low BC subtype, we also looked at TJ markers and found that Cld1 and Cld3 were strongly reduced in all clones and occludin decreased in 3 out 4 clones (**Fig. 5A**). We also confirmed these results by analyzing the HMLE clones. Although, there was no switch of cadherin expression, we noticed a strong increase of VIM accompanied by a slight but robust decrease of Cld3 (**Fig. 5B**). Confocal immunofluorescence analysis of MCF10 WT and EFA6B KO 55 cells grown in 3D-collagen confirmed the cadherin switch at cell-cell junctions (**Fig. 5C**). N-cadherin was described to provide weaker homotypic interaction between adjacent cells (Cavallaro and Dejana, 2011). We thus assessed the cell-to-cell affinity by using the hanging-drop assay in which cells were submitted to gravity in a drop of medium to facilitate cell-cell contacts within a monolayer. Lining the bottom of the drop, MCF10 WT cells formed compact monolayers while EFA6B KO 55 cells formed lacy monolayers indicative of loose cell-cell contacts (**Fig. 5D**). These results indicated that the loss of EFA6B reduced cell-cell adhesion facilitating pro-migratory cell movements, while maintaining enough connection between cells to invade through a collective mode of invasion.

We also analyzed by FACS the expression levels of the cell surface markers, EpCAM and CD49f. In the EFA6B KO 55 cells, we found an overall decrease of both markers of 66.9±7.2% for EpCAM and 41.4±9.6% for CD49f together with the emergence of a new population (11,7% of total cells, red gate) characterized by a very low EpCAM expression suggestive of a loss of epithelial identity (**Fig. 5E**). Further analysis by RT-qPCR confirmed the switch of E/N-cadherin, and the decrease of CD49f and occludin. It also revealed that Cld7 expression was down-regulated confirming the effect on TJ components. We also looked at the CK14 which down-regulation was recently shown to mark an advanced mesenchymal state in melanoma (Pastushenko et al., 2018) (**Fig. 5F**). All our results indicated that loss of EFA6B had engaged the cells into an EMT program. Thus, we analyzed the expression of the known EMT-TF in BC and found a significant increase of SNAI, TWIST1 and ZEB1, and to a lower extent of SLUG and TWIST2 (**Fig. 5F**). Next, we tested the implication of the most relevant EMT-TFs in invasion and found that siRNA-mediated down-regulation of Twist1, Snail and Slug but not ZEB1 blocked the EFA6 KO invasion (**Fig. 5G, H**).

We concluded that the knock-out of EFA6B induced the expression of EMT-TFs that promoted EMT and collective invasion.

EFA6B knock-out stimulates cellular contractility and invasion through Cdc42

Our results showed that loss of EFA6B promotes collective invasion through activation of an EMT transcriptional program, alteration of the matrisome including the integrin repertoire. All of these modifications can be directly linked to a change in cell contractility behavior.

We thus explored the contractility capacity of our cells by first looking at the organization of the collagen surrounding the cell aggregates by reflectance (**Fig. 6A**). We did not observe a particular orientation of the collagen fibers around the WT cell aggregates. In contrast, reflectance signals showed accumulation of collagen fibers at the periphery of invading EFA6B KO 55 cells, and more interestingly, a radial distribution of aligned collagen fibers from leading cells. Thin membrane filopodial structures were prolonged by collagen fibers detected by reflectance (**Fig. 6A, inset arrows**). We then quantified the contractility activity by using collagen gel contraction assay (**Fig. 6B**). EFA6AB KO cells were at least twice more contractile than their WT counterparts. Cell contractility is dependent

upon the activation of the myosin II through the phosphorylation of the myosin light chain (MLC) (Vicente-Manzanares et al., 2009). Concomitant with the results of the contraction assay, whole cell lysate showed that EFA6B KO 55 cells presented higher levels of pMLC than control cells (**Fig. 6C**). All these observations indicated that the EFA6B KO 55 cells were more contractile that the WT cells. Small G proteins of the Rho family are known to control cell contractility (Zegers and Friedl, 2014); thus by siRNA-mediated down-regulation (**Fig. 6D**), we searched for the small G proteins that could mediate the augmented contractility of the EFA6B KO 55 cells. Using gel contraction assays, we found that the downregulation of Cdc42, but not RhoA or Rac1, altered the contractility of the EFA6B KO 55 cells (**Fig. 6B**). Next, we observed that the down-regulation of Cdc42 was the most effective at blocking invasion, while again RhoA and Rac1 had no effect (**Fig. 6E**). Pull-down experiments were conducted to determine whether any of the small G proteins were over-activated in the EFA6B KO 55 cells compared to WT (**Fig. 6F**). In agreement with the functional assays, we found an upregulation of activated Cdc42, but not of RhoA or Rac1. Overall, these observations point towards a central role for Cdc42 in regulating cell contractility and invasion following EFA6B depletion.

EFA6B knock-out stimulates cellular contractility and invasion through two Cdc42-dependent signaling pathways: Cdc42-MRCK-pMLC and Cdc42-NWASP-Arp2/3

Cdc42 is known to regulate contractility through the recruitment of kinases that phosphorylate MLC (Wilkinson et al., 2005) and to control invadopodia formation by activating the Arp2/3 complex, a regulator of actin dynamics, through N-WASP (Torres and Rosen, 2006). Downstream of Cdc42, the myotonic dystrophy-related Cdc42-binding kinases (MRCK) were shown to phosphorylate directly or indirectly the myosin II regulatory light chains (MLC) (Wilkinson et al., 2005). SiRNA experiments showed that the combined down-regulation of both MRCKα and MRCKβ in EFA6B KO 55 cells reduced both the MLC phosphorylation and cell invasion in collagen I (**Fig. 7A**). We also analyzed the effect of depleting the Ca^{2+}–calmodulin activated myosin light chain kinase (MLCK) that has been proposed to act on the cell peripheral acto-myosin cytoskeleton (Vicente-Manzanares et al., 2009). Down-regulation of MLCK also decreased the MLC phosphorylation but had little effect on invasion indicating that MRCK and MLCK regulate separate pools of MLC (**Fig. 7B**). RhoA activates the Rho-associated protein kinases ROCK1 and ROCK2 believed to phosphorylate MLC in a more central area of the cells. Knock-down of both ROCK1 and ROCK2 had no effect on either phosphorylation of MLC or invasion (**Fig. 7C**). Thus, in EFA6B KO cells, the activated Cdc42 controls phosphorylation of MLC and invasion in an MRCKα/β-dependent manner. Further, siRNA down-regulation of N-WASP and Arp2/3 inhibited invasion (**Fig. 7D**). Altogether, our results unraveled a new pathway regulated by EFA6B, which controls the activation of Cdc42 and two downstream functions: a) contractility through MRCKα/β phosphorylation of MLC and b) invasion through N-WASP and Arp2/3.

Discussion

During this study, we discovered a novel negative regulatory pathway of the collective invasion controlled by the exchange factor of Arf6, EFA6B. In the absence of EFA6B, mammary cells undergo EMT, matrisome remodeling and concomitant activation of a Cdc42-dependent signaling pathway that controls cell contractility and invasion via the formation of ITGB1-based and MMP14-enriched invadopodia.

EFA6B : specificity and haplo-insufficiency

The EFA6 family comprises 4 isoforms among which 3 are expressed in mammary epithelial cells at the exception of the neuronal specific member EFA6C. In MCF10A cells, compared to EFA6B, EFA6A is expressed in similar amount and EFA6D is in large excess (our unpublished results). Since, neither EFA6A nor EFA6D levels of expression were affected upon EFA6B knock-out it indicates that neither one was able to compensate for the absence of EFA6B. On the other hand, EFA6B re-expression in MCF10 EFA6B KO cells was sufficient to revert the invasive phenotype. Thus, in MCF10A cells the EFA6B isoform appears to be selectively regulating the invasive properties. The absence of compensation between the EFA6 isoforms is a general observation made by us and other groups (Luton et al., 2003; Morishige et al., 2008; Théard et al., 2010; Zangari et al., 2014). All four EFA6 members displaying similar Arf6 GEF activities, it suggests that either their subcellular localization is strictly distinct and/or that their functions do not depend only on Arf6 activation but on a combination of signals that they integrate through their other functional domains. We have already reported evidence of the latter model by showing that EFA6 effects on TJ assembly can only be recapitulated by co-expressing an Arf6 constitutive mutant (Arf6T157N) together with the PH-Cterminus of EFA6 (Klein et al., 2008). Finally, the EFA6B substrate Arf6 levels were found to be slightly but reproducibly reduced in MCF10A and HMLE (luminal progenitor) cells while the other members of the family Arf1 and Arf5 were unaffected. In BC patients of the Cld-low subtype this reduction in Arf6 was also observed indicating that there is a specific loop of regulation between EFA6B levels and its substrate Arf6 (Zangari et al., 2014).
Most interesting is the observation that heterozygous KO clones were as invasive as the homozygous ones, emphasizing the importance of the levels of expression of EAF6B in repressing the invasive potential of normal mammary cells. This observation is in agreement with many of the results we have previously obtained by studying EFA6A and EFA6B in different cellular models that demonstrated that the functions of EFA6 proteins are dependent on their expression level. First, using an inducible system to control EFA6Avsvg levels of expression in the MDCK cells, we observed that EFA6A stimulating effects on the assembly of the TJ is dose-dependent (Luton et al., 2003). Second, at the onset of epithelial polarization following the engagement of the E-cadherin molecules, the levels of endogenous EFA6B are transiently and dramatically increased at cell-cell contacts to help assemble the TJ (Luton et al., 2003; Théard et al., 2010). Third, at steady state the levels of expression of the endogenous EFA6B are maintained low by a finely-tuned balance between high rates of protein synthesis and degradation by the ubiquitin-proteasome system (Théard et al., 2010). Fourth, although the levels of EFA6B at steady state are low, siRNA-mediated down-regulation weakens the TJ indicating that a minimal level of EFA6B is necessary to maintain a functional TJ (Théard et al., 2010). Fifth, the functional complementation experiments described above indicated that the strength of the signals delivered by the two proteins Arf6T157N and EFA6 PHCter needed to be finely equilibrated to mimic EFA6 effects suggestive of a stoichiometric control (Klein et al., 2008). Finally, in BC patients we found a correlation between the histo-clinical data and the levels of *PSD4*/*EFA6B* (Zangari et al., 2014). Collectively, these results indicate that the levels of expression of EFA6B are critical to its functions. In this manuscript, the results obtained with the knock-out cells deliver a novel information: the *PSD4/EFA6B* gene appears as an haplo-insufficient tumor-antagonist gene.

Invasive properties

MCF10A are the most studied normal epithelial human mammary cells. Yet, although they polarize around hollow lumens when grown in Matrigel as expected from luminal cells, their transcriptomic signature is that of a basal cell line suggesting that these cells may represent a multipotent lineage (Neve et al., 2006). To analyze the effect of EFA6B knock-out selectively in basal and luminal cells, we carried out the CRISPR/Cas9-mediated knock-out of EFA6B after sorting both populations from the immortalized mammary epithelial cells HMLE (Elenbaas et al., 2001). We observed that the two isolated homozygous KO clones derived from each population as well as the heterozygous KO luminal

clone were all invasive, though the basal EFA6B KO cells appeared slightly less invasive. Further, regardless of their basal or luminal origin, the KO cells displayed similar EMT profiles with no sign of E-Cadh/N-Cadh switch but a strong increase in vimentin and a slight decrease of the Cld3 protein. Although based on few clones, our results indicate that EFA6B depletion in luminal and basal cells induces EMT and invasion in collagen I. It is admitted that basal breast cancers are more aggressive than luminal ones. However, very little is known about how the differentiation state of the cancer cell impacts the acquisition of metastatic capacities. The EMT observed in our luminal clones may endow them with invasive properties (Cheung et al., 2013).

A large body of evidence obtained from *in vitro* and *in vivo* studies demonstrated that the MMP14 metalloprotease is instrumental to enabling normal mammary gland development and BC collective invasion (Feinberg et al., 2016, 2018; Friedl and Gilmour, 2009; Ghajar and Bissell, 2008). Looking for the protease responsible for invasion in MCF10A KO cells, we found that MMP14 was required. Yet, the total level of expression is comparable between MCF10A WT and EFA6B KO cells. Since, invasion is a regulated process based on the organization of specialized invasive structures called invadopodia, we looked at the cell surface distribution of MMP14 and for the presence of invadopodia. In MCF10 WT cells, the MMP14-mCherry was found mostly in an intracellular peri-nuclear compartment with little MMP14 at the cell surface. In contrast, in EFA6B KO cells, the MMP14 was found enriched in large dotted structures labelled for ITGB1 and cortactin marking the presence of invadopodia. Hence, EFA6B KO cells invade by stimulating the formation of invadopodia enriched in MMP14.

The fact that our cells display thin filopodia at the front of the leader cells, express MMP14 and sustain invasive protrusions in collagen I is reminiscent of a mechanism of invasion by cancer cells. Indeed, the collective invasion during mammary tubulogenesis occurs without actin-based protrusions extending into ECM (Ewald et al., 2012). Further, MMP14 is not expressed by the normal epithelial cells during mammary gland branching but is expressed by the invading BC cells (Feinberg et al., 2018). Finally, normal cells would only invade collagen I transiently before producing their basement membrane that blocks invasion (Nguyen-Ngoc et al., 2012).

EFA6B KO cells keep on invading the collagen I even mixed with Matrigel indicating that they do not respond to the arrest signal provided by the matrix and/or do not produce a normal matrix. Gene profiling expression analyses showed that the EFA6B KO cells had a major change in their matrisome. We have made the same observation in MCF7 cells down-regulated for EFA6B using constitutive expression of a specific shRNA (our unpublished results). Nevertheless, immunoblot analyses did not detect significant changes of expression of the major laminins expressed by our cells. When spheroids of MCF10 WT and EFA6B KO cells were placed in collagen I, we observed staining of similar intensities for laminins (LAMα5 and LAMγ2) deposited around the core of the spheroids indicating that the KO EFA6B cells were capable of producing, secreting and assembling normal levels of laminins. However, while MCF10 WT cells did not invade the collagen I passed their basement membrane, the EFA6B KO cells disseminated from the spheroids most likely by digesting their basement membrane that was no longer recognized as a stop signal.

The Cdc42 signaling pathway

In MCF10A cells, the absence of EFA6B led to a strong activation of Cdc42 but not Rac1 nor RhoA. *In vitro* and *in vivo* studies have shown important roles for Cdc42 in regulating diverse cellular processes such as cell cycle progression and mitosis, polarity, survival, differentiation and stem cell function (Stengel and Zheng, 2011). Transgenic overexpression of Cdc42 in the mammary gland produced hyperbranched ductal trees and abnormal acini with altered epithelial-stromal interactions (Bray et al., 2013). Although Cdc42 is found hyperactivated in breast tumors (Fritz et al., 1999, 2002), activating mutations in Cdc42 have not been found (Rihet et al., 2001) suggesting that its activating pathways

must be altered. We propose that loss of expression of EFA6B alters a Cdc42 activating pathway contributing to Cdc42 hyperactivation in human BC.

How is Cdc42 activated upon EFAB KO? In other words, how EFA6B and/or Arf6 activation inhibits Cdc42 in non-tumoral cells? The most direct pathway would be through the recruitment of a Cdc42-GAP of the ARH-GAP family, which members bind to activated Arf-GTP molecules. For instance, ARHGAP10 was shown to be recruited by Arf1-GTP in the Golgi to repress Cdc42 functions (Dubois et al., 2005). ARHGAP10 appears to be Golgi-specific but other members of the ARHGAP would be good candidates to mediate Cdc42 inhibition downstream of EFA6B/Arf6. Alternatively, another EFA6B/Arf6-associated signaling pathway may eventually recruit one of the many Cdc42-GAPs to mediate its inhibition. Also, indirectly the EMT transcriptional program or change in matrisome may have induced the increased expression of a Cdc42-GAP.

From *in vitro* studies, Cdc42 is a known pro-invasive protein that can induce the formation of filopodia, invadopodia and can regulate cellular contractility (Stengel and Zheng, 2011). We found that knock-down of Cdc42 abrogates contractility and invasion of the EFA6B KO cells. We determined that Cdc42 promotes increased contractility through MLC phosphorylation via the MRCK proteins. In contrast, the major RhoA/ROCK contractility pathway did not appear to play a major role. Interestingly, ECM rigidity and cellular contractility were shown to regulate the formation of invadopodia (Alexander et al., 2008; Parekh and Weaver, 2016) suggesting that in EFA6B KO cells Cdc42 activation might facilitate the formation of invadopodia by increasing cell contractility. EFA6B knock-out cell contractility may also be the consequence of an alteration of the matrisome that might have increased the ECM rigidity, for instance through the observed up-regulation of the LOX protein (Table 1).

Further, Cdc42 plays an essential role in invadopodia formation (Stengel and Zheng, 2011; Yamaguchi et al., 2005) and maturation by maintaining the activation of N-WASP-Arp2/3 complex, which nucleates actin polymerization (Eddy et al., 2017). In addition, Cdc42 can promote the recruitment of MMP14 to the plasma membrane at invadopodia (Castro-Castro et al., 2016). Since the invasion of our EFA6B KO cells is dependent on N-WASP, Arp2/3 and MMP14 we propose that Cdc42 is the major effector of their invasive behavior.

EFA6B/Arf6 and breast cancer

Our previous study indicated that the loss of EFA6B expression in BC patients is correlated with poor prognosis and the metastatic subtype Claudin-low characterized by the loss of expression of all cell junction constituents and an EMT signature (Zangari et al., 2014). Here, we show that the loss of EFA6B expression induces an EMT and endows the cells with invasive properties. There have been no genomic studies showing EFA6B to be an oncosuppressor, and our orthotopic xenograft experiments of EFA6B KO cells in immunosuppressed mice did not lead to the formation of any tumor demonstrating that the loss of EFA6B is not a driver mutation. Yet, other so-called secondary driver mutations, although non-transforming on their own, can provide selective advantages to transformed cells (Nik-Zainal and Morganella, 2017). We propose that the loss of expression or activity of EFA6B is a secondary driver mutation that confers invasive properties and high metastatic susceptibility to cancer cells.

The loss of expression or activity of EFA6B may occur in several ways. In BC, mutations within the *PSD4/EFA6* gene are very rare and mostly found outside the catalytic site, or within domains not known to control its GEF activity or its association with known interactors (Zangari et al., 2014). It therefore seems more likely that the loss of EFA6B expression is due to events altering biological processes that control its messenger or protein abundance. We propose that the loss of EFA6B expression observed in Cld-low tumors is due to either alteration of its regulation by the ubiquitin proteasome system, by non-coding RNAs (miRNAs and ceRNAs), or by mutations in its promoter that could mediate haplo-insufficiency in the event that only one promoter is affected. In any case, our results indicate that reduction of EFA6B protein levels below a minimum threshold induces invasive behavior. Yet, we do

not exclude that a gradual loss of EFA6B expression may correlate with the progressive acquisition of increasing invasive properties. They are now accumulating evidence emphasizing the role of heterozygosity in tumor progression and showing that a reduction of the amount of highly interconnected proteins, such as EFA6B, may change the networks response resulting in a high amount of damage (Berger et al., 2011; Smilenov, 2006).
In general, Arf6 is considered as a pro-tumoral factor although only few studies provided mechanistic details of its contribution. The work from the group of Sabe described a signaling pathway activated by the EGF whereby the EGFR would recruit the Arf-GEF BRAG2/GEP100 to activate Arf6, which then recruits in cascade the Arf-GAP AMAP1, cortactin and the mesenchymal protein EPB41L5. *In vivo*, this pathway would regulate the invasive properties of EGFR positive BCs (Li et al., 2017; Sabe et al., 2009). In TNBCs, the group of Chavrier reported the implication of Arf6 in facilitating the trafficking of the MMP14 to the invadopodia through the adaptor JIP3/4 and kinesin 1 (Marchesin et al., 2015). However, another study described an opposite effect where Arf6 recruited by NEDD9 would negatively control the trafficking of active MMP14 to the cell surface and block invasion (Loskutov et al., 2015). More recently, it was found that the endocytic protein Numb controls negatively the acquisition of migratory and invasive properties by activating EFA6B/Arf6 in response to growth factors (Zobel et al., 2018).

In summary, we found that the depletion of EFA6B stimulates an epithelial-to-mesenchymal transition concomitant to an alteration of the matrisome and the acquisition of collective invasive properties. The collective invasion of the EFA6B KO cells is dependent on the activation of Cdc42. The activated Cdc42 elicits two signaling pathways that first increase cellular contractility dependent on the MRCK proteins, and second the formation of invadopodia enriched in N-WASP, Arp2/3 and the protease MMP14. Together with others, these results indicate that the loss of EFA6B expression might contribute to the high metastatic propensity of Claudin-low breast cancers. A better understanding of the molecular mechanisms leading to EFA6B depletion as well as its consequences should offer new opportunities to fight breast cancer.

Methods

CRISPR/Cas9 knock-out
Two guided RNAs targeting the exon 1 of human *PSD4* were selected from the crispr.mit.edu/ and crispor.tefor.net/ websites. The guided RNAs were cloned separately into the vector pSpCas9(BB)-2A-GFP (PX458 - Addgene) encoding for Cas9 and GFP. Sequences were as follow: PSD4-Z1T8-pX458-FOR1 forward 5'-3' CACCgaggatccaccggagcctttcg, PSD4-Z1T8-pX458-REV1 reverse 5'-3' AAACcgaaaggctccggtggatcctc, PSD4-Z2T36-pX458-FOR2 forward 5'-3' CACCgttctctgagcaaggactcgcc, PSD4-Z2T36-pX458-REV2 reverse 5'-3' AAACggcgagtccttgctcagagaac.
HMLE and MCF10-A cells were first transfected with the two plasmids using Lipofectamin 3000 (Invitrogen) according to manufacturer's recommendations. 24 hours later, GFP positive cells were sorted and cloned in 96 wells culture plates using the BD FACSAria III (BD Biosciences). Knock-out and heterozygous clones were screened by immunoblot. Further validation was carried out using the Surveyor® assay (Integrated DNA Technologies) and genomic sequencing of the targeted sequence. Of note, the three different populations of HMLE were sorted according to their expression of EpCAM and CD49f as shown in figure 2 before next-day transfection.

Transient transfection
Transient transfection was performed using RNAiMAX (Invitrogen) according to the manufacturer instructions. All siRNAs were purchased from Dharmacon ON-TARGETplus collection.

Stable transfection
HEK-293T cells were transfected with the human PSD4 containing pLV lentivirus (VB160428-1095xdp – Vector Builder) together with the 3rd generation lentiviral packaging plasmid (Addgene): pMDLG/pRRE (Gag and Pol), pRSV-Rev (Rev), and pMD2.G (VSV-G envelope) using JETPEI (Polypus Transfection). Supernatants containing the lentiviruses were collected at 48h and 72h post-transfection. MCF10-A cells were transduced with the filtered supernatants in the presence of 10 μg/ml of Polybrene (Sigma-Aldrich). Transduced cells were selected with 250 μg/ml of G418 (Sigma).

3D culture
3D culture was performed using Rat tail Collagen I (Corning®). The collagen I solution was neutralized using 1N NaOH and diluted in PBS to a final concentration of 1mg/ml for the contractility assay, and 1.5 mg/ml for the invasion assay, otherwise specified. Matrigel (Corning®) matrix was used alone at 2mg/ml for cell polarization or at 1mg/ml mixed to 1mg/ml collagen matrix to measure invasion.

Contractility assay
70 μl of collagen mixed with human mammary cells (700 cells/μl) were plated in 96-well plates, and incubated for 30 min at 37°C in 5% CO2 before addition of complete medium. The collagen gels were detached from the plastic using a pipet cone. Collagen area was quantified using Image J software.

Invasion assay
Cells transfected with siRNA were plated in collagen 24h after transfection. Human mammary individual cells (100 cells/μl) resuspended in 200 μl of collagen were plated in chambered cover glass (Lab-Tek, Thermo Fisher Scientific), and incubated for 30 min at 37°C in 5% CO2 before addition of complete medium. After 48h, protrusions were quantified using a phase contrast microscope (Leica) by counting 100 cellular aggregates per well. Cells with at least one membrane extension of at least 2 microns' length were considered protrusive.

Immunoblot
Cells grown on plastic dishes were washed 3 times with phosphate buffered saline (PBS) and lysed with a SDS lysis buffer containing 0.5% SDS, 150 mM NaCl, 5 mM EDTA, 20 mM Triethanolamine–HCl pH 8.1, 1 mM PMSF. The lysate was heated at 95°C for 10 minutes and then thoroughly shaken for 15 minutes. After a 20 minutes centrifugation at 16,000 *g* at room temperature, supernatant was transferred into new tubes containing 5 × Laemmli buffer and further boiled 5 min. For protein analysis, cell lysates were loaded into SDS-PAGE and transferred onto a nitrocellulose membrane. Membrane blocking and secondary antibodies dilutions were done in PBS 5% non-fat dry milk, primary antibodies were diluted in PBS containing 3% BSA. The proteins were revealed by chemiluminescence (ECL™, Amersham France) using secondary antibodies directly coupled to HRP. The membranes were analyzed with the luminescent image analyzer Fusion (VILBER, France).

Pull down assay
MCF10-A cells were lysed at 4°C in 0.5% Nonidet P-40, 20 mM Hepes pH 7.4, 125 mM NaCl, 1 mM phenylmethylsulphonyl fluoride (PMSF) and a cocktail of protease inhibitors (Complete, Roche Diagnostics). The cleared lysates containing the protein of interest were incubated 4 h at 4°C with 1.5 μM of the indicated GST-fused proteins and 30 μl of glutathione-sepharose CL-4B beads. After three washes in lysis buffer, the beads were boiled in Laemmli buffer, submitted to SDS–PAGE and the indicated proteins were revealed by immunoblot. To pull-down Arf6GTP, Rac1GTP, Cdc42GTP and RhoAGTP, we fused Gst to the Arf6-GTP binding domain of ARHGAP10, the Cdc42/Rac binding domain of PAK, or the Rho binding domain of Rhotekin, respectively.

RNA isolation and RT-qPCR

Total mRNA was isolated using the Tri Reagent (Sigma-Aldrich) and treated with Ambion™ Dnase I (Invitrogen) following the manufacturers' instructions. 2 μg of total RNAs was denatured at 65°C for 10 min and incubated for 1h at 50°C in the presence of 2.5 mM dNTP, 100 U Superscript III (Invitrogen) using 0.5 μg oligo(dT)15 primer in a total volume of 20 μl, followed by an inactivation step of 15 min at 70°C. A negative control lacking RT enzyme was also performed in each assay (NRT). A control PCR reaction of the reverse transcription was performed with human GAPDH (forward) gaacatcatccctgcatcc, (reverse) ccagtgagcttcccgttca primers with Q5 High fidelity DNA polymerase according to the standard protocol described by the manufacturer (New England BioLabs®). The PCR products obtained after 35 cycles were separated through a 1% agarose gel, visualized under UV after staining with ethidium bromide. Real-time PCR was carried out with The LightCycler® 480 SYBR Green I Master (Roche Life Science) in triplicates and analyzed using LightCycler® 480 Software, Version 1.5 (Roche). The expression of each gene was normalized to the HPRT1 housekeeping gene and relative levels were calculated on the basis of the comparative cycle threshold Ct method (2-ΔΔCt) where ΔΔCt is the difference in Ct between target and reference gene.

Flow cytometry

Cells were detached using Accutase (STEMCELL technology) and washed 3 times in PFE (PBS, 2mM EDTA, 2% Foetal Bovine Serum). The cells were incubated at 4°C for 30 minutes in the presence of the indicated antibodies diluted in PFE. After washes, cells resuspended in cold PFE were examined by BD LSRII Fortessa™ cell analyser. Results were processed using Kaluza or FlowJo softwares.

Fluorescent gelatin degradation assay

Oregon Green 488-labeled gelatin was obtained from Molecular Probes. Sterilized coverslips (18-mm diameter) were coated with 50 μg/ml poly-L-lysine for 20 min at RT, washed with PBS, and fixed with 0.5% glutaraldehyde for 10 minutes. After 3 washes with PBS coverslips were inverted on a 40-μl drop of 0.2% fluorescently labeled gelatin in 2% sucrose in PBS and incubated for 10 min at RT. After washing with PBS, coverslips were incubated in a 5mg/ml solution of borohydride for 3 min, washed three times in PBS, and incubated with 1 ml of complete medium for 30 minutes. 5 x 10^4 cells per 12-well were plated on the fluorescent gelatin-coated coverslips and incubated at 37°C for 48 h. Cells were then washed three times with PBS and fixed with 4% PFA for 20 minutes and processed for labeling with Texas Red-Phalloidin and DAPI. The coverslips were mounted with Mowiol mounting medium. Cells were imaged on a confocal microscope (Leica TCS-SP5). For the quantification of the gelatin degradation, the total area of degraded matrix measured with ImageJ software was divided by the total area of each phalloidin-labeled cell. A total of 90 cells were analyzed in three independent experiments.

Quantification of cellular collagenolysis

2 x 10^4 MCF10A cells were re-suspended in 0.2 ml of 2 mg/ml collagen I solution loaded on an LabTek 8-well chambered cover-glass. After gelling for 1 h at 37°C, a complete DMEM-F12 medium was added, and collagen-embedded cells were incubated 48 h at 37°C in 1% CO_2. After fixation in 4% PFA for 20 min, samples were incubated with collagen type I cleavage site antibody (Col1-2/3 C) diluted 1:200 in PBS (5 μg/ml, 24 h at 4°C), washed extensively with PBS, and counterstained with Cy5-conjugated anti-rabbit IgG antibodies, DAPI and Texas Red-phalloidin. Images acquisition was performed with a confocal microscope (Leica TCS-SP5) with a 60x oil objective. Quantification of degradation spots was performed with a homemade ImageJ program as described by Marchesin et al., 2015. The degradation index is the number of degradation spots divided by the number of cells in each cluster present in the field. A total of 90 cells clusters were counted in 3 independent experiments.

Integrin antibody blocking assay

MCF10A cells were detached using trypsin, washed with PBS and re-suspended in complete DMEM-F12 medium. The cells were then incubated for 30 min at 37°C to allow for recovery of cell surface receptors. 5 x 10^4 cells were re-suspended in 0.2 μl of a 2 mg/ml collagen I solution and control or

blocking antibodies were added. Cell suspension was loaded on an 8-well Lab-tek chambered cover-glass and left to gelify for 1 h at 37°C. Complete DMEM-F12 medium containing the control or blocking antibodies was added on top of collagen-embedded cells. The samples were incubated 48 h at 37°C in 1% CO_2. The development of protrusions was quantified as described above by counting 100 cell clusters, in 3 independent experiments.

Immunofluorescence

Cells were fixed in 4% paraformaldehyde for 20 minutes, washed three times in PBS and permeabilized in PBS containing 0.05% saponin, 0.5% horse serum for 30 min at 37°C. Then the cells were incubated with primary antibodies over-night and counterstained with appropriate fluorescent secondary antibodies, DAPI or phalloidin. Images acquisition was performed with a confocal microscope (Leica TCS-SP5) with a 60x oil objective.

Confocal reflectance microscopy

MCF10A spheroids were embedded in collagen I for 48 h at 37°C, then spheroids were fixed and IF was performed as indicated above. The imaging of the orientation of the collagen matrix fibers was performed by confocal reflectance microscopy using a scanning confocal microscope (Leica TCS-SP5). The collagen gels were excited with 488 nm laser, and signal between 485 nm and 495 nm was collected.

Statistics

Experiments were performed at least three times independently. The number of repeats is indicated in the legend as (n). Error bars represent ± standard error of the mean (S.E.M) or standard deviation (SD) as indicated in the legend. Statistical significance was determined using a Student *t*-test and one-way ANOVA, in which *P* values < 0.05 were considered statistically significant. All statistical analyses have been performed with GraphPad Prism software.

References

1. Alexander, N.R., Branch, K.M., Parekh, A., Clark, E.S., Iwueke, I.C., Guelcher, S.A., and Weaver, A.M. (2008). Extracellular Matrix Rigidity Promotes Invadopodia Activity. Curr. Biol. *18*, 1295–1299.

2. Berger, A.H., Knudson, A.G., and Pandolfi, P.P. (2011). A continuum model for tumour suppression. Nature *476*, 163–169.

3. Bonnans, C., Chou, J., and Werb, Z. (2014). Remodelling the extracellular matrix in development and disease. Nat. Rev. Mol. Cell Biol. *15*, 786–801.

4. Bray, F., Ferlay, J., Soerjomataram, I., Siegel, R.L., Torre, L.A., and Jemal, A. (2018). Global cancer statistics 2018: GLOBOCAN estimates of incidence and mortality worldwide for 36 cancers in 185 countries. CA. Cancer J. Clin. *68*, 394–424.

5. Bray, K., Gillette, M., Young, J., Loughran, E., Hwang, M., Sears, J.C., and Vargo-Gogola, T. (2013). Cdc42 overexpression induces hyperbranching in the developing mammary gland by enhancing cell migration. Breast Cancer Res. *15*.

6. Bryant, D.M., and Mostov, K.E. (2008). From cells to organs: building polarized tissue. Nat. Rev. Mol. Cell Biol. *9*, 887–901.

7. Castro-Castro, A., Marchesin, V., Monteiro, P., Lodillinsky, C., Rossé, C., and Chavrier, P. (2016). Cellular and Molecular Mechanisms of MT1-MMP-Dependent Cancer Cell Invasion. Annu. Rev. Cell Dev. Biol. *32*, 555–576.

8. Cavallaro, U., and Dejana, E. (2011). Adhesion molecule signalling: not always a sticky business. Nat. Rev. Mol. Cell Biol. *12*, 189–197.

9. Cheung, K.J., and Ewald, A.J. (2014). Illuminating breast cancer invasion: diverse roles for cell-cell interactions. Curr. Opin. Cell Biol. *30*, 99–111.

10. Cheung, K.J., Gabrielson, E., Werb, Z., and Ewald, A.J. (2013). Collective Invasion in Breast Cancer Requires a Conserved Basal Epithelial Program. Cell *155*, 1639–1651.

11. Drost, J., and Clevers, H. (2018). Organoids in cancer research. Nat. Rev. Cancer *18*, 407.

12. Dubois, T., Paléotti, O., Mironov Jr, A.A., Fraisier, V., Stradal, T.E.B., De Matteis, M.A., Franco, M., and Chavrier, P. (2005). Golgi-localized GAP for Cdc42 functions downstream of ARF1 to control Arp2/3 complex and F-actin dynamics. Nat. Cell Biol. *7*, 353–364.

13. Eddy, R.J., Weidmann, M.D., Sharma, V.P., and Condeelis, J.S. (2017). Tumor Cell Invadopodia: Invasive Protrusions that Orchestrate Metastasis. Trends Cell Biol. *27*, 595–607.

14. Elenbaas, B., Spirio, L., Koerner, F., Fleming, M.D., Zimonjic, D.B., Donaher, J.L., Popescu, N.C., Hahn, W.C., and Weinberg, R.A. (2001). Human breast cancer cells generated by oncogenic transformation of primary mammary epithelial cells. Genes Dev. *15*, 50–65.

15. Ewald, A.J., Huebner, R.J., Palsdottir, H., Lee, J.K., Perez, M.J., Jorgens, D.M., Tauscher, A.N., Cheung, K.J., Werb, Z., and Auer, M. (2012). Mammary collective cell migration involves transient

loss of epithelial features and individual cell migration within the epithelium. J. Cell Sci. *125*, 2638–2654.

16. Feinberg, T.Y., Rowe, R.G., Saunders, T.L., and Weiss, S.J. (2016). Functional roles of MMP14 and MMP15 in early postnatal mammary gland development. Dev. Camb. Engl. *143*, 3956–3968.

17. Feinberg, T.Y., Zheng, H., Liu, R., Wicha, M.S., Yu, S.M., and Weiss, S.J. (2018). Divergent Matrix-Remodeling Strategies Distinguish Developmental from Neoplastic Mammary Epithelial Cell Invasion Programs. Dev. Cell *47*, 145-160.e6.

18. Fletcher Alexander G., Cooper Fergus, and Baker Ruth E. (2017). Mechanocellular models of epithelial morphogenesis. Philos. Trans. R. Soc. B Biol. Sci. *372*, 20150519.

19. Friedl, P., and Gilmour, D. (2009). Collective cell migration in morphogenesis, regeneration and cancer. Nat. Rev. Mol. Cell Biol. *10*, 445–457.

20. Fritz, G., Just, I., and Kaina, B. (1999). Rho GTPases are over-expressed in human tumors. Int. J. Cancer *81*, 682–687.

21. Fritz, G., Brachetti, C., Bahlmann, F., Schmidt, M., and Kaina, B. (2002). Rho GTPases in human breast tumours: expression and mutation analyses and correlation with clinical parameters. Br. J. Cancer *87*, 635–644.

22. Ghajar, C.M., and Bissell, M.J. (2008). Extracellular matrix control of mammary gland morphogenesis and tumorigenesis: insights from imaging. Histochem. Cell Biol. *130*, 1105–1118.

23. Heerboth, S., Housman, G., Leary, M., Longacre, M., Byler, S., Lapinska, K., Willbanks, A., and Sarkar, S. (2015). EMT and tumor metastasis. Clin. Transl. Med. *4*, 6.

24. Howard, B.A., and Lu, P. (2014). Stromal regulation of embryonic and postnatal mammary epithelial development and differentiation. Semin. Cell Dev. Biol. *25–26*, 43–51.

25. Klein, S., Partisani, M., Franco, M., and Luton, F. (2008). EFA6 Facilitates the Assembly of the Tight Junction by Coordinating an Arf6-dependent and -independent Pathway. J. Biol. Chem. *283*, 30129–30138.

26. Ladoux, B., and Mège, R.-M. (2017). Mechanobiology of collective cell behaviours. Nat. Rev. Mol. Cell Biol. *18*, 743–757.

27. Lecuit, T., and Le Goff, L. (2007). Orchestrating size and shape during morphogenesis. Nature *450*, 189–192.

28. Li, R., Peng, C., Zhang, X., Wu, Y., Pan, S., and Xiao, Y. (2017). Roles of Arf6 in cancer cell invasion, metastasis and proliferation. Life Sci. *182*, 80–84.

29. Loskutov, Y.V., Kozyulina, P.Y., Kozyreva, V.K., Ice, R.J., Jones, B.C., Roston, T.J., Smolkin, M.B., Ivanov, A.V., Wysolmerski, R.B., and Pugacheva, E.N. (2015). NEDD9/Arf6-dependent endocytic trafficking of matrix metalloproteinase 14: a novel mechanism for blocking mesenchymal cell invasion and metastasis of breast cancer. Oncogene *34*, 3662–3675.

30. Luton, F., Klein, S., Chauvin, J.-P., Le Bivic, A., Bourgoin, S., Franco, M., and Chardin, P. (2003). EFA6, Exchange Factor for ARF6, Regulates the Actin Cytoskeleton and Associated Tight Junction in Response to E-Cadherin Engagement. Mol. Biol. Cell *15*, 1134–1145.

31. Macias, H., and Hinck, L. (2012). Mammary gland development: Mammary gland development. Wiley Interdiscip. Rev. Dev. Biol. *1*, 533–557.

32. Marchesin, V., Castro-Castro, A., Lodillinsky, C., Castagnino, A., Cyrta, J., Bonsang-Kitzis, H., Fuhrmann, L., Irondelle, M., Infante, E., Montagnac, G., et al. (2015). ARF6–JIP3/4 regulate endosomal tubules for MT1-MMP exocytosis in cancer invasion. J Cell Biol *211*, 339–358.

33. Martin, P., and Parkhurst, S.M. (2004). Parallels between tissue repair and embryo morphogenesis. Dev. Camb. Engl. *131*, 3021–3034.

34. Martín-Belmonte, F., and Rodríguez-Fraticelli, A.E. (2009). Chapter 3 Acquisition of Membrane Polarity in Epithelial Tube Formation: Patterns, Signaling Pathways, Molecular Mechanisms, and Disease. In International Review of Cell and Molecular Biology, (Academic Press), pp. 129–182.

35. Milanini, J., Fayad, R., Partisani, M., Lecine, P., Borg, J.-P., Franco, M., and Luton, F. (2018). EFA6 proteins regulate lumen formation through α-actinin 1. J Cell Sci *131*, jcs209361.

36. Monteiro, P., Rossé, C., Castro-Castro, A., Irondelle, M., Lagoutte, E., Paul-Gilloteaux, P., Desnos, C., Formstecher, E., Darchen, F., Perrais, D., et al. (2013). Endosomal WASH and exocyst complexes control exocytosis of MT1-MMP at invadopodia. J. Cell Biol. *203*, 1063–1079.

37. Morishige, M., Hashimoto, S., Ogawa, E., Toda, Y., Kotani, H., Hirose, M., Wei, S., Hashimoto, A., Yamada, A., Yano, H., et al. (2008). GEP100 links epidermal growth factor receptor signalling to Arf6 activation to induce breast cancer invasion. Nat. Cell Biol. *10*, 85–92.

38. Neve, R.M., Chin, K., Fridlyand, J., Yeh, J., Baehner, F.L., Fevr, T., Clark, L., Bayani, N., Coppe, J.-P., Tong, F., et al. (2006). A collection of breast cancer cell lines for the study of functionally distinct cancer subtypes. Cancer Cell *10*, 515–527.

39. Nguyen-Ngoc, K.-V., Cheung, K.J., Brenot, A., Shamir, E.R., Gray, R.S., Hines, W.C., Yaswen, P., Werb, Z., and Ewald, A.J. (2012). ECM microenvironment regulates collective migration and local dissemination in normal and malignant mammary epithelium. Proc. Natl. Acad. Sci. *109*, E2595–E2604.

40. Nik-Zainal, S., and Morganella, S. (2017). Mutational Signatures in Breast Cancer: The Problem at the DNA Level. Clin. Cancer Res. Off. J. Am. Assoc. Cancer Res. *23*, 2617–2629.

41. Parekh, A., and Weaver, A.M. (2016). Regulation of invadopodia by mechanical signaling. Exp. Cell Res. *343*, 89–95.

42. Pastushenko, I., Brisebarre, A., Sifrim, A., Fioramonti, M., Revenco, T., Boumahdi, S., Van Keymeulen, A., Brown, D., Moers, V., Lemaire, S., et al. (2018). Identification of the tumour transition states occurring during EMT. Nature *556*, 463–468.

43. Poincloux, R., Lizárraga, F., and Chavrier, P. (2009). Matrix invasion by tumour cells: a focus on MT1-MMP trafficking to invadopodia. J Cell Sci *122*, 3015–3024.

44. Rihet, S., Vielh, P., Camonis, J., Goud, B., Chevillard, S., and Gunzburg, J. (2001). Mutation status of genes encoding RhoA, Rac1, and Cdc42 GTPases in a panel of invasive human colorectal and breast tumors. J. Cancer Res. Clin. Oncol. *127*, 733–738.

45. Sabe, H., Hashimoto, S., Morishige, M., Ogawa, E., Hashimoto, A., Nam, J.-M., Miura, K., Yano, H., and Onodera, Y. (2009). The EGFR-GEP100-Arf6-AMAP1 Signaling Pathway Specific to Breast Cancer Invasion and Metastasis†. Traffic *10*, 982–993.

46. Sakakura, T., Suzuki, Y., and Shiurba, R. (2013). Mammary stroma in development and carcinogenesis. J. Mammary Gland Biol. Neoplasia *18*, 189–197.

47. Shamir, E.R., and Ewald, A.J. (2015). Adhesion in Mammary Development. In Current Topics in Developmental Biology, (Elsevier), pp. 353–382.

48. Smilenov, L.B. (2006). Tumor development: Haploinsufficiency and local network assembly. Cancer Lett. *240*, 17–28.

49. Stengel, K., and Zheng, Y. (2011). Cdc42 in oncogenic transformation, invasion, and tumorigenesis. Cell. Signal. *23*, 1415–1423.

50. Théard, D., Labarrade, F., Partisani, M., Milanini, J., Sakagami, H., Fon, E.A., Wood, S.A., Franco, M., and Luton, F. (2010). USP9x-mediated deubiquitination of EFA6 regulates de novo tight junction assembly. EMBO J. *29*, 1499–1509.

51. Thiery, J.P., Acloque, H., Huang, R.Y.J., and Nieto, M.A. (2009). Epithelial-Mesenchymal Transitions in Development and Disease. Cell *139*, 871–890.

52. Torres, E., and Rosen, M.K. (2006). Protein-tyrosine Kinase and GTPase Signals Cooperate to Phosphorylate and Activate Wiskott-Aldrich Syndrome Protein (WASP)/Neuronal WASP. J. Biol. Chem. *281*, 3513–3520.

53. Vicente-Manzanares, M., Ma, X., Adelstein, R.S., and Horwitz, A.R. (2009). Non-muscle myosin II takes centre stage in cell adhesion and migration. Nat. Rev. Mol. Cell Biol. *10*, 778–790.

54. Wilkinson, S., Paterson, H.F., and Marshall, C.J. (2005). Cdc42–MRCK and Rho–ROCK signalling cooperate in myosin phosphorylation and cell invasion. Nat. Cell Biol. *7*, 255–261.

55. Yamaguchi, H., Lorenz, M., Kempiak, S., Sarmiento, C., Coniglio, S., Symons, M., Segall, J., Eddy, R., Miki, H., Takenawa, T., et al. (2005). Molecular mechanisms of invadopodium formation: the role of the N-WASP-Arp2/3 complex pathway and cofilin. J. Cell Biol. *168*, 441–452.

56. Zangari, J., Partisani, M., Bertucci, F., Milanini, J., Bidaut, G., Berruyer-Pouyet, C., Finetti, P., Long, E., Brau, F., Cabaud, O., et al. (2014). EFA6B Antagonizes Breast Cancer. Cancer Res. *74*, 5493–5506.

57. Zegers, M.M., and Friedl, P. (2014). Rho GTPases in collective cell migration. Small GTPases *5*, e983869.

58. Zobel, M., Disanza, A., Senic-Matuglia, F., Franco, M., Colaluca, I.N., Confalonieri, S., Bisi, S., Barbieri, E., Caldieri, G., Sigismund, S., et al. (2018). A NUMB–EFA6B–ARF6 recycling route controls apically restricted cell protrusions and mesenchymal motility. J Cell Biol *217*, 3161–3182.

Figure legends

Fig1: CRISPR/Cas9-mediated knock-out of the EFA6B encoding gene *PSD4* in MCF10A cells induces collective invasion in collagen I. **A**) The MCF10A WT, the homozygous EFA6B KO 55, EFA6B KO 50, EFA6B KO 2, the heterozygous EFA6B KO 2.9 and the EFA6B KO 55 over-expressing EFA6B-vsvg cells (Rescue) were solubilized in SDS-lysis buffer and the expression of the indicated proteins analyzed by immunoblot. Actin served as a loading control **B**) Representative images of the MCF10A WT, the homozygous EFA6B KO 55, the heterozygous EFA6B KO 2.9 and the EFA6B KO 55 over-expressing EFA6B-vsvg placed in collagen for 7 days (upper panels) or 2 days (middle and bottom panels). The cells were processed for immunofluorescence to label the endogenous F-actin (red) and the nuclei (blue). The bottom panels are brightfield phase contrast images of the corresponding immunofluorescence images shown in the middle panels. Scale bars 20 μm. **C**) Lysates of MCF10A WT and EFA6B KO 55 cells were reacted with Gst or Gst-ABD (Arf6GTP-binding domain of ARHGAP10) prebound to glutathione-sepharose beads. The whole lysates and bound proteins were analyzed by immunoblotting with an anti-Arf6 antibody. **D**) Quantification of the percentage of cell aggregates with invasive protrusions of the indicated cell lines grown in collagen for 2 days. n=6, average ±SD, Student's *t*-test *p* values were ****, $p < 0.0001$.

Fig2: CRISPR/Cas9-mediated knock-out of the EFA6B encoding gene *PSD4* in HMLE sub-populations induces collective invasion in collagen I. **A**) The cell surface marker EpCAM and CD49f were used to sort three epithelial cell populations including the luminal, luminal progenitors and mature basal cells. These cells were immediately processed for CRISPR/Cas9-mediated *PSD4* knock-out. **B**) The HMLE WT population, the luminal progenitor WT clone 23, heterozygous EFA6B KO 25, homozygous EFA6B KO 3 and the mature basal WT clone 2", homozygous EFA6B-KO 1" cells were solubilized in SDS-lysis buffer and the expression of the indicated proteins analyzed by immunoblot. Actin served as a loading control. **C**) Representative images of the indicated cells grown 5 days in collagen I are shown. The cells were processed for immunofluorescence to label the endogenous F-actin (red) and the nuclei (blue). Scale bars 20 μm. **D**) Quantification of the percentage of cell aggregates with invasive protrusions of the indicated cell lines grown in collagen I for 5 days. n=3, average ±SD, Student's *t*-test *p* values were * $p < 0.05$; **, $p < 0.01$.

Fig3: EFA6B knock-out stimulates matrices degradation and invasion in a MMP14-dependent manner, and leads to loss of collective apico-basal polarization in 3D-Matrigel. **A**) Representative images of MCF10WT and EFA6B KO 55 cells placed on Oregon488-gelatin (green) coated coverslips and stained for F-actin (red) and nuclei (blue). Areas devoid of fluorescent signal indicate degradation of the fluorescent gelatin. Scale bars 20 μm. **B**) Quantification of the gelatin degradation. Values are mean degradation area per cell ± SEM. 90 cells were analyzed for each cell population in three independent experiments. ****, $p < 0.0001$. **C**) Representative images of MCF10WT and EFA6B KO 55 cells grown in collagen I for 3 days and stained for cleaved collagen I with the Col1-$^{3/4}$C antibody (white in middle panel and green in left merge panel). The cells were also labelled for F-actin (red) and nuclei (blue). Scale bars 20 μm. **D**) Quantification of the collagen degradation. Values are mean degradation index ± SEM. 90 cells were analyzed for each cell population in three independent experiments. ***, $p < 0.001$. **E**) MCF10A WT and EFA6B KO 55 cells were solubilized in SDS-lysis buffer and the expression of MMP14 analyzed by immunoblot. Hsp60 served as a loading control. **F**) MCF10A WT and EFA6B-KO 55 cells were transfected with siRNA control or directed against MMP14. 48 h post-transfection, the cells were solubilized in SDS lysis buffer and the expression of MMP14 was analyzed by immunoblot. Hsp60

served as a loading control. **G**) Quantification of the percentage of cell aggregates with invasive protrusions of the indicated cell lines grown in collagen I for 2 days. n=4, ****, *p < 0.0001*. **H**) Quantification of the percentage of cell aggregates with membrane and cell protrusions of the indicated cell lines grown in collagen I (1mg/ml) or collagen I/Matrigel (1:1, 1mg/ml) for 4 days. n=3, *, *p < 0.05*; **, *p < 0.01*; ***, *p < 0.001*. Right panels show representative images of MCF10WT and EFA6B KO 55 cell aggregates grown in collagen I/Matrigel. Arrow points toward a cell protrusion and arrowheads to membrane protrusions. **I**) Representative images of MCF10A WT and EFA6B KO 55 cells grown 5 days in Matrigel (2mg/ml). Arrow points to the central lumen (L) only visible in MCF10A WT cell aggregates.

Fig4: EFA6B knock-out promotes a change in the integrin (ITG) repertoire and stimulates the formation of ITGB1-based degradative invadopodia. **A**) Cell surface expression of ITG molecules in MCF10A WT and EFA6B KO 55 cells analyzed by FACS. **B**) Quantification of MCF10A WT and EFA6B-KO 55 cell aggregates with invasive protrusions incubated in the presence of pre-immune serum (Ctl) or the indicated anti-ITG antibodies for 2 days. Values are percentages of total cell aggregates ± SD. 300 cell aggregates were analyzed for each cell population in three independent experiments. *, *p < 0.05*; **, *p < 0.01*. **C**, **D**) MCF10A WT and EFA6B KO 55 cells were solubilized in SDS-lysis buffer and the expression of ITGB1 and ITGB4 (**C**), or LAMγ2, LAMβ1 and fibronectin (FN) (**D**) analyzed by immunoblot. Hsp60 served as a loading control. **E**) Representative images of the indicated spheroids grown 2 days in collagen I are shown. The spheroids were processed for immunofluorescence to label the indicated ITG. Scale bars 20 μm. **F**) Representative images of the indicated cells grown 2 days on coverslips coated with Oregon488-gelatin (green) are shown. The cells were processed for immunofluorescence to label cortactin (blue) and F-actin (red). Co-localization in large dots of both markers appears as a pink staining at the periphery of EFA6B-KO cells within areas of Oregon488-gelatin degradation. Scale bars 20 μm. **G**, **H**) Representative images of the indicated cells grown 2 days on collagen I-coated coverslips are shown. The cells were processed for immunofluorescence to label cortactin (blue) and MMP14-mCherry (red) (**G**), or ITGB1 (blue) and MMP14-mCherry (red) (**H**). Co-localization of the markers appears as an intense pink staining in EFA6B KO 55 cells. Scale bars 20 μm. **I**) Representative images of the indicated spheroids grown 4 days in collagen I are shown. The cells were processed for immunofluorescence to label the indicated LAM (green) and the nuclei (blue). Arrows point to the absence of LAM staining where EFA6B KO 55 cells invade the collagen I. Scale bars 20 μm.

Fig5: EFA6B knock-out induces the expression of EMT transcription factors that promote collective invasion of MCF10A and HMLE WT cells in collagen I. **A**) The MCF10A WT, the homozygous EFA6B KO 55, EFA6B-KO 50, EFA6B-KO 2 and the heterozygous EFA6B KO 2.9 cells were solubilized in SDS-lysis buffer and the expression of the indicated proteins analyzed by immunoblot. Actin served as a loading control. **B**) The HMLE WT population, the luminal progenitor WT clone 23, heterozygous EFA6B KO 25, homozygous EFA6B KO 3 and the mature basal WT clone 2", homozygous EFA6B-KO 1" cells were solubilized in SDS-lysis buffer and the expression of the indicated proteins analyzed by immunoblot. Actin served as a loading control. **C**) Representative images of the indicated spheroids grown 2 days in collagen I are shown. The cells were processed for immunofluorescence to label E-cadherin or N-cadherin. Scale bars 20 μm. **D**) Representative brightfield phase contrast images of the indicated cells grown 2 days in hanging-drops are shown. Scale bars 20 μm. **E**) The MCF10A WT (blue) and EFA6B-KO 55 (green) cells were labeled for the cell surface markers EpCAM and CD49f. The red dotted line circles a new de-differentiated population $EpCAM^{-/low}$ and $CD49f^{low}$ (11.7%) appearing in the EFA6B KO 55 cell line. **F**) Expression of EMT-associated genes by qPCR analysis in EFA6B KO 55 cells normalized to MCF10A WT. **G**) Quantification of the percentage of aggregates with invasive protrusions of MCF10A WT and EFA6B KO 55 cells grown in collagen I for 2 days after transfection of the indicated siRNAs. n=3,

average ±SD, Student's *t*-test *p* values were * *p < 0.05*; **, *p < 0.01*; ****, *p < 0.0001*, non-significant (ns). **H**) Expression of the indicated EMT-TF genes by qPCR analysis 2 days after transfection of their corresponding specific siRNAs in EFA6B KO 55 cells normalized to siCtl. Folds < 1 represent a downregulation of gene expression and folds > 1 represent an upregulation of the corresponding gene compared to WT cells gene expression.

Fig6: EFA6B knock-out stimulates cellular contractility and invasion through Cdc42. **A**) Representative images of the MCF10A WT and EFA6B KO 55 spheroids embedded 2 days in collagen I are shown. The cells were processed for immunofluorescence to label F-actin (red). The organization of the collagen I fibers surrounding the cell aggregates was imaged by confocal reflectance microscopy (green). Scale bars 20 μm. **B**) Quantification of the contractility of MCF10A WT (WT) and EFA6B KO 55 (KO) cells transfected with a control siRNA, and EFA6B KO 55 cells transfected with the indicated siRNA evaluated by a collagen gel contraction assay. Values are mean surface area of the collagen gel ± SEM. n=3, Student's *t*-test *p* values were * *p < 0.05*; ** *p < 0.01*. **C**) MCF10A WT and EFA6B KO 55 cells were solubilized in SDS-lysis buffer and the expression of pMLC and total MLC analyzed by immunoblot. **D**) Two days post-transfection with the indicated siRNAs, EFA6B KO 55 cells were solubilized in SDS-lysis buffer and the expression of the corresponding protein analyzed by immunoblot. Hsp60 served as a loading control. **E**) Quantification of the percentage of aggregates with invasive protrusions of EFA6B KO 55 cells grown in collagen I for 2 days after transfection of the indicated siRNAs. n=3, average ±SD, Student's *t*-test *p* values were **** *p < 0.0001*: ns: non-significant. **F**) Lysates of MCF10A WT and EFA6B KO 55 cells were reacted with Gst, Gst-CRIB (Cdc42GTP- and Rac1GTP-intercating domain of PAK) or Gst-RBD (RhoGTP-binding domain of rhotekin) prebound to glutathione-sepharose beads. The whole lysates and bound proteins were analyzed by immunoblotting with the indicated antibodies.

Fig7: EFA6B knock-out stimulates cellular contractility and invasion through two Cdc42-dependent signaling pahways: Cdc42-MRCK-pMLC and Cdc42-N-WASP-Arp2/3. **A**) Left upper panel: Expression of MRCKα and MRCKβ genes by qPCR analysis 2 days after transfection of their corresponding specific siRNAs alone or in combination in EFA6B KO 55 cells normalized to siCtl. siMRCKα+β/α indicates the gene expression level of MRCKα after transfection of siRNAs against both MRCKs. siMRCKα+β/β indicates the gene expression level of MRCKβ after transfection of siRNAs against both MRCKs. Right upper panel: two days post-transfection with the indicated siRNAs as in left panel, EFA6B-KO 55 cells were solubilized in SDS-lysis buffer and the expression of pMLC and total MLC was analyzed by immunoblot. Bottom panel: quantification of the percentage of aggregates with invasive protrusions of EFA6B KO 55 cells grown in collagen I for 2 days after transfection of the indicated siRNAs. n=3, average ±SD, Student's *t*-test *p* values were * *p < 0.05*. **B**) Upper panel: two days post-transfection with the indicated siRNAs, EFA6B KO 55 cells were solubilized in SDS-lysis buffer. The down-regulation of MLCK and the expression of pMLC compared to total MLC was analyzed by immunoblot. The p85 regulatory subunit of the PI3K served as a loading control. Bottom panel: quantification of the percentage of aggregates with invasive protrusions of EFA6B KO 55 cells grown in collagen I for 2 days after transfection of the indicated siRNAs as in the upper panel. n=3, average ±SD, Student's *t*-test *p* values were non-significant (ns). **C**) two days post-transfection with the indicated siRNAs directed against ROCK1, ROCK2 or both (ROCK1+2), EFA6B KO 55 cells were solubilized in SDS-lysis buffer. The expression of the proteins ROCK1 and ROCK2 compared to the loading control hsp60, as well as pMLC compared to total MLC was analyzed by immunoblot. Right panel: quantification of the percentage of aggregates with invasive protrusions of EFA6B KO 55 cells grown in collagen I for 2 days after transfection of the indicated siRNAs as in the upper panel. n=3, average ±SD, Student's *t*-test *p* values were non-significant (ns). **D**) Left panel: two days post-transfection with N-WASP targeted siRNAs, EFA6B KO 55 cells were solubilized in SDS-lysis buffer. The

down-regulation of N-WASP was analyzed by immunoblot. Actin served as a loading control. Right panel: quantification of the percentage of aggregates with invasive protrusions of EFA6B KO 55 cells grown in collagen I for 2 days after transfection of N-WASP-directed siRNAs. n=3, average ±SD, Student's *t*-test *p* values were ** $p < 0.01$; ***, $p < 0.001$). **E**) Right panels: two days post-transfection with a specific Arp2/3 siRNA, EFA6B KO 55 cells were solubilized in SDS-lysis buffer. The down-regulation of Arp2/3 was analyzed by immunoblot. Hsp60 served as a loading control. Quantification of the percentage of aggregates with invasive protrusions of EFA6B KO 55 cells grown in collagen I for 2 days after transfection. n=3, average ±SD.

Figure 1

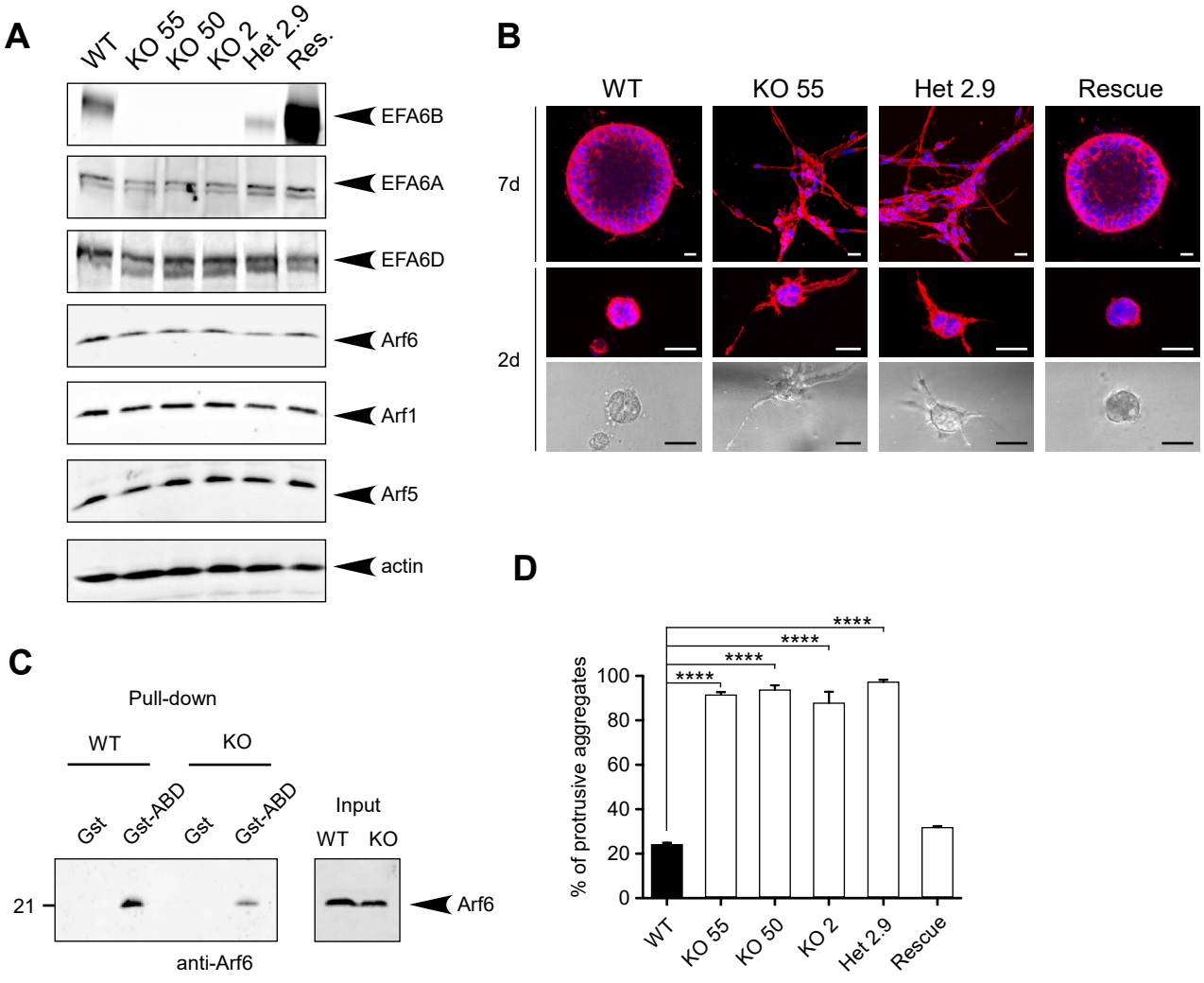
A
WT
KO 55
KO 50
KO 2
Het 2.9
Res.
EFA6B
EFA6A
EFA6D
Arf6
Arf1
Arf5
actin
B
WT
KO 55
Het 2.9
Rescue
7d
2d
C
Pull-down
WT
KO
Gst
Gst-ABD
Gst
Gst-ABD
Input
WT
KO
21
Arf6
anti-Arf6
D
% of protrusive aggregates
100
80
60
40
20
0
****
****
****
****
WT
KO 55
KO 50
KO 2
Het 2.9
Rescue

Figure 2

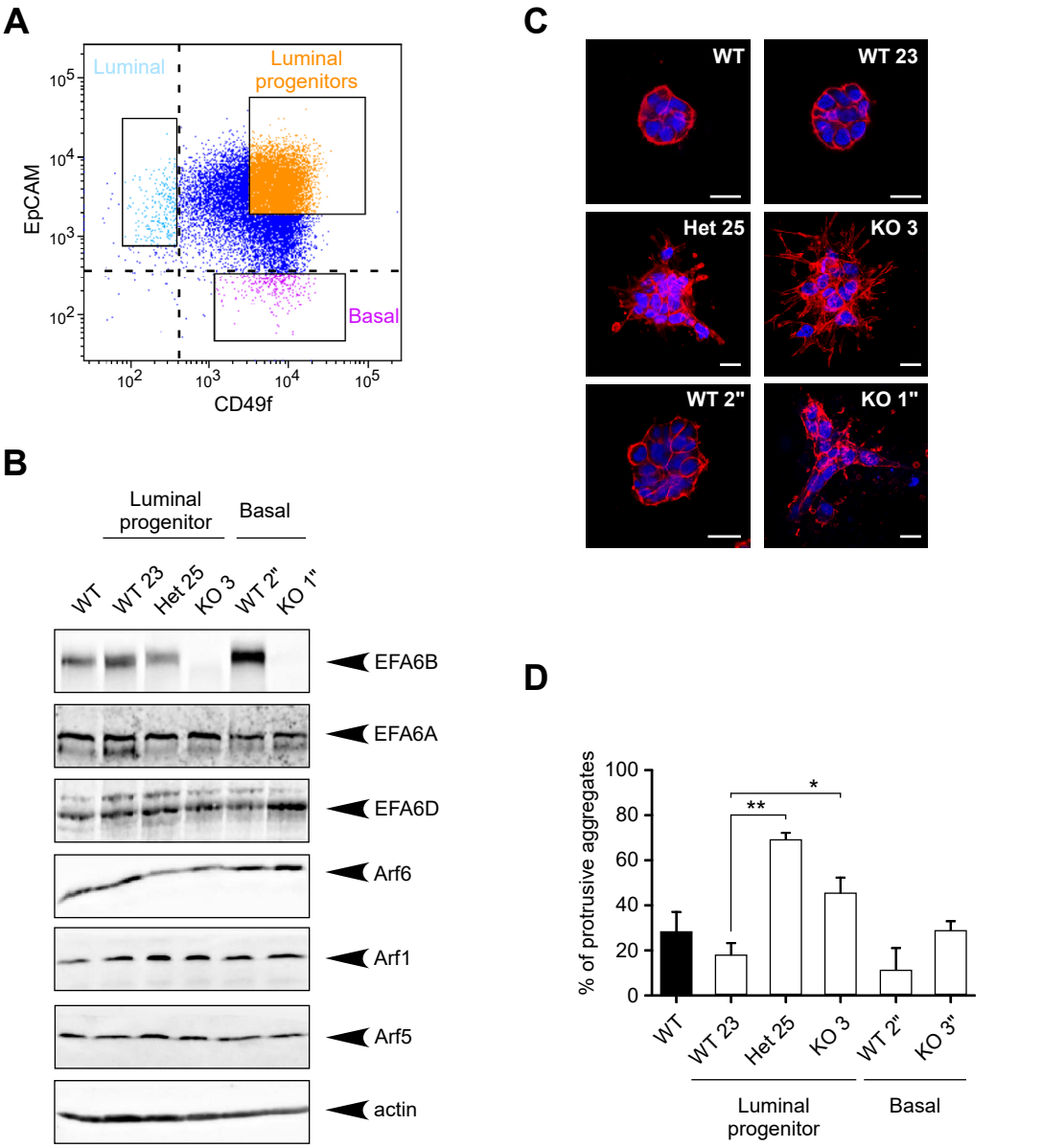
A
Luminal
Luminal progenitors
Basal
EpCAM
CD49f
B
Luminal progenitor
Basal
WT
WT 23
Het 25
KO 3
WT 2"
KO 1"
EFA6B
EFA6A
EFA6D
Arf6
Arf1
Arf5
actin
C
WT
WT 23
Het 25
KO 3
WT 2"
KO 1"
D
% of protrusive aggregates
Luminal progenitor
Basal
KO 3"

Figure 3

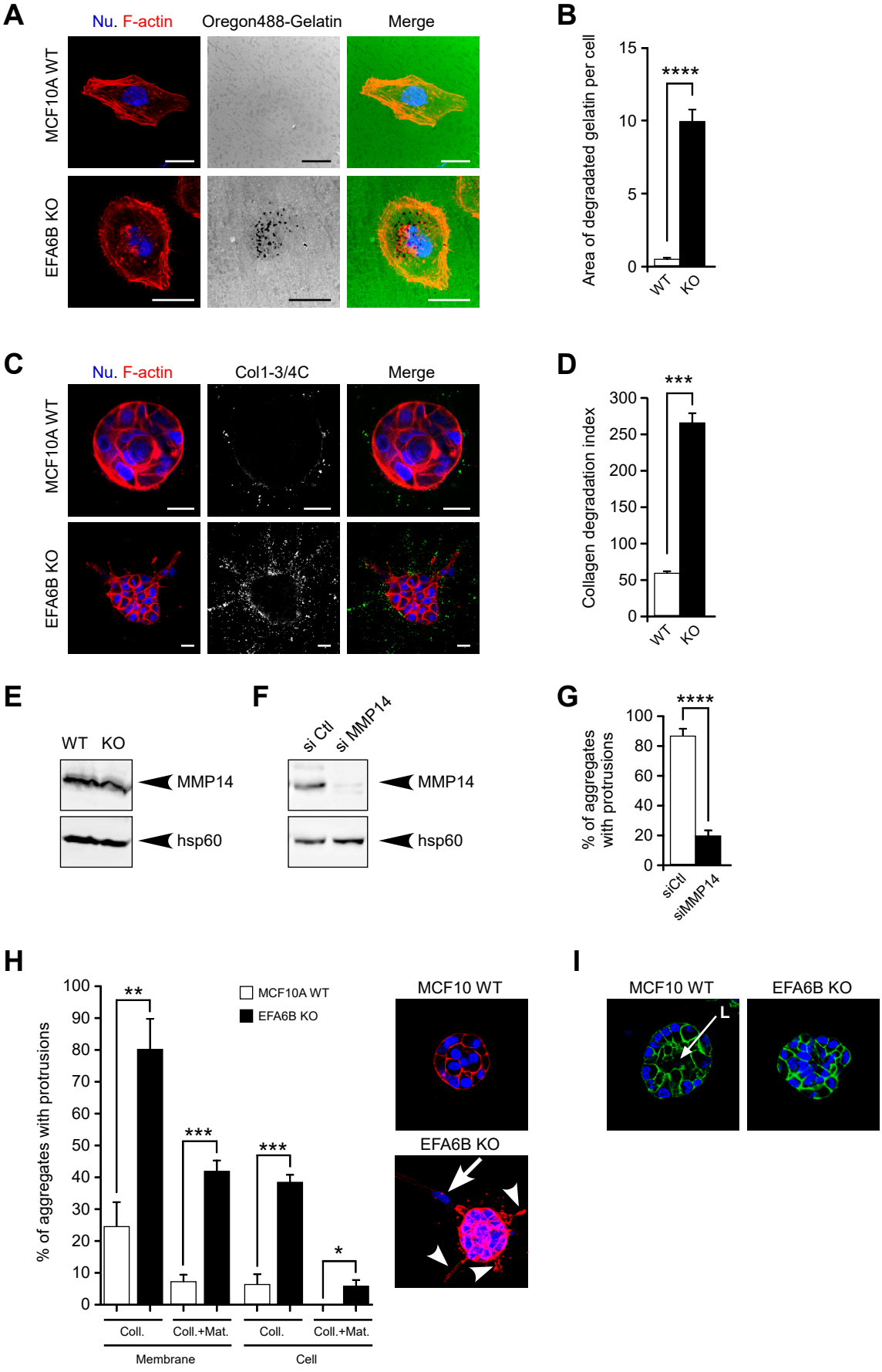
A
Nu. F-actin
Oregon488-Gelatin
Merge
MCF10A WT
EFA6B KO
B
Area of degradated gelatin per cell
****
WT
KO
C
Nu. F-actin
Col1-3/4C
Merge
MCF10A WT
EFA6B KO
D
Collagen degradation index
***
WT
KO
E
WT KO
MMP14
hsp60
F
si Ctl
si MMP14
MMP14
hsp60
G
% of aggregates with protrusions
****
siCtl
siMMP14
H
MCF10A WT
EFA6B KO
% of aggregates with protrusions
**
***
***
*
Coll.
Coll.+Mat.
Coll.
Coll.+Mat.
Membrane
Cell
MCF10 WT
EFA6B KO
I
MCF10 WT
EFA6B KO
L

Figure 4

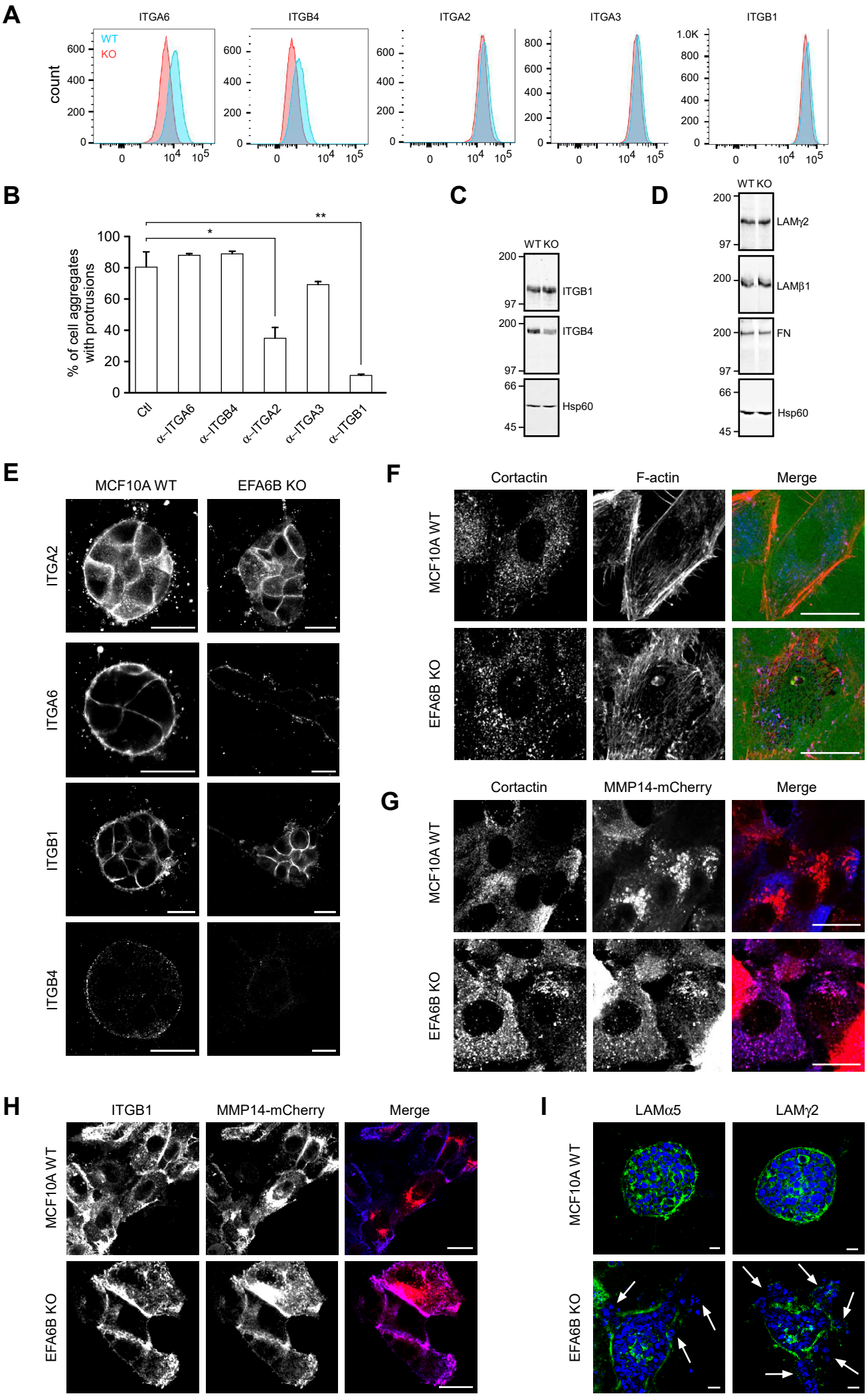
A
ITGA6
ITGB4
ITGA2
ITGA3
ITGB1
WT
KO
count
B
% of cell aggregates with protrusions
Ctl
α–ITGA6
α–ITGB4
α–ITGA2
α–ITGA3
α–ITGB1
C
WT KO
ITGB1
ITGB4
Hsp60
D
WT KO
LAMγ2
LAMβ1
FN
Hsp60
E
MCF10A WT
EFA6B KO
ITGA2
ITGA6
ITGB1
ITGB4
F
Cortactin
F-actin
Merge
MCF10A WT
EFA6B KO
G
Cortactin
MMP14-mCherry
Merge
MCF10A WT
EFA6B KO
H
ITGB1
MMP14-mCherry
Merge
MCF10A WT
EFA6B KO
I
LAMα5
LAMγ2
MCF10A WT
EFA6B KO

Figure 5

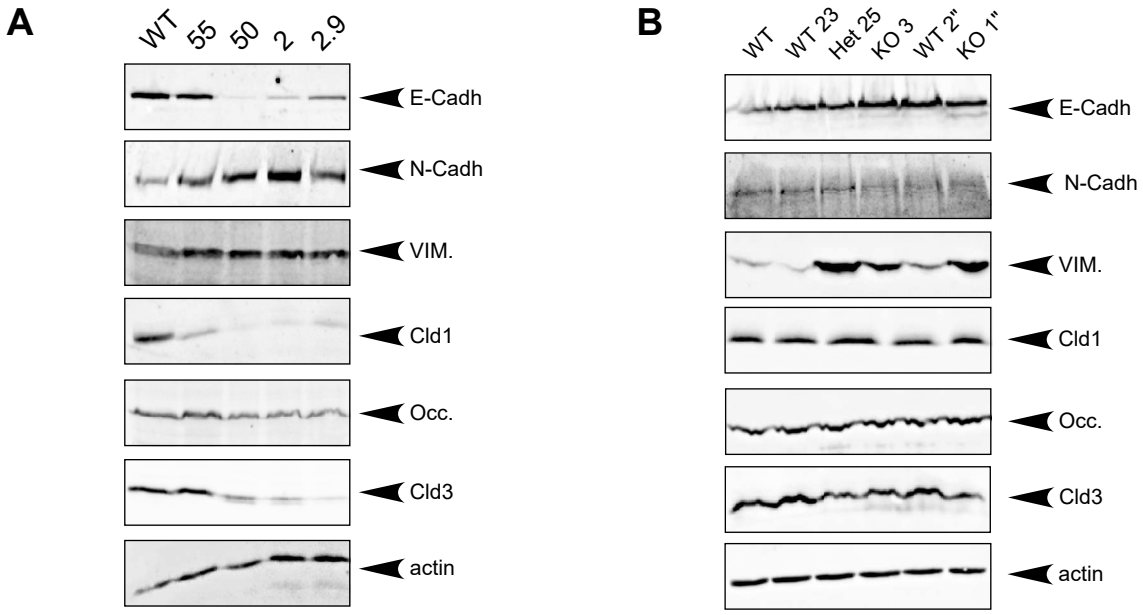
A
WT
55
50
2
2.9
E-Cadh
N-Cadh
VIM.
Cld1
Occ.
Cld3
actin
B
WT
WT 23
Het 25
KO 3
WT 2"
KO 1"
E-Cadh
N-Cadh
VIM.
Cld1
Occ.
Cld3
actin

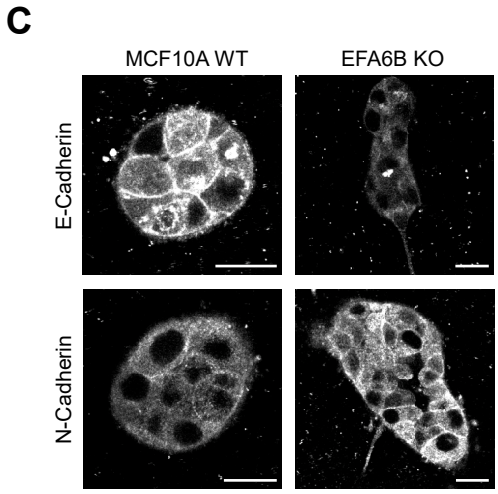
C
MCF10A WT
EFA6B KO
E-Cadherin
N-Cadherin

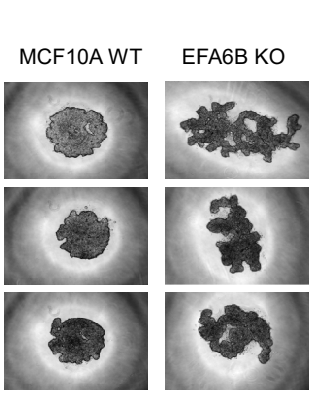
D
MCF10A WT
EFA6B KO

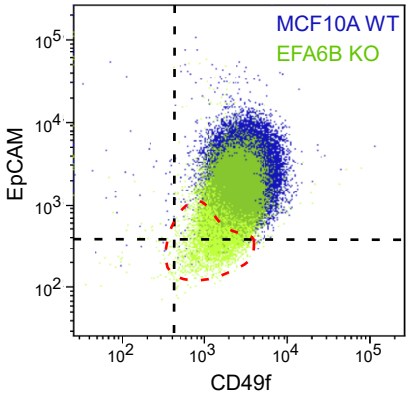
E
MCF10A WT
EFA6B KO
EpCAM
CD49f

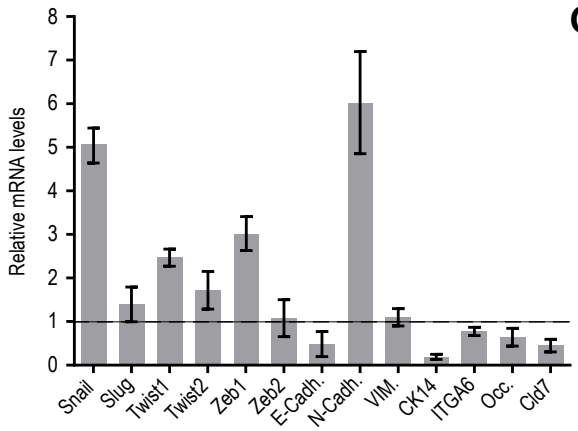
F
Relative mRNA levels
Snail
Slug
Twist1
Twist2
Zeb1
Zeb2
E-Cadh.
N-Cadh.
VIM.
CK14
ITGA6
Occ.
Cld7

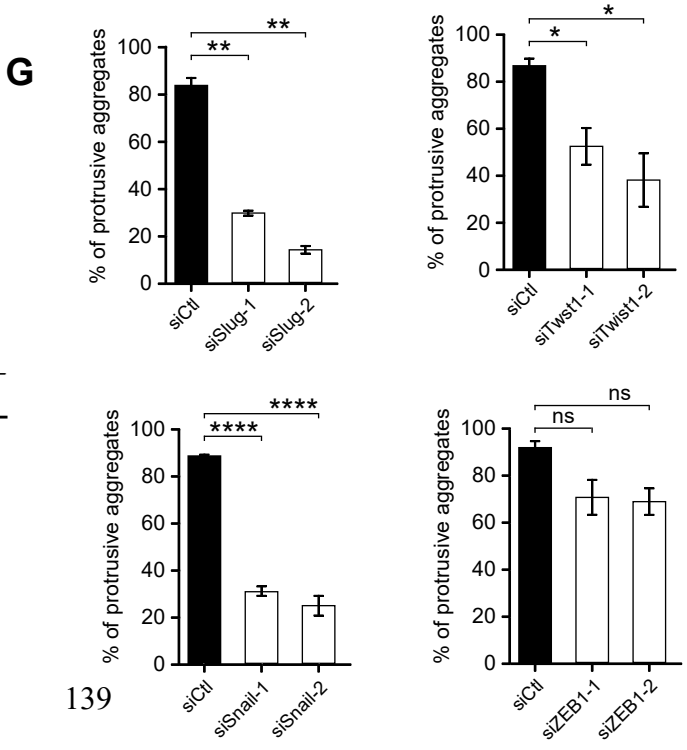
G
% of protrusive aggregates
siCtl
siSlug-1
siSlug-2
siTwist1-1
siTwist1-2
siSnail-1
siSnail-2
siZEB1-1
siZEB1-2
ns

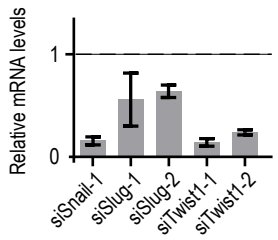
H
Relative mRNA levels
siSnail-1
siSlug-1
siSlug-2
siTwist1-1
siTwist1-2

Figure 6

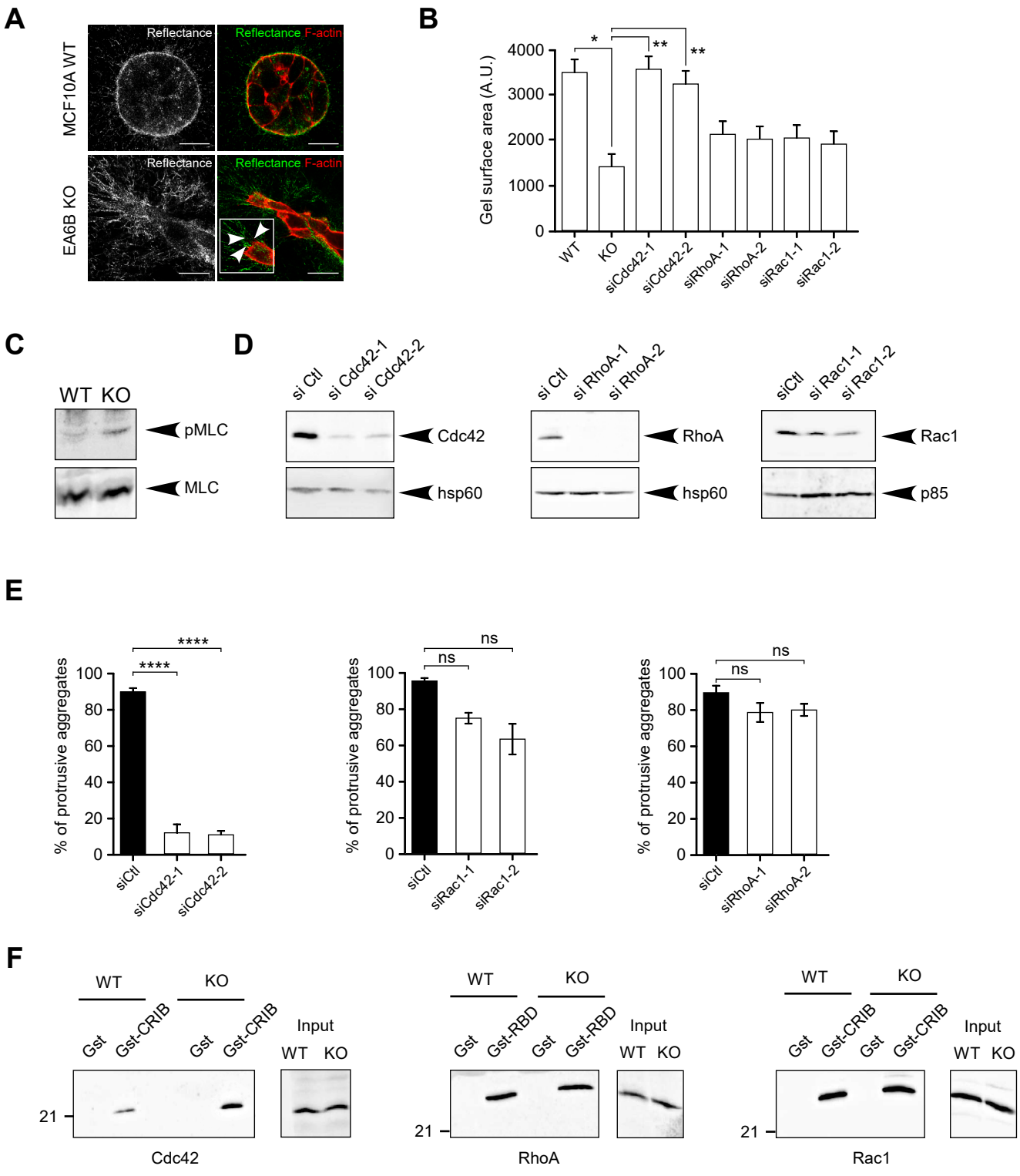
A
MCF10A WT
EA6B KO
Reflectance
Reflectance F-actin
B
Gel surface area (A.U.)
4000
3000
2000
1000
0
*
**
**
WT
KO
siCdc42-1
siCdc42-2
siRhoA-1
siRhoA-2
siRac1-1
siRac1-2
C
WT KO
pMLC
MLC
D
si Ctl
si Cdc42-1
si Cdc42-2
Cdc42
hsp60
si Ctl
si RhoA-1
si RhoA-2
RhoA
hsp60
siCtl
si Rac1-1
si Rac1-2
Rac1
p85
E
% of protrusive aggregates
100
80
60
40
20
0
****
****
siCtl
siCdc42-1
siCdc42-2
ns
ns
siCtl
siRac1-1
siRac1-2
ns
ns
siCtl
siRhoA-1
siRhoA-2
F
WT
KO
Gst
Gst-CRIB
Gst
Gst-CRIB
Input
WT KO
21
Cdc42
Gst
Gst-RBD
Gst
Gst-RBD
RhoA
Gst
Gst-CRIB
Gst
Gst-CRIB
Rac1

Figure 7

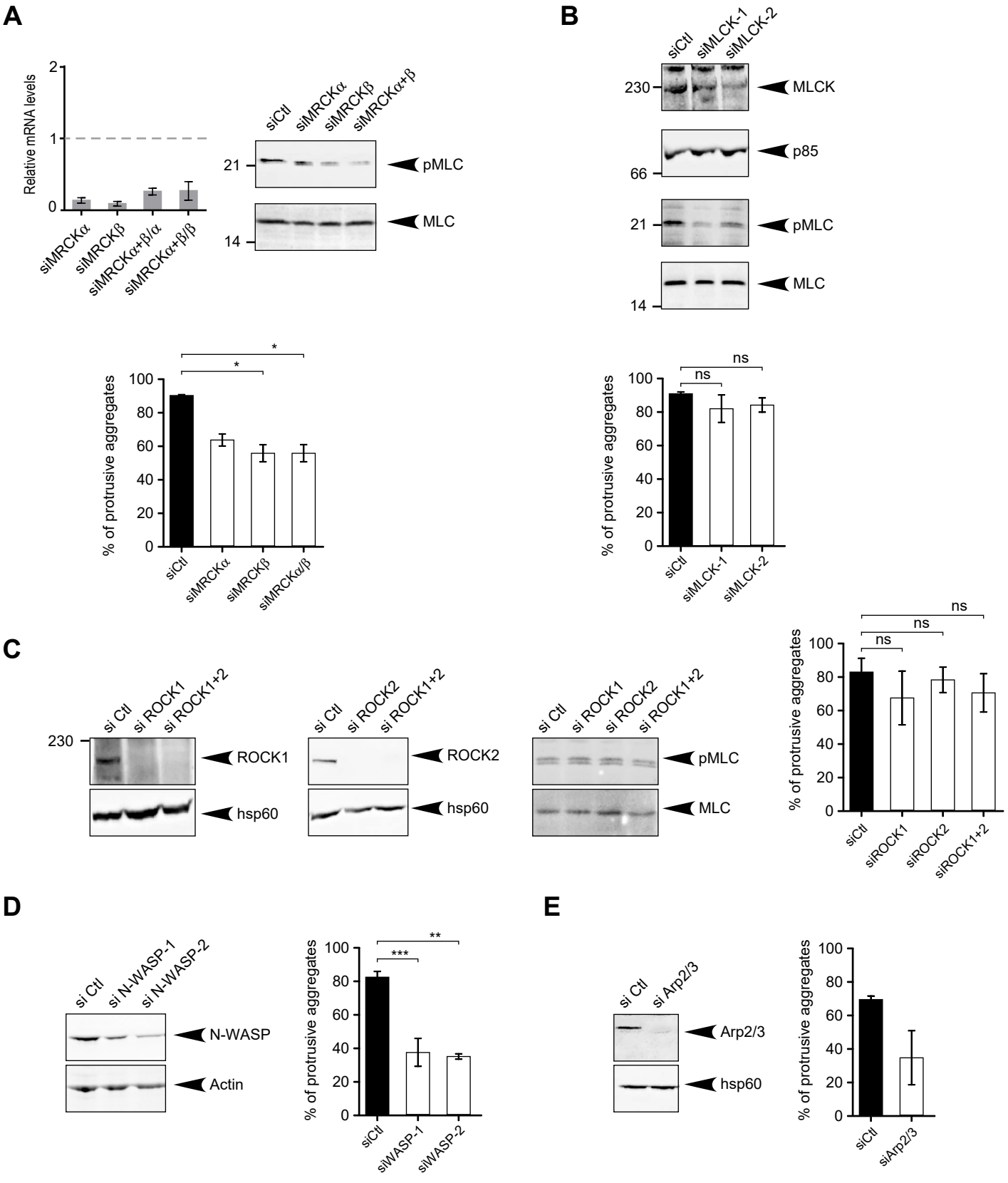
A
Relative mRNA levels
2
1
0
siMRCKα
siMRCKβ
siMRCKα+β/α
siMRCKα+β/β
siCtl
siMRCKα
siMRCKβ
siMRCKα+β
21
14
pMLC
MLC
% of protrusive aggregates
100
80
60
40
20
0
*
*
siCtl
siMRCKα
siMRCKβ
siMRCKα/β
B
siCtl
siMLCK-1
siMLCK-2
230
66
21
14
MLCK
p85
pMLC
MLC
ns
ns
siCtl
siMLCK-1
siMLCK-2
C
si Ctl
si ROCK1
si ROCK1+2
si ROCK2
230
ROCK1
ROCK2
hsp60
pMLC
MLC
ns
ns
ns
siCtl
siROCK1
siROCK2
siROCK1+2
D
si Ctl
si N-WASP-1
si N-WASP-2
N-WASP
Actin
**
***
siCtl
siWASP-1
siWASP-2
E
si Ctl
si Arp2/3
Arp2/3
hsp60
siCtl
siArp2/3

Supplementary Table 1

Gene symbol	Gene description	KO 55+Het 2.9 vs WT	Matrisome category
ANGPT1	angiopoietin 1	up	Secreted Factors
DCN	decorin	up	Proteoglycans
SFTPB	surfactant protein B	up	ECM-affiliated protein
SERPINB4	serpin peptidase inhibitor, clade B, 4	up	ECM Regulators
SERPINB3	serpin peptidase inhibitor, clade B, 3	up	ECM Regulators
HMMR	hyaluronan-mediated motility receptor	up	Glycoprotein receptor
GDF15	growth differentiation factor 15	up	Secreted Factors
ADAMTS12	ADAM with thrombospondin type 1 motif, 12	up	ECM Regulators
S100A8	S100 calcium binding protein A8	up	Secreted Factors
S100A7	S100 calcium binding protein A7	up	Secreted Factors
CLEC2B	C-type lectin domain family 2, B	up	ECM-affiliated Protein
MUC1	mucin 1, cell surface associated	up	ECM-affiliated protein
LAMB1	laminin, beta 1	up	ECM glycoPn
SERPINA3	serpin peptidase inhibitor, member 3	up	ECM Regulators
LOX	lysyl oxidase	up	ECM Regulators
CTSK	cathepsin K	up	ECM Regulators
CYR61	cysteine-rich, angiogenic inducer, 61	down	ECM glycoPn
FGFBP1	fibroblast growth factor binding protein 1	down	secreted factors
SERPINB2	serpin peptidase inhibitor, clade B, 2	down	ECM Regulators
MMP2	matrix metallopeptidase 2	down	ECM Regulators
CLCF1	cardiotrophin-like cytokine factor 1	down	Secreted factors
INHBA	inhibin, beta A	down	Secreted factors
THBS1	thrombospondin 1	down	ECM glycoPn
SERPINE1	serpin peptidase inhibitor, clade E, 1	down	ECM Regulators
PLAT	plasminogen activator, tissue	down	ECM regulators
WNT9A	wingless-type, 9A	down	Secreted factors
S100A10	S100 calcium binding protein A10	down	Secreted Factors
PXDN	peroxidasin homolog	down	ECM glycoPn
LAMC2	laminin, gamma 2	down	ECM glycoPn
IL8	interleukin 8	down	Secreted Factors
SMOC1	SPARC related modular calcium binding 1	down	ECM glycoPn
FN1	fibronectin 1	down	ECM glycoPn
PRG2	proteoglycan 2	down	Proteoglycans
LEPREL1	leprecan-like 1	down	ECM regulators
SPARC	secreted protein, acidic, cysteine-rich	down	ECM glycoPn
TNC	tenascin C	down	ECM glycoPn
SULF2	sulfatase 2	down	ECM Regulators
FST	follistatin	down	Secreted Factors
CTSL2	cathepsin L2	down	ECM regulators
S100A2	S100 calcium binding protein A2	down	Secreted Factors
NRG1	neuregulin 1	down	Secreted factors
AREG	amphiregulin	down	Secreted factors
ADAMTSL5	ADAMTS-like 5	down	ECM Regulators
PLXNA2	plexin A2	down	ECM-affilitaed proteins
SDC1	syndecan 1	down	ECM-affilitaed proteins
S100A3	S100 calcium binding protein A3	down	Secreted Factors
IGFBP7	insulin-like growth factor binding protein 7	down	ECM glycoPn

Gene set enrichment analysis of the Matrisome signature comparing the expression profiles of MCF10A EFA6B KO 55 + Het 2.9 cells vs. MCF10A WT cells

Supplementary Figure 1

A

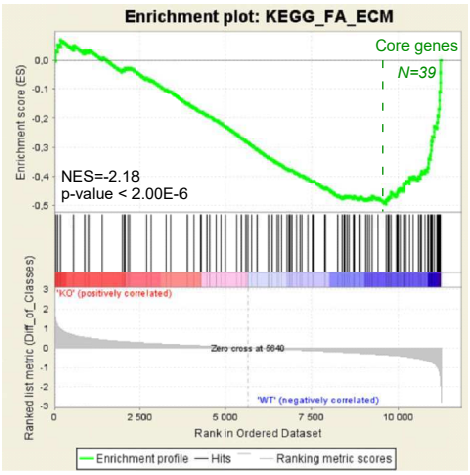

Gene symbol	Gene name
ITGB4	integrin subunit beta 4
MAPK8	mitogen-activated protein kinase 8
CAPN2	calpain 2
VASP	vasodilator-stimulated phosphoprotein
ITGB5	integrin subunit beta 5
COL4A1	collagen, type IV, alpha 1
COL4A6	collagen, type IV, alpha 6
CCND1	cyclin D1
ITGA5	integrin subunit alpha 5
PXN	paxillin
VAV2	vav guanine nucleotide exchange factor 2
CD44	CD44 molecule (Indian blood group)
ACTN4	actinin alpha 4
SRC	SRC proto-oncogene, non-receptor tyrosine kinase
PDGFA	platelet derived growth factor subunit A
HRAS	HRas proto-oncogene, GTPase
PIP5K1C	phosphatidylinositol-4-phosphate 5-kinase type 1 gamma
CAV2	caveolin 2
ITGA3	integrin subunit alpha 3
CAV1	caveolin 1
ITGA10	integrin subunit alpha 10
CCND2	cyclin D2
ELK1	ELK1, ETS transcription factor
MYL12B	myosin light chain 12B
FLNA	filamin A
SDC1	syndecan 1
HSPG2	heparan sulfate proteoglycan 2
ACTG1	actin gamma 1
ITGA6	integrin subunit alpha 6
ITGA2	integrin subunit alpha 2
VCL	vinculin
ITGB6	integrin subunit beta 6
ZYX	zyxin
LAMC2	laminin subunit gamma 2
ITGA4	integrin subunit alpha 4
MYL9	myosin light chain 9
TNC	tenascin C
FN1	fibronectin 1
THBS1	thrombospondin 1

B

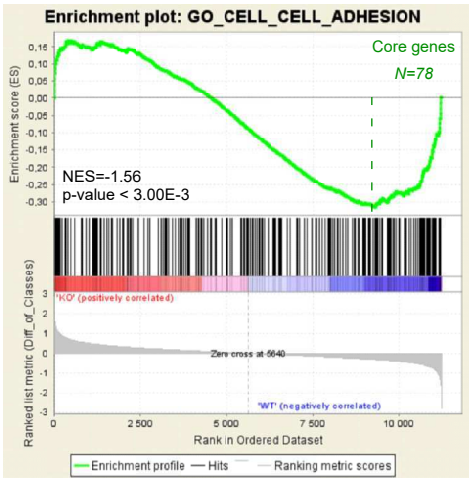

Gene symbol	Gene name
CD24	CD24 molecule
TACSTD2	tumor associated calcium signal transducer 2
SOX9	SRY-box 9
CYR61	cysteine rich angiogenic inducer 61
MYL9	myosin light chain 9
PCDH7	protocadherin 7
ITGA4	integrin subunit alpha 4
CLDN1	claudin 1
PTGER4	prostaglandin E receptor 4
FBLIM1	filamin binding LIM protein 1
STK10	serine/threonine kinase 10
FZD8	frizzled class receptor 8
VCL	vinculin
IGSF9B	immunoglobulin superfamily member 9B
EPCAM	epithelial cell adhesion molecule
EOMES	eomesodermin
MYH9	myosin heavy chain 9
ACTG1	actin gamma 1
FLNA	filamin A
CDH1	cadherin 1
STXBP1	syntaxin binding protein 1
SRF	serum response factor
FAT1	FAT atypical cadherin 1
CHD7	chromodomain helicase DNA binding protein 7
FNDC3A	fibronectin type III domain containing 3A
NECTIN2	nectin cell adhesion molecule 2
JAG2	jagged 2
CSTA	cystatin A
CSRP1	cysteine and glycine rich protein 1
SMAD3	SMAD family member 3
FZD7	frizzled class receptor 7
CELSR2	cadherin EGF LAG seven-pass G-type receptor 2
NECTIN1	nectin cell adhesion molecule 1
CDK6	cyclin dependent kinase 6
FZD5	frizzled class receptor 5
LEF1	lymphoid enhancer binding factor 1
CLDN7	claudin 7
LGALS7B	galectin 7B
CELSR1	cadherin EGF LAG seven-pass G-type receptor 1
ZFP36L1	ZFP36 ring finger protein like 1
PIP5K1C	phosphatidylinositol-4-phosphate 5-kinase type 1 gamma
PLEKHA7	pleckstrin homology domain containing A7
LCP1	lymphocyte cytosolic protein 1
CADM4	cell adhesion molecule 4
DSC3	desmocollin 3
SRC	SRC proto-oncogene, non-receptor tyrosine kinase
JUP	junction plakoglobin
CLDN19	claudin 19
CD44	CD44 molecule (Indian blood group)
EZR	ezrin
ITGA5	integrin subunit alpha 5
CD276	CD276 molecule
CERCAM	cerebral endothelial cell adhesion molecule
CDH3	cadherin 3
PVR	poliovirus receptor
PSMB10	proteasome subunit beta 10
FGFRL1	fibroblast growth factor receptor-like 1
ELF4	E74 like ETS transcription factor 4
ITGB5	integrin subunit beta 5
FAT2	FAT atypical cadherin 2
SMAGP	small cell adhesion glycoprotein
RC3H1	ring finger and CCCH-type domains 1
FAS	Fas cell surface death receptor
PKNOX1	PBX/knotted 1 homeobox 1
NOV	nephroblastoma overexpressed
CDSN	corneodesmosin
RAP2B	RAP2B, member of RAS oncogene family
RELB	RELB proto-oncogene, NF-kB subunit
NPTN	neuroplastin
CLSTN1	calsyntenin 1
GATA1	GATA binding protein 1
CD58	CD58 molecule
AMIGO1	adhesion molecule with Ig like domain 1
NT5E	5'-nucleotidase ecto
CDK5R1	cyclin dependent kinase 5 regulatory subunit 1
PKP2	plakophilin 2

Supp. Materials and Methods: List of Antibodies

Antigen	Antibody source and reference	Application
MMP-14	Millipore, MAB3328	Immunoblot
Integrin-β1	Santa Cruz, sc-13590	Flow cytometry Immunofluorescence
Integrin-β4	BD Biosciences, 611232	Flow cytometry Immunofluorescence
Integrin-α2	Santa Cruz, sc-53502	Flow cytometry Immunofluorescence
Integrin-α3	Millipore, MAB2057	Flow cytometry Immunofluorescence
Integrin-α6	BD Biosciences, 555734	Flow cytometry Immunofluorescence
EpCAM/CD326	BD Biosciences, 563181	Flow cytometry
CD49f	BD Biosciences, 562582	Flow cytometry
Lamininα5	BIO-RAD, 5620-0436	Immunofluorescence
Lamininγ2	Santa Cruz, sc-25341	Immunofluorescence Immunoblot
Lamininβ1	R&D Systems, MAB25491	Immunofluorescence
Lamininβ1	Santa Cruz, sc-17763	Immunoblot
Col1-3/4C	Immuno Globe, 0217-050	Immunofluorescence
N-cadherin	BD Biosciences, 610921	Immunofluorescence Immunoblot
E-cadherin	Thermo Scientific, 33-4000	Immunofluorescence
E-cadherin	BD Biosciences, 610182	Immunoblot
Vimentin	Sigma, V6389	Immunoblot
Claudin 1	ZYMED Laboratories, 51-9000	Immunoblot
Occludin	Thermo Scientific, 40-4700	Immunoblot
Actin	Sigma, A4700	Immunoblot
Claudin 3	Millipore, 2819163	Immunoblot
Arf6	Gift from Dr. Bourgoin	Immunoblot
EFA6A	Gift from Dr. Sakagami	Immunoblot
EFA6B	Sigma, HPA034722	Immunoblot
EFA6D	Gift from Dr. Sakagami	Immunoblot
Hsp60	Sigma, SAB4501464	Immunoblot
Cdc42	BD Biosciences, 610928	Immunoblot
N-WASP	Cell Signaling, 4848	Immunoblot
Arp2/3	BD Biosciences, 612134	Immunoblot
MLCK	Santa Cruz, sc-365352	Immunoblot
p85	Millipore, ABS1856	Immunoblot
pMLC	Cell Signaling, 3671 & 3675	Immunoblot
MLC	Sigma, M4401	Immunoblot
RhoA	Santa Cruz, sc-418	Immunoblot
ROCK 1	Santa Cruz, sc-17794	Immunoblot
ROCK 2	Santa Cruz, sc-398519	Immunoblot
Rac 1	BD Biosciences, 610650	Immunoblot
Arf1	Novus Biologicals, NB100-55421	Immunoblot
Arf5	Abnova, H00000381-M01	Immunoblot
Fibronecin	BD Biosciences, 610077	Immunoblot
Cortactin	Millipore, 05-180	Immunoblot

3. Discussion of Article 1

In the above section, I presented the major results of my thesis in the form of an article; however, kindly note that it is not the final publishable version. Here, I will be discussing on-going and future experiments essential to validate some hypothesis proposed and push our research towards more complex models (in vivo).

In the present work, we identified *PSD4* (EFA6B) as a secondary oncogenic driver gene providing when altered normal cells with invasive properties in a CDC42 dependent manner.

We showed that the loss of EFA6B was able to strongly deregulate the epithelial homeostasis of normal mammary cell lines at different levels. First, deleting EFA6B allowed the formation of invadopodia rich in ITGB1 and MMP14. The invasion capacity of these cells is Cdc42 dependent. We suppose that EFA6B KO cells invasion is supported by the contractility, and the formation of protrusive branched structures ensured most-likely by Cdc42/MRCK and Cdc42/N-WASP/Arp2/3 activation, respectively. Second, we showed that the loss of EFA6B is associated with the engagement of EFA6B KO cells in EMT, shown by a clear cadherin switch and an upregulation of mesenchymal TFs. Third, coherently with EFA6B roles on junction assembly, its deletion prevented MCF10A cells from polarizing correctly and forming normal acini with central lumens. Lastly, in agreement with a previous correlation with Cld-low BC patients, our EFA6B KO cells presents a decrease in TJ proteins expression, EMT properties and invasion capacities consistent with the Cld-low subtype characteristics.

Taken together, our results suggest that the loss of EFA6B impacts negatively the epithelial integrity of normal mammary cells and drive them towards invasiveness.

I can propose a scenario showing a dual effect of the loss of EFA6B. On one hand the disassembly of adhesion complexes induced by the loss of EFA6B leads to the activation of a transcriptional program increasing the expression of EMT-TFs. This can result in the detected modifications of the matrisome transcriptomics and its receptors (mainly integrins). On the other hand, EFA6B upregulates Cdc42 activity, promoting the increase in contractility and invadopodia formation.

It is hard at this stage to define the chronological order of EFA6B loss consequences. Further studies and investigations are needed to better understand the order of emergence of these events.

In the following, I will expose three different experiments that should be performed to better elucidate the impact of the loss of EFA6B on normal mammary epithelial cells. First, we need to

show the direct link between Cdc42 and invadopodia formation in the KO cells. Second, we will tackle the *in vivo* experiments that I have already started in order to study the role of EFA6B deletion on tumor invasion and how can we improve our models. And lastly, how can we use the data we have to better stratify BC patient, and find new therapeutic targets.

Cdc42 and invadopodia:

The major result of this work is the impressive invasive capacity acquired by normal cells upon the loss of EFA6B. Downregulation experiments have clearly shown the leading role of Cdc42 signaling in supporting and mediating this phenotype.

What we actually showed is that downregulating Cdc42 in the KO cells decreased contractility as well as the formation of protrusive degradative structures. However, an essential information is missing in order to directly link Cdc42 to the formation of invadopodia. Invadopodia are actin-rich specialized structures, important for migration and invasion in cancer cells, that are dependent mainly on actin-regulatory protein. We have already confirmed the presence of invadopodia upon the loss of EFA6B by staining for cortactin that co-localized with integrin β1and MMP-14.

Cdc42 was reported to be important for invadopodia formation by sustaining actin nucleation through the recruitment of N-WASP/Arp2/3 (Stengel and Zheng, 2011). First, we need to look for N-WASP/Arp2/3 localization at the invadopodia level. Second, we will verify if the downregulation of Cdc42 alter invadopodia formation quantified using a with cortactin, and N-WASP/Arp2/3 staining, characteristic of these structures.

***In vivo* models: Unpublished data and perspectives**

We have proposed that the alterations of PSD4 (EFA6B) gene can be considered as a secondary driver mutation providing cells with invasive advantages.

-Transformed or not?

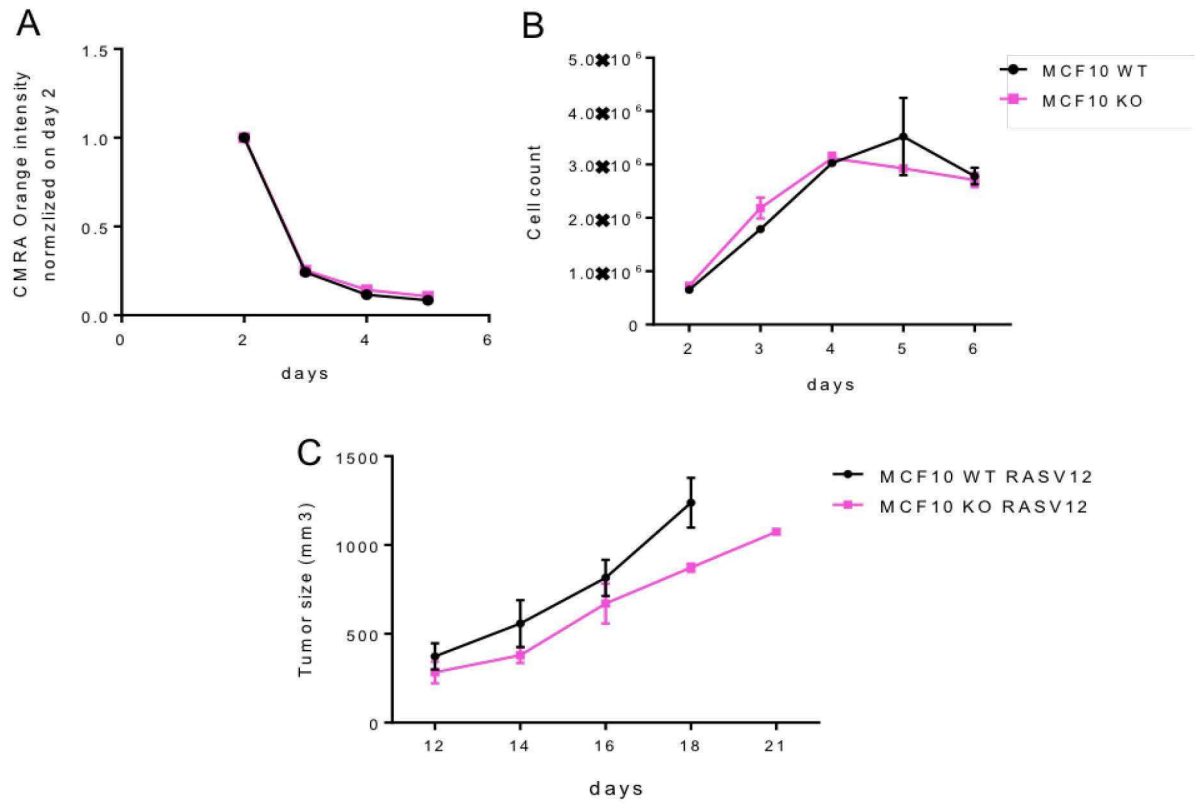

Figure 26: EFA6B knock-out does not affect cell proliferation in vitro and no differences observed in vivo when EFA6B KO is combined with the expression of activated form of the oncogene RAS, RASV12.

A) *Cell proliferation of MCF10A WT and EFA6B KO 55 cells measured by FACS using an intracellular staining CMRA Orange that decreases with each cell division for 5 consecutive days (N=1).* ***B)*** *Cell proliferation of MCF10A WT and EFA6B KO 55 cells measured by Cell LUNA counter for 6 consecutive days (N=1).* ***C)*** *Orthotopic xenografts of MCF10A WT and EFA6B KO 55 cells infected with a lentivirus expressing RASV12. 800 000 cells were injected in each mammary gland of the fourth pair in NOD/SCID female mice. Tumor growth was measured with a caliper (3 mice for each group, N=1).*

Indeed, our EFA6B knock-out did not transform MCF10A normal cell line. *In vitro*, I tested first if cells had an increased proliferation or a decrease in apoptosis, two main strategies used by transformed cells to form a tumor (**Figure 26**). I used two techniques to follow cells' proliferation rates for 5 consequent days, first by counting cells grown in 2D culture with the LUNA™ cell counter (Logos Biosystems) and second by staining cells with the CellTracker™ Orange CMRA, a fluorescent dye measured by flow cytometry. Both methods showed no proliferative differences between WT and EFA6B KO MCF10A cells. Apoptosis was examined using the annexin-V staining assay measured as well by flow cytometry. Similarly, we had insignificant difference in apoptosis rates between our two MCF10A cell lines (<3%). We tested the renewing capacity of KO cells as well using a mammosphere assay that did not show any differences with WT cells. Most importantly, when injected in the mammary glands of an immunodeficient xenograft mice model (NOD/SCID mice), EFA6B KO and WT MCF10A cells did not

show any tumor growth. The result of this *in vivo* experiment validates that MCF10A normal cells are not transformed by the loss of EFA6B.

The loss of EFA6B is not an oncogenic driver but still has provided cells with remarkable invasive capacities. Hence our hypothesis of EFA6B acting when altered as a secondary oncogenic driver, giving cells pro-invasive properties.

-Aim of the in vivo xenografts and the insertion of an oncogene

After revealing these properties *in vitro*, it was interesting to look at the impact of the loss of EFA6B on invasion *in vivo*. Thus, we decided to add an oncogenic gene to our WT and EFA6B KO MCF10A cells in order to transform them into cancer cells capable of proliferating and forming a primary tumor. The major goal of this experiment was to see if cells deleted for EFA6B would be more apt of leaving the primary tumor and invading surrounding tissues or even metastasizing to distant organs. We would expect that the KO cells having degradative capacities (MMP-14), upregulated contractility and invasive structures would breach the endogenous physical barriers (basal membrane and the ECM) and ultimately exhibit secondary site colonization, metastasis. Collected tumors can be then classified by BC subtype. One can expect that a higher frequency of Cld-low tumors would emerge from the EFA6B KO cells.

-Adapted oncogenic choices

We chose to decrease the expression separately of TP53 and PTEN, two tumor suppressors found in human breast tumors, especially in Cld-low. Mutations of *TP53* are estimated to occur in approximately 20%–30% of breast cancers (Hollstein et al., 1991) and the frequency of PTEN loss is 30%-40% in sporadic breast cancer (Milella et al., 2015). We also decided expressing RASV12 an activated form of Ras that has been frequently used in xenograft breast cancer models.

I infected MCF10A cells separately with three lentiviruses carrying each one of the aforementioned oncogenes/tumor suppressors. When injected orthotypically in the mammary gland of immunodeficient mice, MCF10A WT and EFA6B KO cells downregulated for PTEN or TP53 did not show any tumor growth even with 10^6 cells injected.

Cells infected with RASV12 injected in the mammary gland of NOD/SCID mice rapidly developed primary tumor (**Figure 26**)(the regulatory tumor size limit (1000mm^3) attained in 17 days). The oncogenic impact of RASV12 was very intense and we think that it has masked the potential effect expected for the cells deleted for EFA6B. The RASV12 WT and KO cells did not show anymore the protrusive differences when plated in collagen, collagen mixed with Matrigel or Matrigel alone. The fast tumor growth observed in our RASV12 WT and KO cells can be due to the high expression level of RASV12. It would be then interesting to select clones having a mild expression of this oncogene.

-Other in vivo models' suggestions:

Our cell models combined with these specific transformative genes did not allow us to investigate the role of the loss of EFA6B *in vivo*. Therefore, I think that we need to adapt better our *in vivo* models by choosing oncogenes that will have a moderate transformative effect on cells. I can propose two mice models that will probably allow us to answer our question. First, we can use a syngeneic P53 null mouse mammary gland transplant model of BALB/c mice suggested to mimic more closely human breast cancer than other models (Zhang et al., 2008). Here, we will recover the mammary cells downregulated for P53 and downregulate *in vitro* EFA6B. Cells KO for both P53 and EFA6B will then be injected in the clear fat pad of syngeneic wild-type recipient mice. Second, we can test other oncogenes and make sure to control the amount of transfected viral particles. The ideal oncogene should transform the MCF10A or HMLE cells in order to see a slow growth of a primary tumor. We can use a combined deletion of PTEN and P53 that was shown to cluster with human Cld-low (Liu et al., 2014). Another possibility is to upregulate cyclin E in the HMLE cell line (Morel et al., 2017); of note cyclin E overexpression was identified in 20%-30% of breast cancer (Keyomarsi et al., 2002). In both models, we will track tumor growth and the emergence of metastasis and then check if the tumors present a Cld-low transcriptional signature.

The injection method can be as well reviewed. Previously, I used to inject the cells in the fat pad of the mammary gland. Another more precise way in order to see if cells will manage to breach the endogenous basal membrane is to inject directly in the nipple and then check for local invasions by immunohistochemistry.

Currently, knock-outs of EFA6 in mice are being established in the laboratory of our collaborator H. Sakagami in Japan which will open new possibilities and tools for further studies of these GEFs.

-How can we use our data to better stratify BC in patients?

In collaboration with the genomic platform of IPC in Marseille and the team of Dr. Daniel Birnbaum, we are actually trying to further analyze the transcriptional data we have for our EFA6B KO MCF10A cells. It would be interesting to propose a transcriptomic signature that would help stratify better the Cld-low patients, especially by integrating the matrisome analysis. Another important analysis would be to check if we can find an upregulation of Cdc42 signaling pathway signature in the Cld-low patients who have a downregulation of EFA6B. Moreover, we are interested in finding therapeutic targets for the Cld-low subtype. Since EFA6B is downregulated, it cannot be used directly targeted. Thus, on the basis of the transcriptomic data of our EFA6B KO cells combined to that of Cld-low patients, we will propose, as potential therapeutic targets, a list of genes which expression levels inversely correlate with the downregulation of EFA6B.

THESIS . ARTICLE 2

Article 2

1. Objectives of Article 2

EFA6 belongs to the EFA6/PSD exchange factors family comprising four different isoforms coded by different genes: PSD (EFA6A), PSD4 (EFA6B), PSD2 (EFA6C) and PSD3 (EFA6D). They have similar structures with a sec7 catalytic domain responsible for activating Arf6 (GEF activity), a PH domain that localize them at the plasma membrane, a variable N-terminal domain for which roles have not yet been granted and a conserved C-terminal (Cter) domain that can bind multiple effectors (e.g. actin, β-arrestin, etc.).

Since its discovery, EFA6 effects have always been presented as the resultant of EFA6 exchange activity for Arf6 in coordination with EFA6 C-terminal domain activity. Indeed, the formation of actin-based membrane ruffles was more enhanced by the exogenous expression of the Ph-Cter of EFA6A than by overexpressing an activated mutant of Arf6 (Franco et al., 1999). Knowing the importance of EFA6 Cterminus *per se*, our research group was interested in identifying partners that can bind this domain in order to further understand and characterize its mechanism of action. For this purpose, a two-hybrid screening was conducted with the EFA6A C-ter domain from which actinin was sorted as the best candidate. Shortly after, a similar interaction was suggested by Sakagami et al, only on the basis of an observation of overlapping staining between EFA6 and α-actinin in dendritic spines of hippocampal neurons (Sakagami et al., 2007)

After validating the binding of actinin to EFA6A *in vitro*, we were interested in investigating the impact of the EFA6B-actinin interaction on cellular physiology, more specifically epithelial polarity and lumen formation.

Indeed, EFA6 was strongly established as a regulator of epithelial cell polarity and cytoskeleton rearrangement (Klein et al., 2008a; Luton et al., 2003; Théard et al., 2010; Zangari et al., 2014). In addition, we had shown that the overexpression of EFA6B in a tumorigenic mammary cell line restored the formation of a normal lumen in 3D culture (Zangari et al., 2014). We know that these effects are in part mediated by the activation of Arf6, and by the EFA6 Cter domain. However which effectors are engaged by the EFA6 C-terminus to fulfil these functions was not yet determined.

Interestingly, the non-muscular α-actinin1 (ACTN1) and 4 (ACTN4) had already been associated to the apical acto-myosin ring supporting the adherens junctions, but only few studies linked them to tight junctions. The apical localization of actinin is close to EFA6 spatial distribution, and therefore both

molecules were suspected to have a collaborative role on luminogenesis, a process that requires vesicular trafficking, actin cytoskeleton rearrangement and the remodeling of adhesion complexes.

Hence the objective of this work is to identify the role and mechanism of action of this interesting interaction between actinin and EFA6 on luminogenesis, in a normal epithelial cell line (MDCK) and in another model of weakly tumorigenic epithelial mammary cell line (MCF7).

This project has started few years before my arrival. My contribution consisted in elucidating the role and interaction of EFA6B/ACTN1in MCF7 cells (figures 5 and 6).

Thesis . Article 2 . Results

© 2018. Published by The Company of Biologists Ltd | Journal of Cell Science (2018) 131, jcs209361. doi:10.1242/jcs.209361

RESEARCH ARTICLE

EFA6 proteins regulate lumen formation through α-actinin 1

Julie Milanini[1], Racha Fayad[1], Mariagrazia Partisani[1], Patrick Lecine[2,*], Jean-Paul Borg[2], Michel Franco[1] and Frédéric Luton[1,‡]

ABSTRACT

A key step of epithelial morphogenesis is the creation of the lumen. Luminogenesis by hollowing proceeds through the fusion of apical vesicles at cell–cell contacts. The small nascent lumens grow through extension, coalescence and enlargement, coordinated with cell division, to give rise to a single central lumen. Here, by using MDCK cells grown in 3D-culture, we show that EFA6A (also known as PSD) participates in luminogenesis. EFA6A recruits α-actinin 1 (ACTN1) through direct binding. In polarized cells, ACTN1 was found to be enriched at the tight junction where it acts as a primary effector of EFA6A for normal luminogenesis. Both proteins are essential for the lumen extension and enlargement, where they mediate their effect by regulating the cortical acto-myosin contractility. Finally, ACTN1 was also found to act as an effector for the isoform EFA6B (also known as PSD4) in the human mammary tumoral MCF7 cell line. EFA6B restored the glandular morphology of this tumoral cell line in an ACTN1-dependent manner. Thus, we identified new regulators of cyst luminogenesis essential for the proper maturation of a newly-formed lumen into a single central lumen.

KEY WORDS: Epithelium, Lumen, EFA6, ACTN1, Contractility

INTRODUCTION

During organogenesis, the coordinated establishment of the apico-basal polarity with the *de novo* formation of an apical luminal space is fundamental to the emergence of the different types of epithelia. In adult organisms, the aptitude of the internal organs, which are lined with epithelial tissues, to ensure specific functions relies on the preservation of these characteristics. The failure in doing so is associated with a large variety of diseases (Blasky et al., 2015; Datta et al., 2011; Sigurbjörnsdóttir et al., 2014). In particular, these features are often compromised in carcinomas and tumors are formed of non-polarized cell aggregates incapable of collectively organizing a lumen (Martin-Belmonte and Perez-Moreno, 2011; Tanos and Rodriguez-Boulan, 2008; Wang et al., 2012). However, compelling tumoral cells to maintain their normal epithelial phenotype can help them override the power of oncogenes (DuFort et al., 2011; Weaver et al., 1997). Thus, it is important to decipher the molecular programs that instruct epithelial cells to collectively organize around lumens in order to maintain their physiological homeostasis.

For most epithelial tissues, the *de novo* formation of a lumen is generated by hollowing. In this process, apical vesicles are delivered to a focal point of the cell–cell contact named the apical membrane initiation site (AMIS) to give rise to the apical plasma membrane and a facing hollow cavity. The nascent lumen appears first as a closed elongated space named the pre-apical patch (PAP), which is limited by tight junctions. The PAP will then open and expand through a combination of events: the delivery of vesicular membranes, the repulsion of the apposed membrane by highly charged molecules, the increase of hydrostatic pressure, the coalescence of mini-lumens and, eventually, expansion through cell division. This process is closely synchronized with a profound rearrangement of the actin cytoskeleton into discrete structures essential for the attachment of structural and signaling apical proteins. These proteins will then yield a scaffold to shape the lumen and form an acto-myosin ring in support of the circumferential apical junctional complexes (AJCs), which are made of adherens junctions (AJs) and the apical tight junctions (TJs) that outline the luminal space (Datta et al., 2011; Sigurbjörnsdóttir et al., 2014). The organization and functions of the acto-myosin ring attached to the AJ have been extensively studied (Arnold et al., 2017; Braga, 2016; Grikscheit and Grosse, 2016; Lecuit and Yap, 2015); however, far less is known about the actin cytoskeleton associated to the TJ. Nevertheless, it is likely that both structures are somehow intermingled within the so-called apical perijunctional acto-myosin ring (PAMR) (Ebrahim et al., 2013; Sluysmans et al., 2017). The PAMR is described as a sarcomeric-like belt made of F-actin bundles containing myosin-II, which confers contractile properties, and bundling proteins, such as the non-muscle α-actinins, which stiffen the structure. The balance of both activities is believed to determine the flexibility of this belt, its mechanosensitivity and the tension forces exerted on the cell surface (Foley and Young, 2014; Martin and Goldstein, 2014; Murrell et al., 2015; Röper, 2015). The existence of a central apical acto-myosin network with radial contractility has also been reported (Coravos and Martin, 2016).

The α-actinin (ACTN) family comprises four members, the muscle ACTN2 and ACTN3, and the non-muscle ACTN1 and ACTN4, which are expressed in most other cell types. They share a common primary structure with a N-terminal actin-binding domain (ABD) and a C-terminal calmodulin-like domain (CAMD) separated by a central repeat of four spectrin-like domains (spectrin repeats domain; SRD). ACTN molecules form antiparallel dimers through their rigid SRD allowing for the cross-linking of actin filaments by the ABD positioned on either end. In comparison with the filamin proteins, which orthogonally cross-link actin filaments, non-muscle ACTNs form linear F-actin bundles, which increase the stiffness (Jahed et al., 2014; Stossel et al., 2001). They are believed to contribute to myosin-II-driven contractility by facilitating force transmission (Le Clainche and

[1]Université Côte d'Azur, CNRS, Institut de Pharmacologie Moléculaire et Cellulaire (IPMC), Valbonne, F-06560, France. [2]Centre de Recherche en Cancérologie de Marseille (CRCM), 'Cell Polarity, Cell Signalling and Cancer', Equipe Labellisée Ligue Contre le Cancer, Inserm U1068, Marseille, F-13009, France; CNRS, UMR7258, Marseille, F-13009, France; Institut Paoli-Calmettes, Marseille, F-13009, France; Aix-Marseille University, UM105, Marseille, F-13284, France.
*Present address: BIOASTER, Lyon, F-69007, France.

‡Author for correspondence (luton@ipmc.cnrs.fr)

J.M., 0000-0002-5861-2830; J.-P.B., 0000-0001-8418-3382; M.F., 0000-0003-1853-8661; F.L., 0000-0001-6868-4654

Received 3 August 2017; Accepted 11 December 2017

Journal of Cell Science (2018) 131, jcs209361. doi:10.1242/jcs.209361

Carlier, 2008). ACTNs also act as a mechanical linker between actin filaments and cell–cell and cell–extracellular matrix (ECM) adhesion complexes. Besides its structural roles, ACTNs could also serve to couple actin nucleation to assembly at cell–cell contacts (Tang and Brieher, 2012) and contribute to the maturation of cell–ECM focal adhesion by transmitting mechanical forces (Iskratsch et al., 2014; Jahed et al., 2014; Parsons et al., 2010; Ye et al., 2014). Both ACTN1 and ACTN4 were found at the apical acto-myosin ring in association with the AJ (Honda et al., 1998; Tang and Brieher, 2012), whereas a few studies suggested a link with the TJ (Chen et al., 2006; Geiger et al., 1979; Nakatsuji et al., 2008). Nevertheless, the repertoire of ACTN molecules associated with the various F-actin structures is poorly defined and is made even more complex by the existence of ACTN1–ACTN4 heterodimers (Foley and Young, 2013). Moreover, it is not completely clear how ACTNs are recruited to cell–cell contacts. Thus, much remains to be discovered about the role of ACTNs at the AJC as well as their role during luminogenesis.

Small G-proteins of the Rho family and their partners are key regulators in the assembly and maintenance of the PAMR. In particular, RhoA contributes to the constitution of the contractile apical acto-myosin array through the localization and activation of the formin proteins and the activation of the motor protein myosin-II by the Rho-associated coiled-coil kinase effectors ROCK1 and ROCK2 (hereafter denoted ROCK) (Arnold et al., 2017; Quiros and Nusrat, 2014; Sluysmans et al., 2017; Takeichi, 2014). Tension forces are necessary for the establishment and functioning of the AJC, as they support the changes in cell shape occurring during epithelial morphogenesis (Coravos et al., 2017; Lecuit and Yap, 2015; Takeichi, 2014). However, how contractility and its regulators are impacting epithelial cell luminogenesis is an issue of ongoing debate.

Another small G-protein that regulates the cortical cytoskeleton is the ADP ribosylation factor 6 (Arf6). It plays a pivotal role in a wide variety of cellular events including cell surface trafficking, phagocytosis, cell–cell adhesion, and tumor cell migration and invasion (D'Souza-Schorey and Chavrier, 2006; Gillingham and Munro, 2007; Jaworski, 2007; Sabe et al., 2009; Schweitzer et al., 2011). In epithelial cells, Arf6 was initially shown to regulate vesicular trafficking to the apical pole of the cell (Altschuler et al., 1999) and later to impact the turnover of the AJ (Palacios et al., 2001, 2002, 2005), the establishment of the TJ (Klein et al., 2008; Luton et al., 2004), cyst morphogenesis (Tushir et al., 2010) and HGF-induced tubulogenesis (Tushir and D'Souza-Schorey, 2007). Consistent with these observations, the exchange factor for Arf6 (EFA6; also known as PSD) was found to be enriched at the apical pole and at the TJ in fully polarized MDCK cells (Luton et al., 2004). During early epithelial polarization, EFA6 is recruited to the cell–cell contact in a manner that is dependent on E-cadherin engagement, where it contributes to the formation of the TJ by stabilizing the apical acto-myosin ring (Théard et al., 2010). Expression of EFA6B (also known as PSD4) in the mammary tumoral MCF7 cell line restored a normal glandular phenotype, with the formation of lumens delineated by TJs (Zangari et al., 2014). Conversely, knockdown of EFA6B expression drives various mammary cell lines into epithelial-to-mesenchymal transition (Zangari et al., 2014). In breast cancer patients, the loss of EF6AB expression is associated with the claudin-low subtype characterized by the loss of expression of all the TJ components and a poor prognosis (Zangari et al., 2014).

The EFA6 family consists of four isoforms (EFA6A–EFA6D; EFA6C is also known as PSD2, and EFA6D as PSD3) sharing a general structure that comprises a variable N-terminal domain, a catalytic Sec7 domain bearing the nucleotide exchange activity, a PH domain responsible for their plasma membrane localization and a conserved C-terminal region involved in actin cytoskeleton rearrangement (Derrien et al., 2002; Franco et al., 1999; Sakagami, 2008; Sironi et al., 2009). In a previous study, we found that mutations that abolish the nucleotide exchange activity or delete the C-terminal domain abrogated the stimulatory effects of EFA6, indicating that both Arf6 activation and the C-terminal domain are necessary for epithelial polarization (Luton et al., 2004). In addition, complementation experiments demonstrated a finely tuned cooperation between the two signaling pathways associated with the activated Arf6 and with the EFA6 C-terminus (Klein et al., 2008).

In this study, we aimed to determine the signaling pathway associated to EFA6 C-terminus that contributes to its action on epithelial morphogenesis. Our data showed that: (1) ACTN1 is a direct partner of EFA6A C-terminal domain, (2) EFA6A is a crucial regulator of luminogenesis for which ACTN1 is the major effector, (3) together, they stimulate the formation and enlargement of a single lumen with a proper round shape, (4) they act by regulating cortical acto-myosin contractility, and finally (5) ACTN1 is also a partner of the EFA6B isoform in the promotion of lumen formation in the mammary tumoral cells MCF7.

RESULTS

EFA6A binds directly to ACTN1

Looking for functional partners of EFA6A in epithelial cells, we performed a two-hybrid screen of an epithelial library using the C-terminus (Cter) of EFA6A as a bait, and identified ACTN1 as the major interacting protein. A similar result was found by Sakagami et al. in a previous screen using a neuronal library (Sakagami et al., 2007). A pulldown assay was used to confirm that the Cter of EFA6A could bind exogenously expressed ACTN1–GFP (Fig. 1A). We then further characterized this interaction by assessing whether the two proteins could bind directly. We found that both GST–ACTN1 and GST–ACTN4 could pulldown full-length His–EFA6A (Fig. 1B), and that the central SRD of ACTN1 binds directly to His–EFA6A (Fig. 1C). In BHK cells, GFP–EFA6A co-immunoprecipitated endogenous ACTN1 (Fig. 1D), and Myc–EFA6A re-localized the endogenous ACTN1 to F-actin-enriched lamellipodia as well as to the cell surface microspikes induced by Myc–EFA6A (Fig. 1E; Derrien et al., 2002; Macia et al., 2008). We conclude that, *in vitro*, ACTN and EFA6A can bind directly through their respective spectrin and C-terminal domains, and that, *in vivo*, EFA6A can recruit the endogenous ACTN1 to cortical F-actin structures. In agreement with our previous reports (Luton et al., 2004; Théard et al., 2010; Zangari et al., 2014), during lumen formation mRFP–EFA6A was transiently found to be enriched at the AMIS and the opened PAP before its expression at the apical surface decreased to the low level found in mature cyst (Fig. S1A). We also examined the localization of ACTN1 and ACTN4 in polarized cysts formed by MDCK cells. ACTN1–GFP was diffused within the cytoplasm and enriched at the apex of cell-cell junctions (Fig. S1A). Colocalization of ACTN1–GFP with occludin (Fig. 1Fa–a″) indicated its accumulation at the TJ. In contrast, ACTN4–GFP was not consistently observed at the TJ at above the level of the GFP control (Fig. S1A; Fig. 1Fc–c″). In addition, ACTN1–GFP was found to be enriched at the nascent lumen formed in between two cells and its surrounding TJ (Fig. 1Fb–b″), whereas ACTN4–GFP was found on the newly formed luminal membrane and also was enriched along the cell–cell contact (Fig. 1Fd–d″).

Journal of Cell Science (2018) 131, jcs209361. doi:10.1242/jcs.209361

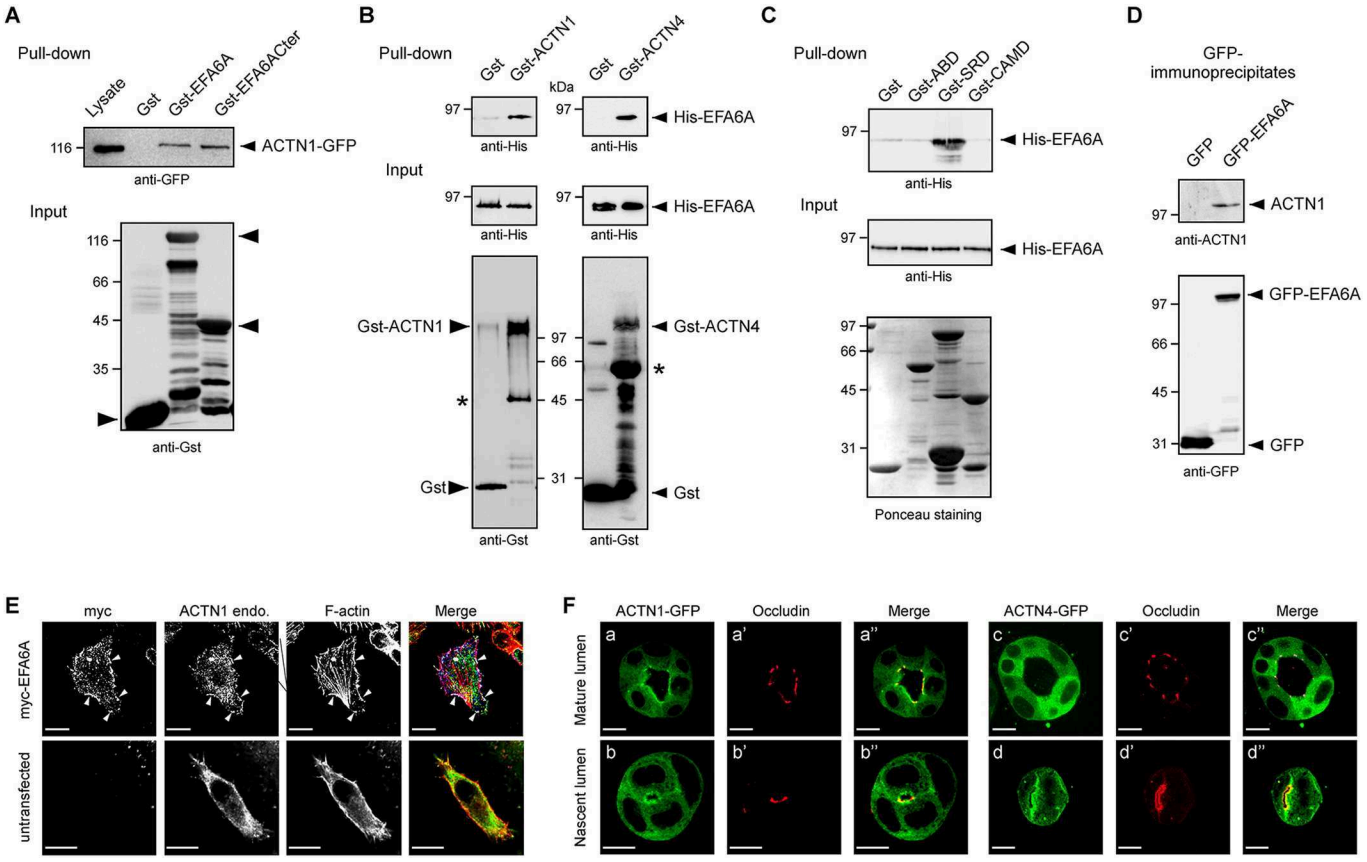

Fig. 1. EFA6A binds directly to ACTN1. (A) Lysate of MDCK cells expressing ACTN1–GFP was reacted with GST, GST–EFA6A or GST–EFA6ACter prebound to glutathione–sepharose beads. The top arrowhead points to GST–EFA6A and the bottom arrowhead to GST–EFA6ACter. (B) Purified GST, GST–ACTN1 and GST–ACTN4 prebound to glutathione–sepharose beads were reacted with purified (6xHis)–EFA6A. The asterisk highlights a main purification contaminant. (C) Purified GST, GST–ABD, GST–SRD and GST–CAMD (fragments of ACTN1) prebound to glutathione–sepharose beads were reacted with purified (6xHis)-EFA6A. In A–C, the input or whole lysate and bound proteins were analyzed by immunoblotting with the indicated antibodies. (D) GFP or GFP–EFA6A expressed in BHK cells were immunoprecipitated using an anti-GFP antibody and the co-precipitation of endogenous ACTN1 was assessed by immunoblotting. (E) BHK cells expressing or not expressing Myc–EFA6A were processed for immunofluorescence and stained for Myc (blue), F-actin (red) and the endogenous ACTN1 (ACTN1 endo., green). Arrowheads point to EFA6A-induced lamellipodia where the endogenous ACTN1 is recruited. (F) MDCK cells expressing ACTN1–GFP (green; a–b″) or ACTN4–GFP (green; c–d″) were processed for immunofluorescence to label the endogenous occludin (red) in mature or nascent lumens. Scale bars: 10 µm.

Later, in mature cysts, ACTN4–GFP appeared to be more enriched in AJs stained for E-cadherin (Fig. S1B). Given the enrichment of ACTN1 at the TJ, we focused our study on the importance of its role as an effector of EFA6.

EFA6A recruits ACTN1 in a regulated manner

EFA6A and ACTN1 are cortical actin regulators and both partially localize to the TJ in polarized epithelial cells; we thus investigated the mechanism of their direct interaction. ACTN1 could serve as a receptor to recruit EFA6A to the TJ. However, EFA6A localization to the plasma membrane was shown to rely on its phosphatidylinositol 4,5-bisphosphate (PIP2)-specific PH domain and its capacity to bind to F-actin (Macia et al., 2008). Furthermore, the EFA6A mutant deleted of its C-terminus, which no longer binds ACTN1, has been shown to localize at the plasma membrane in a similar manner to the full-length protein (Franco et al., 1999; Macia et al., 2008). In contrast, as shown above (Fig. 1E) ACTN1 was re-localized to Myc–EFA6A-induced membrane ruffles, suggesting that ACTN1 can be used as an effector of EFA6A in order to remodel the cortical actin cytoskeleton.

To further analyze the binding of ACTN1 to EFA6A and its functional properties in living cells, we ectopically expressed EFA6A away from the plasma membrane. We fused EFA6A to the mitochondrial-targeting peptide ActA and determined whether EFA6A–ActA was capable of re-localizing the endogenous ACTN1 to the outer membrane of mitochondria, from which it is normally absent. Since ACTN1 binds to the C-terminal domain of EFA6A, we first studied the EFA6ACter fused to mRFP and ActA (named hereafter EFA6ACter–mRFP–ActA). As previously observed by others, depending on the expression rate and construct used, in cells transfected with ActA chimeras the mitochondrial network tended to aggregate around the nucleus (Bubeck et al., 1997; Moeller et al., 2004; Reinhard et al., 1999; Zhang et al., 2009). Nevertheless, all constructs localized to the mitochondria as assessed by monitoring colocalization with the mitochondrial protein Hsp60 (also known as HSPD1) (Fig. S2A). When expressed in BHK cells, EFA6ACter–mRFP–ActA localized to the mitochondria (Fig. S2A) and recruited endogenous ACTN1 (Fig. 2A; magnification in Fig. S2B). In contrast, the control mRFP–ActA construct, which also localized to the mitochondria (Fig. S2A), did not recruit ACTN1 (Fig. 2A). Interestingly, the full-length EFA6A–mRFP–ActA localized to the mitochondria (Fig. S2A) but did not re-localize ACTN1 (Fig. 2A). This observation suggests that the Cter was not available for ACTN1 binding in the full-length EFA6A. Our previous work indicates that EFA6A exists in a closed conformation where the Cter is folded

Journal of Cell Science (2018) 131, jcs209361. doi:10.1242/jcs.209361

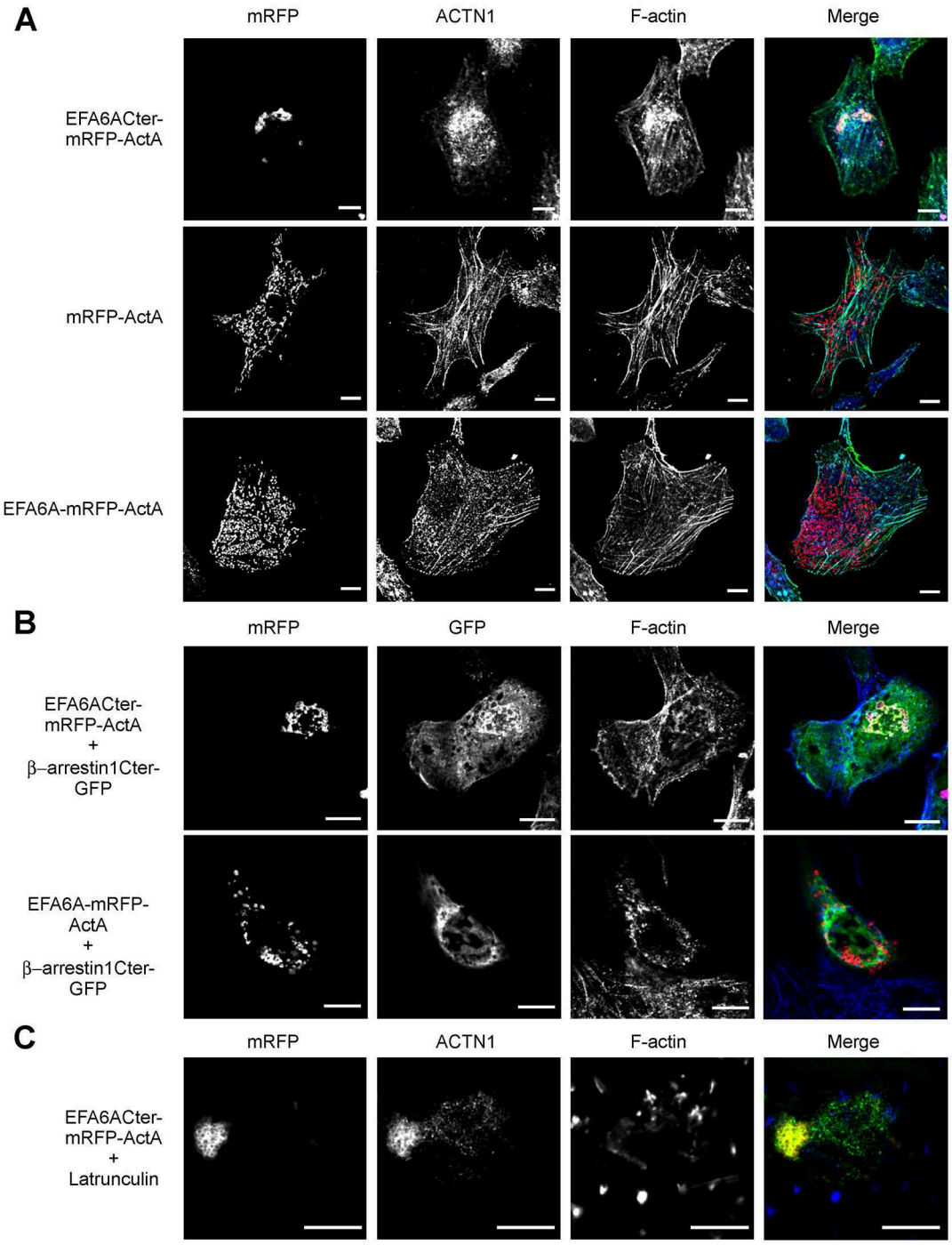

Fig. 2. EFA6A recruits ACTN1 in a regulated manner. (A) BHK cells expressing EFA6ACter–mRFP–ActA, mRFP–ActA and EFA6A–mRFP–ActA were processed for immunofluorescence to label the endogenous ACTN1 and F-actin. In merge images, mRFP is colored red, ACTN1 blue and F-actin green. (B) BHK cells co-expressing β-arrestin1Cter–GFP (green) with EFA6ACter–mRFP–ActA (red) or with the full-length EFA6A–mRFP–ActA (red) were processed for immunofluorescence to label the endogenous F-actin (blue). (C) BHK cells expressing EFA6ACter–mRFP–ActA were exposed to Latrunculin A (2 µM) for 2 h. The cells were processed for immunofluorescence to label the endogenous ACTN1 (green) and F-actin (blue). Scale bars: 10 µm.

back onto the PH domain, preventing its association with the C-terminus of β-arrestin1 (denoted β-arrestin1Cter), another EFA6ACter ligand (Macia et al., 2012). To test whether the EFA6A–mRFP–ActA was in a locked conformation, we co-expressed β-arrestin1Cter–GFP with EFA6ACter–mRFP–ActA or the full-length EFA6A–mRFP–ActA constructs. Similar to what was observed with ACTN1, β-arrestin1Cter–GFP could only bind to EFA6ACter–mRFP–ActA (Fig. 2B) indicating that the binding of ACTN1 to EFA6A is regulated, and requires the release of its C-terminal domain.

Some F-actin staining was observed colocalized together with EFA6ACter–mRFP–ActA and the endogenous ACTN1 at the mitochondria (Fig. 2A; magnification in Fig. S2B). When the cells were treated with Latrunculin A, F-actin was absent from the mitochondria whereas the endogenous ACTN1 was still efficiently recruited by EFA6Cter–ActA (Fig. 2C). Thus, independently of the

Journal of Cell Science (2018) 131, jcs209361. doi:10.1242/jcs.209361

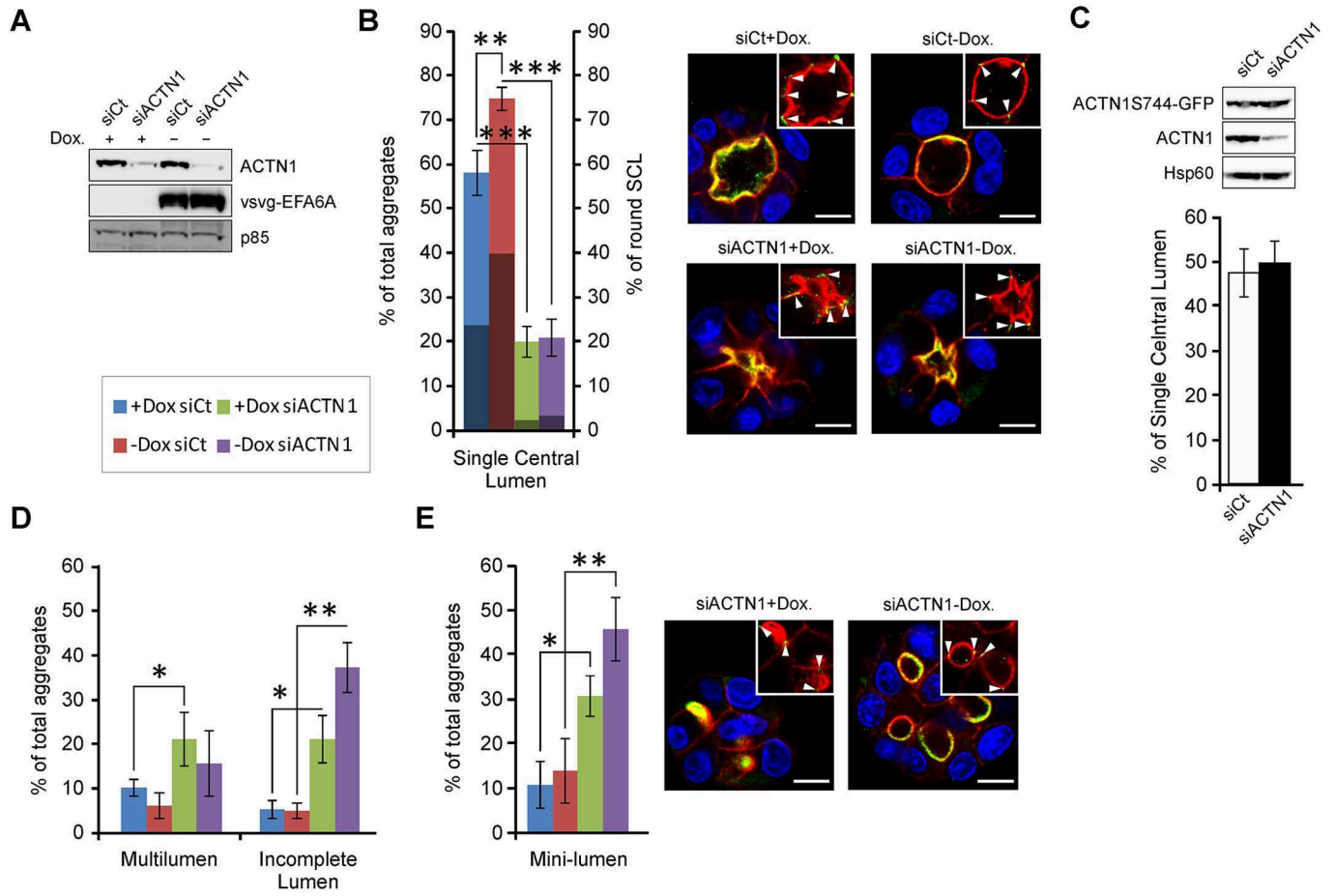

Fig. 3. Depletion of ACTN1 inhibits normal EFA6A-induced luminogenesis. (A) MDCK cells expressing inducible VSV-G–EFA6A were transfected with siRNA directed against ACTN1 (siACTN1; #2225) or with control siRNA (siCt), and were grown without or with doxycycline (Dox) to induce or not the expression of VSV-G–EFA6A, respectively. At 48 h post transfection, the cells were solubilized in SDS lysis buffer and the expression of the indicated proteins was analyzed by immunoblotting. The p85 regulatory subunit of PI3K served as a loading control. (B) Left, quantification of the percentage of cell aggregates with a SCL (left *y*-axis). Shaded areas indicate the percentage of those SCL aggregates with a round lumen (right *y*-axis). Results are mean±s.d., *n*=5. Right, representative images of the four cell types labeled for the nuclei (blue), apical marker PDX (green) and F-actin (red) are shown. The insets display an image of the same lumens stained for F-actin (red) and the TJ marker occludin (green). Arrowheads point to the TJs. (C) MDCK cells expressing ACTN1S744–GFP were transfected with siCt or siACTN1 (#2225). Top panel, the cells were solubilized in SDS lysis buffer and the expression of the indicated proteins analyzed by immunoblotting. Hsp60 served as a loading control. Bottom panel, quantification of the percentage of aggregates with a SCL. No significant difference was measured. Results are mean±s.d., *n*=3. (D) Quantification of the percentage of aggregates with multilumens or incomplete lumens for the indicated conditions. Results are mean±s.d., *n*=5. (E) Quantification of the percentage of aggregates with mini-lumens for the indicated conditions. Representative images of cells depleted in ACTN1, and expressing or not expressing VSV-G–EFA6A, labeled for the nuclei (blue), the apical marker PDX (green) and F-actin (red). The insets display an image of the same mini-lumens stained for F-actin (red) and the TJ marker occludin (green). Arrowheads point to the TJ. **P*≤0.05; ***P*≤0.01; ****P*≤0.001 (Student's *t*-test). Scale bars: 10 µm.

presence of F-actin, EFA6A can directly recruit ACTN1, which in turn might function as an effector to organize EFA6A-regulated actin-based structures.

Depletion of ACTN1 inhibits normal EFA6A-induced luminogenesis

We have previously shown that expression of EFA6A tagged with the G glycoprotein of the vesicular stomatitis virus (VSV-G) (VSV-G–EFA6A) stimulates apical polarity development and TJ formation in MDCK cells (Klein et al., 2008; Luton et al., 2004). To assess the role of ACTN1 as an effector of EFA6A, we analyzed the effects of its downregulation in cells grown in a 3D-culture system in Matrigel. Several siRNAs against ACTN1 were tested for their efficiency to downregulate its expression (Fig. S3A). ACTN1 knockdown was carried out in MDCK cells in which the expression of VSV-G–EFA6A is under the control of the tetracycline (Dox)-repressible transactivator (hereafter denoted MDCK-VSV-G–EFA6A cells) (Luton et al., 2004). Fig. 3A is a representative immunoblot analysis of ACTN1 depletion and VSV-G–EFA6A expression in the presence or absence of doxycycline.

We first examined whether EFA6A overexpression stimulated epithelial polarity in MDCK cells grown in Matrigel over 3 days. Cysts of homogenous size (from 4 to 15 cells) were analyzed for the formation of one or multiple lumens and for their shape. They were also characterized for extension and expansion. Extension refers to the opening of the lumen to all the cells of the aggregates, while expansion refers to the enlargement of the luminal space. Upon VSV-G–EFA6A expression (−Dox) we observed an increase in the formation of cysts displaying a single central lumen (SCL). In addition, the luminal space became more round with an almost doubling (from 23% to 40%) of the SCL, with it displaying a round shape upon VSV-G–EFA6A expression (Fig. 3B, shaded bars and upper right panel). In contrast, depletion of ACTN1 in control conditions (+Dox) reduced the number of cysts with a SCL and

severely altered the shape of the lumen such that the lumens adopted an 'octopus-like' shape with a small central opening from which closed or barely opened luminal extensions reached in between the cells (Fig. 3B, shaded bars and lower left panel). Depletion of ACTN1 in cells expressing VSV-G–EFA6A also impaired enlargement of the lumens, although the opening was more visible (Fig. 3B, shaded bars and bottom right panel). Thus, ACTN1 is required for the stimulatory effects found for EFA6A on SCL formation and on the rounding of the luminal space of multicellular cysts. However, in all conditions, the cells remained well polarized as indicated by the correct localization of the apical podocalyxin (PDX; also known as PODXL) and basolateral (E-cadherin) markers (Fig. S3B), and by the basal positioning of the nuclei, the general F-actin organization and the apical assembly of the TJ (Fig. 3B). To confirm that the phenotypes induced by the siRNA against ACTN1 (siACTN1) were due to ACTN1 depletion we carried out a rescue experiment. MDCK cells expressing an ACTN1–GFP which is insensitive to the siACTN1 (ACTN1S744–GFP) did not display any defect in lumen formation upon depletion of the endogenous ACTN1 (Fig. 3C).

The loss of cysts with SCLs in the ACTN1-depleted cells was counterbalanced by an increase of cell aggregates with multiple lumens and others with incomplete extension to all of the cells (Fig. 3D, see Materials and Methods). In both cases, the lumens displayed the distorted octopus-like shape. The extension defect was further reflected by a strong increase in the number of aggregates displaying multiple lumens that only opened in between two cells (hereafter called mini-lumens) that were often blocked at the PAP stage with no visible opening (Fig. 3E), which suggests that ACTN1 depletion might favor the early formation of an initial lumen. VSV-G–EFA6A expression did not significantly alter the phenotypic changes imposed upon ACTN1-depletion; however, it stimulated the enlargement and rounding of the mini-lumens blocked at the two-cell stage (Fig. 3E, right panel). Thus, as opposed to what is seen for mature lumens, EFA6A can stimulate the volumetric enlargement of nascent mini-lumens in an ACTN1-independent manner. Taken together, these observations suggest that ACTN1 is dispensable for the formation of the initial lumen in between two cells but is required later on for its extension and enlargement (see Discussion section for further comments). In summary, depletion of ACTN1 blocked both the effects of VSV-G–EFA6A on luminogenesis, that is, the formation of fully extended SCL and its expansion as regular round lumen. This suggests that ACTN1 acts as an effector downstream of EFA6A that is important for luminogenesis.

ACTN1 acts as an effector of EFA6A to promote normal luminogenesis

If EFA6A controls luminogenesis and ACTN1 acts as an effector, then EFA6A depletion should hamper luminogenesis, and when combined with ACTN1 depletion there should have no additional effect. MDCK-VSV-G–EFA6A cells grown in the absence or presence of doxycycline were submitted to siRNA against EFA6A (siEFA6A)-, siACTN1- or simultaneous siEFA6A- and siACTN1-mediated depletion. The efficient knockdown of the indicated proteins and the induction of the expression of VSV-G–EFA6A were analyzed by immunoblotting (Fig. 4A; Fig. S4).

Depletion of the endogenous EFA6A was accompanied by a reduction in the amount of cell aggregates with a SCL demonstrating that EFA6A is required for luminogenesis (Fig. 4B). Expression of the exogenous human VSV-G–EFA6A, which is insensitive to the canine-specific siRNA, rescued the normal phenotype, thus controlling for the specificity of EFA6A knockdown (Fig. 4B). As shown in Fig. 3, ACTN1 depletion hampered luminogenesis and blocked the VSV-G–EFA6A stimulation. However, ACTN1 depletion did not have any additional effect when the endogenous EFA6A was knocked down (Fig. 4B). In addition, the exogenous expression of VSV-G–EFA6A in the double knockdown cells could not rescue the normal phenotype (Fig. 4B). In addition, we analyzed the consequences on the lumen formation of expressing a mutant of EFA6A deleted of its C-terminus (EFA6AΔC), which contains the ACTN1-binding site. Expression of VSV-G–EFA6AΔC impaired normal luminogenesis and caused the formation of lumens with an octopus-like shape (Fig. 4C). Although the C-terminus of EFA6A likely interacts with other molecules, it is important to note that its truncation generated lumens with shapes that were similar to those observed in ACTN1-depleted cells. Taken together, these observations indicate that EFA6A mediates luminogenesis in MDCK cells and that ACTN1 is a crucial effector for this process.

ACTN1 is an effector of EFA6B for luminogenesis induction in MCF7 breast cancer cells

We have reported that the EFA6B isoform is an antagonist of breast cancer development (Zangari et al., 2014). Tumoral MCF7 cells grown in 3D-culture systems form compact aggregates with no lumen (Han et al., 2010; Kenny et al., 2007). The exogenous expression of VSV-G–EFA6B in the tumoral MCF7 cells restores an epithelial phenotype characterized by the appearance of aggregates with extended lumens (although not often a SCL), delineated by functional TJs (Zangari et al., 2014). Thus, we asked whether ACTN1 was required downstream of EFA6B to contribute to luminogenesis in MCF7 cells.

We first verified that ACTN1 could also bind to the EFA6B isoform (Fig. S5). Next, we analyzed the effect of ACTN1 depletion in both control MCF7 and MCF7-VSV-G–EFA6B cells grown in Matrigel. An immunoblot analysis demonstrated the efficient knockdown of ACTN1 in both cell lines (Fig. 5A). We quantified the number of aggregates with extended lumens opened to at least four cells, as opposed to mini-lumens opened in between only two cells. As previously reported, MCF7 control cells do not form cysts with lumens (Han et al., 2010; Kenny et al., 2007; Zangari et al., 2014), whereas exogenous expression of VSV-G–EFA6B induced the formation of cysts with extended lumens (Fig. 5B; Zangari et al., 2014). We observed that ACTN1 depletion blocked the formation of extended lumens induced by EFA6B indicating that, in MCF7 cells, ACTN1 is also a crucial effector of EFA6B-induced lumen formation (Fig. 5B). In addition, although control MCF7 cell aggregates did not form extended lumens, in ∼20% of the aggregates one or several mini-lumens were observed (Fig. 5C,D). Upon ACTN1 depletion, the number of these mini-lumens increased in both the VSV-G–EFA6B-expressing and non-expressing MCF7 cell lines. However, in VSV-G–EFA6B-expressing cells aggregates the luminal space was enlarged while in MCF7 controls cells the mini-lumens were seen as PAPs (Fig. 5C,D). Thus, similar to what we had observed in MDCK cells, ACTN1 depletion facilitates the initial lumen formation in between two cells but then hampers both extension and enlargement.

EFA6A and ACTN1 control apical contractility contributing to luminogenesis

The PAMR and ventral stress fibers (SFs) are sarcomere-like actin-based structures capable of contractility that have been implicated in epithelial morphogenesis. Contractile actin bundles are formed by aligned fibers cross-linked by a periodic distribution of ACTNs that alternates with myosin-II (Burridge and Wittchen, 2013; Sluysmans

Journal of Cell Science (2018) 131, jcs209361. doi:10.1242/jcs.209361

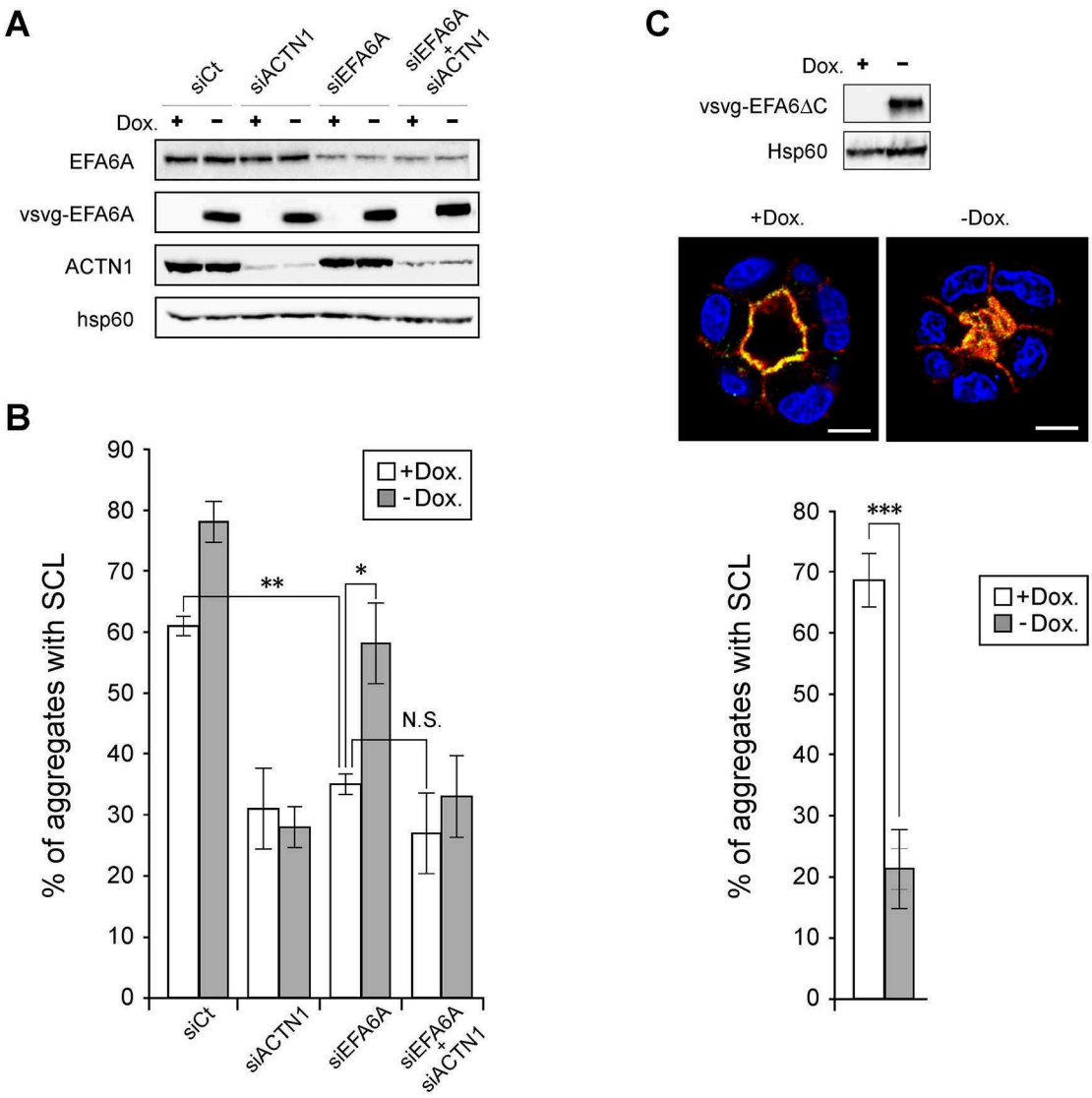

Fig. 4. ACTN1 acts as an effector of EFA6A to promote normal luminogenesis. (A) MDCK cells expressing inducible VSV-G–EFA6A were transfected with siRNA control (siCt), siRNA directed against ACTN1 (siACTN1; #2225) or EFA6A (siEFA6A; #2661), or both siACTN1 and siEFA6A, and then grown without or with doxycycline (Dox) to induce or not the expression of VSV-G–EFA6A, respectively. At 48 h post transfection the cells were solubilized in SDS lysis buffer and the expression of the indicated proteins analyzed by immunoblotting. Hsp60 served as a loading control. (B) Quantification of the percentage of cell aggregates with a SCL. Results are mean±s.d., *n*=4. (C) MDCK cells expressing inducible VSV-G–EFA6AΔC were grown with or without Dox. Top panel, at 48 h post transfection the cells were solubilized in SDS lysis buffer and the expression of VSV-G–EFA6AΔC analyzed by immunoblotting. Hsp60 served as a loading control. Middle panel, representative images of cell aggregates grown with or without Dox labeled for the nuclei (blue), apical marker PDX (green) and F-actin (red). Bottom panel. quantification of the percentage of cell aggregates with a SCL. Results are mean±s.d., *n*=3. **P*≤0.05; ***P*≤0.01; ****P*≤0.001; N.S., not significant (Student's *t*-test). Scale bars: 10 µm.

et al., 2017). RhoA and its effectors (ROCK and mDia1) have been recognized as major regulators of the contractile properties of the acto-myosin cytoskeletons (Arnold et al., 2017; Quiros and Nusrat, 2014; Sluysmans et al., 2017; Takeichi, 2014). Thus, we tested the possibility that EFA6A and ACTN1 regulate luminogenesis by contributing to the PAMR contractility. First, we used an antibody directed against the phosphorylated regulatory myosin light chain 2 (pMLC, also known as MYL2) as a proxy to evaluate the tension forces in response to modulating EFA6A and ACTN1 expression. Fig. 6B shows a representative immunoblot analysis of ACTN1 depletion and VSV-G–EFA6A expression in the presence or absence of doxycycline. In control cells, the pMLC staining appeared as small intracellular dots, as well as larger dots located in proximity to the apical membrane. Under conditions of EFA6A or ACTN1 depletion, this apical staining disappeared and the pMLC distribution became more diffuse. Upon VSV-G–EFA6A expression the proportion of apical pMLC was increased and its staining was evenly distributed all around the luminal cortex. In ACTN1-depleted cells, the VSV-G–EFA6A-induced apical accumulation of pMLC was abrogated (Fig. 6A). These results suggest that EFA6A can modulate the apical tension forces in an ACTN1-dependent manner.

We investigated the contribution of ACTN1 by first analyzing the effect of its depletion on the RhoA-stimulated ventral SFs in MDCK cells by expressing the N-terminal Myc-tagged constitutively active mutant of RhoA (Myc–RhoAV14) under the control of the inducible Tet-off system. The levels of expression of the proteins in different conditions were analyzed by immunoblotting (Fig. 6C). We monitored the Myc–RhoAV14-induced SF contractility by immunofluorescence. We looked at the F-actin organization and the

Journal of Cell Science (2018) 131, jcs209361. doi:10.1242/jcs.209361

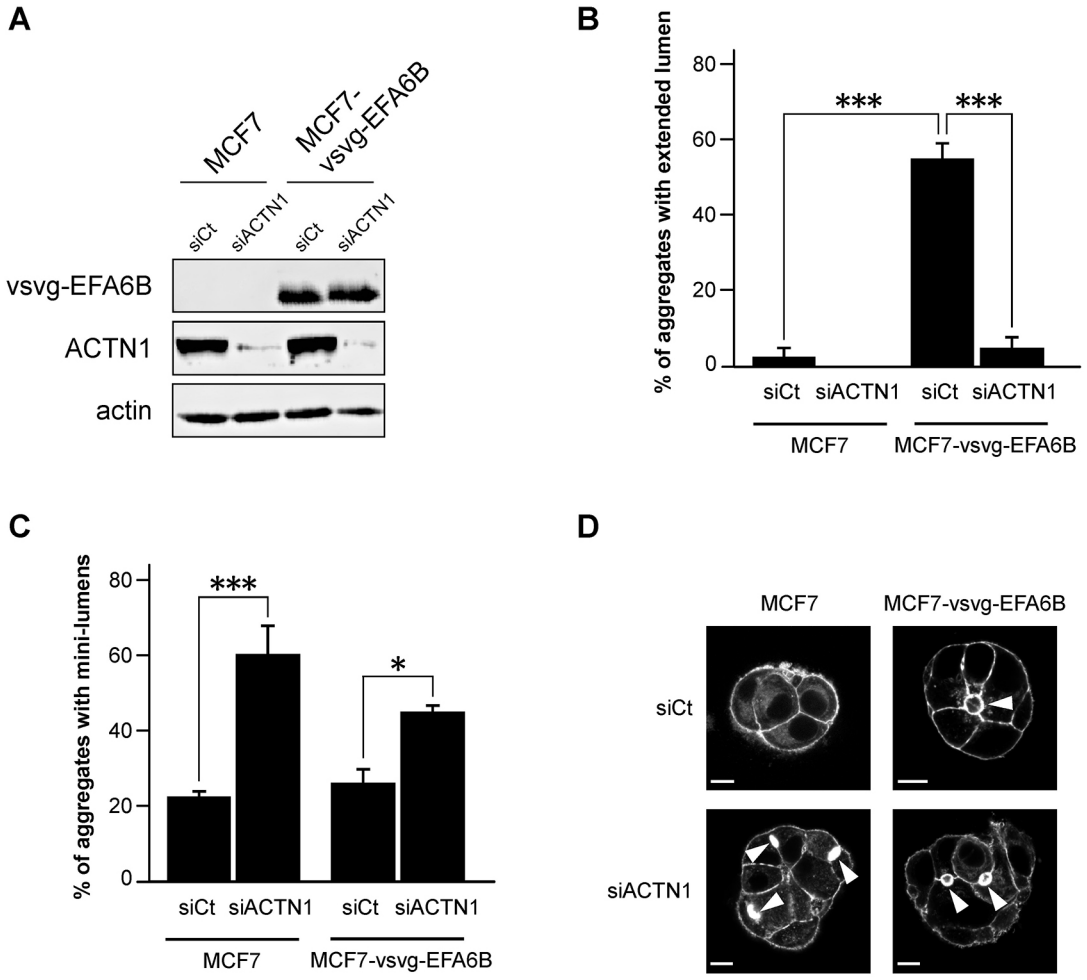

Fig. 5. ACTN1 is an effector of EFA6B that acts to induce luminogenesis in the MCF7 breast cancer cell line. (A) Control and VSV-G–EFA6B-expressing MCF7 cells were transfected with siRNA control (siCt) or siRNA directed against ACTN1 (siACTN1). At 48 h post transfection the cells were solubilized in SDS lysis buffer and the expression of the indicated proteins analyzed by immunoblotting. Actin served as a loading control. (B) Quantification of the percentage of the indicated cell aggregates with extended lumens. (C) Quantification of the percentage of the indicated cell aggregates with mini-lumens. Results in B and C are mean±s.d., n=3. *P≤0.05; ***P≤0.001 (Student's t-test). (D) Representative images of cells depleted or not for ACTN1 and expressing or not expressing VSV-G–EFA6B. The cell aggregates were processed for immunofluorescence by labeling cytoskeletal F-actin with fluorescent phalloidin. Arrowheads point to PAPs. Scale bars: 10 µm.

contractility status by following the distribution of pMLC and paxillin, a marker of the focal adhesions (Fig. 6D). As expected, the expression of Myc–RhoAV14 (−Dox) stimulated the formation of SFs that appeared as thick bundles of parallel F-actin going across the whole cell cluster (Fig. 6Db). In Myc–RhoAV14-expressing cells, pMLC was redistributed all along the SFs (Fig. 6Db′) while in control cells pMLC was enriched at the periphery of the cell cluster and excluded from cell–cell contacts (Fig. 6Da′). Concomitantly, paxillin was re-localized to the periphery of the cell cluster mostly decorating the focal adhesions at the extremity of the SF (Fig. 6Db″). As previously observed by others (Oakes et al., 2012), depletion of ACTN1 in control cells (+Dox) led to the loss of bundles or shortening of radial F-actin bundles resembling transverse arcs (Fig. 6Dc). These structures were stained for pMLC, which remained absent from cell–cell contacts (Fig. 6Dc′). The paxillin signal increased but was still homogeneously distributed within each cell of the cluster similar to what was seen in control cells (Fig. 6Dc″). Depletion of ACTN1 blocked the effects of Myc–RhoAV14, leading to cells displaying a phenotype that was comparable to that of the control cells with respect to all three markers (Fig. 6Dd–d″). We conclude that ACTN1 can balance the contractility status of RhoA-dependent SFs in MDCK cells.

Interfering with the RhoA–ROCK–myosin-II contractility pathway has been shown to alter luminogenesis in MDCK cells (Ferrari et al., 2008; Kim et al., 2015; Rodríguez-Fraticelli et al., 2012). In particular, under permissive conditions, the constitutively active RhoAV14 mutant blocks the initial step of lumen formation (Ferrari et al., 2008). We thus asked whether ACTN1 depletion could prevent the Myc–RhoAV14 inhibitory effect on luminogenesis. In our 3D cell culture conditions, Myc–RhoAV14 expression abrogated lumen formation. The cells became round and loosely attached, forming aggregates almost exclusively without lumens and that displayed an inverted polarity, as judged by the peripheral localization of the apical PDX marker (Fig. 6E,F). ACTN1 depletion partially rescued the formation of lumens (Fig. 6E). We observed aggregates with multilumens or incomplete lumen formation, essentially as mini-lumens (Fig. 6E). The cells adopted a more cuboidal shape and formed more-compact aggregates (Fig. 6F). These results suggest that the knockdown of ACTN1 acts to reduce the strong

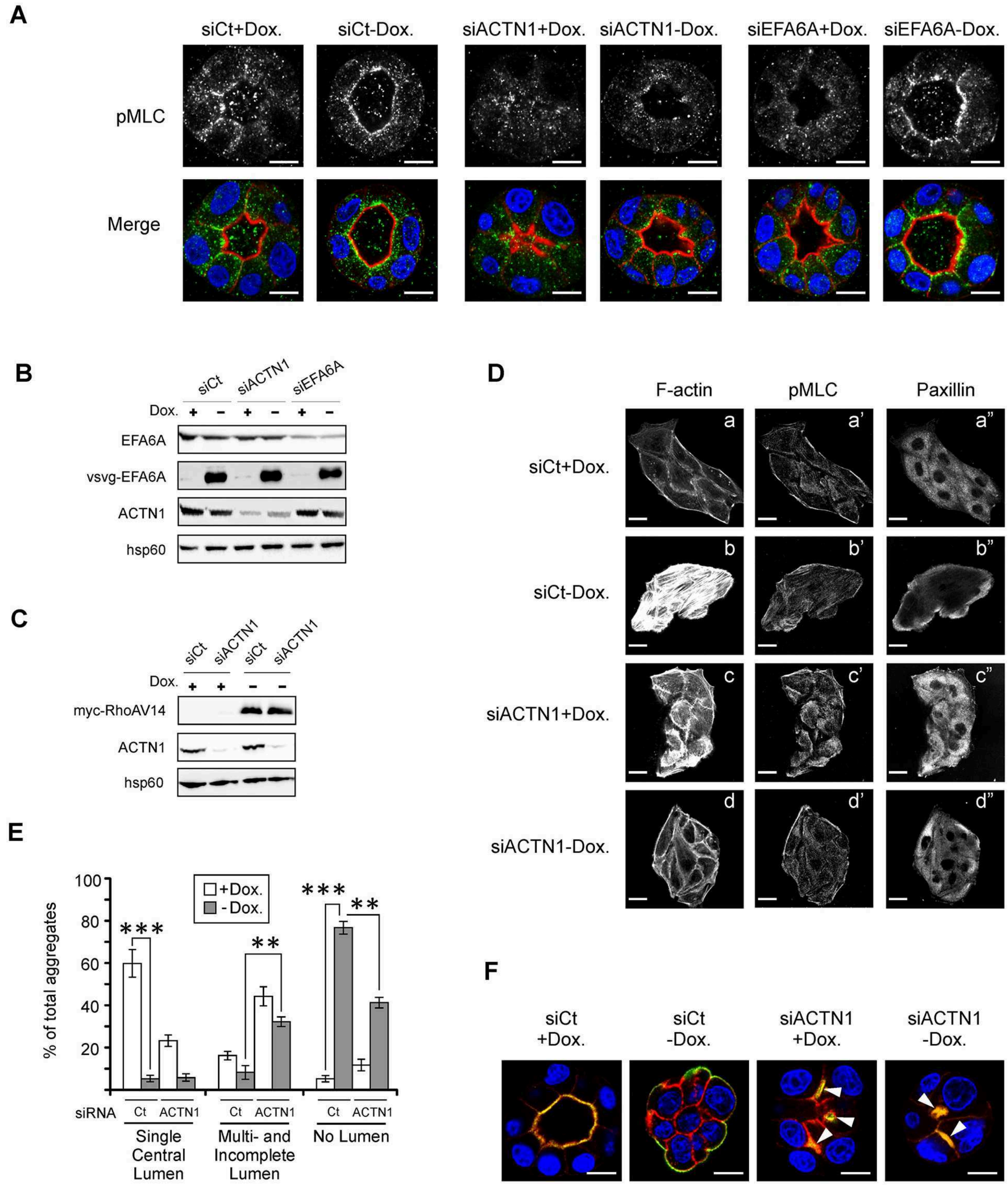

Fig. 6. EFA6A and ACTN1 control apical contractility, thereby contributing to luminogenesis. (A,B) MDCK cells expressing inducible VSV-G–EFA6A were transfected with siRNA control (siCt), or siRNA directed against ACTN1 (siACTN1; #2225) or EFA6A (siEFA6A; #2661) and then grown without or with doxycycline (Dox) to induce or not the expression of VSV-G–EFA6A, respectively. (A) Representative images of the aggregates labeled for pMLC, F-actin and the nuclei. Top panels, pMLC staining alone. Bottom panels show the corresponding merged images; pMLC is colored in green, F-actin in red and the nuclei in blue. Scale bars: 10 µm. (B) At 48 h post transfection the cells were solubilized in SDS lysis buffer and the expression of the indicated proteins analyzed by immunoblotting. Hsp60 served as a loading control. (C) MDCK cells expressing inducible Myc–RhoAV14 were transfected with siCt or siACTN1 (#2225) and grown with or without doxycycline. At 48 h post transfection the cells were solubilized in SDS lysis buffer and the expression of the indicated proteins was analyzed by immunoblotting. Hsp60 served as a loading control. (D) MDCK cells expressing inducible Myc–RhoAV14 were transfected with siCt or siACTN1 (#2225) and grown on coverslips with or without doxycycline. At 48 h post transfection the cells were processed for immunofluorescence and labeled for F-actin (a–d), pMLC (a′–d′) and the focal adhesion protein paxillin (a″–d″). Scale bars: 20 µm. (E) MDCK cells expressing inducible Myc-RhoAV14 were transfected with siCt or siACTN1 (#2225), and grown with or without doxycycline in Matrigel. Quantification of the indicated cell aggregates for SCLs, multilumens and incomplete lumens or no lumen is reported in the bar graph. Results are mean±s.d., *n*=3. ***P*≤0.01; ****P*≤0.001 (Student's *t*-test). (F) Representative images MDCK cells with inducible Myc–RhoAV14 depleted or not for ACTN1 (#2225) and grown for 4 days in Matrigel with or without doxycycline. The cell aggregates were processed for immunofluorescence and labeled for the nuclei (blue), the apical marker PDX (green) and the F-actin (red). Arrowheads point to PAPs and mini-lumens. Scale bars: 10 µm.

contractility imposed by Myc–RhoAV14, thus allowing the initiation of lumen formation. This is in agreement with previous studies that show that reduction of the myosin-II contractility stimulates the initial early step of lumen opening at the two-cell stage (Ferrari et al., 2008; Rodríguez-Fraticelli et al., 2012). However, the extension and enlargement of the lumens, which we demonstrate to be dependent on ACTN1, were both still compromised upon reduction of contractility induced by ACTN1 depletion. Thus, our findings support a model whereby the initial stage of the lumen formation is facilitated by the absence of ACTN1, followed by lumen maturation, which is ACTN1 dependent.

Taken together, our data suggest that EFA6A and its effector ACTN1 contribute to SCL formation through the regulation of the cell surface tension forces within the cell aggregate.

DISCUSSION

In this study, we aimed to define the role of EFA6, a regulator of epithelial polarization, in lumen formation by using a 3D epithelial cell culture system. Given the importance of the reorganization of the actin cytoskeleton during cystogenesis, we were particularly interested in deciphering the signaling pathway associated with the EFA6 C-terminal domain that is capable of remodeling the cortical actin independently of EFA6 GEF activity.

Searching for partners of EFA6ACter, we find that EFA6A binds directly to the non-muscular ACTN member ACTN1. We characterized this interaction in living cells by using a mitochondrial-targeting system, and observed that it is likely regulated by the structural conformation of the EFA6A C-terminus. This observation confirms our previous results obtained with another EFA6Cter ligand, β-arrestin1 (Macia et al., 2012), and implies the existence of a common regulatory mechanism whereby binding to EFA6ACter requires an opening signal. A possible candidate for mediating this signal is Arf6-GTP, the product of EFA6A Sec7-dependent nucleotide exchange activity. ARNO (also known as CYTH2), another Sec7 family guanine nucleotide exchange factor for Arf1, was shown to adopt an auto-inhibited conformation where its short C-terminus downstream of the PH domain interferes with the catalytic Sec7 domain (DiNitto et al., 2007). Arf6-GTP binds to the PH domain of ARNO and stimulates, in synergy with plasma membrane lipids, the nucleotide exchange activity of ARNO on Arf1 (Cohen et al., 2007b; Stalder et al., 2011). We found that Arf6-GTP binds to the PH-C-terminal region of EFA6 (Padovani et al., 2014). Thus, by analogy with ARNO, one could speculate that Arf6-GTP, by binding to the PH domain of EFA6, could release the C-terminus and allow for ACTN1 binding.

We had previously reported that EFA6A is present at and regulates the TJ (Luton et al., 2004; Théard et al., 2010), where we now find ACTN1. Our results support the hypothesis that it is EFA6A that recruits ACTN1. The re-localization experiments performed in the presence of Latrunculin B indicate that the binding between EFA6A and ACTN1 is independent of F-actin. However, F-actin is found around the mitochondria together with EFA6ACter–ActA and ACTN1 suggesting that the EFA6A and ACTN1 couple could organize actin filament structures or even contribute to their nucleation, as proposed for ACTN4 at the AJ (Tang and Brieher, 2012). ARNO was also found to bind directly to ACTN1, through its C-terminal extremity, to modulate neurite extension, suggesting that ACTNs could be a general player in the Arf-regulated actin cytoskeleton (Torii et al., 2012).

Since EFA6A recruits ACTN1, we hypothesized that ACTN1 was acting as its effector. In the past, studying monolayers of MDCK cells, we had found that overexpression of EFA6A accelerates the general program of epithelial polarization, including the assembly of functional TJs (Klein et al., 2008; Luton et al., 2004). Part of the contribution of EFA6A has been attributed to its ability to stabilize the PAMR. Here, by using a 3D cell culture system together with siRNA-mediated depletion, we show that EFA6A is necessary for normal luminogenesis in MDCK cells. Conversely, overexpression of EFA6A increased the proportion of cysts with a SCL and stimulated their enlargement. Thus, we asked whether ACTN1 was acting as an effector to transduce some of the effects of EFA6A on luminogenesis. Indeed, we observed that depletion of ACTN1 blocked the stimulatory effect of EFA6A on both the formation and enlargement of the round SCL. In further support of this idea, depletion of ACTN1 had no additional disruptive impact on cells knocked down for EFA6A. This addition, expression of a mutant of EFA6A deleted of its C-terminus, which contains the ACTN1-binding site, impaired normal luminogenesis. These results demonstrate that ACTN1 is a crucial effector of EFA6A whose function is to promote normal luminogenesis.

To understand the roles of ACTN1, we analyzed in detail the defects induced upon its depletion. In the absence of ACTN1, there was an increase in cysts with multiple lumens, mostly as mini-lumens formed between two cells, or cysts with lumens that failed to extend to all cells. We propose that, in the absence of ACTN1, the initial fusion event to form a PAP is facilitated; however, the subsequent coalescence and extension of lumens to all cells of the aggregate is precluded. In addition, the volumetric growth of the lumens is impaired. In the ACTN1 knockdown cells, the mini-lumens appeared to be essentially blocked at the PAP stage and, in larger cysts, the extended lumens and SCL adopted an octopus-like shape rather than a nice round hollow. Interestingly, in both MDCK and MCF7 cells, in the absence of ACTN1, EFA6 overexpression is capable of rescuing enlargement of the mini-lumens. However, at later stages EFA6A overexpression cannot rescue the enlargement because ACTN1 is required as an effector downstream of EFA6. This implies that the enlargement of the luminal space relies on different molecular machinery at different stages along the process of lumen formation. Thus, ACTN1 is dispensable at the initial stage to create the nascent lumens, but it is essential downstream of EFA6A at later stages for the coalescence, extension and enlargement of the lumens.

ACTN1 is an actin-bundling protein known to regulate the contractility and stiffness of acto-myosin. It competes with myosin-II to bind F-actin in order to maintain a complementary periodicity, which results in linear F-actin bundles with contractile properties. The ratio and distribution of these two proteins determines the overall contractility and rigidity of F-actin cytoskeletons, including that of the PARM (Arnold et al., 2017; Ferrari et al., 2008; Sluysmans et al., 2017). Thus, ACTN1 could act by regulating tension forces at the surface of the developing lumen. Several observations support of this hypothesis. First, EFA6A and ACTN1 depletion reduced the amount of apical pMLC, whereas EFA6A expression stimulated its accumulation at the apical pole in an ACTN1-dependent manner. Second, upon ACTN1 depletion in both MDCK and MCF7 cells, we observed two defects: (1) a stimulatory effect on the initial formation of lumens as indicated by the rapid accumulation of multiple mini-lumens and, (2) at later stages, a defect of maturation (coalescence and extension) that leads to large cysts with several lumens or incomplete lumens. These results are consistent with a role for ACTN1 on contractility or stiffness. Indeed, several independent studies have shown that

decreasing contractility through treatment with blebbistatin, ROCK inhibitors, or downregulation of LKB1 (also known as STK11), an upstream regulator of RhoA, stimulates the initial formation of a lumen at the two-cell stage (Cohen et al., 2007a; Ferrari et al., 2008; Rodríguez-Fraticelli et al., 2012; Taniguchi et al., 2015). Less appreciated is the impact of contractility at later stages. We found that similar to what is seen upon ACTN1 depletion, blebbistatin leads to large cysts with multiple lumens (our unpublished results). A similar observation was made by reducing contractility through depletion of LKB1, which first stimulates the initial formation of lumens but then prevents their coalescence into a SCL (Rodríguez-Fraticelli et al., 2012). Third, supplemental evidence for the role of ACTN1 on contractility came from its effects in RhoAV14-expressing cells. The small G protein RhoA, through its action on the apical PAMR, is a general regulator of the assembly and maintenance of the AJ (Lecuit and Yap, 2015) and TJ (Terry et al., 2010). We showed that ACTN1-depletion could counterbalance the RhoAV14-mediated contractility. We also found that ACTN1-depletion rescued the initial formation of lumens inhibited by RhoAV14 expression. Taken together, these results indicate that luminogenesis is regulated by acto-myosin contractility and stiffness, which should be kept low for the initial formation of a mini-lumen, and then be increased to allow for their coalescence and extension to form a SCL in larger multicellular aggregates.

The implementation of tension forces relies on molecular pickets, which are usually transmembrane proteins that anchor the acto-myosin structures. In polarized epithelial cells, the AJ and TJ are anchor points for the PAMR. It is noteworthy that neither EFA6A nor ACTN1 appeared to be essential for the assembly and positioning of the AJ and TJ, nor the establishment and maintenance of the asymmetry along the apico-basal axis. Thus, EFA6A and its effector ACTN1 modulate the contractility by affecting the activity and/or organization of the apical acto-myosin cytoskeleton and not the anchoring junctional complexes.

Not all the functions of ACTN1 appeared to be mediated through regulating contractility. ACTN1 depletion prevented the luminal enlargement, while the inhibition of contractility by inhibiting myosin-II or LKB1 depletion (Rodríguez-Fraticelli et al., 2012) did not affect the luminal enlargement. Enlargement has been proposed to depend on apical membrane transport involving the delivery of highly charged molecules, hydrostatic pressure mediated by ion channels and coalescence of multilumens. In ACTN1-depleted cells, the surface of the apical membrane appears large enough to accommodate a bigger luminal volume. In addition, the highly charged PDX protein is properly delivered and coalescence is not relevant when considering SCLs with an octopus-like shape. However, ACTN1 could help to retain polycystins, which are implicated in intercellular mechanotransduction (Li et al., 2005); Wilson, 2001), as well as ion channels. In fact, many ion channels have been shown to bind or to require ACTNs in order for them to be retained at the cell surface (Cukovic et al., 2001; Lu et al., 2009; Maruoka et al., 2000; Sadeghi et al., 2002; Schnizler et al., 2009; Wyszynski et al., 1997; Ziane et al., 2010). EFA6A was also shown to bind the ion channels TWIK1 and Kir3.4 (Decressac et al., 2004; Gong et al., 2007). Furthermore, it has been reported that ACTN4 regulates the outwards water transport in a process called regulatory volume decrease in response to osmotic swelling (Ando-Akatsuka et al., 2012). In summary, together with EFA6A, the recruitment of ACTN1 to the apical surface might help stabilize ion channels regulating fluid influx and consequently lumen enlargement.

Alternatively, ACTN1 could serve to organize a non-contractile scaffold to help support the spherical architecture of the luminal membrane. To do so, ACTN1 could participate by bundling F-actin filaments into rigid structures and/or could serve to link or even nucleate actin filaments at the AJ or TJ to anchor the luminal actin cytoskeleton. Such a role has been proposed for ACTN4 at the level of the AJ (Tang and Brieher, 2012).

Finally, we examined the role of ACTN1 in the human tumoral mammary cell line MCF7. When grown in 3D culture, these cells fail to assemble TJ, form a lumen or polarize (Han et al., 2010; Kenny et al., 2007; Zangari et al., 2014). Only a small fraction of cell aggregates display one or several mini-lumens. As shown in the past, EFA6B expression stimulated the formation of extended lumens and restored an epithelial-like phenotype. So, in contrast to MDCK cells, the formation of extended lumens in MCF7 is strictly dependent on the expression of VSV-G–EFA6B. Thus, these cells make a good model to study the role of ACTN1 downstream of EFA6B. Indeed, ACTN1 depletion totally blocked lumen formation, demonstrating that ACTN1 is a crucial effector for EFA6B in the induction of luminogenesis. Furthermore, ACTN1-depletion in wild-type MCF7 cells stimulated the formation of multiple mini-lumens that were blocked at the PAP stage. EFA6B expression did not rescue the formation of extended lumens but did enlarge their volume. Thus, in agreement with our observations in MDCK cells, ACTN1 depletion favors the initial formation of lumens in between two cells but prevents their coalescence and enlargement.

In conclusion, we show that ACTN1 is an effector of EFA6A and EFA6B to promote luminogenesis in normal and tumoral cell models. We propose a scenario whereby, at the onset of luminogenesis, the acto-myosin contractility and rigidity must be kept low to relax the sub-membranous actin cytoskeleton where vesicle fusion occurs at the AMIS. At this stage, EFA6 proteins have a stimulatory effect on the formation and the enlargement of the mini-lumens suggesting that it acts through an effector other than ACTN1; perhaps through Arf6, which has already been shown to be involved in luminogensis (Tushir et al., 2010; Zangari et al., 2014). At a later stage, EFA6 proteins recruit ACTN1 to contribute to the coalescence of the mini-lumens, their extension to neighboring cells and enlargement. We do not exclude the possibility that EFA6 proteins could recruit other effectors to mediate its effects. Nevertheless, ACTN1 is certainly a primary effector that might act by modulating the contractility of the acto-myosin ring and thereby mediating its effects on coalescence and extension (by helping to pull the lumens together and breaking through the junctional complexes). Given these results, the EFA6A–ACTN1 pathway might be important for tubulogenesis occurring through the cord hollowing mechanism, where multiple mini-lumens are formed along the tubular structure and subsequently fuse to coalesce in a single lumen, in a ROCK–myosin II-dependent manner (Bernascone et al., 2017; Kim et al., 2015; Sigurbjörnsdóttir et al., 2014).

In summary, we identified and characterized the role of two new regulators of luminogenesis: EFA6A and ACTN1. ACTN1 behaves as an effector to transduce the stimulating effect of EFA6A on the formation of a single and well-expanded central lumen by facilitating the extension and enlargement stages. The EFA6A–ACTN1 couple acts, at least in part, by balancing the contractility of the cortical acto-myosin cytoskeleton. In the tumoral MCF7 cells, this pathway has the capacity to restore the apico-basal polarization, TJ assembly and collective cellular organization into a cyst with a central lumen pointing to new directions for cancer research and therapy.

Journal of Cell Science (2018) 131, jcs209361. doi:10.1242/jcs.209361

MATERIALS AND METHODS

Cells, media and transfection

BHK cells were grown in Glasgow's minimum essential medium (GMEM; Invitrogen, Paris, France) supplemented with 5% heat decomplemented fetal calf serum (FCS; Biowest-Abcys, Nuaillé, France) and penicillin-streptomycin (Invitrogen). Transient transfection was performed by lipofection using JETPEI (Polyplus Transfection, Illkirch, France). MDCK clone II cells expressing VSV-G–EFA6A, VSV-G–EFA6AΔC (Luton et al., 2004) or Myc-RhoAV14 (Jou and Nelson, 1998) under the control of the tetracycline-repressible transactivator were grown in MEM (Sigma-Aldrich, Saint-Quentin-Fallavier, France), 5% decomplemented FCS (Biowest-Abcys), penicillin-streptomycin and 20 ng/ml doxycycline. Expression of EFA6A and RhoAV14 was induced upon removal of doxycycline. Plasmids and siRNA transfections were performed by nucleofection (Nucleofector™; Lonza, Köln, Germany). For stable expression of ACTN1–GFP, ACTN4–GFP and ACTN1S744–GFP, the cells were selected with geneticin (Invitrogen) 2 days after transfection. MCF7 and MCF7-VSV-G–EFA6B (Zangari et al., 2014) were grown in Dulbecco's modified Eagle's medium (DMEM; Sigma-Aldrich) containing 10% decomplemented FCS (Hyclone™, GE Healthcare, France), supplemented with insulin, transferrin, selenium, glutamine, sodium pyruvate, MEM non-essential amino-acids and penicillin-streptomycin (all from Invitrogen). Transient transfection was performed by nucleofection. For 3D cell culture, 10^4 cells were mixed with 20 µl of 5 mg/ml Matrigel (BD Biosciences, Le Pont de Claix, France) deposited as a drop on a 12 mm glass coverslip. The BHK and MCF7 cells were obtained from the ATCC and authenticated by short tandem repeat profiling by the vendor. The parental MDCK II cell line was from Dr Keith Mostov (University of California, San Francisco, USA). MDCK and derived cell lines were tested for species specificity. Newly thawed cells from frozen stocks were tested for absence of mycoplasma contamination and used for 10 passages before replacement.

Antibodies and reagents

Rabbit polyclonal sera specific for EFA6B (HPA034722; Sigma-Aldrich), occludin (71-1500, Invitrogen), phosphorylated (Thr18/Ser19) myosin light chain 2 (3674, Cell Signaling Technology, Leiden, The Netherlands), the PI3K p85 regulatory subunit (ABS234, Millipore, Molsheim, France), Hsp60 (Ab46798, Abcam, Paris, France), GST (27-4577-01, GE Healthcare) were used. Mouse monoclonal antibodies specific for gp135/podocalyxin (3B8; gift from George Ojakian, State University of New York Downstate Medical Center), the VSV-G tag (P5D4; Roche Diagnostics, Mannheim, Germany), actin (AC-40; Sigma-Aldrich), E-cadherin (36; Invitrogen), paxillin (610052, BD Biosciences), the 6× histidine tag (HIS1; Sigma-Aldrich), the Myc tag (9E10 and rat hybridoma 3F10; Roche Diagnostics), GFP (7.1, Roche Diagnostics), ACTN1 (BM75.2; Sigma-Aldrich and H-2; Santa Cruz Biotechnology, Heidelberg, Germany) were used. The rabbit polyclonal anti-EFA6A was as described elsewhere (Sakagami et al., 2007). The horseradish peroxidase (HRP)-coupled and fluorescent probes (secondary antibodies, phalloidin and DAPI) were from Jackson ImmunoResearch Labs (Suffolk, UK) and Molecular Probes (Eugene, Oregon, USA), respectively. Full details of antibodies, including dilutions used are given in Table S1. All other reagents and chemicals were from Sigma-Aldrich.

DNA constructs and siRNA

Constructs for the expression of the following proteins have been described elsewhere: GFP–EFA6A (Decressac et al., 2004), mRFP–EFA6A (Théard et al., 2010), GST–EFA6A, GST–EFA6ACter (Macia et al., 2008), (6xhis)–EFA6A (Macia et al., 2008), βarrestin1Cter–GFP (Scott et al., 2002), the GST–ABD [amino acids (aa) 1–269], GST–SRD (aa 218–749) and GST–CAMD (aa 713–887) fragments of ACTN1 (Fraley et al., 2003), ACTN1–GFP (Rajfur et al., 2002), GST–ACTN4 (Khurana et al., 2011), ACTN4–HA and ACTN4–GFP (Michaud et al., 2006). The GST–ACTN1 construct was prepared by PCR amplification of full-length ACTN1 from pEGFP-ACTN1 and cloned into EcoR1 and Xho1 sites of the pGEX4T1 using the following primers:5′-GATCGATCGAATTCATGGACCATTATGATTCTCAG-3′ and 5′-TGTATCACTCGAGTTAGAGGTCACTCTCGCCGTAC-3′. The siRNA #2225 insensitive ACTN1–GFP was generated by introducing silent mutations at positions 2236, 2237 and 2238 (aa Ser744) using the QuikChange mutagenesis kit (Agilent Technologies, Courtabœuf, France) using the following primers 5′-GCCAAGGGCATCTCGCAGGAGCAGATGAATG-3′ and 5′-CATTCATCTGCTCCTGCGAGATGCCCTTGGC-3′. The resulting plasmid was termed ACTN1S744–GFP. Full-length EFA6A and EFA6ACter were cloned into mRFP-N1-ActA (Benjamin et al., 2010) by PCR amplification at the EcoRI and SacII sites. Primers used to amplify and clone the full-length EFA6A were 5′-GATCGATCGAATTCGCCGCCACCATGCCTCTCAAGTCACCTGTG-3′ and 5′-GATCGATCCCGCGGGGGCTTCCGCCGCCCACTGCC-3′, and those for the EFA6ACter fragment were 5′-GATCGATCGAATTCGCCGCCACCATGTTCTCTGCGCCCCCCTTCC-3′ and 5′-GATCGATCCCGCGGGGGCTTCCGCCGCCCACTGCC-3′. The resulting plasmids were termed EFA6A–mRFP–ActA and EFA6ACter–mRFP–ActA.

The specific and control siRNAs were designed and obtained from Eurogentec (Angers, France) and Sigma-Aldrich. The silencing efficiency of several siRNAs per target was assessed by immunoblotting (Figs S3 and S4). Knockdown of canine EFA6A and ACTN1 expression in MDCK cells was carried out using the siRNA #2661 5′-CCUAUCAGAGGCGGAGCUA-3′ or #1440 5′-CUCUUUCAGUUGUGUGUUU-3′ and siRNA #2225 5′-GCAUCAGCCAGGAGCAAAU-3′ or #594 5′-GGACGACCCACUCACAAAU-3′, respectively. Knockdown of human ACTN1 expression in MCF7 cells was carried out using the siRNA #1789 5′-CCUCAGGAGAUCAAUGGCAAA-3′. Silencing specificity was verified with control siRNAs, rescue experiments (Fig. 3C and Fig. 4B) and additional independent siRNA (Fig. S4).

Recombinant proteins, pull-down assay and immunoprecipitation

The induction and purification of GST constructs with glutathione–sepharose CL-4B beads (GE Healthcare) was as previously described (Macia et al., 2008). The N-terminal 6×his–EFA6A was purified on Ni-NTA columns according to the manufacturer's instructions (Qiagen, Courtabœuf, France). For the GST-EFA6A pull-down from cell lysates, MDCK-ACTN1–GFP cells were lysed at 4°C in 0.5% Nonidet P-40, 20 mM Hepes pH 7.4, 125 mM NaCl, 1 mM phenylmethylsulphonyl fluoride (PMSF) and a cocktail of protease inhibitors (Complete™, Roche Diagnostics). The cleared lysates were incubated for 4 h at 4°C with 1.5 µM of the indicated GST-fused proteins and 30 µl of glutathione-sepharose CL-4B beads. After three washes in lysis buffer, the beads were boiled in Laemmli buffer, submitted to SDS-PAGE and the proteins revealed by immunoblotting. For the GST pull-down of purified His–EFA6A, 10 µM of the indicated GST fusion proteins and 10 µM of His–EFA6A were incubated together for 2 h at 4°C, and the experiments carried on as described above. For all GST pulldown experiments, an aliquot of the mixture was analyzed by SDS-PAGE followed by immunoblotting to estimate the total amount of the added proteins. For immunoprecipitation, cells were solubilized in ice-cold Triton X-100 lysis buffer (1% Triton X-100, 150 mM NaCl, 5 mM EDTA, 20 mM Triethanolamine-HCl pH 8.1 and 1 mM PMSF). After centrifugation for 20 min at 16,000 ***g*** at 4°C, the supernatants were pre-cleared at 4°C for 10 min, centrifuged for 10 min at 16,000 ***g*** and combined with protein A–sepharose and the indicated antibody overnight at 4°C. The beads were then washed three times in washing buffer (1% Triton X-100, 0.2% SDS, 150 mM NaCl, 5 mM EDTA, 8% sucrose, 1 mM PMSF and the cocktail of protease inhibitors) and washed once in washing buffer without detergent. The immunoprecipitates were then resuspended and boiled for 5 min in Laemmli buffer before SDS-PAGE and immunoblot analysis.

Immunoblotting

Samples were resolved on SDS-PAGE and proteins transferred onto a nitrocellulose membrane. Membrane blocking (30 min at room temperature) and antibody dilutions were performed in PBS with 5% non-fat dried milk. The membranes were incubated overnight at 4°C with the indicated antibody. The proteins were revealed by chemiluminescence (ECL, Amersham, GE Healthcare) using secondary antibodies directly coupled

to HRP. The membranes were analyzed with the luminescent image analyzer LAS-3000 (Fujifilm, Saint-Quentin-en-Yvelines, France).

Immunofluorescence

Cells were fixed in 4% PFA, the samples processed as previously described (Luton et al., 2004) and imaged on a confocal microscope (Leica TCS-SP5, Nanterre, France and Zeiss LSM780, Marly-le-Roi, France). Images were processed for presentation using NIH Image and Adobe® Photoshop® CS2 software.

Quantification of luminogenesis

Unless specified, all quantifications were from cysts of 4–15 cells obtained after 48 to 72 h growth in Matrigel. Experiments were repeated at least three times in triplicate and a minimum of 100 cysts per experimental replicate were analyzed. Each cell aggregate was scanned by using confocal microscopy to analyze the shape of the lumens and determine the presence of a single lumen or multiple lumens. Cysts were classified within five categories: cysts with a single central opened lumen (SCL), two or more lumens regardless of their shape (multilumen), with an opened lumen but that was not extended to all cells (incomplete lumen), with an optically closed lumen (otherwise named pre-apical patch, PAP), and with no lumen. Within the SCL class, we discriminated those lumens that were well enlarged from those that were barely opened and not expanded displaying an 'octopus-like' shape (see Fig. 3B). Note, that cysts with dividing cells or with lumen-containing cells and/or nuclei were not included. In addition, a separate quantification was performed for a lumen opened only in between two cells (mini-lumen) as they fell in the multilumen, incomplete and optically closed lumen categories (see Fig. 3E). Enlargement refers to the increase of the luminal volume. When enlargement was compromised there was an octopus-like lumen. Extension refers to the opening of a lumen (in general starting in-between two cells) to all the cells of the cell aggregate or coalescence of multiple small lumens to eventually form a single lumen. When extension was compromised it led to an incomplete lumen and/or to the presence of multiple lumens including mini-lumens (see Fig. 3D,E).

Statistics

The experiments were performed at least three times in triplicate, and data from all experiments were combined. Values are mean±s.d. Statistical significance was calculated with a two-tailed Student's *t*-test. Non-significant difference (N.S.) are $P>0.05$; *$P\leq0.05$; **$P\leq0.01$; ***$P\leq0.001$.

Acknowledgements

We thank Drs Hiroyuki Sakagami (Kitasato University, Japan) for the EFA6A-specific anti-serum, James Nelson (Stanford University, USA) for the MDCK-RhoAV14 cells and the ActA–mRFP plasmid, Dr Jeffery Greenwood (Oregon State University, USA) for the plasmids encoding the three fragments of GST–ACTN1 and GFP–ACTN1, Dr Chris Kennedy (University of Ottawa, Canada) for plasmids encoding HA–ACTN4 and GFP–ACTN4, and Dr Hung-Ying Kao (Case Western Reserve University, USA) for plasmid encoding GST–ACTN4. We are grateful to K. L. Singer for critical reading of the manuscript.

Competing interests

The authors declare no competing or financial interests.

Author contributions

Conceptualization: J.M., F.L.; Methodology: J.M., R.F., M.P., P.L., F.L.; Validation: J.M., M.P., P.L., F.L.; Formal analysis: J.M., R.F., M.P., P.L., J.-P.B., M.F., F.L.; Investigation: J.M., F.L.; Data curation: J.M., F.L.; Writing - original draft: J.M., F.L.; Writing - review & editing: J.M., R.F., M.F.; Visualization: M.F., F.L.; Supervision: J.-P.B., M.F., F.L.; Project administration: F.L.; Funding acquisition: J.-P.B., M.F., F.L.

Funding

This work was supported by Fondation ARC pour la Recherche sur le Cancer, and Agence Nationale de la Recherche (ANR) through the 'Investments for the Future' LABEX SIGNALIFE (program reference ANR-11-LABX-0028-01). R.F. was the recipient of a PhD fellowship from the Labex SIGNALIFE program. J.-P.B. is funded by La Ligue Contre le Cancer, Cancéropôle PACA and SIRIC (INCa-DGOS-Inserm 6038). J.-P.B. is a scholar of Institut Universitaire de France.

Supplementary information

Supplementary information available online at
http://jcs.biologists.org/lookup/doi/10.1242/jcs.209361.supplemental

References

Altschuler, Y., Liu, S.-H., Katz, L., Tang, K., Hardy, S., Brodsky, F., Apodaca, G. and Mostov, K. (1999). ADP-ribosylation factor 6 and endocytosis at the apical surface of Madin-Darby canine kidney cells. *J. Cell Biol.* **147**, 7-12.

Ando-Akatsuka, Y., Shimizu, T., Numata, T. and Okada, Y. (2012). Involvements of the ABC protein ABCF2 and alpha-actinin-4 in regulation of cell volume and anion channels in human epithelial cells. *J. Cell. Physiol.* **227**, 3498-3510.

Arnold, T. R., Stephenson, R. E. and Miller, A. L. (2017). Rho GTPases and actomyosin: partners in regulating epithelial cell-cell junction structure and function. *Exp. Cell Res.* **358**, 20-30.

Benjamin, J. M., Kwiatkowski, A. V., Yang, C., Korobova, F., Pokutta, S., Svitkina, T., Weis, W. I. and Nelson, W. J. (2010). AlphaE-catenin regulates actin dynamics independently of cadherin-mediated cell-cell adhesion. *J. Cell Biol.* **189**, 339-352.

Bernascone, I., Hachimi, M. and Martin-Belmonte, F. (2017). Signaling networks in epithelial tube formation. *Cold Spring Harb. Perspect. Biol.* **9**, pii: a027946.

Blasky, A. J., Mangan, A. and Prekeris, R. (2015). Polarized protein transport and lumen formation during epithelial tissue morphogenesis. *Annu. Rev. Cell Dev. Biol.* **31**, 575-591.

Braga, V. (2016). Spatial integration of E-cadherin adhesion, signalling and the epithelial cytoskeleton. *Curr. Opin. Cell Biol.* **42**, 138-145.

Bubeck, P., Pistor, S., Wehland, J. and Jockusch, B. M. (1997). Ligand recruitment by vinculin domains in transfected cells. *J. Cell Sci.* **110**, 1361-1371.

Burridge, K. and Wittchen, E. S. (2013). The tension mounts: stress fibers as force-generating mechanotransducers. *J. Cell Biol.* **200**, 9-19.

Chen, V. C., Li, X., Perreault, H. and Nagy, J. I. (2006). Interaction of zonula occludens-1 (ZO-1) with alpha-actinin-4: application of functional proteomics for identification of PDZ domain-associated proteins. *J. Proteome Res.* **5**, 2123-2134.

Cohen, D., Tian, Y. and Musch, A. (2007a). Par1b promotes hepatic-type lumen polarity in Madin Darby canine kidney cells via myosin II- and E-cadherin-dependent signaling. *Mol. Biol. Cell* **18**, 2203-2215.

Cohen, L. A., Honda, A., Varnai, P., Brown, F. D., Balla, T. and Donaldson, J. G. (2007b). Active Arf6 recruits ARNO/cytohesin GEFs to the PM by binding their PH domains. *Mol. Biol. Cell* **18**, 2244-2253.

Coravos, J. S. and Martin, A. C. (2016). Apical sarcomere-like actomyosin contracts nonmuscle Drosophila epithelial cells. *Dev. Cell* **39**, 346-358.

Coravos, J. S., Mason, F. M. and Martin, A. C. (2017). Actomyosin pulsing in tissue integrity maintenance during morphogenesis. *Trends Cell Biol.* **27**, 276-283.

Cukovic, D., Lu, G. W.-K., Wible, B., Steele, D. F. and Fedida, D. (2001). A discrete amino terminal domain of Kv1.5 and Kv1.4 potassium channels interacts with the spectrin repeats of alpha-actinin-2. *FEBS Lett.* **498**, 87-92.

D'Souza-Schorey, C. and Chavrier, P. (2006). ARF proteins: roles in membrane traffic and beyond. *Nat. Rev. Mol. Cell Biol.* **7**, 347-358.

Datta, A., Bryant, D. M. and Mostov, K. E. (2011). Molecular regulation of lumen morphogenesis. *Curr. Biol.* **21**, R126-R136.

Decressac, S., Franco, M., Bendahhou, S., Warth, R., Knauer, S., Barhanin, J., Lazdunski, M. and Lesage, F. (2004). ARF6-dependent interaction of the TWIK1 K+ channel with EFA6, a GDP/GTP exchange factor for ARF6. *EMBO Rep.* **5**, 1171-1175.

Derrien, V., Couillault, C., Franco, M., Martineau, S., Montcourrier, P., Houlgatte, R. and Chavrier, P. (2002). A conserved C-terminal domain of EFA6-family ARF6-guanine nucleotide exchange factors induces lengthening of microvilli-like membrane protrusions. *J. Cell Sci.* **115**, 2867-2879.

DiNitto, J. P., Delprato, A., Gabe Lee, M.-T., Cronin, T. C., Huang, S., Guilherme, A., Czech, M. P. and Lambright, D. G. (2007). Structural basis and mechanism of autoregulation in 3-phosphoinositide-dependent Grp1 family Arf GTPase exchange factors. *Mol. Cell* **28**, 569-583.

DuFort, C. C., Paszek, M. J. and Weaver, V. M. (2011). Balancing forces: architectural control of mechanotransduction. *Nat. Rev. Mol. Cell Biol.* **12**, 308-319.

Ebrahim, S., Fujita, T., Millis, B. A., Kozin, E., Ma, X., Kawamoto, S., Baird, M. A., Davidson, M., Yonemura, S., Hisa, Y. et al. (2013). NMII forms a contractile transcellular sarcomeric network to regulate apical cell junctions and tissue geometry. *Curr. Biol.* **23**, 731-736.

Ferrari, A., Veligodskiy, A., Berge, U., Lucas, M. S. and Kroschewski, R. (2008). ROCK-mediated contractility, tight junctions and channels contribute to the conversion of a preapical patch into apical surface during isochoric lumen initiation. *J. Cell Sci.* **121**, 3649-3663.

Foley, K. S. and Young, P. W. (2013). An analysis of splicing, actin-binding properties, heterodimerization and molecular interactions of the non-muscle alpha-actinins. *Biochem. J.* **452**, 477-488.

Foley, K. S. and Young, P. W. (2014). The non-muscle functions of actinins: an update. *Biochem. J.* **459**, 1-13.

Franco, M., Peters, P. J., Boretto, J., van Donselaar, E., Neri, A., D'Souza-Schorey, C. and Chavrier, P. (1999). EFA6, a sec7 domain-containing exchange

factor for ARF6, coordinates membrane recycling and actin cytoskeleton organization. *EMBO J.* **18**, 1480-1491.
Fraley, T. S., Tran, T. C., Corgan, A. M., Nash, C. A., Hao, J., Critchley, D. R. and Greenwood, J. A. (2003). Phosphoinositide binding inhibits alpha-actinin bundling activity. *J. Biol. Chem.* **278**, 24039-24045.
Geiger, B., Tokuyasu, K. T. and Singer, S. J. (1979). Immunocytochemical localization of alpha-actinin in intestinal epithelial cells. *Proc. Natl. Acad. Sci. USA* **76**, 2833-2837.
Gillingham, A. K. and Munro, S. (2007). The small G proteins of the Arf family and their regulators. *Annu. Rev. Cell Dev. Biol.* **23**, 579-611.
Gong, Q., Weide, M., Huntsman, C., Xu, Z., Jan, L. Y. and Ma, D. (2007). Identification and characterization of a new class of trafficking motifs for controlling clathrin-independent internalization and recycling. *J. Biol. Chem.* **282**, 13087-13097.
Grikscheit, K. and Grosse, R. (2016). Formins at the Junction. *Trends Biochem. Sci.* **41**, 148-159.
Han, J., Chang, H., Giricz, O., Lee, G. Y., Baehner, F. L., Gray, J. W., Bissell, M. J., Kenny, P. A. and Parvin, B. (2010). Molecular predictors of 3D morphogenesis by breast cancer cell lines in 3D culture. *PLoS Comput. Biol.* **6**, e1000684.
Honda, K., Yamada, T., Endo, R., Ino, Y., Gotoh, M., Tsuda, H., Yamada, Y., Chiba, H. and Hirohashi, S. (1998). Actinin-4, a novel actin-bundling protein associated with cell motility and cancer invasion. *J. Cell Biol.* **140**, 1383-1393.
Iskratsch, T., Wolfenson, H. and Sheetz, M. P. (2014). Appreciating force and shape – the rise of mechanotransduction in cell biology. *Nat. Rev. Mol. Cell Biol.* **15**, 825-833.
Jahed, Z., Shams, H., Mehrbod, M. and Mofrad, M. R. K. (2014). Mechanotransduction pathways linking the extracellular matrix to the nucleus. *Int. Rev. Cell Mol. Biol.* **310**, 171-220.
Jaworski, J. (2007). ARF6 in the nervous system. *Eur. J. Cell Biol.* **86**, 513-524.
Jou, T.-S. and Nelson, W. J. (1998). Effects of regulated expression of mutant RhoA and Rac1 small GTPases on the development of epithelial (MDCK) cell polarity. *J. Cell Biol.* **142**, 85-100.
Kenny, P. A., Lee, G. Y., Myers, C. A., Neve, R. M., Semeiks, J. R., Spellman, P. T., Lorenz, K., Lee, E. H., Barcellos-Hoff, M. H., Petersen, O. W. et al. (2007). The morphologies of breast cancer cell lines in three-dimensional assays correlate with their profiles of gene expression. *Mol. Oncol.* **1**, 84-96.
Khurana, S., Chakraborty, S., Cheng, X., Su, Y. T. and Kao, H. Y. (2011). The actin-binding protein, actinin alpha 4 (ACTN4), is a nuclear receptor coactivator that promotes proliferation of MCF-7 breast cancer cells. *J. Biol. Chem.* **286**, 1850-1859.
Kim, M., Shewan, A. M., Ewald, A. J., Werb, Z. and Mostov, K. E. (2015). p114RhoGEF governs cell motility and lumen formation during tubulogenesis through a ROCK-myosin-II pathway. *J. Cell Sci.* **128**, 4317-4327.
Klein, S., Partisani, M., Franco, M. and Luton, F. (2008). EFA6 facilitates the assembly of the tight junction by coordinating an Arf6-dependent and -independent pathway. *J. Biol. Chem.* **283**, 30129-30138.
Le Clainche, C. and Carlier, M.-F. (2008). Regulation of actin assembly associated with protrusion and adhesion in cell migration. *Physiol. Rev.* **88**, 489-513.
Lecuit, T. and Yap, A. S. (2015). E-cadherin junctions as active mechanical integrators in tissue dynamics. *Nat. Cell Biol.* **17**, 533-539.
Li, Q., Montalbetti, N., Shen, P. Y., Dai, X.-Q., Cheeseman, C. I., Karpinski, E., Wu, G., Cantiello, H. F. and Chen, X.-Z. (2005). Alpha-actinin associates with polycystin-2 and regulates its channel activity. *Hum. Mol. Genet.* **14**, 1587-1603.
Lu, L., Timofeyev, V., Li, N., Rafizadeh, S., Singapuri, A., Harris, T. R. and Chiamvimonvat, N. (2009). Alpha-actinin2 cytoskeletal protein is required for the functional membrane localization of a Ca2+-activated K+ channel (SK2 channel). *Proc. Natl. Acad. Sci. USA* **106**, 18402-18407.
Luton, F., Klein, S., Chauvin, J. P., Le Bivic, A., Bourgoin, S., Franco, M. and Chardin, P. (2004). EFA6, exchange factor for ARF6, regulates the actin cytoskeleton and associated tight junction in response to E-cadherin engagement. *Mol. Biol. Cell* **15**, 1134-1145.
Macia, E., Partisani, M., Favard, C., Mortier, E., Zimmermann, P., Carlier, M.-F., Gounon, P., Luton, F. and Franco, M. (2008). The pleckstrin homology domain of the Arf6-specific exchange factor EFA6 localizes to the plasma membrane by interacting with phosphatidylinositol 4,5-bisphosphate and F-actin. *J. Biol. Chem.* **283**, 19836-19844.
Macia, E., Partisani, M., Paleotti, O., Luton, F. and Franco, M. (2012). Arf6 negatively controls the rapid recycling of the beta2 adrenergic receptor. *J. Cell Sci.* **125**, 4026-4035.
Martin, A. C. and Goldstein, B. (2014). Apical constriction: themes and variations on a cellular mechanism driving morphogenesis. *Development* **141**, 1987-1998.
Martin-Belmonte, F. and Perez-Moreno, M. (2011). Epithelial cell polarity, stem cells and cancer. *Nat. Rev. Cancer* **12**, 23-38.
Maruoka, N. D., Steele, D. F., Au, B. P.-Y., Dan, P., Zhang, X., Moore, E. D. W. and Fedida, D. (2000). alpha-actinin-2 couples to cardiac Kv1.5 channels, regulating current density and channel localization in HEK cells. *FEBS Lett.* **473**, 188-194.
Michaud, J. L., Chaisson, K. M., Parks, R. J. and Kennedy, C. R. (2006). FSGS-associated alpha-actinin-4 (K256E) impairs cytoskeletal dynamics in podocytes. *Kidney Int.* **70**, 1054-1061.
Moeller, M. J., Soofi, A., Braun, G. S., Li, X., Watzl, C., Kriz, W. and Holzman, L. B. (2004). Protocadherin FAT1 binds Ena/VASP proteins and is necessary for actin dynamics and cell polarization. *EMBO J.* **23**, 3769-3779.
Murrell, M., Oakes, P. W., Lenz, M. and Gardel, M. L. (2015). Forcing cells into shape: the mechanics of actomyosin contractility. *Nat. Rev. Mol. Cell Biol.* **16**, 486-498.
Nakatsuji, H., Nishimura, N., Yamamura, R., Kanayama, H. O. and Sasaki, T. (2008). Involvement of actinin-4 in the recruitment of JRAB/MICAL-L2 to cell-cell junctions and the formation of functional tight junctions. *Mol. Cell. Biol.* **28**, 3324-3335.
Oakes, P. W., Beckham, Y., Stricker, J. and Gardel, M. L. (2012). Tension is required but not sufficient for focal adhesion maturation without a stress fiber template. *J. Cell Biol.* **196**, 363-374.
Padovani, D., Folly-Klan, M., Labarde, A., Boulakirba, S., Campanacci, V., Franco, M., Zeghouf, M. and Cherfils, J. (2014). EFA6 controls Arf1 and Arf6 activation through a negative feedback loop. *Proc. Natl. Acad. Sci. USA* **111**, 12378-12383.
Palacios, F., Price, L., Schweitzer, J., Collard, J. G. and D'Souza-Schorey, C. (2001). An essential role for ARF6-regulated membrane traffic in adherens junction turnover and epithelial cell migration. *EMBO J.* **20**, 4973-4986.
Palacios, F., Schweitzer, J. K., Boshans, R. L. and D'Souza-Schorey, C. (2002). ARF6-GTP recruits Nm23-H1 to facilitate dynamin-mediated endocytosis during adherens junctions disassembly. *Nat. Cell Biol.* **4**, 929-936.
Palacios, F., Tushir, J. S., Fujita, Y. and D'Souza-Schorey, C. (2005). Lysosomal targeting of E-cadherin: a unique mechanism for the down-regulation of cell-cell adhesion during epithelial to mesenchymal transitions. *Mol. Cell. Biol.* **25**, 389-402.
Parsons, J. T., Horwitz, A. R. and Schwartz, M. A. (2010). Cell adhesion: integrating cytoskeletal dynamics and cellular tension. *Nat. Rev. Mol. Cell Biol.* **11**, 633-643.
Quiros, M. and Nusrat, A. (2014). RhoGTPases, actomyosin signaling and regulation of the epithelial Apical Junctional Complex. *Semin. Cell Dev. Biol.* **36**, 194-203.
Rajfur, Z., Roy, P., Otey, C., Romer, L. and Jacobson, K. (2002). Dissecting the link between stress fibres and focal adhesions by CALI with EGFP fusion proteins. *Nat. Cell Biol.* **4**, 286-293.
Reinhard, M., Zumbrunn, J., Jaquemar, D., Kuhn, M., Walter, U. and Trueb, B. (1999). An alpha-actinin binding site of zyxin is essential for subcellular zyxin localization and alpha-actinin recruitment. *J. Biol. Chem.* **274**, 13410-13418.
Rodríguez-Fraticelli, A. E., Auzan, M., Alonso, M. A., Bornens, M. and Martín-Belmonte, F. (2012). Cell confinement controls centrosome positioning and lumen initiation during epithelial morphogenesis. *J. Cell Biol.* **198**, 1011-1023.
Röper, K. (2015). Integration of cell-cell adhesion and contractile actomyosin activity during morphogenesis. *Curr. Top. Dev. Biol.* **112**, 103-127.
Sabe, H., Hashimoto, S., Morishige, M., Ogawa, E., Hashimoto, A., Nam, J.-M., Miura, K., Yano, H. and Onodera, Y. (2009). The EGFR-GEP100-Arf6-AMAP1 signaling pathway specific to breast cancer invasion and metastasis. *Traffic* **10**, 982-993.
Sadeghi, A., Doyle, A. D. and Johnson, B. D. (2002). Regulation of the cardiac L-type Ca2+ channel by the actin-binding proteins alpha-actinin and dystrophin. *Am. J. Physiol. Cell Physiol.* **282**, C1502-C1511.
Sakagami, H. (2008). The EFA6 family: guanine nucleotide exchange factors for ADP ribosylation factor 6 at neuronal synapses. *Tohoku J. Exp. Med.* **214**, 191-198.
Sakagami, H., Honma, T., Sukegawa, J., Owada, Y., Yanagisawa, T. and Kondo, H. (2007). Somatodendritic localization of EFA6A, a guanine nucleotide exchange factor for ADP-ribosylation factor 6, and its possible interaction with alpha-actinin in dendritic spines. *Eur. J. Neurosci.* **25**, 618-628.
Schnizler, M. K., Schnizler, K., Zha, X. M., Hall, D. D., Wemmie, J. A., Hell, J. W. and Welsh, M. J. (2009). The cytoskeletal protein alpha-actinin regulates acid-sensing ion channel 1a through a C-terminal interaction. *J. Biol. Chem.* **284**, 2697-2705.
Schweitzer, J. K., Sedgwick, A. E. and D'Souza-Schorey, C. (2011). ARF6-mediated endocytic recycling impacts cell movement, cell division and lipid homeostasis. *Semin. Cell Dev. Biol.* **22**, 39-47.
Scott, M. G., Benmerah, A., Muntaner, O. and Marullo, S. (2002). Recruitment of activated G protein-coupled receptors to pre-existing clathrin-coated pits in living cells. *J. Biol. Chem.* **277**, 3552-3559.
Sigurbjörnsdóttir, S., Mathew, R. and Leptin, M. (2014). Molecular mechanisms of de novo lumen formation. *Nat. Rev. Mol. Cell Biol.* **15**, 665-676.
Sironi, C., Teesalu, T., Muggia, A., Fontana, G., Marino, F., Savaresi, S. and Talarico, D. (2009). EFA6A encodes two isoforms with distinct biological activities in neuronal cells. *J. Cell Sci.* **122**, 2108-2118.
Sluysmans, S., Vasileva, E., Spadaro, D., Shah, J., Rouaud, F. and Citi, S. (2017). The role of apical cell-cell junctions and associated cytoskeleton in mechanotransduction. *Biol. Cell* **109**, 139-161.
Stalder, D., Barelli, H., Gautier, R., Macia, E., Jackson, C. L. and Antonny, B. (2011). Kinetic studies of the Arf activator Arno on model membranes in the presence of Arf effectors suggest control by a positive feedback loop. *J. Biol. Chem.* **286**, 3873-3883.

Stossel, T. P., Condeelis, J., Cooley, L., Hartwig, J. H., Noegel, A., Schleicher, M. and Shapiro, S. S. (2001). Filamins as integrators of cell mechanics and signalling. *Nat. Rev. Mol. Cell Biol.* **2**, 138-145.

Takeichi, M. (2014). Dynamic contacts: rearranging adherens junctions to drive epithelial remodelling. *Nat. Rev. Mol. Cell Biol.* **15**, 397-410.

Tang, V. W. and Brieher, W. M. (2012). alpha-Actinin-4/FSGS1 is required for Arp2/3-dependent actin assembly at the adherens junction. *J. Cell Biol.* **196**, 115-130.

Taniguchi, K., Shao, Y., Townshend, R. F., Tsai, Y.-H., DeLong, C. J., Lopez, S. A., Gayen, S., Freddo, A. M., Chue, D. J., Thomas, D. J. et al. (2015). Lumen formation is an intrinsic property of isolated human pluripotent stem cells. *Stem Cell Reports* **5**, 954-962.

Tanos, B. and Rodriguez-Boulan, E. (2008). The epithelial polarity program: machineries involved and their hijacking by cancer. *Oncogene* **27**, 6939-6957.

Terry, S., Nie, M., Matter, K. and Balda, M. S. (2010). Rho signaling and tight junction functions. *Physiology (Bethesda)* **25**, 16-26.

Théard, D., Labarrade, F., Partisani, M., Milanini, J., Sakagami, H., Fon, E. A., Wood, S. A., Franco, M. and Luton, F. (2010). USP9x-mediated deubiquitination of EFA6 regulates de novo tight junction assembly. *EMBO J.* **29**, 1499-1509.

Torii, T., Miyamoto, Y., Nakamura, K., Maeda, M., Yamauchi, J. and Tanoue, A. (2012). Arf6 guanine-nucleotide exchange factor, cytohesin-2, interacts with actinin-1 to regulate neurite extension. *Cell. Signal.* **24**, 1872-1882.

Tushir, J. S. and D'Souza-Schorey, C. (2007). ARF6-dependent activation of ERK and Rac1 modulates epithelial tubule development. *EMBO J.* **26**, 1806-1819.

Tushir, J. S., Clancy, J., Warren, A., Wrobel, C., Brugge, J. S. and D'Souza-Schorey, C. (2010). Unregulated ARF6 activation in epithelial cysts generates hyperactive signaling endosomes and disrupts morphogenesis. *Mol. Biol. Cell* **21**, 2355-2366.

Wang, C.-C., Jamal, L. and Janes, K. A. (2012). Normal morphogenesis of epithelial tissues and progression of epithelial tumors. *Wiley Interdiscip. Rev. Syst. Biol. Med.* **4**, 51-78.

Weaver, V. M., Petersen, O. W., Wang, F., Larabell, C. A., Briand, P., Damsky, C. and Bissell, M. J. (1997). Reversion of the malignant phenotype of human breast cells in three-dimensional culture and in vivo by integrin blocking antibodies. *J. Cell Biol.* **137**, 231-245.

Wilson, P. D. (2001). Polycystin: new aspects of structure, function, and regulation. *J. Am. Soc. Nephrol.* **12**, 834-845.

Wyszynski, M., Lin, J., Rao, A., Nigh, E., Beggs, A. H., Craig, A. M. and Sheng, M. (1997). Competitive binding of alpha-actinin and calmodulin to the NMDA receptor. *Nature* **385**, 439-442.

Ye, N., Verma, D., Meng, F., Davidson, M. W., Suffoletto, K. and Hua, S. Z. (2014). Direct observation of alpha-actinin tension and recruitment at focal adhesions during contact growth. *Exp. Cell Res.* **327**, 57-67.

Zangari, J., Partisani, M., Bertucci, F., Milanini, J., Bidaut, G., Berruyer-Pouyet, C., Finetti, P., Long, E., Brau, F., Cabaud, O. et al. (2014). EFA6B antagonizes breast cancer. *Cancer Res.* **74**, 5493-5506.

Zhang, L., Li, L., Liu, H., Borowitz, J. L. and Isom, G. E. (2009). BNIP3 mediates cell death by different pathways following localization to endoplasmic reticulum and mitochondrion. *FASEB J.* **23**, 3405-3414.

Ziane, R., Huang, H., Moghadaszadeh, B., Beggs, A. H., Levesque, G. and Chahine, M. (2010). Cell membrane expression of cardiac sodium channel Na(v)1.5 is modulated by alpha-actinin-2 interaction. *Biochemistry* **49**, 166-178.

Supplementary figures

Figure S1

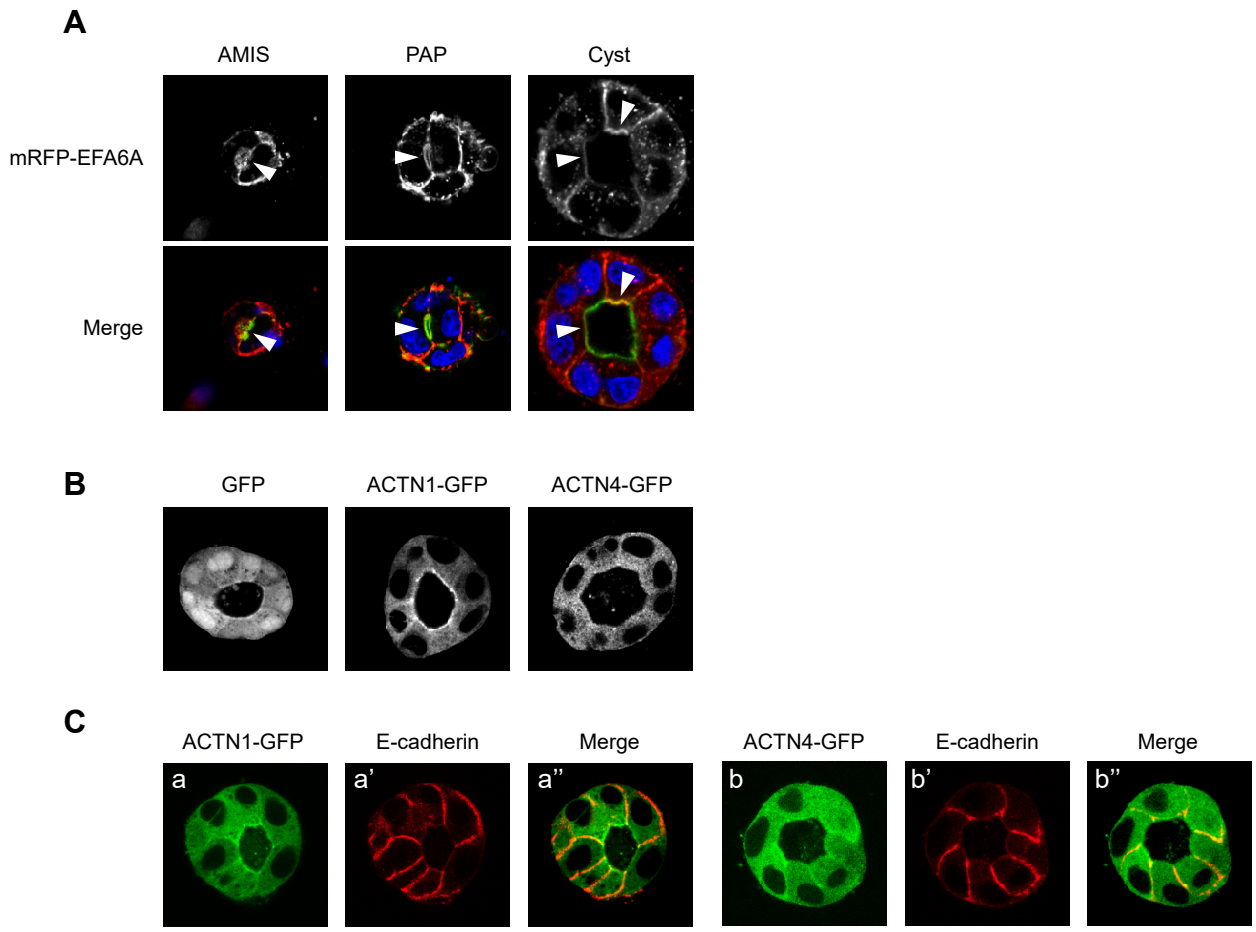

Figure S1. **Subcellular localization of mRFP-EFA6A, ACTN1-GFP and ACTN4-GFP**. **A**) MDCK cells expressing mRFP-EFA6A were grown in Matrigel and processed for immunofluorescence to label F-actin and the nuclei. The top panels show the mRFP-EFA6A staining alone and the bottom panels the corresponding merged images with mRFP-EFA6A colored in red, F-actin in green and the nuclei in blue. Scale bars 10μm. **B**) MDCK cells expressing GFP, ACTN1-GFP and ACTN4-GFP were grown in Matrigel and processed for immunofluorescence. **C**) MDCK cells expressing ACTN1-GFP (green; a-a'') or ACTN4-GFP (green; b-b'') were processed for immunofluorescence to label the endogenous E-cadherin (red). Scale bars 10μm.

Figure S2

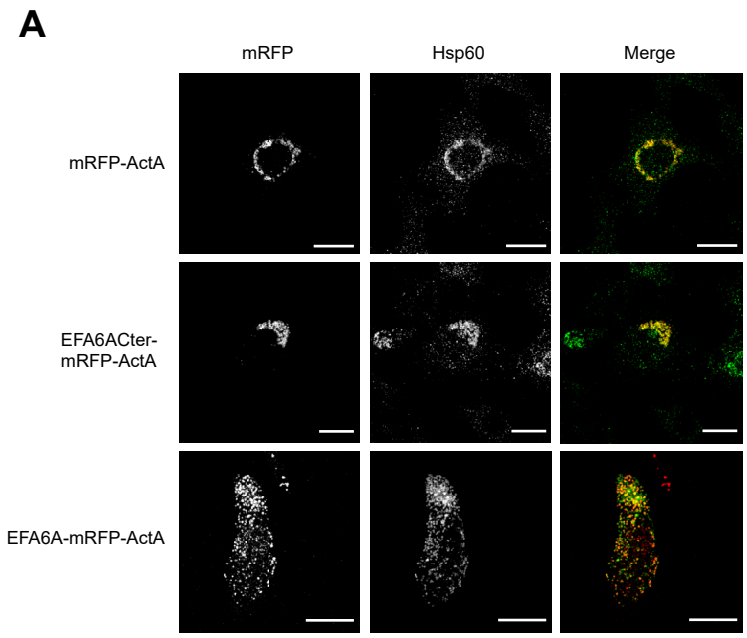

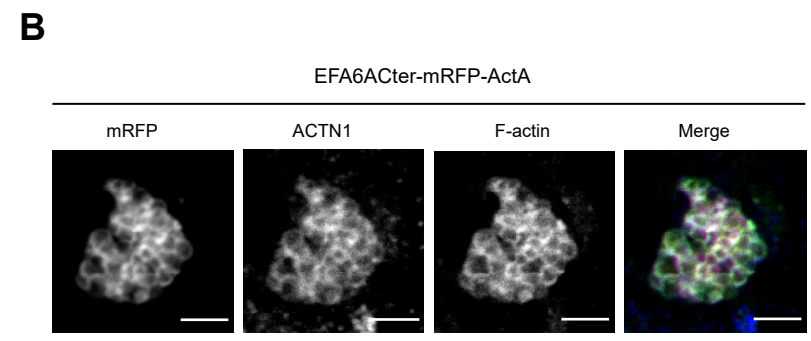

Figure S2. **A**) **The mRFP-ActA constructs localized to mitochondria**. BHK cells expressing mRFP-ActA, EFA6ACter-mRFP-ActA and the full-length EFA6A-mRFP-ActA were processed for immunofluorescence to label the endogenous mitochondrial protein Hsp60. In merge images, mRFP is colored red and Hsp60 is colored green; thus, yellow pixels indicate co-localization demonstrating that the fusion proteins are localized to the mitochondria. **B**) **Co-localization of EFA6ACter-mRFP-ActA with the endogenous ACTN1 and F-actin**. Magnified image of BHK cells expressing EFA6ACter-mRFP-ActA stained for the endogenous ACTN1 and F-actin. In the merge image, mRFP is colored red, ACTN1 is colored blue and F-actin is colored green. Overlap of expression appears white in the merge color image and indicates triple co-localization. Scale bars 10μm.

Journal of Cell Science • Supplementary information

Figure S3

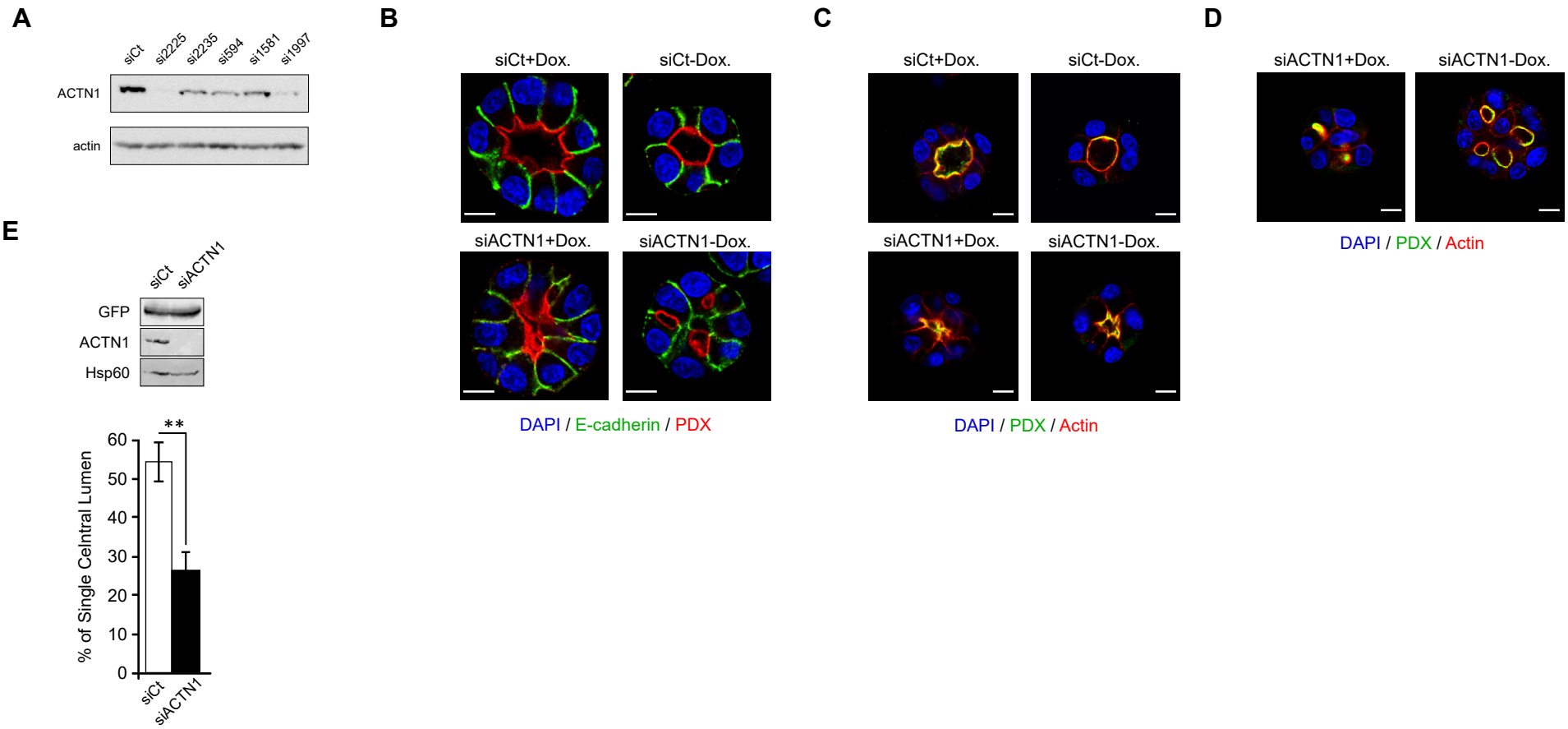

Figure S3. **A**) **siRNA-mediated ACTN1 depletion**. MDCK cells were transfected with siRNA control or siRNAs directed against ACTN1. 48 hr post-transfection the cells were solubilized in SDS lysis buffer and the expression of ACTN1 analyzed by immunoblot. Actin served as a loading control. **B**) **ACTN1 depletion does not affect the apico-basal polarity**. Inducible vsvg-EFA6A MDCK expressing cells were transfected with siRNA control or directed against ACTN1 and grown in the presence or absence of doxycycline. At day four, the cells were processed for immunofluorescence and labeled for the nuclei (blue), the AJ marker E-cadherin (green) and the apical marker PDX (red). Scale bars 10μm. **C,D**) Uncropped images shown in Fig. 3B and Fig. 3E. **E**) MDCK cells expressing GFP were transfected with siRNA control or directed against ACTN1. Top panel: the cells were solubilized in SDS lysis buffer and the expression of the indicated proteins analyzed by immunoblot. Hsp60 served as a loading control. Bottom panel: quantification of the percentage of aggregates with a SCL. Statistical significance was calculated using the Student's t-test. *n=3, p*<0.01.

Journal of Cell Science • Supplementary information

Figure S4

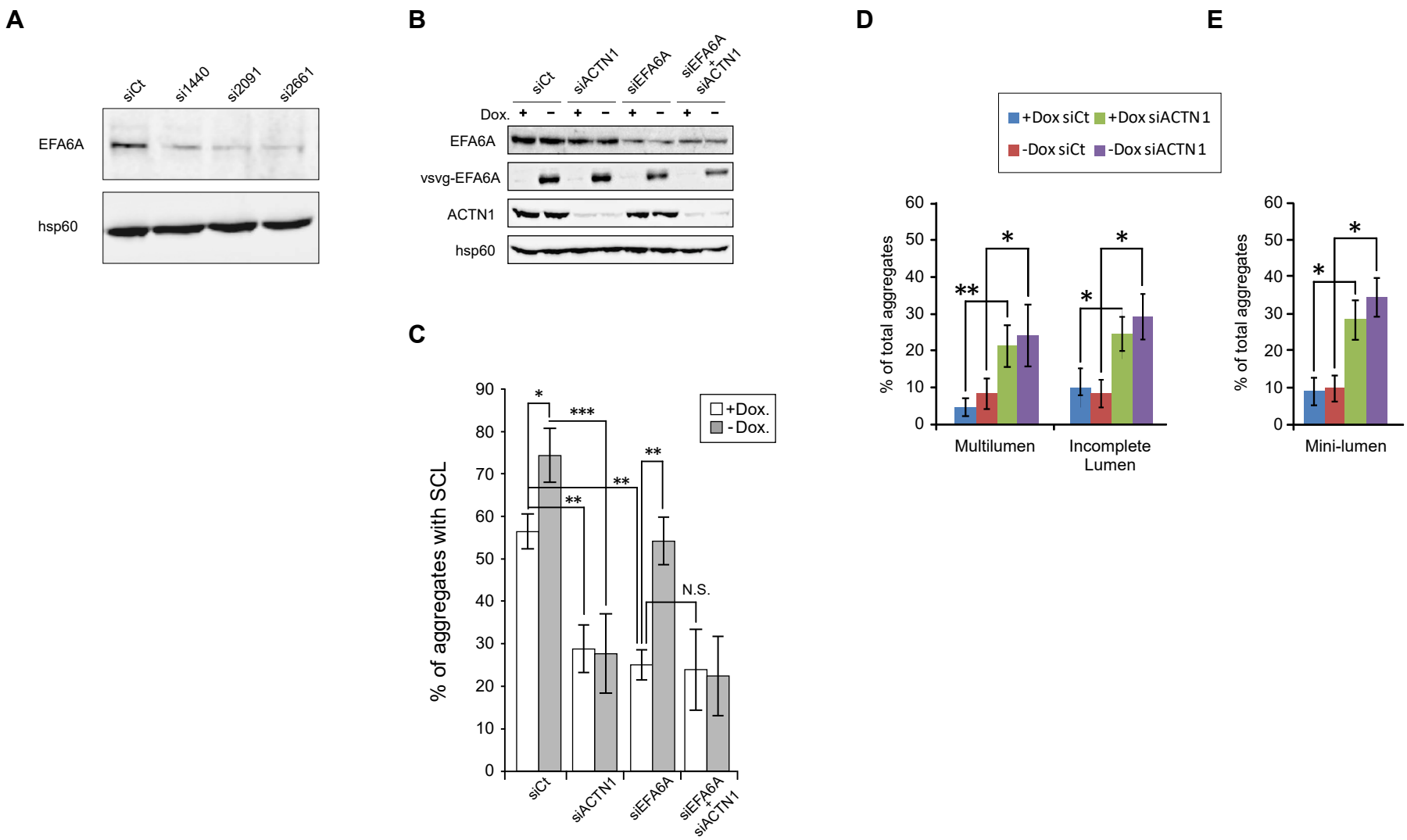

Figure S4. **siRNA-mediated EFA6A depletion.** MDCK cells were transfected with siRNA control or siRNAs directed against EFA6A. 48 hr post-transfection the cells were solubilized in SDS lysis buffer and the expression of EFA6A analyzed by immunoblot. Hsp60 served as a loading control. **B-E**) Experiments presented in Fig. 3A,B,D,E and Fig. 4A,B were repeated with alternate siRNAs directed against EFA6A (#1440) or ACTN1 (#594). *n=3, p*-values of the main results discussed in the text are indicated on the graphs.

Figure S5

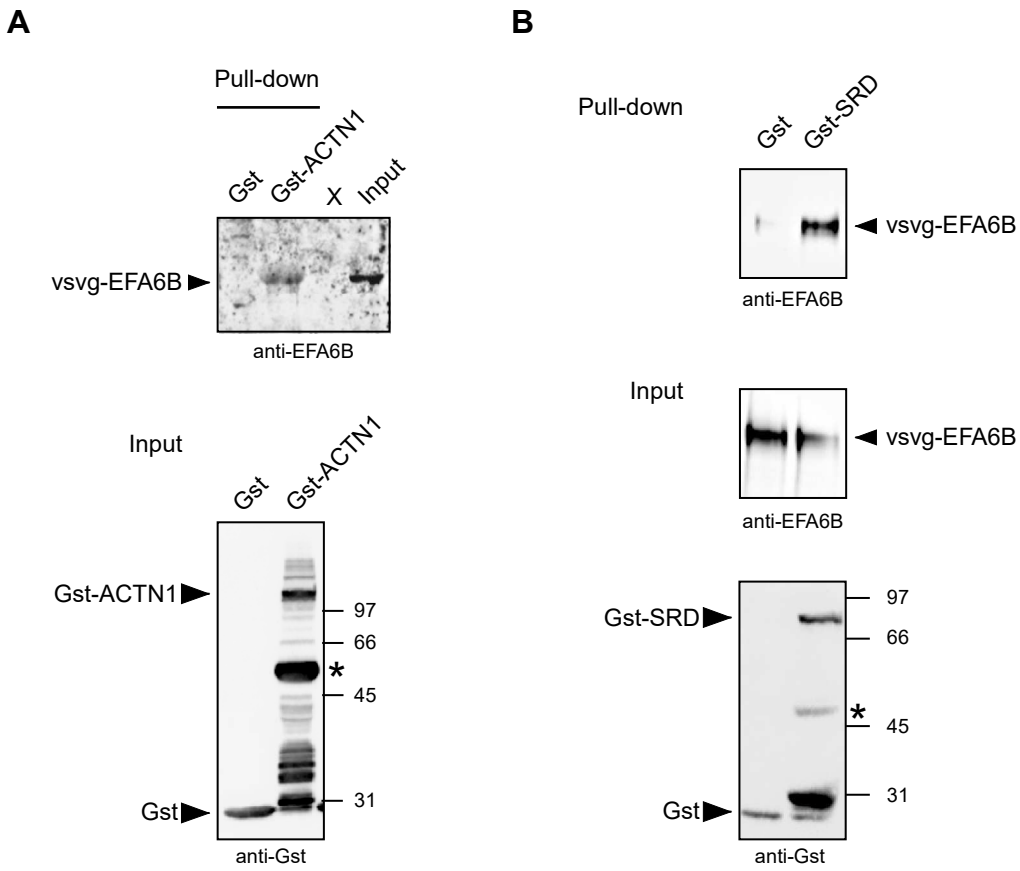

Figure S5. **EFA6B binds to ACTN1 SRD**. Lysate of MCF-10 cells expressing vsvg-EFA6B was reacted with Gst-ACTN1 (**A**) and Gst-SRD (**B**) or control Gst (**A,B**) prebound to glutathione Sepharose 4B beads. The input, whole lysate and bound proteins were analyzed by immunoblotting with the indicated antibodies. * Main purification contaminant.

Table S1. Antibodies used in this study.

Antigen	Antibody source and reference	Application	Dilution or concentration
EFA6B	Sigma-Aldrich, HPA034722	Immunoblotting	1/250
Occludin	Invitrogen, 71-1500	Immunofluorescence	1/100
pMLC	Cell Signaling Technology, 3674	Immunofluorescence	1/50
p85	Millipore, ABS234	Immunoblotting	1/500
Hsp60	Abcam, Ab46798	Immunoblotting	1/10,000
GST	GE Healthcare, 27-4577-01	Immunoblotting	1/2,000
PDX	Dr. GK Ojakian, 3B8 ascite	Immunofluorescence	1/50
VSV-G	Roche Diagnostics, P5D4	Immunoblotting	1/200
Actin	Sigma-Aldrich, AC-40	Immunoblotting	1/1,000
E-cadherin	Invitrogen, 36	Immunofluorescence	1/200
Paxillin	BD Biosciences, 610052	Immunofluorescence	1/5,000
6xHis	Sigma-Aldrich, HIS1	Immunoblotting	1/3,000
GFP	Roche Diagnostics, 7.1	Immunoblotting	1/5,000
Myc	Roche Diagnostics, 3F10	Immunofluorescence	1/100
ACTN1	Sigma-Aldrich, BM75.2	Immunoblotting	1/200
ACTN1	Santa Cruz Biotechnology, H-2	Immunofluorescence	1/100
EFA6A	Dr. H. Sakagami, immunopurified	Immunoblotting	10μg/ml

Journal of Cell Science • Supplementary information

3. Discussion of Article 2

This work has allowed the identification of EFA6 and ACTN1 as two new regulators of luminogenesis. We show that ACTN1 acts as a crucial effector of EFA6A and EFA6B for this process in a normal epithelial cell model and a tumorigenic context, respectively. Our findings suggest a scenario whereby the initial formation of lumen is ensured by ACTN1-independent EFA6 activity, whereas lumen maturation is EFA6-ACTN1-dependent. More specifically, the role of EFA6 in lumen initiation and enlargement is facilitated by the absence of ACTN1. Indeed, the formation of mini-lumens required a relaxed apical actomyosin contractility in order to allow vesicular fusion important to establish the apical plasma membrane. However, the tension forces generated in an EFA6-ACTN1 dependent manner are essential to favor the extension and enlargement of mini-lumens into single mature central lumens.
We can notice that this article revealed not only the role of EFA6A-ACTN1 cascade in luminogenesis but also highlighted the fact that both proteins have some independent chronologically different roles mediated by probably other effectors in the same process. This notion led us once again to the importance of a fine regulation of each and every protein activity. Spatio-temporal protein regulations can be achieved through a wide variety of strategies: conformational change, phosphorylation, intermediate proteins recruiting, scaffolds, etc. I will discuss hereafter two unpublished results that can give some insights on how EFA6 and ACTN1 are regulated.

Unpublished results and potential new roles of ACTN1 on EFA6

May ACTN1 be a possible conformational regulator of EFA6?

After finding that EFA6A binds directly to the non-muscular ACTN1, their interaction was characterize using a mitochondrial-targeting system. Notably, only the PH-Cter construction but not the full length of EFA6A was able to recruit ACTN1 meaning that EFA6A is likely regulated by the structural conformation of its Cter domain. This is in agreement with previous results of the lab on β-arrestin1, another effector of EFA6A, suggesting that EFA6 is present in a close conformation where the Cter domain is folded on the PH domain (Macia et al., 2012). Thus, the binding of EFA6 to its effectors needs an opening signal. In the paper's discussion, we propose Arf6GTP as a possible candidate for mediating the opening signal on the basis of: 1- a published mechanism of activation of the inactivated conformation of ARNO, an exchange factor for Arf1 deriving from the same Sec7 family of ArfGEFs, by ARf1GTP (Cohen et al., 2007; DiNitto et al., 2007; Stalder et al., 2011) , 2- previous results of our research group showing that Arf6GTP can bind the PH-Cter region of EFA6A (Padovani et al., 2014).

An unpublished preliminary result complementary to the present work suspects ACTN1 as another potential candidate to stimulate the opening of EFA6 closed conformation. Indeed, the PH-Cter region of EFA6A managed to bind a conformation sensible effector of EFA6, here the β-arrestin1, only when pre-incubated with ACTN1. This suggests that ACTN1 by binding to this EFA6 region could release the Cter domain and allow the binding of another effector.

Thus, ACTN1 might regulate the opening of the PH-Cter region and stimulate EFA6 functions.

May ACTN1 recruitEFA6 recruiter?

After seeing that the PH-Cter region of EFA6A can target ACTN1 to the mitochondria, we proposed that EFA6A, maintained normally at the apical domain of the cell, is responsible of recruiting the ubiquitous ACTN1 which will induce the maturing of mini-lumens.

Another unpublished piece of data indicated that we cannot exclude the opposite scenario. We found by fusing ACTN1 to the mitochondrial-targeting peptide ActA, that ACTN1 is also capable of relocating EFA6A to the outer membrane of mitochondria. This experiment suggested that ACTN1 might also recruit EFA6A. We think that both scenarios may be actually feasible: in a cell and that both proteins at different times can recruit each other. Hence one can imagine that, for example, that ACTN1 normally present at the level of newly formed adherens junctions will recruit EFA6 to the adhesion complex in order to allow the segregation and formation of tight junctions followed by positive feedback loops enhancing the recruitment of actinin through EFA6.

We believe that EFA6 and actinin collaborate in order to regulate the actin cytoskeleton rearrangement, the formation of adhesion complexes and luminogenesis among others. Further understanding of their interaction and its regulation can be important not only to better understand these functions essential for epithelial establishment and homeostasis, but as well to understand their implications in tumorigenesis.

General Discussion

General discussion

1. General context:

Understanding how normal cells keep their homeostasis through the intense dynamics of the developmental cycles is crucial to better interpret the molecular events inducing breast cancer.
I have started my introduction by presenting the mammary gland morphogenesis, in which epithelial cells communicate with their surrounding stroma in order to orchestrate the formation of a functional organ. In fact, the mechanisms described in cancer responsible for its initiation and progression largely co-opt the finely regulated complex processes of mammary gland development. For instance, mammary cells undergo multiple cycles of proliferation, EMT/MET, migration and invasion by integrating various internal and external signals. Even though typically found in cancer cells, these aforementioned pathways occur in a regulated manner during development, a key notion differentiating a normal tissue from a cancerous one. Regulation includes controlling key epithelial features (apico-basal polarity, cohesion between epithelial cells, lumen formation, etc.) responsible for maintaining the overall epithelial integrity. Here stands our protein of interest, EFA6B, at the core of these structural features, and hence our interest in studying its role in mammary epithelial cells.

So, what did we learn from the present work about the impact of EFA6B in mammary epithelial cells? And what is the relevance of this work to breast cancer?

In the course of this PhD work, using the mammary gland as a study model, we have described the important role of EFA6B in regulating and maintaining epithelial tissue homeostasis.

In the first article, we show that the loss of EFA6B can severely disrupt the epithelial state of normal mammary cells. Indeed, EFA6B KO MCF10A and HMLE cells displayed mesenchymal characteristics and invasive capacities. They present significant modifications of their extracellular matrix components and their integrin repertoire, and they have lost in part their epithelial status by engaging into EMT (upregulation of EMT-TFs, E-cadh/N-cadh switch). EFA6B KOs presented a collective dissemination regulated by the activation of Cdc42 responsible for actin nucleation (via N-WASP/Arp2/3) essential for invadopodia formation (Yamaguchi et al., 2005). Cdc42 upregulation also contributed to cell mobility and invadopodia formation by contracting and aligning the collagen fibers (via MRCK/MLC) (Fraley et al., 2015). In support to this conclusion, deleting EFA6B allowed the formation of invasive structures, invadopodia, rich in ITGB1 and MMP14. All of these newly acquired properties converge into a pro-invasive phenotype. In addition, these results are in agreement with a previous correlation

between low level of expression of EFA6B and Cld-low BC patients. In fact, this subtype is characterized by high metastatic rates and EMT signature. Thus, the loss of EFA6B may have caused the acquisition of the Cld-low invasive properties.

In the second article, consistent with the importance of EFA6 in establishing a normal epithelial tissue, we identified α-actinin1 as an effector of EFA6A in normal epithelial cells and EFA6B in a tumorigenic mammary cell line, MCF7. We showed that both EFA6B/ACTN1 coordination regulates the establishment of apico-basal polarity and luminogenesis, two essential processes for functional epithelia, via apical cellular contractility. Similarly, we found that MCF10A KO cells were not able to polarize and form a lumen. We can definitely suggest that in the absence of EFA6B, actinin is not recruited to the apical acto-myosin cytoskeleton and therefore the absence of contractility, crucial for lumen enlargement and maturation. It is interesting to note that actin might also be playing a cooperative role with Cdc42 in cells deleted for EFA6B, hence the increased contractility. Further investigations are needed to validate these hypotheses.

Altogether, these results strikingly show that the KO of EFA6B is capable of turning normal cells into invasive ones, and to modify their microenvironment (contractility, degradative invadopodia, alteration of the matrisome). We propose *PSD4* (EFA6B) as an invasion-suppressor gene that will preserve cells from losing their epithelial features in order to maintain tissue integrity.

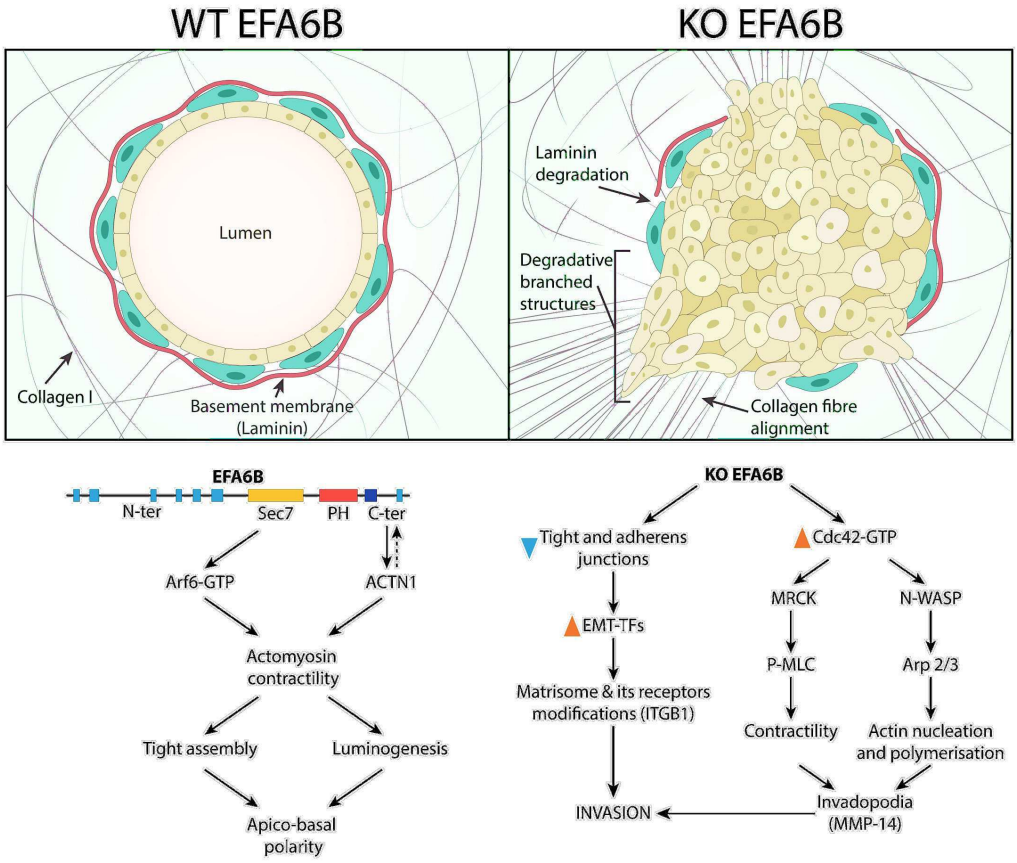

Figure 27: Model for signaling pathways mediating EFA6B roles in epithelial cells.

In mammary epithelial cells, EFA6B activates Arf6 through its sec7 catalytic domain and recruits ACTN1 by its C-terminal domain. We suggest that first both effectors will regulate cell contractility through apical actin cytoskeleton rearrangement. This contractility is important for tight junctions' assembly that was shown to require EFA6B expression and its activated substrate Arf6 in epithelial cells. In parallel, EFA6B/ACTN1 mediated contractility is crucial for the formation of central mature lumen, a characteristic of normal acini. The overall functions of EFA6B will ensure the establishment and maintenance of the apico-basal polarity in epithelial cells. In the absence of EFA6B, cells acquire a degradative invasive phenotype associated with an increased contractility, invadopodia formation and alteration of the matrisome. We suggest that EFA6B loss activates two different pathways: a) The downregulation of EFA6B causes the disassembly of tight and adherens junctions that is probably enhanced by the decreased levels and activity of Arf6 and the lack of ACTN1 recruitment in the absence of EFA6B. In this case, components of adherens junctions such as catenins can be translocated to the nucleus and stimulate new transcriptional programs that will affect the expression of EMT-TFs. EMT-TFs have been shown to engage cells in an epithelial-mesenchymal transition but can be also responsible for the alteration of the matrisome composition and the integrin expression. Given the role of Arf6 in vesicular trafficking, the transport of some integrins can be as well altered in the EFA6B KO cells. b) In parallel, EFA6B deletion induced a clear upregulation of Cdc42, that can be mediated by one of the members of ARH GAP family. We suggest that the overactivation of Cdc42 stimulates MRCK that can phosphorylate the MLC which in turn will increase cellular contractility. In parallel, it will stabilize the N-WASP/Arp2/3 complex and enable actin nucleation and polymerization. Contractility and actin polymerization where both shown to be important for the formation of invadopodia. The collective invasion observed in the absence of EFA6B is the result of both MMP14 rich invadopodia that will degrade the ECM and possible changes in the matrix stiffness and density perceived by the new repertoire of integrins. Of note, inhibiting any of these two Cdc42 dependent and independent pathways

can block invasion. We postulate that both pathways have cooperative functions and therefore are crucial for providing invasive advantages for EFA6B KO cells.

A step back: what is then the importance of EFA6B, in a normal context, on epithelial homeostasis?

Collectively our data suggest that epithelial cells cannot afford to lose EFA6B. It protects normal cells from losing their epithelial identity. Here's some examples of EFA6 proteins functions among others that would illustrate their importance.

First important role for EFA6B in maintaining the epithelial homeostasis is the assembly of TJs and the establishment of apico-basal polarity. Indeed, a previous study of our research group shows that exogenous expression of EFA6B is able of blocking the TGF-β induced EMT (Zangari et al., 2014), and here we show that its absence facilitates an EMT engagement. In fully polarized cells, the presence of EFA6B at the TJs might serve to preserve the apico-basal polarity and TJs in place. The disassembly of adhesion complexes activates different signaling pathways that can disrupt vital cellular functions. For example, E-cadherin, once removed from the plasma membrane, activates transcriptional programs mainly translocating β-catenin to the nucleus. Associated to TJs, we can find the transcription factor ZONAB that can affect cell proliferation by accumulating in the nucleus (Balda et al., 2003).

The second aspect, related to the apico-basal polarity, ensured by EFA6B and its effector a-actinin1 expression is luminogenesis. Luminogenesis is a fundamental property of epithelial cells and tube formation, and a key step of the mammary gland development and milk secretion. A deregulation of lumen formation can be at the origin of human diseases like polycystic kidney disease, cystic fibrosis and certain cancer metastasis (Willenborg and Prekeris, 2011).

Lastly, EFA6 proteins are believed to coordinate the organization of the actin cytoskeleton and cell surface trafficking (endocytosis, exocytosis, secretion, recycling). Taking for instance just the regulation of receptors expression on cell surface, EFA6 can cover a wide panel of cellular roles. EFA6A was shown to control the recycling of β2 adrenergic receptor, a GPCR implicated in controlling vision, insulin secretion, heart muscle contraction, etc. (Boulakirba et al., 2014b; Macia et al., 2012). In another project in the lab to which I participated (appendix I), EFA6A appears to be important for rhodopsin transport and a key player for ciliogenesis by regulating vesicular fusion, two biological processes important for vision (shown *in vitro* in epithelial retinal cells and *in vivo* in the retina of mice).

Being implicated in basic cell functions (actin cytoskeleton organization, cell surface trafficking) and providing fundamental properties (epithelial cell junctions, apico-basal polarity, lumen formation) for epithelial cells, EFA6 proteins should be given more importance when studying epithelial tissues.

***

The whole of this work leaves some questions unanswered, and opens various perspectives for future investigation. I will present some of the possible areas of improvement and some hanging questions that we still need to tackle in order to better elucidate the roles of EFA6B and its mechanisms of action. Seeing the importance of EFA6B in maintaining epithelial cell physiology, I would like first to discuss what could be the upstream regulators allocated to prevent EFA6B downregulation in a normal context. Then, I would like to tackle the possible links that exists between EFA6B and its effector Cdc42, an interesting area for future research, and to bring up where our results stand in the midst of the controversies related to the role of EFA6B substrate, Arf6, in cancer. Lastly, I will try to further elaborate on the matrisome modifications induced by EFA6B loss: could it be a consequence or the cause of other modifications? And what other components would be interesting to consider?

1. 1. Upstream EFA6B: Regulation at its best

Another compelling discovery from this present work is the importance of the level of expression of EFA6B. As seen in both MCF10A and HMLE cell lines, heterozygous clones presented similar invasive characteristics to the full EFA6B KO cells. With only half of the expression of EFA6B, cells cannot function correctly meaning that a certain level of activity is required to maintain the epithelial homeostasis of normal cells. In BC patients, EFA6B is not frequently found mutated which suggests that regulatory pathways are responsible for this downregulation.

After these observations, a natural question comes to mind: what regulates the expression levels of EFA6B?

Regulation is definitely of extreme importance in this case and our research group has previously shown that EFA6B proteins are regulated at the protein level by ubiquitination/deubiquitination cycles. The levels of EFA6 are critical for TJs biogenesis and are controlled by the deubiquitinating enzyme USP9x. In polarized cells, a low level of EFA6 is maintained by an equilibrium between high protein synthesis and constitutive ubiquitination and turn over by the proteasome. However, while establishing new contacts, epithelial cells require higher levels of EFA6 guaranteed by the USP9x-mediated deubiquitination that protects EFA6 from proteosomal degradation at the nascent cell-cell contact where TJs are assembled (Théard et al., 2010).

Other cooperative mechanism can be put in place by cells to regulate EFA6B on a transcriptional level. First, by looking at the promoter of EFA6B, we noted several consensus sequences that can allow the binding of several transcription factors. Second, methylation sites have been observed offering another strategy of regulating the transcriptional expression of EFA6B (data not shown).

The level of EFA6B expression seems to be crucial for mediating its protective role against cells gaining invasive properties**.** We can suspect that one of these mechanisms is disrupted in tumor cells expressing low EFA6B levels. Understanding better the EFA6B regulation process can help control the invasive capacity of tumor cells.

1. 2. Downstream EFA6B: Cdc42 and Arf6

Arf6 and controversies

EFA6B effects are mediated by the regulation of Arf6 activation, in coordination with the recruitment of effector proteins by the C-terminal domain or other domains of EFA6B. In our EFA6B KO cells, we have clearly shown a reduced expression and activity of Arf6 which is probably in part responsible for the invasive properties present in our cells. In the same line of thoughts, our research group has previously shown a downregulation of Arf6 in Cld-low BC patients expressing lower levels of EFA6B. According to our data, Arf6 activation is more likely to play a protective role against the cells gaining mesenchymal and invasive features. In support to this conclusion, a recent study has identified that the downregulation of Arf6 by NEDD9, a maker of invasive and metastatic cancers, increased the pool of active MMP-14. Thus, the activation of Arf6 maintains MMP-14 in an inactive state that was correlated to a decrease in invasion (Loskutov et al., 2015).

However, this does not fit with the results suggested by two research groups showing mainly that the activation of Arf6 is associated with the acquisition of pro-tumorigenic properties manifested by the formation of invadopodia and the trafficking of MMP-14 to these structures (Hashimoto et al., 2011, 2004, 2005; Marchesin et al., 2015a). Importantly, the paper of Hashimoto et al (2004) shows that the expression of a constitutively active Arf6 can also reduce the invasion of these cells (Hashimoto et al., 2004). This suggests that any deregulation of the cycle activation/deactivation of Arf6 can aberrantly affect the tumorigenic phenotype of cells. In fact, previous results of the lab have shown that expressing a continuously activated Arf6 alone gave opposite results on TJ assembly than when expressed with the PH-Cterminal of EFA6 (Klein et al., 2008a). These data suggested that the role of Arf6 should be studied in the presence of its exchange factor which mimics a more physiological context. Another explanation for the controversies related to Arf6 role in cancer is how invasive the cellular model used is. For instance, the overexpression of EFA6B in weakly tumorigenic cell lines (e.g. MCF7) could revert the

epithelial phenotype in 3D culture, however, this was not possible in aggressive tumor cells (MDA-MB231) (Zangari et al., 2014). This suggested that Arf6 might have different roles depending on the tumor stage.

Which domains of EFA6B are responsible for the protrusion formation?

EFA6 family comprise four isoforms and 4 different domains (N-terminal, C-terminal, PH, Sec7) (**Figure 23**). We first confirmed the specificity of EFA6B by generating a rescue clone in MCF10A. However, it is important to validate whether EFA6B regulates this protrusive phenotype through the activation of Arf6, the C-terminal domain or other domains or by the coordination of both events. The most straightforward approach would be to express EFA6B mutants deleted for the different domains individually and measure the effect on the formation of the protrusive structures. These experiments are planned for the near future in order to validate to what extent Arf6 activation or the C-terminal domain alone can revert the invasive features of our EFA6B KO cells.

From EFA6B to Cdc42: what are the missing links?

The impact of the loss of EFA6B was mediated in part by the remarkable upregulation in Cdc42 activity. Interestingly, a study conducted on normal mammary cells overexpressing Cdc42, using *in vitro* and *in vivo* approaches, presents similar results to our present work: they show that the upregulation of Cdc42 induces an increase in branching and MMP-14 activity/expression, an increased contractility and more importantly stromal alterations (Bray et al., 2013). The most surprising common phenotype is the modifications of the stromal components seen upon Cdc42 upregulation. This study validates the effects we have upon the loss of EFA6B and the consequences of the upregulation of Cdc42: the loss of EFA6B induces the upregulation of Cdc42 that will increase cell contractility, invadopodia formation and invasion and lastly, act on the transcriptional level to modify the ECM. Bray et al identified MAPK pathway activated in parallel to the upregulation of Cdc42, thus it would be interesting to test if the increase of Cdc42 due to the loss of EFA6B has the same effect.

We should note that some characteristics were specific to our model such as the EMT engagement and loss of TJs proteins that are probably activated through other pathways, probably by the upregulated EMT-TFs or the downregulation of Arf6.

Now, our next target should be to characterize the actors that are regulating Cdc42 activation in the absence of EFA6B. A plethora of indirect activation could be possible, however if we want to suggest that there is a direct regulator affected by the loss of EFA6B then we have to consider the upstream regulators of Cdc42, GEFs and GAPs. Loss of function of Rho GAPs and upregulation of Rho GEFs have been observed in various patient tumors. Based on in vitro experiments linking these Rho GEFs/GAPs to Cdc42, I can suggest the following potential candidates: from Rho GEFs, the Dbl family

GEF ARH GEF7 (β-PIX) is one of the most extensively studied for its roles in cell migration and invasion, and from Rho GAPs family srGAP3, a member of the Slit-Robo significantly reduced in a panel of breast cancer cell (Arias-Romero and Chernoff, 2013; Lawson and Ridley, 2018).

More concretely, ARHGAP10, is probably the only Rho GAP for which it was previously shown as an effector of Arf1 creating therefore a link between Arf proteins and Rho family, particularly Arf1 to Cdc42 (Kumari and Mayor, 2008). I suggest starting by investigating members of the ARHGAP family, mainly ARHGAP10, and validate if they are mediating the upregulation of Cdc42 in the absence of EFA6B.

1. 3. EFA6B and the matrisome

Interestingly, the loss of EFA6B have affected the matrisome composition, with 48 out of 475 modified genes. It is striking that around 10 % of the transcriptional changes in the EFA6B KO are on the ECM, an aspect gaining in importance in cancer research considering the increasing evidence of its impact on promoting tumorigenesis. Many candidates seem interesting to further investigate, more specifically the upregulation of lysyl oxidase (LOX). LOX has been shown to increase matrix stiffness by crosslinking collagen fibers contributing to invadopodia formation (Menon and Beningo, 2011) and to promote tumor invasion and metastasis by engaging integrin signaling (Kirschmann et al., 2002; Levental et al., 2009; Wan et al., 2013).

As I mentioned before, on the basis of Bayer et al (2013) study, we can propose that the Cdc42 upregulation is responsible for these matrisomal changes. However, we should keep in mind that cells can always amplify these modifications on the basis of the mechanoreciprocity principle between ECM and epithelial cells, meaning that physical forces applied by either side can trigger considerable changes [discussed in depth in V.Weaver reviews (Butcher et al., 2009; Paszek and Weaver, 2004)]. Thus, inversely, changes in the matrisome may have activated Cdc42.

We thought that the upregulation of LOX would induce an increase in matrix rigidity that can activate some signaling pathways, so we started by testing the YAP/TAZ pathway, shown to respond to stiffness. By immunofluorescence in 2D, we did not see any differences in YAP translocation to the nucleus (preliminary data). More experiments held on 3D cultured KO cells would help investigate the implication of the YAP/TAZ pathway. Another interesting experiment is to put the KO cells in matrixes with increasing stiffness and see if our cells are sensitive to matrix rigidity.

2. Conclusion

In conclusion, this PhD work allowed us to reveal the importance of EFA6B in maintaining the epithelial integrity in normal cells. We have also elucidated the impact of its loss on driving normal cells towards invasiveness in a Cdc42 dependent manner. Deleting EFA6B provided mammary epithelial cells with contractile and degrading capacities as well as a remarkable modification of their stromal compartment, all of which contribute to an invasive advantage. These properties provided by EFA6B loss can be *in vivo* the needed modifications to allow transformed cells to metastasize. EFA6B loss can be classified as a secondary driver gene capable of pushing cancer cells a step further in the tumorigenesis process and drive them towards invasion. In patients, the downregulation of EFA6B might be in part responsible for the evolution of breast cancer tumors into the aggressive claudin-low subtype.

After all, the development of breast cancer treatments is still limited by the lack of complete knowledge of the molecular and cellular mechanisms responsible for mammary tumorigenesis. In addition to that, it is essential to better understand the microenvironment properties that can affect treatment efficiency. Thus, identifying in our EFA6B KO cell model the signaling pathways involved and their regulators might disclose new therapeutic targets for invasive breast cancer, more specifically claudin-low.

Appendix 1

EFA6A plays a key role in retinal function by controlling ciliogenesis.

Mariagrazia Partisani[1*], Carole L. Baron[1*], Rania Ghossoub[2], Mohammed Ettaiche[1], Racha Fayad[1], Emmanuelle Silvy[1], Sophie Pagnotta[3], Frédéric Brau[1], Sandra Lacas-Gervais[3], Carole Rovere[1], Alexandre Benmerah[4,5], Frédéric Luton[1], Michel Franco[1*]

[1] Institut de Pharmacologie Moléculaire et Cellulaire (IPMC), UMR 7275 CNRS-Université de Nice-Sophia Antipolis, 660, route des lucioles, 06560 Valbonne, France
[2]Centre de Recherche en Cancérologie de Marseille (CRCM), Inserm, U1068-CNRS UMR7258, Aix-Marseille Université, Institut Paoli-Calmettes, 13009 Marseille, France.
[3]Centre Commun de Microscopie Appliquée (CCMA), Université de Nice-Sophia Antipolis Parc Valrose, 06103 Nice cedex 2.
[4]INSERM, UMR 1163, Laboratory of Inherited Kidney Diseases, 75015 Paris, France
[5]Paris Descartes - Sorbonne Paris Cité University, Imagine Institute, 75015 Paris, France

Short title: EFA6A controls ciliogenesis

Abstract

Ciliogenesis is a coordinated process, initiated at the mother centriole by the formation of a large ciliary vesicle through molecular mechanisms that remain unclear. Here, we report that EFA6A, an exchange factor for Arf6, controls ciliogenesis at early stage by promoting the fusion of small distal appendage vesicles *via* the recruitment of Arl13b and the exocyst complex and by removing the inhibitory protein CP110 from the mother centriole. At a later stage, and similar to Arl13b and Sec10 findings, expression levels of EFA6A regulate the length of the cilium. *In vivo,* EFA6A is essential for visual function, which depends on the highly specialized photoreceptor cilium. We show that EFA6A depletion from mouse retina resulted in morphological alterations of photoreceptors reminiscent of defects observed in retinal ciliopathies. Our results uncover novel fusion machinery comprised of EFA6A, Arl13b and the exocyst complex, which controls the assembly, the maintenance and the physiological function of primary cilia

Introduction

The primary cilium (PC) is a microtubule-based structure found in most eukaryotic cells. Originally considered to be a vestigial organelle, it is now the object of intense interest because of its essential roles in cell homeostasis and development. Also, defects in PC assembly or function cause a wide variety of diseases called ciliopathies. They include skeletal defects, limb and digit development disorders, cystic renal diseases, neurodevelopmental disorders (cerebellar ataxia, acrocallosal syndrome) and retinal degeneration [1-3]. Considered as a group, the prevalence rate of ciliopathies is relatively high (1 in 2000 adults)[4]. These disorders are due to mutations in genes that encode proteins localized to the PC and which play an important role in its function.

The outer segment (OS) of photoreceptor cells is a highly specialized PC that converts light signals into an electrical output in a process called phototransduction [5, 6]. This dynamic cilium is subjected to constant renewal to compensate for the shedding and phagocytosis of its distal tip by the retinal pigment epithelium (RPE). Its resident proteins, particularly the light sensitive receptor rhodopsin, are continuously transported from the

proximal inner segment (IS) to the OS through the connecting cilium (CC). Most of the ciliopathies, including Joubert, Meckel, Senior-Loken and Bardet-Biedl syndromes lead to the retinal degeneration that is associated with classical disorders such as renal cystic disease, obesity, and mental retardation [7]. The gene products implicated in these retinal illnesses are also expressed in the primary cilium of other tissues, which explains their pleiotropic phenotype.

The PC is formed at the distal end of the mother centriole (m-centriole) during quiescence or the G0 phase of the cell cycle [8-10]. The assembly of PC starts with the formation of a large ciliary vesicle (CV) docked to the m-centriole as described more than 50 years ago by Sergei Sorokin [11]. This step is followed by the dissociation of the inhibitory CP110-CEP97 complex from the distal end allowing axoneme extension and the eventual formation of the cilium (reviewed in [8, 10]). Clearly the biogenesis of the CV is not fully understood. Recent reports describe the presence of small preciliary vesicles docked onto the distal appendages (called DAV for distal appendage vesicles) that precede the formation of the CV, probably through their fusion[12, 13].The DAV fusion is driven by the proteins EHD1/3 and the SNARE SNAP29, at the very least [12]. Then, the ciliary membrane biogenesis and extension is achieved by vesicular membrane trafficking controlled by a cascade of small G proteins, including Rab11, Rab8 and its Guanine Nucleotide Exchange Factor (GEF) Rabin8 [14-16]. More recently, the exocyst, an octameric protein complex implicated in the tethering and fusion of post-Golgi and recycling-compartment-derived vesicles has also been shown to control ciliogenesis and ciliary membrane extension [17, 18]. Indeed, the exocyst complex localizes to the PC, and knockdown of Sec10, one of the eight exocyst subunits, strongly inhibits ciliogenesis whereas its overexpression increases PC assembly and length [17, 19]. Moreover, Sec15, another exocyst subunit, interacts with Rab proteins including Rab8 and Rab11 (reviewed in [20]). Arl13b is another small G protein that is involved in membrane transport, and a set of mutations in the corresponding gene has been linked to the Joubert syndrome ciliopathy, indicating that it plays a role in ciliogenesis [21-23]. Arl13b regulates the ciliary length by controlling ciliary membrane extension [24]. In addition, Arl13b acts as an Arl3 GEF to control the ciliary targeting of lipidated protein cargo, and the assembly of Intra-Flagellar Transport (IFT) -A and -B complexes required for the intra-cilium transport [25]. Interestingly, Arl13b directly binds two exocyst complex subunits, Sec5 and Sec8, suggesting that Arl13b and the exocyst function together to control ciliary membrane extension *via* the tethering of membrane vesicles [26].

The EFA6 family belongs to the Sec7-domain containing proteins that act as nucleotide exchange factors for the small G proteins of the Arf group [27]. Humans express four tissue specific EFA6 isoforms, which are encoded by four different genes [28, 29]. While they display highly divergent N-terminal domains, they share a common C-terminal structure [30]. Despite their homology and frequent co-expression, it remains unclear whether the different EFA6 proteins play specific or overlapping roles. EFA6A, is mostly expressed in the brain, small intestine and colon [30]. It controls the endocytic trafficking of different cargos such as GPCRs, the transferrin receptor, ion channels [27, 31-33] and the transport of membrane vesicles to form the apical lumen in mammary epithelial cells [34]. In addition, EFA6A drives actin cytoskeleton reorganization, at least in part, by interacting with F-actin and α-actinin [35-37]. Its exogenous expression leads to the formation of membrane ruffles in various cell types, the stabilization of the apical actomyosin ring in polarized epithelial cells [27, 30, 38], the formation of neurite and dendritic spines [36, 39, 40] and axon regeneration [41].

Here, we describe the role of EFA6A as an essential regulator of ciliogenesis and vision. In human cells, EFA6A is required for the removal of the ciliation inhibitor CP110 and acts together with Arl13b and the exocyst complex to assemble the ciliary vesicle by fusion of DAVs. In mouse retina, EFA6A controls morphology and electrical activity of the photoreceptor OS. Considered together, our results indicate that EFA6A plays a key role in photoreceptor function by controlling early steps of ciliogenesis and cilia maintenance.

RESULTS

EFA6A localizes to photoreceptor and RPE cells in mouse retina

EFA6A protein is particularly enriched in the brain but its functions in neurons has not been clearly established [27]. Here, we looked for a role of EFA6A in the mouse retina. First, immuno-histochemistry analyses localized the EFA6A protein in RPE cells, the outer and inner segments (OS and IS respectively) of the photoreceptors, in some cells of the inner nuclear and plexiform layers (INL and IPL) and in ganglion cell layer (GCL) (Fig. 1A and Supp. Fig. 1A). EFA6A mRNA localization was subsequently determined by *in situ* hybridization on frozen sections of retinas. In accordance with the immuno-histochemistry results, a specific antisense oligonucleotide probe revealed mRNA expression in the ganglion cell layer, inner and outer nuclear layers, and in RPE cells to some extent (Supp. Fig. 1B). We conclude that EFA6A is present in most cell layers of the retina including photoreceptors and RPE.

Depletion of EFA6A leads to morphological alterations in mouse retina

EFA6A depletion, obtained by intravitreal siRNA application, was used to explore the role of EFA6A on the morphology and ultrastructural organization of the mouse retina. EFA6A siRNA efficiency was analyzed by WB and RT-PCR (Supp. Fig.1 C and D). Using light microscopy, we observed severe retinal detachment in numerous retinal sections of the si-EFA6A-treated groups (Fig. 1B a, b white arrowhead). This was accompanied by the loss of some OS (Fig. 1B b black arrowhead) and the loss of nuclei in the outer nuclear layer (ONL) (Fig. 1B).

Electron microscopy (EM) further confirmed that the photoreceptor OS organization was severely disrupted in the siEFA6A injected eyes at day 7 (Fig. 1C a and b). In contrast to the control groups, the OS were not regularly aligned and packed (Fig. 1C a,b) and the interface with the RPE was not tight (Supp. Fig. 1E a,b). Large holes were observed in the OS layer probably as a result of a defect in OS growth (Fig. 1C b white arrowhead). Moreover, the alteration to photoreceptor cell structure observed by EM in the siEFA6A-treated retinas was associated with mislocalization of rhodopsin (Supp. Fig.1F b compared to a). Rhodopsin staining was not uniformly distributed throughout the retinas, suggesting inhibition of IS to OS transport. This fault in rhodopsin transport can be explained by the disorganization of the membrane, or connecting cilium (CC), that joins the inner and the outer segments (Fig. 1C b black arrowheads). In fact, the CC was less visible in the siEFA6A-treated tissue, compared to the control (Fig.1C b compared to a). Interestingly, in further support of these EM observations, acetylated-tubulin staining, which is particularly enriched in the CC and in the RPE of control retinas, was significantly disturbed and attenuated in siEFA6A-treated retinas (Fig. 1D a, b).

Finally, ultrastructural analysis of ONL showed degenerative cell bodies in rod (*) and cone photoreceptors (**) in siEFA6A-treated retinas compared to the control (Supp. Fig. 1E c, d) indicating that EFA6A depletion resulted in photoreceptor cell degeneration.

To summarize, EFA6A depletion in mouse retina provoked profound morphological alterations mainly in the outer segment and in the RPE layers. It resulted in the degeneration and the loss of photoreceptor outer segments, a mislocalization of rhodopsin, and a loss of connecting cilia (Supp. Fig.1G for an illustration). Thus, from these results, we conclude that EFA6A plays an important role in organizing the CC and the OS of the photoreceptor cells.

Depletion of EFA6A leads to functional alterations of mouse retina

The modified structural integrity of EFA6A-depleted retinas prompted us to test for alterations to their physiological electrical response. To explore the functional status of the siEFA6A-treated retinas, we recorded electro-retinograms (ERG) in scotopic (to measure the activity of rod cells, Fig. 1E and Fig Supp.2A,B,C) and photopic (to measure the activity of cone cells, Fig. 1F and Fig Supp.2D,E,F) conditions seven days after siRNA injection. In all cases, ERG showed no alteration between untreated (control) and siRNA-control-treated groups. However, siEFA6A-treated retinas exhibited a severe decrease in ERG response under both conditions.

In scotopic conditions and at high stimuli intensity (1.87 log scot troland.s), the a-wave amplitude, generated by the rod cells, declined to 38% and 45% at day 7 for siRNA #a and #b respectively compared to control (Fig. 1E and Supp. Fig. 2A). These results are consistent with a degenerated and dysfunctional photoreceptor layer. The b-wave, which is generated by the bipolar cells immediately following the a-wave, was also affected by the siEFA6A treatment (Supp. Fig. 2B). The maximum saturated scotopic b-wave (Vmax) was significantly reduced ($p<0.001$); approximately 40% (#a) and 43% (#b) lower at day 7 in the siEFA6A-treated groups, compared to the control. However the b/a wave ratio was conserved between the four groups (Supp. Fig. 2C), indicating that the degeneration preferentially occurs in the outer retina and is not the consequence of degeneration in other retinal cells.

In photopic conditions, and at high intensity stimuli (1.87 log scot troland.s), the a-wave amplitudes decreased significantly ($p< 0.001$) to 31% and 27% at day 7 for siRNA #a and #b compared to the control groups (Fig. 1F). Concomitantly, the overall difference in the photopic b-wave was also significant ($p< 0.001$) and the b-wave amplitudes decreased to 27% and 30% at day 7 in siRNA #a and #b compared to the control groups (Supp. Fig. 2E). However the b/a ratio, under photopic condition, was not significantly affected (absence of negative-type ERGs b/a wave ratio< 1) by siEFA6A treatment, confirming that photoreceptor alteration was the main cause for the decrease in the retinal electrical response (Supp. Fig. 2F).

In conclusion, our data demonstrate that EFA6A is required *in vivo* for the morphological integrity and functional activity of the photoreceptors.

EFA6A controls ciliogenesis

As EFA6A depletion from the retina phenocopied ciliopathies i.e. loss of visual activity and degeneration of photoreceptor outer segments [42-44], we looked for a role of EFA6A in primary cilium biogenesis. We determined the localization of exogeneous EFA6A expressed at low levels in hTert-RPE-1 (RPE-1) cells after serum starvation to induce ciliogenesis. In addition to its classical plasma membrane localization, EFA6A was detected along the entire primary cilium where it colocalized with Arl13b, a protein essential to ciliogenesis and whose localization is restricted to the ciliary membrane (Fig. 2A).

In RPE-1 cells, small interfering RNA (siRNA) mediated depletion of EFA6A strongly inhibited ciliogenesis, as assessed by acetylated tubulin staining (70.1% of ciliated cells in the control compared to 6.1% in EFA6A siRNA pool treated cells; Fig. 2B and C and Supplementary Fig. 3A and B). Similar results were obtained with Arl13b labeling, which confirmed that EFA6A depletion affected ciliogenesis (Fig. 2D). In contrast, EFA6A depletion did not affect centrosome assembly as controlled by the centrosomal/satellite localization of PCM1 (Fig. 2B), nor was Golgi apparatus morphology affected as indicated by p23 labeling (Supplementary Fig. 3C). These results suggest a specific role for EFA6A in the assembly of the primary cilium.

RPE-1 cells expressed two other EFA6 isoforms, EFA6B and EFA6D (Supplementary Fig. 3A, B). Knockdown of either one had no effect on the presence or morphology of primary cilia (Fig. 2D, E and Supplementary Fig. 3A, B). This result indicates that ciliogenesis is specifically controlled by the EFA6A isoform in RPE-1 cells.

To determine if EFA6A plays a general role in ciliogenesis and PC maintenance, we turned to the MDCK renal epithelial cell model. The exogenous and inducible expression (Tet-Off system) of a human vsv-g-tagged EFA6A (Supplementary Fig. 3D) significantly increased the percentage of ciliated cells and unexpectedly increased the cilium length as well (Fig. 3A, B). The cilia elongation mediated by EFA6A was also observed in MDCK cells grown in 3D culture indicating that this stimulatory property also occurs in near physiological conditions (Fig. 3C). Furthermore, siRNA-mediated EFA6A depletion inhibited ciliogenesis, which was rescued by the expression of the human vsv-g-tagged EFA6A, resistant to the canine-specific siRNA (Fig. 3D and Supplementary Fig. 3E). Thus, cilia-localized EFA6A appears to act as a general regulator of ciliogenesis and controls both cilium assembly and maintenance.

EFA6A depletion prevents the removal of CP110 from the m-centriole

We investigated the molecular mode of action of EFA6A in ciliogenesis, and given that EFA6A depletion totally abolished the formation of primary cilia, we focused on the early steps of ciliogenesis. The CP110 protein caps the distal end of both centrioles and its removal from the mother centriole is required for the initiation of ciliogenesis [45]. In serum-starved RPE-1 cells, EFA6A siRNA-treatment significantly increased the proportion of cells containing two CP110-capped centrioles (63.4% vs 30.6% in control cells; Fig. 4A a). This observation suggested that EFA6A depletion may have blocked cilia formation at least in part by inhibiting the dissociation of CP110 from the m-centriole. CP110 removal is known to be driven by the centriole distal appendage protein CEP164 and the recruitment of the serine/threonine kinase TTBK2 to the sub-distal appendages (for review [46]). EFA6A depletion did not inhibit the accumulation of either CEP164 or TTBK2 at the centrioles (Fig. 4A b and c). These observations indicate that EFA6A does not regulate the localization of CEP164 and TTBK2 to the m-centriole. However, in the absence of EFA6A, their recruitment is not sufficient to promote the release of the ciliation inhibitor CP110.

EFA6A controls the fusion of vesicles by regulating the function of Arl13b

We subsequently considered whether EFA6A depletion could interfere with membrane vesicle delivery to the m-centriole. As Arl13b is a membrane ciliary marker that is required for ciliary membrane formation and extension, we looked for the presence of Arl13b positive structures at the m-centrioles. Using immuno-fluorescence after serum-starvation, we observed Arl13b-positive staining close to the centriole in EFA6A-depleted cells (Fig. 4B a). This result suggested that, even if it led to the inhibition of PC, EFA6A depletion was not preventing the formation or the docking of Arl13b-positive vesicles to the m-centriole.

To test this hypothesis, we investigated the effect of EFA6A depletion at the ultrastructural level by EM on serum-starved RPE-1 cells (Fig. 4B b). Control cells exhibited a typical PC comprised of a basal body with distal appendages and a long axoneme surrounded by a proximal ciliary pocket [47]. In contrast, EFA6A-depleted cells rarely exhibited fully assembled cilia or CV-docked basal bodies. In most of the cells small vesicles (between 50 and 100 nm diameter) were found very close to the m-centrioles, likely docked to the distal appendages (Fig. 4B b, and Fig. 5 G for quantification), which is consistent with the Arl13b-positive vesicles observed by immunofluorescence (Fig. 4B a). These vesicles

resembled m-centriole-docked DAVs prior to fusion and CV assembly [12]. Collectively, our data demonstrate a role for EFA6A in the fusion of the DAVs and in the removal of the CP110 negative regulator.

Several lines of evidence prompted us to look for a link between EFA6A and Arl13b. Indeed, EFA6A depletion led to the inhibition of ciliogenesis as observed in Arl13b deficient cells, and to photoreceptor cells degeneration as noted in patients with the Arl13b-associated Joubert Syndrome. Moreover, similar to Arl13b, overexpression of EFA6A increased PC length. Using GST pull-down experiments, we demonstrated that full-length EFA6A, and to a lesser extent its catalytic Sec7 and PH domains, were able to specifically pull-down Arl13b-GFP from RPE-1 cell lysate (Fig.5A and Supp. Fig. 4A). GST pull-down experiments with purified proteins revealed that the two proteins were able to directly interact (Fig. 5B). EFA6A preferentially bound the GTP-loaded form of Arl13b but did not act as an Arl13b-GEF (Supp. Fig. 4B, C). We considered whether Arl13b could act downstream of EFA6A. Overexpression of Arl13b-GFP partially rescued the inhibition of ciliogenesis induced by EFA6A depletion (Fig.5D and E), indicating that a lower amount of EFA6A could be counterbalanced by a higher expression of Arl13b. In contrast, EFA6A overexpression could not rescue the inhibition of ciliogenesis caused by Arl13b depletion (Supp. Fig. 4D). One explanation could be that EFA6A recruits Arl13b to promote the fusion of the DAVs. If this were the case, the depletion of Arl13b would lead to the same phenotype as that observed for EFA6A, namely an absence of CV but the presence of DAVs in the vicinity of m-centrioles. Indeed, electron microscopy imaging showed that, similarly to EFA6A, Arl13b depletion resulted in a majority of m-centrioles surrounded with small membrane vesicles (Fig. 5F and G for quantification). Our results show that EFA6A interacts with Arl13b to regulate the fusion of DAVs to assemble the PC.

Among the different Arl13b interactors, only the exocyst complex could play a role in DAVs fusion. Indeed, the exocyst complex is involved in the tethering and the fusion of recycling vesicles and is also known to be required for PC and photoreceptor outer segment assembly [17, 18]. Interestingly, we observed that EFA6A pull-downed the Sec10 and Exo84 but not Exo70 exocyst complex subunits (Fig.5C and Supp. Fig. 4D, E, F). The interaction with Sec10 is direct as indicated by the pull-down experiment with the purified proteins (Fig.5B). Altogether our data demonstrate that EFA6A and Arl13b, most likely through their interaction with the exocyst complex, regulate the fusion of DAVs to form the ciliary vesicle.

Discussion

Biogenesis of the primary cilium is an important and intricate process that has been the object of numerous studies. The hierarchical series of events from the conversion of the centriole to the cilium extension have been well established, yet the detailed molecular mechanisms and the different partners involved in each step are poorly described. Here, we describe a novel molecular cascade that regulates primary cilium formation and maintenance.

EFA6A functions in retina activity

We observed that EFA6A is present in almost all mouse retina cells, including photoreceptors and RPE. The localization of EFA6A in photoreceptors has been previously reported, but its role in retina function was not addressed [48]. Here, we demonstrate that EFA6A is required for vision. In mouse retina, EFA6A depletion led to a strong alteration of visual electrical activity. ERG analyses indicated that the photoreceptors, both cones and rods, were at the root of the defect. The electrical alterations were coupled to morphological damage, which was visible in the organization of the photoreceptor cell layer. The localization of rhodopsin was markedly affected and the rods were less compact, with a loss of outer segments. These alterations could arise from a defect in lipid and protein transport toward the cilium and would be compatible with a role for EFA6A in the delivery and the fusion of membrane vesicles at the basis of the OS. Moreover, EFA6A depletion resulted in the morphological alteration of the connecting cilium as revealed by the loss of tubulin acetylation labeling and confirmed at the ultrastructure level by EM. This indicated that EFA6A is involved in the assembly and the stability of the connecting cilium. As the latter plays a critical function in the transport of proteins toward the outer segment, the photoreceptor degeneration observed in the absence of EFA6A might also result from the inability to transport key OS components through the deficient connecting cilium. In any case, a defect in rhodopsin transport toward the outer segment is a well-described causal mechanism for severe diseases, such as autosomal dominant Retinitis Pigmentosa and its associated photoreceptor degeneration [7, 49, 50].

A role for EFA6A in CP110 release and CV formation

EFA6A depletion in MDCK and RPE1 cell models abolished the formation of PC induced by serum starvation. This demonstrates a conserved and essential role of EFA6A in ciliogenesis. More precisely, our data show that EFA6A is required to remove the negative regulator, CP110, from the m-centriole and is thus indispensable in the early stages of ciliogenesis. The persistence of CP110 could explain the absence of ciliogenesis in EFA6A-depleted cells. However, EFA6A depletion did not affect the recruitment to the basal body of CEP164 or the kinase TTBK2, two proteins required for the removal of CP110. These results suggest that EFA6A could either regulate the kinase activity of TTBK2 or control the release of CP110 by an unknown mechanism.

Immuno-fluorescence analyses in EFA6A-depleted cells revealed the accumulation of small Arl13b-positive structures in the vicinity of the centrioles. EM studies confirmed the presence of small vesicles (DAV) docked or very close to the m-centrioles. These results indicate that docking of DAV to the distal appendages of the m-centriole is not an EFA6A-dependent process. Yet, there was no evidence for a large CV cap at the distal end of the m-centriole, which indicates that the fusion of the DAVs into a larger CV requires EFA6A. The

direct binding of EFA6A to Arl13b and to the exocyst subunit Sec10 could explain the role of EFA6A in CV formation. Surprisingly, we found that EFA6A depletion could be bypassed by overexpression of Arl13b. This observation suggests that EFA6A may act as an anchor for Arl13b. We hypothesize that EFA6A may regulate the formation of a complex between Arl13b and the exocyst in order to favor the fusion of the DAV. Arl13b and Arf6, the substrate of EFA6, are known to regulate the endocytic recycling traffic [23, 51-53]. Moreover, it has been shown that Arf6 regulates the post-endocytic recycling through its interaction with Sec10 [54]. Thus, we propose that EFA6A controls the fusion of vesicular membranes during ciliogenesis *via* the formation of a complex including Arf6, Arl13b and the exocyst.

Another protein involved in vesicular transport, EHD1/3, was recently found to be necessary for CV assembly [12]. Much like EFA6A, EHD1 appears to be essential for both the fusion of the DAV and the removal of CP110. This suggests the existence of an unexpected link whereby the assembly of the CV would control the CP110 release from the m-centriole, a crucial step for the subsequent elongation of the axoneme. The authors proposed that EHD1/3 regulates the fusion of the DAV through SNAP29, a SNARE membrane fusion regulator. To date no connections between EFA6A and EHD proteins nor between EFA6A and SNAP29 have been reported. Yet, EHD1 and Arf6 have been implicated in the recycling of MHC-I to the plasma membrane [55] suggesting that both proteins could be part of the same transport machinery. As the exocyst complex is thought to bridge the v- and t-SNAREs from opposing membranes, the interaction between EFA6A and Arl13b would occur prior to the interaction between EHD1/3 and the t-SNARE SNAP29.

EFA6A expression controls PC maintenance

The primary cilium is a dynamic structure whose size and shape is controlled by extracellular signals. This is emphasized in the outer segments of photoreceptors cells, which are continually renewed to counterbalance cell shedding and RPE phagocytosis. The fact that EFA6A depletion in adult mice retina resulted in the alteration of the CC and OS of photoreceptors indicates that EFA6A also controls the maintenance of the PC. Analogous to its role in DAVs fusion and CV formation, we propose that EFA6A-mediated membrane vesicle fusion plays a major role in PC maintenance. It is noteworthy that the overexpression of EFA6A (this study), as observed for Arl13b and Sec10 [17, 24], increases the cilium length. One can speculate that EFA6A and Arl13b regulate the delivery of membrane, through interactions with the vesicle tethering exocyst complex, to the base of the growing cilia where the exocyst has been found to be enriched [26]. It would be now interesting to study a putative link between the EFA6A/Arl13b/exocyst machinery and the Rab11/Rabin8/Rab8 equivalent, which has been clearly shown to be involved in the delivery of vesicular membrane during ciliogenesis (reviewed in [20, 56]).

In summary, EFA6A is essential during the initiation steps of ciliogenesis and in the control of PC length. EFA6A could assume both of these functions by regulating membrane vesicles fusion during ciliogenesis.

Loss of EFA6A function, a cause of ciliopathy?

Although ciliopathies are individually relatively rare disorders (incidence of individual ciliopathies ranges from around 1 in 1000 for autosomal dominant polycystic kidney disease to 1 in 150000 [3]), taken as a group their high frequency has a significant impact on human health. In the absence of effective treatments, they remain a serious public health challenge. Mutations in genes that encode cilia components account for most of ciliopathies. Here, we have observed that the exogenously expressed EFA6A is localized throughout the primary

cilium in RPE-1 cells, and immuno-histochemistry analyses revealed that the endogenous EFA6A was abundant in the photoreceptor cell layer of mouse retina. EFA6A was also identified in a proteomic analysis of the mouse photoreceptor sensory cilium complex [57]. In addition to its retinal localization, we found EFA6A to be essential for cilium assembly, as well as photoreceptor maintenance and function. We observed that EFA6A depletion in retinas leads to progressive degeneration of photoreceptors. Thus, aberrant alleles of the PSD gene, which encodes EFA6A, are a strong candidate for retinal ciliopathies. Given that the molecular mechanisms of primary cilium assembly are highly conserved we predict that PSD gene mutations will be the source of pleiotropic disorders. We also predict that strong alterations in the PSD post-transcriptional gene regulatory mechanisms affecting the cellular expression level of EFA6A protein could also lead to ciliopathies.

METHODS

Antibodies and reagents.
Mouse monoclonal antibodies (mAb) against vsv-g epitope (clone P5D4, Roche Diagnostics GmbH, Mannheim, Germany), α-Tubulin, γ-Tubulin, acetylated-Tubulin, syntaxin, PKCα, calbindin monoclonal D-28K antibody (Sigma Chemical St. Louis, MO), RPE65 (Novus Biological), rhodopsin (Millipore). Rabbit antisera against Arl13b and CP110 (Proteintech Europe Manchester, United Kingdom), EFA6B, TTBK2 and CEP164 (Sigma), P23 and PCM1 (Abcam). Rat monoclonal anti–Thy1.2 antibody (Abcam). Goat anti-peanut agglutinin antibody (Vector Laboratories). Fluorescent conjugated secondary antibodies from donkey and cross absorbed for the other species were from Jackson Immuno-Research (West Grove PA) or Molecular Probes (Invitrogen, Cergy Pontoise France). DAPI (4', 6-diamidino-2-phenylindole) was from Sigma. Fluorescent labeled Phalloïdin (Molecular Probes). Purified rabbit anti-EFA6A antibodies were prepared against a C-terminal peptide (LQPKPSSQPRAQRHS) (Eurogentec).

DNA constructs
Plasmids encoding vsv-g-tagged EFA6A, EGFP-EFA6A, His-EFA6A, His-EFA6AΔN, GST-EFA6A-Sec7, GST-EFA6A, GST-EFA6A-Cter, GST-EFA6A-PHCter and Arf6-His have been described elsewhere [35]. Plasmid encoding Arl13b-EGFP [58], plasmids encoding GST-CrArl13b(18-278), called GST-Arl13b in the text, was kindly provided by A. Whittinghofer and C. Koerner (MPI Dortmund, Germany). Plasmids encoding, Sec10-mCherry, Exo70-mCherry and Exo84-mCherry were kindly provided by Dr. P. Chavrier (Institut Curie, Paris).

Expression and purification of recombinant proteins
For the *in vitro* binding assays, recombinant Arf6 wild-type with a C-terminal hexa-his tag (Arf6-His) and recombinant N-terminal his-tagged EFA6AΔN (His-EFA6AΔN) were produced in *Escherichia coli* and purified on Ni/NTA resin according manufacturer's instructions (Qiagen). The different GST fusion proteins were also produced in *Escherichia coli* and purified by affinity chromatography on gluthatione sepharose beads (GE Healthcare). After elution with glutathione, the purified proteins were dialysed against 20 mM Tris-HCl pH 8.0, 100 mM NaCl, 1 mM MgCl2, 1 mM DTT, and 10% glycerol (dialysis buffer), and stored at -80 °C.

Cell culture and transfections.
All cell culture reagents were from Invitrogen/Thermofisher, unless indicated. Filtered FBS was from Perbio Thermo Scientific. All cell lines were grown in 10% FBS at 37°C in 5% CO2 incubator. RPE-1 cells (from ATCC) were cultured in DMEM/F12 (1:1). For cilia formation, RPE-1 cells were serum deprived overnight before fixation.
MDCKII cells stably expressing vsvg tagged-EFA6A under the control of the tetracycline-repressible transactivator were grown in MEM (Sigma), 5% decomplemented FCS (Biowest-Abcys), penicillin-streptomycin 100 U/ml and 100 μg/ml [38]. When indicated cells were grown on transparent permeable filters (Costar, Corning, NY) at $2x10^5$ cells/12 mm filter. For 3D cell culture, cells were grown in Matrigel (BD Biosciences, San Jose, CA). $2x10^3$ cells were mixed with 20 µl of Matrigel and deposited as a drop on a 12 mm glass coverslip placed in a 24-well plate and fed with regular medium.

siRNAs and mammalian expression constructs.
SiRNA duplexes (SiGenome smart pool) targeting human Arl13b, Sec10 (ExoC5), EFA6A, EFA6B and EFA6D and the four individual siRNA-EFA6A were purchased from Dharmacon.

SiRNA control was from Sigma. The siRNA#2661 ccuaucagaggcggagcua targeting the canine EFA6A transcript was from Eurogentec.
Small siRNA targeting mouse EFA6A for intravitreal injection siRNA#1:ccaagugggaauucuu and siRNA#2: ggugcuaccgagagac (Eurogentec)
SiRNA transfection in RPE-1 cells was performed using RNAiMAX (Invitrogen) following the manufacturer's instructions and the transfected cells were incubated for 3 days at 37 °C.
SiRNA transfection in MDCK cells was performed by nucleofection (AMAXA, Lonza Group Ltd, Switzerland) according to the manufacturer's instructions.

All cDNA transfections were performed with Jet-PEI (Polyplus transfection, Illkirch, France) and the transfected cells were incubated for 24 h or 48 h at 37 °C. All cDNAs were amplified in DH5α *Escherichia coli* (Invitrogen) and prepared following the manufacturer's instructions (Qiagen).

RNA isolation, RT-PCR and QRT-PCR.
Total mRNA was isolated according the Chowynski method using Fast Prep apparatus (Q-Biogen). 2 μg of total RNA was denatured at 65 °C for 10 min and incubated for 1 h at 50 °C in presence of 2.5 mM dNTP, 100 U Superscript III (Invitrogen) using 0.5 μg oligo$(dT)_{15}$ primer in a total volume of 20 μl, followed by an inactivation step of 15 min at 70 °C. A negative control lacking RT enzyme was also performed in each assay (NRT).

The PCR was performed with mouse EFA6A (forward) atctctgttgcgcccc, (reverse) gggcggcggaagccctga and GAPDH (forward) gaacatcatccctgcatcc, (reverse) ccagtgagcttcccgttca primers with HotStartTaq DNA polymerase according to the standard protocol described by the manufacturer (Q-Biogen). The PCR products obtained after 35 cycles were separated through a 1% agarose gel, visualized under UV after staining with ethidium bromide. The PCR fragments of expected sizes for EFA6A and GAPDH mRNA-derived PCR products were obtained.

Quantitative real-time PCR was carried out with The LightCycler® 480 SYBR Green I Master (Roche Life Science) in triplicate and analyzed using LightCycler® 480 Software, Version 1.5 (Roche). Primers sequences were as followed:
Human EFA6A: Forward: AGGGCATGATCCTCTACCTG
Reverse: ATGCTGATGGCATTCTTGAG
Canine EFA6A: Forward: CAACGGGCAGAAAGCAGACC
Reverse: CTTGAGGTACTCGCCAGCCA
Human EFA6B: Forward: AGCTGGAAAGTGAGCCAGAT
Reverse: CAGCAGATGGAGTGTGGTTT
Human EFA6D: Forward: AAGGCCTTGTCTGAAGAGGA
Reverse: CTCTGGGCTCTGAGTTTGAA
Human/Canine GAPDH: Forward: TGCCTCCTGCACCACCAACT
Reverse: CCCGTTCAGCTCAGGGATGA
The expression of each gene was normalized to the GAPDH housekeeping gene and relative levels were calculated on the basis of the comparative cycle threshold Ct method ($2^{-\Delta\Delta Ct}$) where ΔΔCt is the difference in Ct between target and reference gene.

Western blot (WB) analysis.
Cells were washed twice in PBS then scrapped and resuspended in lysis buffer (20 mM TriEthanolAmine pH 8.0, 150 mM NaCl, 5 mM EDTA, 0.5% sodium dodecyl sulfate and protease inhibitor cocktail Complete (Roche)). Cell lysates were centrifuged and supernatants were diluted with Laemmli Sample Buffer. The proteins were heat denatured and processed by SDS-PAGE, transferred to nitrocellulose membranes, stained with Ponceau Red and immunoblotted with the indicated Abs. Proteins were detected with SuperSignal western lightning chemiluminescence reagents (ThermoScientific) following the manufacturer's instructions.

Analysis of the protein content of siRNA-treated mouse retinas by WB. Retinas were washed in PBS and resuspended in Lysis Buffer, boiled for 10 min, sonicated for 10 seconds and centrifuged. The resulting lysates were diluted 10 times and the total protein concentrations were determined by the Bradford method. Protein samples (40 μg/lane) were then analyzed as described above.

GST pull-down experiments

RPE-1 cells were transfected with plasmid encoding GFP-Arl13b, Sec10-mCherry, Exo84-mCherry or Exo70-mCherry using Jet-PEI reagent. After 24 h, cells were lysed in 50 mM Tris pH 8.0, 100 mM NaCl, 10 mM $MgCl_2$, 10% glycerol, 1% Triton-X100, 2 mM DTT and a cocktail of protease inhibitors (Roche, Diagnostics GmbH, Mannheim, Germany), and centrifuged at 15,000 g for 10 min at 4 °C. Supernatants were incubated with 0.5 μM GST constructs in the presence of 0.75% BSA and Glutathione Sepharose beads for 4 h at 4 °C.
For the direct binding assay with purified recombinant proteins, 0.2 μM His-EFA6A was incubated in 50 mM Tris pH 8.0, 100 mM NaCl, 10 mM $MgCl_2$, 10% glycerol, 2 mM DTT and a cocktail of protease inhibitors with 0.5 μM GST or GST-Arl13b or GST-Sec10 in the presence of 0.75% BSA and Glutathione Sepharose beads for 1 h at 25 °C.
Beads were washed, and bound proteins were eluted using SDS sample buffer and separated by SDS-PAGE. Their presence in the eluate was detected by western blotting using the anti-tag antibodies.

[35S]GTPγS binding assay

Arf6-His or GST-Arl13b (2 μM) were incubated at 30 °C with [^{35}S]GTPγS (20 μM, ~ 2000 cpm/pmol) in 50 mM Hepes (pH 7.5), 2 mM $MgCl_2$, 100 mM KCl, with azolectin (2 mM) with or without (as indicated in the figure legend) His-tagged EFA6A (0.5 μM). At the indicated times, samples of 25 μl were removed and measured for radioactivity as described previously [27].

Preparation of phospholipid vesicles.

Large unilamellar vesicles of azolectin were prepared as previously described [59], and extruded through a 0.4 μM pore size polycarbonate filter (Isopore, Millipore).

Immunofluorescence and confocal microscopy analysis.

Cultured cells were fixed on 11 mm round glass coverslips with 3 % paraformaldehyde, and processed for immunofluorescence analysis as described previously [60]. Confocal microscopy analysis was carried out with a Leica TCS-SP5 microscope (Leica Microsystems) or a LSM-780 (Zeiss). Images were analyzed using Image J and Adobe Photoshop software.
For centrosomal markers, the cells were fixed in methanol at -20 °C for 4 min, rinsed twice in PBS and processed as above.

Transmission Electron Microscopy.

For ultrastructural analysis, RPE-1 cells were fixed in 1.6% glutaraldehyde in 0.1 M phosphate buffer, rinsed in 0.1 M cacodylate buffer, post-fixed for 1 h in 1% osmium tetroxide and 1% potassium ferrocyanide in 0.1 M cacodylate buffer to enhance the staining of membranes. Cells were rinsed in distilled water, dehydrated in alcohol and lastly embedded in epoxy resin. Contrasted ultrathin sections (70 nm) were analyzed using a JEOL 1400 transmission electron microscope mounted with a Morada Olympus CCD camera.

Quantifications.

Results are the mean of three to five independent experiments. The error bars represent standard deviations within n experiments (n= number of distinct experiments, unless otherwise indicated). Statistical significances (p) were calculated using the Student's t test. *$p<0.05$; **$p<0.01$, ***$p<0.001$ and ****$p<0.0001$.

For cilium length measurement, fluorescence image stacks of MDCK cells obtained by laser scanning confocal microscopy (LSM780, Carl Zeiss, France) were analyzed to measure cilia lengths using a custom-built ImageJ macro program. After maximal projection of the stack, filtering by "background subtraction", segmentation by thresholding and skeletization of the cilia, the length of the skeleton was measured to determine the length of each cilium in the image.

Ethics statement.
All animal experimental procedures were carried out in accordance with French ethical guidelines for laboratory animals (Reference number of the project: 00537.01; Agreement number: C061525 -16/04/2015) and approved by the Animal Care Committee.

Animals.
Adult male C57BL/6J mice (12 weeks old, Charles River, France) were maintained in clear plastic cages and subjected to standard light cycles (12 hours light/12 hours dark cycle) with *ad libitum* access to food and water. Light levels measured from the bottom of cages averaged 40 to 50 lux. Mice were acclimated for 2 weeks before experiments. These studies were performed in accordance with the Association for Research in Vision and Ophthalmology Statement for the Use of Animals in Ophthalmic and Vision Research.

In situ hybridization, immunochemistry and double labeling.
Mice were dark adapted overnight, anesthetized, and killed by cervical dislocation. Eyes were removed, punctured at the limbus, and perfused with ice-cold 4 % paraformaldehyde in phosphate-buffered saline (PBS). After 30 min of fixation, the cornea, the lens, and the vitreous were removed, and the eyecups were cryoprotected in 20 % sucrose in PBS for 1 hour and then embedded (Tissue-Tek; Sakura Finetek, Bayer Diagnostic, France) and snap frozen in liquid nitrogen-cooled isopentane. Frozen 14 µm sections were then prepared.
For *in situ* hybridization, the following antisense oligonucleotide EFA6A was used (5'-GCA-GGT-AGA-GGA-TCA-TCG-CCT-TGA-GGA-TCC-CGT-GGA-AGC-TCT-TCC-3'). A sense oligonucleotide unrelated to EFA6A (5'-GGA-AGA-GCT-TCC-ACG-GGA-TCC-TCA-AGG-GCA-TGA-TCC-TCT-ACC-TGC-3') was used as a negative control. The probes were 3' end-labeled with digoxigenin (DIG)-UTP by a terminal deoxynucleotidyl transferase. The sections were fixed for 20 min in 4% paraformaldehyde in PBS, permeabilized in 0.1% Tween 20 in PBS, and rinsed three times in PBS. The sections were acetylated for 10 min in 0.25% acetic anhydride and 0.1 M triethanolamine, pH 7.5, prehybridized for 10 min at 37 °C in 4X SSC and 12.5% formamide, and hybridized overnight at 42 °C in 4X SSC, 12.5% formamide, 2.5x Denhardt's solution, 250 µg/ml herring sperm DNA, 125 µg/ml yeast tRNA and 22 ng/µl DIG-labeled probe. The slides were washed briefly with 4X SSC and then washed for 10 min with 1XSSC. DIG-labeled probes were detected according to the protocol from Roche Diagnostics. Briefly, the sections were incubated with anti-DIG-alkaline phosphatase for 2 hr at 25 °C, rinsed with washing buffer, and incubated with nitroblue tetrazolium (NBT)–5-bromo-4-chloro-3-indolyl-phosphate (BCIP) for 2 hr in the dark.
For immunochemistry, the frozen retinal sections were immediately permeabilized with 0.1% Triton X-100 in PBS for 15 minutes, subsequently washed in 1X PBS three times, and blocked with 10% horse serum in PBS to avoid nonspecific staining. EFA6A was detected with the rabbit anti–EFA6A antibody (1:250) incubated on sections overnight. Detection was achieved with FITC labeled anti-rabbit IgG antibody (1:300; Vector Laboratories, Burlingame, CA). In double-immunostaining experiments, cell-type marker antibodies were incubated overnight at 4 °C and were detected with an indocarbocyanine (Cy-3)–labeled anti–mouse IgG (1:300; Invitrogen, Cergy Pontoise, France) or anti–rat IgG (1:400; Invitrogen). Control experiments were conducted without primary antibody. Rod and cone inner segments were localized, respectively, with anti-rhodopsin and peanut agglutinin antibodies, horizontal cells with anti-calbindin, bipolar cells with anti-PKCα, amacrine cells with anti–syntaxin, RPE cells with anti-RPE65 and ganglion cells with rat anti–Thy1.2 antibodies. Immunostained retinas on slides were mounted in anti-fade solution containing DAPI for nuclear staining

(Vectashield; VectorLaboratories). Negative controls were used without primary or secondary antibodies (data not shown). Images of retinal sections were acquired and photographed with an imaging microscope (Axioplan2; Zeiss, Thornwood, NY) and analyzed by confocal microscopy (Zeiss, LSM 780).

***Intravitreal injection*.**
Wild-type mice of C57BL/6 strain (4-month-old) were anesthetized by intraperitoneal injection of ketamine/xylazine (ketamine, 100-125 mg/kg; xylazine, 10-12.5 mg/kg). Intravitreal injections were performed under a dissecting microscope with a 33 gauge needle attached to a 10 µl glass syringe (Hamilton, France). The needle was positioned 1 mm posterior to the limbus and 1 µl of the solution was slowly injected (3-5 sec) into the vitreous chamber of the eye using micro-pump (WA 30 second interval was kept before removing the needle).
Intravitreal injections of siRNA were performed as described in [61].

***ERG Recording and Analysis*.**
Photopic and scotopic ERGs were performed according to the procedure previously described [62]. To record conventional ERGs, responses were recorded using a stainless ring electrode that made contact with the corneal surface through a thin layer of 0.7% methylcellulose. Needle electrodes placed in the cheek and the tail served as reference and ground leads, respectively. Responses were differentially amplified (0.3-500 Hz), averaged, and stored using a UTAS Big-Shot signal averaging system (LKC Technologies, Gaithersburg, MD). In scotopic conditions, ERGs were recorded to flash stimuli ranging from -4.72 to 1.87 log (sc td*s) presented, in order of increasing intensity to the dark-adapted eye, in an LKC ganzfeld flashes. Cone ERGs were obtained to flash stimuli ranging between -2.32 to 1.87 log (sc td*s) superimposed on a steady adapting field (44 cd/m^2) after a 7-min adaptation period (Peachey et al. 1993). The a-wave amplitude was measured from the pre-stimulus baseline to the trough of the a-wave. The b-wave amplitude was measured from the trough of the a-wave to the positive peak. The amplitude of the c-wave was measured from the pre-stimulus baseline to the peak of the c-wave. Oscillatory potentials (OPs), which are superimposed over the ascending phase of the ERG b-wave, were extracted for the highest and the lowest stimulus intensity using EM software with two filtering operations equivalent to applying a bandpass filter with corner frequencies of 73 and 500 Hz. For each of the four parameters, the data were plotted against flash luminance to generate the scotopic and photopic luminance response. Two other parameters were derived from the scotopic and photopic luminance response of the b-wave, the V max and logσ.

Histology and transmission electron microscopy. Eyes enucleated from mice killed by anesthetic overdose were placed in fresh fixative (2.5% glutaraldehyde, 2% paraformaldehyde and 100 mM cacodylate, pH 7.4) for 30 min. Tissues were post fixed with 1% OsO4 for 1 h and stained with 2% uranyl-acetate for 30 min, dehydrated in a graded ethanol series, and infiltrated and embedded in medium (Polybed 812; Polysciences, Warrington, PA). Thin sections were cut with an ultramicrotome (MT 7000; Ventana, Tucson, AZ), collected onto nickel grids, stained with 2% uranyl acetate and lead citrate, and imaged in a transmission electron microscope (Morgagni; FEI, Hillsboro,OR) at 80 Kv.

REFERENCES

1. Badano, J.L., Mitsuma, N., Beales, P.L. & Katsanis, N. The ciliopathies: an emerging class of human genetic disorders. *Annu Rev Genomics Hum Genet* **7**, 125-148 (2006).
2. Hildebrandt, F., Benzing, T. & Katsanis, N. Ciliopathies. *N Engl J Med* **364**, 1533-1543 (2011).
3. Tobin, J.L. & Beales, P.L. The nonmotile ciliopathies. *Genet Med* **11**, 386-402 (2009).
4. Quinlan, R.J., Tobin, J.L. & Beales, P.L. Modeling ciliopathies: Primary cilia in development and disease. *Curr Top Dev Biol* **84**, 249-310 (2008).
5. May-Simera, H., Nagel-Wolfrum, K. & Wolfrum, U. Cilia - The sensory antennae in the eye. *Prog Retin Eye Res* (2017).
6. Sung, C.H. & Chuang, J.Z. The cell biology of vision. *J Cell Biol* **190**, 953-963 (2010).
7. Adams, N.A., Awadein, A. & Toma, H.S. The retinal ciliopathies. *Ophthalmic Genet* **28**, 113-125 (2007).
8. Ishikawa, H. & Marshall, W.F. Ciliogenesis: building the cell's antenna. *Nat Rev Mol Cell Biol* **12**, 222-234 (2011).
9. Malicki, J.J. & Johnson, C.A. The Cilium: Cellular Antenna and Central Processing Unit. *Trends Cell Biol* **27**, 126-140 (2017).
10. Sanchez, I. & Dynlacht, B.D. Cilium assembly and disassembly. *Nat Cell Biol* **18**, 711-717 (2016).
11. Sorokin, S. Centrioles and the formation of rudimentary cilia by fibroblasts and smooth muscle cells. *J Cell Biol* **15**, 363-377 (1962).
12. Lu, Q. *et al.* Early steps in primary cilium assembly require EHD1/EHD3-dependent ciliary vesicle formation. *Nat Cell Biol* **17**, 531 (2015).
13. Wu, C.T., Chen, H.Y. & Tang, T.K. Myosin-Va is required for preciliary vesicle transportation to the mother centriole during ciliogenesis. *Nat Cell Biol* **20**, 175-185 (2018).
14. Westlake, C.J. *et al.* Primary cilia membrane assembly is initiated by Rab11 and transport protein particle II (TRAPPII) complex-dependent trafficking of Rabin8 to the centrosome. *Proc Natl Acad Sci U S A* **108**, 2759-2764 (2011).
15. Nachury, M.V. *et al.* A core complex of BBS proteins cooperates with the GTPase Rab8 to promote ciliary membrane biogenesis. *Cell* **129**, 1201-1213 (2007).
16. Knodler, A. *et al.* Coordination of Rab8 and Rab11 in primary ciliogenesis. *Proc Natl Acad Sci U S A* **107**, 6346-6351 (2010).
17. Zuo, X., Guo, W. & Lipschutz, J.H. The exocyst protein Sec10 is necessary for primary ciliogenesis and cystogenesis in vitro. *Mol Biol Cell* **20**, 2522-2529 (2009).
18. Lobo, G.P. *et al.* The exocyst is required for photoreceptor ciliogenesis and retinal development. *J Biol Chem* **292**, 14814-14826 (2017).
19. Rogers, K.K. *et al.* The exocyst localizes to the primary cilium in MDCK cells. *Biochem Biophys Res Commun* **319**, 138-143 (2004).
20. Das, A. & Guo, W. Rabs and the exocyst in ciliogenesis, tubulogenesis and beyond. *Trends Cell Biol* **21**, 383-386 (2011).
21. Sun, Z. *et al.* A genetic screen in zebrafish identifies cilia genes as a principal cause of cystic kidney. *Development* **131**, 4085-4093 (2004).
22. Cantagrel, V. *et al.* Mutations in the cilia gene ARL13B lead to the classical form of Joubert syndrome. *Am J Hum Genet* **83**, 170-179 (2008).
23. Barral, D.C. *et al.* Arl13b regulates endocytic recycling traffic. *Proc Natl Acad Sci U S A* **109**, 21354-21359 (2012).
24. Lu, H. *et al.* A function for the Joubert syndrome protein Arl13b in ciliary membrane extension and ciliary length regulation. *Developmental biology* **397**, 225-236 (2015).

25. Gotthardt, K. *et al.* A G-protein activation cascade from Arl13B to Arl3 and implications for ciliary targeting of lipidated proteins. *Elife* **4** (2015).
26. Seixas, C. *et al.* Arl13b and the exocyst interact synergistically in ciliogenesis. *Mol Biol Cell* **27**, 308-320 (2016).
27. Franco, M. *et al.* EFA6, a sec7 domain-containing exchange factor for ARF6, coordinates membrane recycling and actin cytoskeleton organization. *Embo J* **18**, 1480-1491 (1999).
28. D'Souza-Schorey, C. & Chavrier, P. ARF proteins: roles in membrane traffic and beyond. *Nat Rev Mol Cell Biol* **7**, 347-358 (2006).
29. Sakagami, H. The EFA6 family: guanine nucleotide exchange factors for ADP ribosylation factor 6 at neuronal synapses. *Tohoku J Exp Med* **214**, 191-198 (2008).
30. Derrien, V. *et al.* A conserved C-terminal domain of EFA6-family ARF6-guanine nucleotide exchange factors induces lengthening of microvilli-like membrane protrusions. *J Cell Sci* **115**, 2867-2879. (2002).
31. Decressac, S. *et al.* ARF6-dependent interaction of the TWIK1 K(+) channel with EFA6, a GDP/GTP exchange factor for ARF6. *EMBO Rep* **5**, 1171-1175 (2004).
32. Gong, Q. *et al.* Identification and characterization of a new class of trafficking motifs for controlling clathrin-independent internalization and recycling. *J Biol Chem* **282**, 13087-13097 (2007).
33. Macia, E., Partisani, M., Paleotti, O., Luton, F. & Franco, M. Arf6 negatively controls the rapid recycling of the beta2 adrenergic receptor. *J Cell Sci* **125**, 4026-4035 (2012).
34. Zangari, J. *et al.* EFA6B antagonizes breast cancer. *Cancer Res* **74**, 5493-5506 (2014).
35. Macia, E. *et al.* The pleckstrin homology domain of the Arf6-specific exchange factor EFA6 localizes to the plasma membrane by interacting with phosphatidylinositol 4,5-bisphosphate and F-actin. *J Biol Chem* **283**, 19836-19844 (2008).
36. Sakagami, H. *et al.* Somatodendritic localization of EFA6A, a guanine nucleotide exchange factor for ADP-ribosylation factor 6, and its possible interaction with alpha-actinin in dendritic spines. *Eur J Neurosci* **25**, 618-628 (2007).
37. Milanini, J. *et al.* EFA6 proteins regulate lumen formation through alpha-actinin 1. *J Cell Sci* **131** (2018).
38. Luton, F. *et al.* EFA6, exchange factor for ARF6, regulates the actin cytoskeleton and associated tight junction in response to E-cadherin engagement. *Mol Biol Cell* **15**, 1134-1145 (2004).
39. Choi, S. *et al.* ARF6 and EFA6A regulate the development and maintenance of dendritic spines. *J Neurosci* **26**, 4811-4819 (2006).
40. Sironi, C. *et al.* EFA6A encodes two isoforms with distinct biological activities in neuronal cells. *J Cell Sci* **122**, 2108-2118 (2009).
41. Eva, R., Koseki, H., Kanamarlapudi, V. & Fawcett, J.W. EFA6 regulates selective polarised transport and axon regeneration from the axon initial segment. *J Cell Sci* **130**, 3663-3675 (2017).
42. Rachel, R.A., Li, T. & Swaroop, A. Photoreceptor sensory cilia and ciliopathies: focus on CEP290, RPGR and their interacting proteins. *Cilia* **1**, 22 (2012).
43. Liu, Q., Zhang, Q. & Pierce, E.A. Photoreceptor sensory cilia and inherited retinal degeneration. *Adv Exp Med Biol* **664**, 223-232 (2010).
44. Wheway, G., Parry, D.A. & Johnson, C.A. The role of primary cilia in the development and disease of the retina. *Organogenesis* **10**, 69-85 (2014).
45. Tsang, W.Y. & Dynlacht, B.D. CP110 and its network of partners coordinately regulate cilia assembly. *Cilia* **2**, 9 (2013).
46. Wei, Q., Ling, K. & Hu, J. The essential roles of transition fibers in the context of cilia. *Curr Opin Cell Biol* **35**, 98-105 (2015).
47. Ghossoub, R., Molla-Herman, A., Bastin, P. & Benmerah, A. The ciliary pocket: a once-forgotten membrane domain at the base of cilia. *Biol Cell* **103**, 131-144 (2011).

48. Katsumata, O. *et al.* Predominant localization of EFA6A, a guanine nucleotide exchange factor for ARF6, at the perisynaptic photoreceptor processes. *Brain Res* **1234**, 44-49 (2008).
49. Berson, E.L., Rosner, B., Weigel-DiFranco, C., Dryja, T.P. & Sandberg, M.A. Disease progression in patients with dominant retinitis pigmentosa and rhodopsin mutations. *Invest Ophthalmol Vis Sci* **43**, 3027-3036 (2002).
50. Deretic, D. A role for rhodopsin in a signal transduction cascade that regulates membrane trafficking and photoreceptor polarity. *Vision Res* **46**, 4427-4433 (2006).
51. D'Souza-Schorey, C., Li, G., Colombo, M.I. & Stahl, P.D. A regulatory role for ARF6 in receptor-mediated endocytosis. *Science* **267**, 1175-1178 (1995).
52. Montagnac, G. *et al.* ARF6 Interacts with JIP4 to control a motor switch mechanism regulating endosome traffic in cytokinesis. *Curr Biol* **19**, 184-195 (2009).
53. Radhakrishna, H. & Donaldson, J.G. ADP-ribosylation factor 6 regulates a novel plasma membrane recycling pathway. *J Cell Biol* **139**, 49-61. (1997).
54. Prigent, M. *et al.* ARF6 controls post-endocytic recycling through its downstream exocyst complex effector. *J Cell Biol* **163**, 1111-1121 (2003).
55. Caplan, S. *et al.* A tubular EHD1-containing compartment involved in the recycling of major histocompatibility complex class I molecules to the plasma membrane. *Embo J* **21**, 2557-2567 (2002).
56. Deretic, D. Crosstalk of Arf and Rab GTPases en route to cilia. *Small GTPases* **4**, 70-77 (2013).
57. Liu, Q. *et al.* The proteome of the mouse photoreceptor sensory cilium complex. *Mol Cell Proteomics* **6**, 1299-1317 (2007).
58. Hori, Y., Kobayashi, T., Kikko, Y., Kontani, K. & Katada, T. Domain architecture of the atypical Arf-family GTPase Arl13b involved in cilia formation. *Biochem Biophys Res Commun* **373**, 119-124 (2008).
59. Franco, M., Chardin, P., Chabre, M. & Paris, S. Myristoylation of ADP-ribosylation factor 1 facilitates nucleotide exchange at physiological Mg2+ levels. *J Biol Chem* **270**, 1337-1341 (1995).
60. Franco, M. *et al.* ARNO3, a Sec7-domain guanine nucleotide exchange factor for ADP ribosylation factor 1, is involved in the control of Golgi structure and function. *Proc Natl Acad Sci U S A* **95**, 9926-9931. (1998).
61. Turchinovich, A., Zoidl, G. & Dermietzel, R. Non-viral siRNA delivery into the mouse retina in vivo. *BMC Ophthalmol* **10**, 25 (2010).
62. Ettaiche, M., Fillacier, K., Widmann, C., Heurteaux, C. & Lazdunski, M. Riluzole improves functional recovery after ischemia in the rat retina. *Invest Ophthalmol Vis Sci* **40**, 729-736 (1999).

Acknowledgements

We thank Drs P. Chavrier, C. Koerner, J. Mazella, G. Montagnac, and A. Wittinghofer for the generous gifts of various reagents. We kindly thank Drs P. Chavrier, E. Macia, T.Coppola and S. Martin for critical reading of the manuscript. We thank Dr. Hiroyuki Sakagami (Kitasato University, Japan) for the EFA6A and EFA6D specific anti-serum, This work is supported by the Centre National de la Recherche Scientifique, the Association pour la Recherche contre le Cancer and the Agence Nationale pour la Recherche through the Investissement pour le Futur Labex Signalife Program ref ANR-11Labx-0028-01.

Author contributions

M.P.; C.L.B.; R.G.; M.E.; F.L. and M.F. designed research. M.P.; C.L.B.; R.G.; M.E.; R.F.; E.S.; S.P.; S.L-G.; C.R.; F.L. and M.F. performed experiments. M.P.; C.L.B.; R.G.; M.E.; R.F.; F.B.; S.L-G.; A.B.; F.L. and M.F. analyzed data. R.G.; M.E; A.B.; F.L. and M.F. wrote the paper

Figure legends.

Figure 1. Localization of EFA6A and morphological changes resulting from its depletion in retina. (**A**) Immunolabeling of wild-type retinas with an anti-EFA6A Ab (anti-EFA6A) or an anti-EFA6A Ab after incubation with purified EFA6A protein (control) revealed the specific presence of EFA6A in the retinal pigment epithelium, in photoreceptors (outer and inner segments), in some cells in the inner nuclear and plexiform layer and in the ganglion cell layer. (**B**) Morphology of siRNA control or siEFA6A-injected retinas. Semi-thin retinal sections (1 μm) counterstained with methylene blue-azur II of siRNA control (**a**) and siEFA6A (**b**) treated retinas. Scale bar = 20 μm. (**C)** Electron micrographs of photoreceptor Outer Segments (OS) of siControl (**a**) or siEFA6A (**b**) treated retinas illustrating lack of well-organized OS accompanied with degeneration in siEFA6A retina. (**D**) Mislocalisation of acetylated tubulin in EFA6A depleted retinas. Immunohistochemical analysis of cryosections of siControl (**a**) or siEFA6A (**b**) treated retina using acetylated tubulin antibodies (green). DAPI was used to stain the nuclei (blue). Scale bars: 20 μm. RPE, retinal pigment epithelium; OS, outer segment; CC, connecting cilium; IS, inner segment, ONL, outer nuclear layer; OPL, outer plexiform layer; INL, inner nuclear layer IPL, inner plexiform layer; GCL, ganglion cell layer. (**E, F**) EFA6A depletion on scotopic (E) or photopic (F) luminance-response function: Intensity response curve of the dark adapted (E) or of the light-adapted (F) ERG a-waves in retina of 3-month-old control mice (black square) or subjected to intravitreal injection of siRNA control (gray inverted triangle), siEFA6A#a (black circle) and si-EFA6A#b (gray triangle) respectively. Mean amplitude + SD are plotted; n=3 and ***p <0.001).

Figure 2. EFA6A controls ciliogenesis in RPE-1 cells. (**A**) Localization of GFP-EFA6A transiently expressed in RPE-1 cells for 48 hours, starved for 24 hours and stained with anti-Arl13b. (**B**) EFA6A depletion inhibits ciliogenesis without affecting PCM1 localization. Acetylated Tubulin (Ac.T), and PCM1 were detected in control or EFA6A siRNA treated RPE-1 serum starved for 24 h. (**C**) Ciliation quantification in 48 h siRNA-treated cells (control, EFA6A si-pool, si#2 and si#4) with 24 h serum starvation, followed by staining with acetylated α-tubulin and γ tubulin antibodies. (Means +/- SD from n= 3 to 5 independent experiments are shown, with >200 cells per treatment. For si-pool n=5 and *p*=3.2E-5; for si#2 and si#4 n=3 and *p*=6.3E-3, and *p*=6.5E-3 respectively. (**D**) Analysis of the effect of the EFA6 isoform specificity on ciliogenesis. RPE-1 cells were transfected with siRNA control or siRNA pool against EFA6A or EFA6B or EFA6D for 48 h, with 24 h serum starvation, followed by staining with Arl13b antibodies. (**D**) Quantification of ciliation is shown. Means +/- SD from 3 to 5 independent experiments, t-test *p*=1.3E-4 for siEFA6A; *p*=8.2E-2 for siEFA6B, and *p*=3.6E-2 for siEFA6D.

Figure 3. EFA6A overexpression increases cilium length in 2D and 3D culture systems. (A) MDCK cells overexpressing (-dox) or not (+dox) vsv-g-EFA6A were grown on polycarbonate filters for 10 days then fixed and processed for immuno-fluorescence. (**B**) Quantification of the effect of EFA6A overexpression on the number of cilia/cell and the cilium length observed in (**A**). Mean ± SD, n=4 for Dox and n=5 for no Dox, *p*=0.4 (NS) for nucleus number, *p*=6.7E-05 (****) for cil/nucl % and *p*=0.0004 (***) for average cilium length (μm). (**C**) Ciliogenesis rescued with human vsv-g EFA6A in MDCK treated with siRNA anti-canine EFA6A. MDCK cells were transfected with a control siRNA or a canine EFA6A specific siRNA and grown on polycarboante filters. After 10 days, the fully polarized cells were processed for immunofluorescence and the primary cilia stained with an anti-Arl13b antibody. The experiment was performed three times and data from all three experiments were combined. An average of 4000 cells per sample was analyzed for the presence or absence of a cilium. Values are mean ± SD, n=3, t-test *p*=0.001 for siEFA6A +DOX; *p*=0.04 for siEFA6A -DOX. (**D**) EFA6A overexpression increases cilium size in 3D culture system. MDCK cells overexpressing (-dox) or not (+dox) vsv-g-EFA6A were grown in matrigel for 7 days then fixed and processed for immuno-fluorescence using antibodies anti vsv-g and anti-acetylated α-tubulin antibodies.

Figure 4. Knockdown of EFA6A inhibits the maturation of the basal body (**A**) and the assembly of the ciliary vesicle (**B**). (**A**) EFA6A depletion prevents CP110 release from the mother centrioles (a) but does not impair the recruitment of CEP164 (**b**) or TTBK2 (**c**).). γ tubulin (γ-Tub), CP110, CEP164 and TTBK2 were detected in control or EFA6A siRNA treated RPE-1 cells with 24 h serum starvation. Error bars represent SD (n =3 to 5 independent experiments), *p*=4.9E-5 for CP110, *p*=0.8 and 0.6 for CEP164 and TTBK2 respectively. (**B**) EFA6A depletion does not prevent the accumulation of Arl13b

positive structures at the centriole (a). γ tubulin (γ-Tub) and Arl13b were detected in control or EFA6A siRNA treated RPE-1 cells after 24 h serum starvation. Error bars represent SD (n=3 to 5 independent experiments), *p*=0.3. Representative electron micrographs of RPE-1 cells treated with siRNA control or EFA6A pool for 48 h with serum starvation for the last 24 h (b). Distal appendage vesicles (DAV) are highlighted.

Figure 5. EFA6A interacts with Arl13b and Sec10 a subunit of the exocyst complex. (**A**) GST pull-down of Arl13b-GFP expressed in BHK cells by EFA6A fused to GST. (**B**) GST pull-down of purified His-EFA6A by Arl13b or Sec10 fused to GST. (**C**) GST pull-down of Sec10-mCherry expressed in BHK cells by EFA6A fused to GST. **(D)** Overexpression of Arl13b-GFP partially rescued the inhibition of ciliogenesis induced by EFA6A depletion. RPE-1 cells were transfected or not with pEGFP-Arl13b for 24 h and then transfected with siEFA6A for 48 h, with 24 h serum starvation, followed by staining with acetylated tubulin or Arl13b antibodies. (**D**) Quantification of ciliation is shown. Error bars represent SD, n =3 *p*=1.9E-3 for siEFA6A pool treated sample and p=2.2E-2 for the siEFA6A pool-treated and Arl13b-GFP-expressing sample. (**F**) Representative electron micrographs of RPE-1 cells treated with siRNA control or Arl13b pool for 48 h with serum starvation for the last 24 h. (**G**) Quantification of electron microscopy experiments. Only m-centrioles without elongated cilia are quantified (i.e. about 30% of control cells and 90% of the siEFA6A and siARl13b cells as determined by immunofluorescence experiments). (**H**) Model for the role of EFA6A during intracellular ciliogenesis (modified from [12])

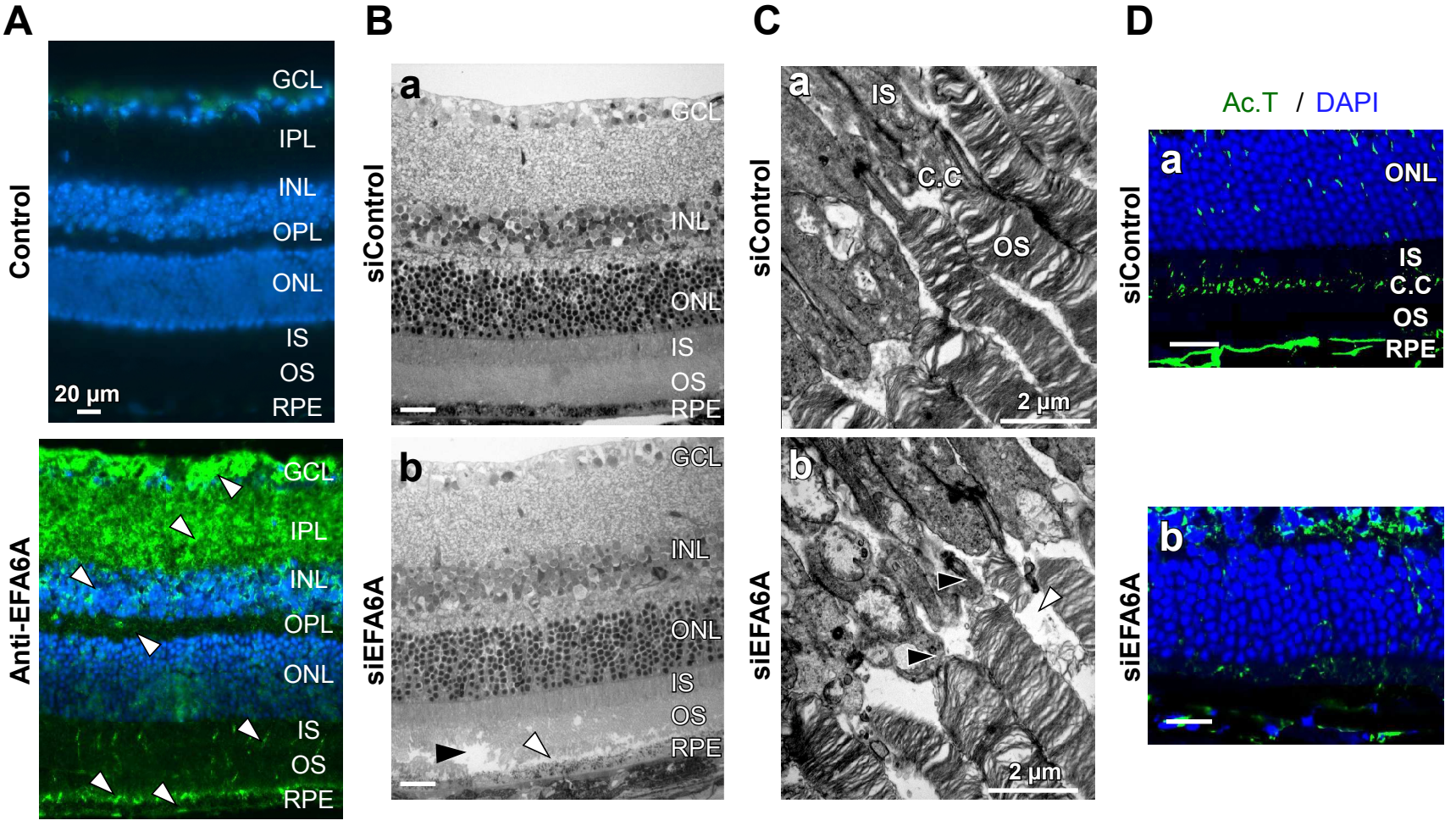
A
Control
GCL
IPL
INL
OPL
ONL
IS
OS
RPE
20 μm
Anti-EFA6A
B
siControl
a
siEFA6A
b
C
siControl
IS
C.C
OS
2 μm
siEFA6A
D
Ac.T / DAPI
siControl
ONL
siEFA6A

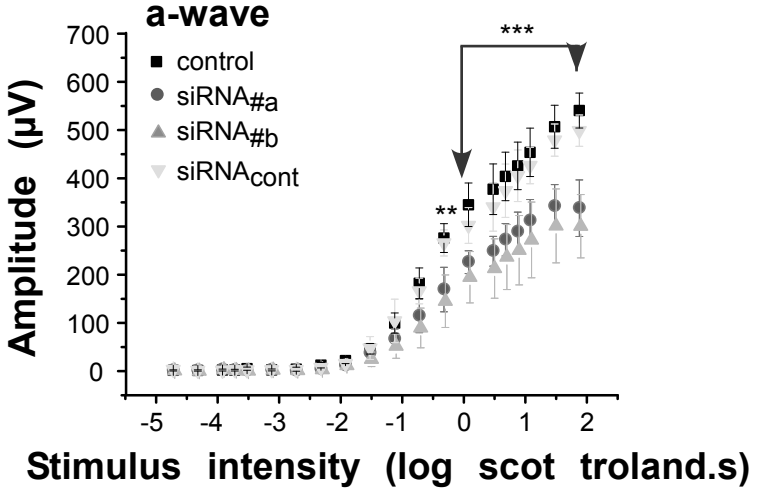
E
Scotopic conditions (Rods)
a-wave
control
siRNA#a
siRNA#b
siRNAcont
Amplitude (μV)
Stimulus intensity (log scot troland.s)

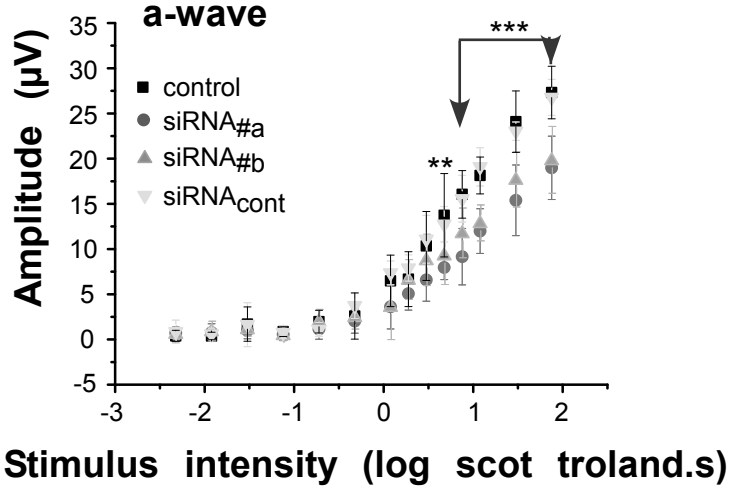
F
Photopic conditions (Cones)
a-wave
control
siRNA#a
siRNA#b
siRNAcont
Amplitude (μV)
Stimulus intensity (log scot troland.s)

Fig. 1

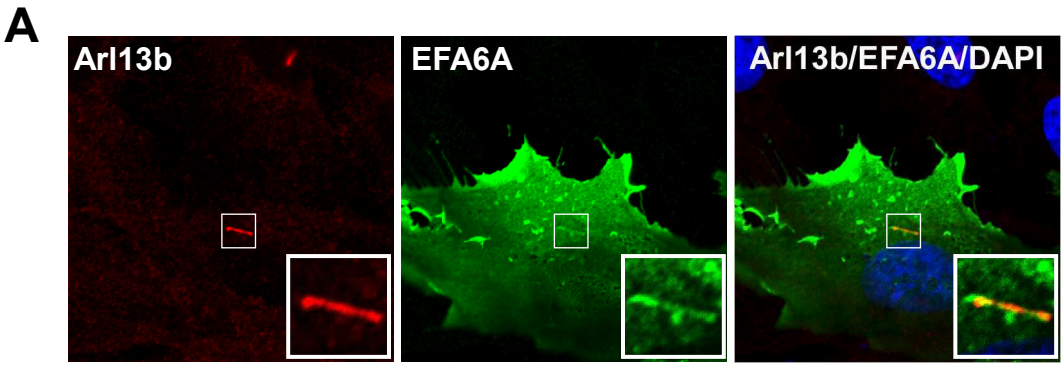
A
Arl13b
EFA6A
Arl13b/EFA6A/DAPI

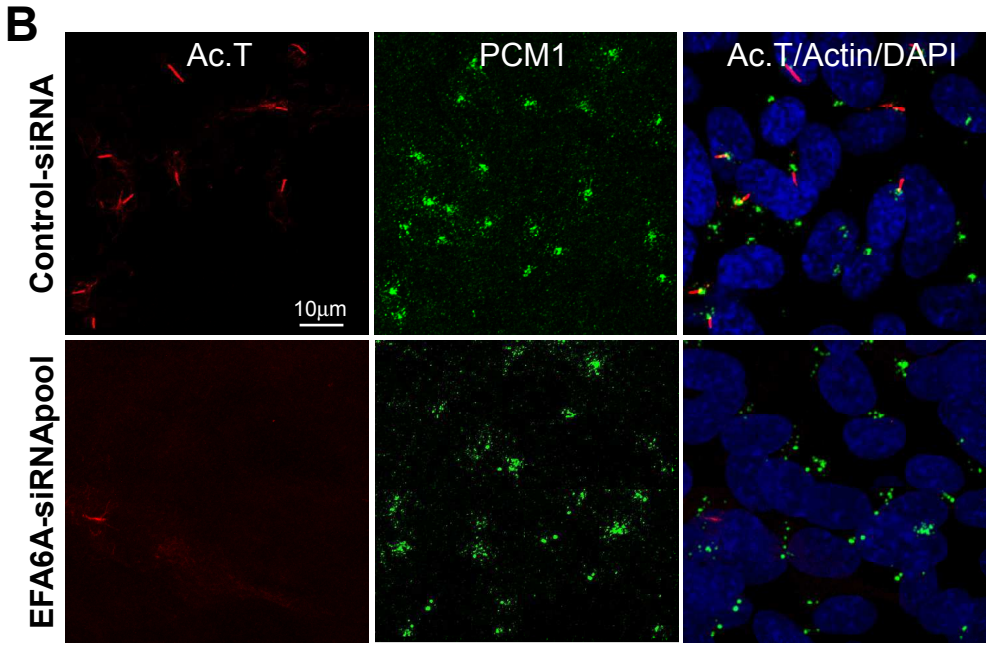
B
Control-siRNA
EFA6A-siRNApool
Ac.T
PCM1
Ac.T/Actin/DAPI
10μm

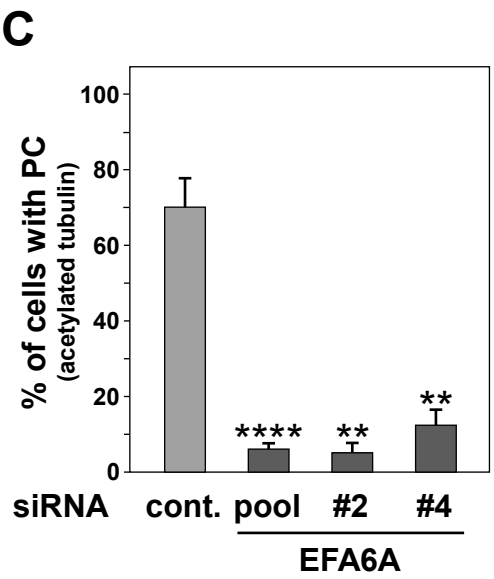
C
% of cells with PC
(acetylated tubulin)
100
80
60
40
20
0
****
**
**
siRNA
cont.
pool
#2
#4
EFA6A

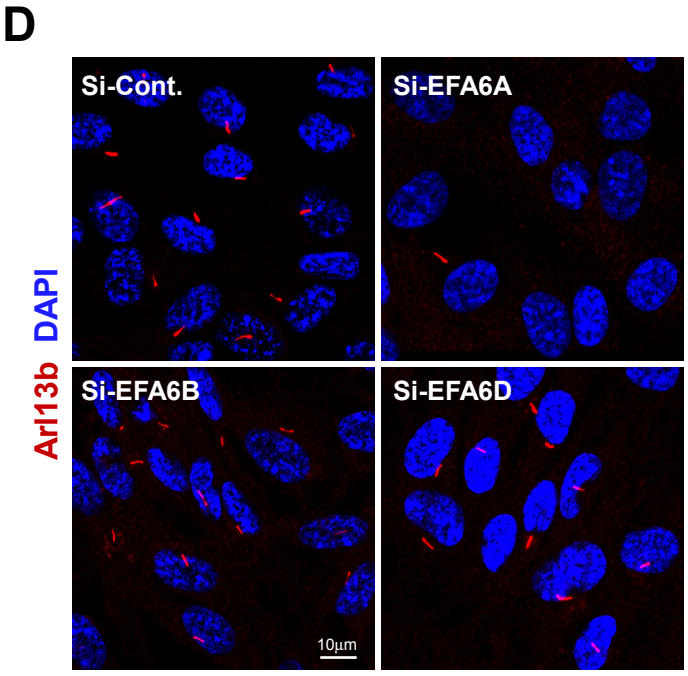
D
Arl13b DAPI
Si-Cont.
Si-EFA6A
Si-EFA6B
Si-EFA6D
10μm

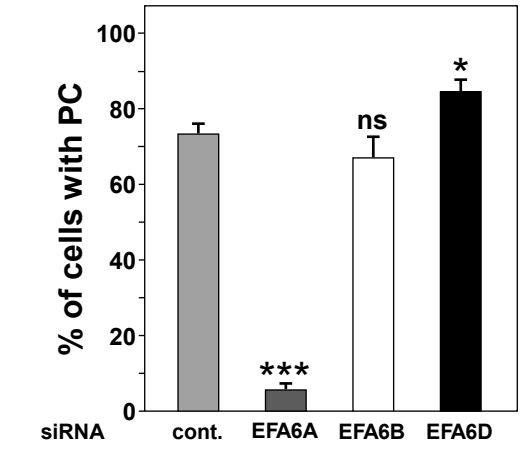
E
% of cells with PC
100
80
60
40
20
0
***
ns
*
siRNA
cont.
EFA6A
EFA6B
EFA6D

Fig.2

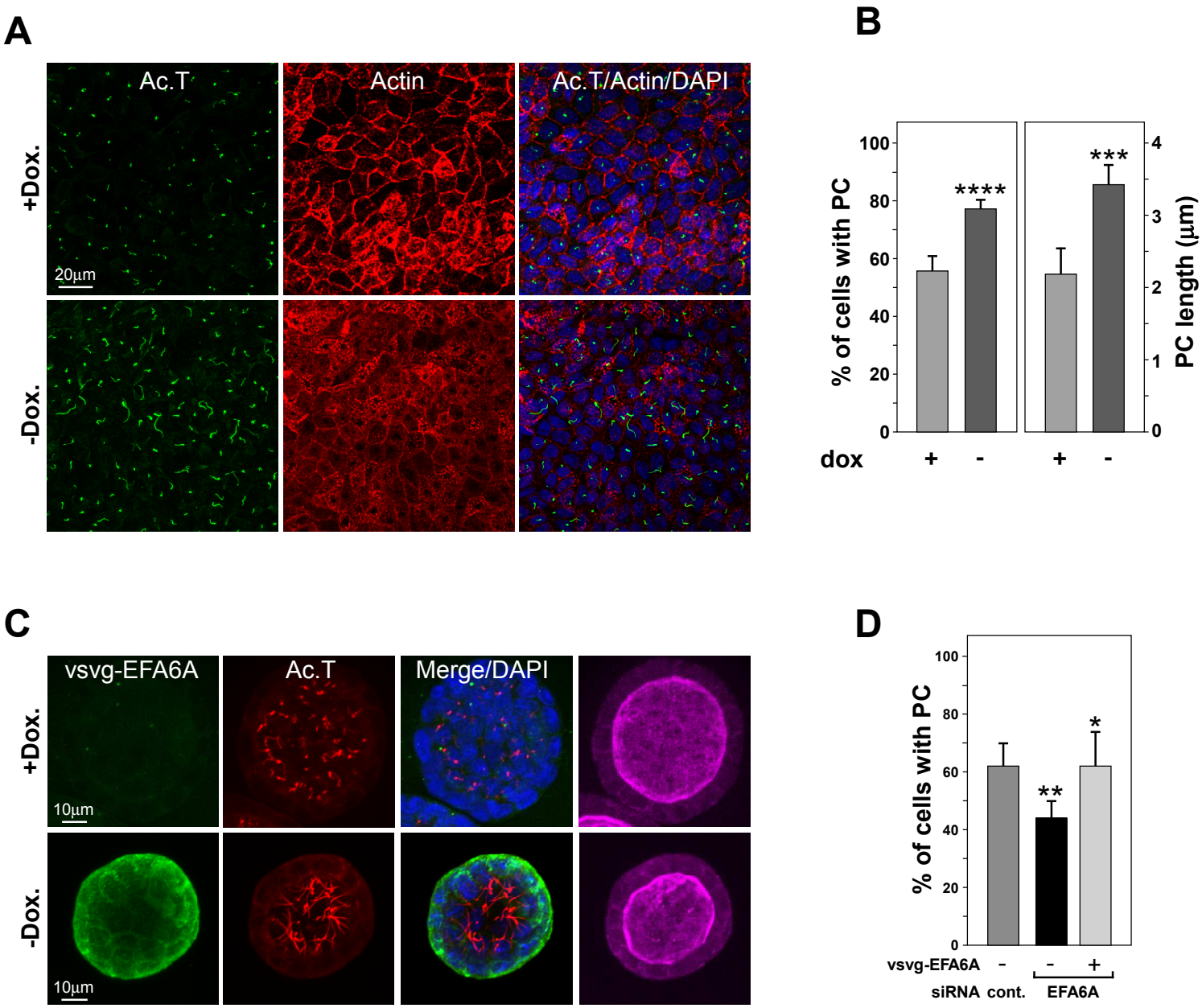
A
Ac.T
Actin
Ac.T/Actin/DAPI
+Dox.
-Dox.
20μm
B
% of cells with PC
PC length (μm)
****
***
dox
+
-
+
-
C
vsvg-EFA6A
Ac.T
Merge/DAPI
+Dox.
-Dox.
10μm
10μm
D
% of cells with PC
**
*
vsvg-EFA6A
-
-
+
siRNA cont.
EFA6A

Fig.3

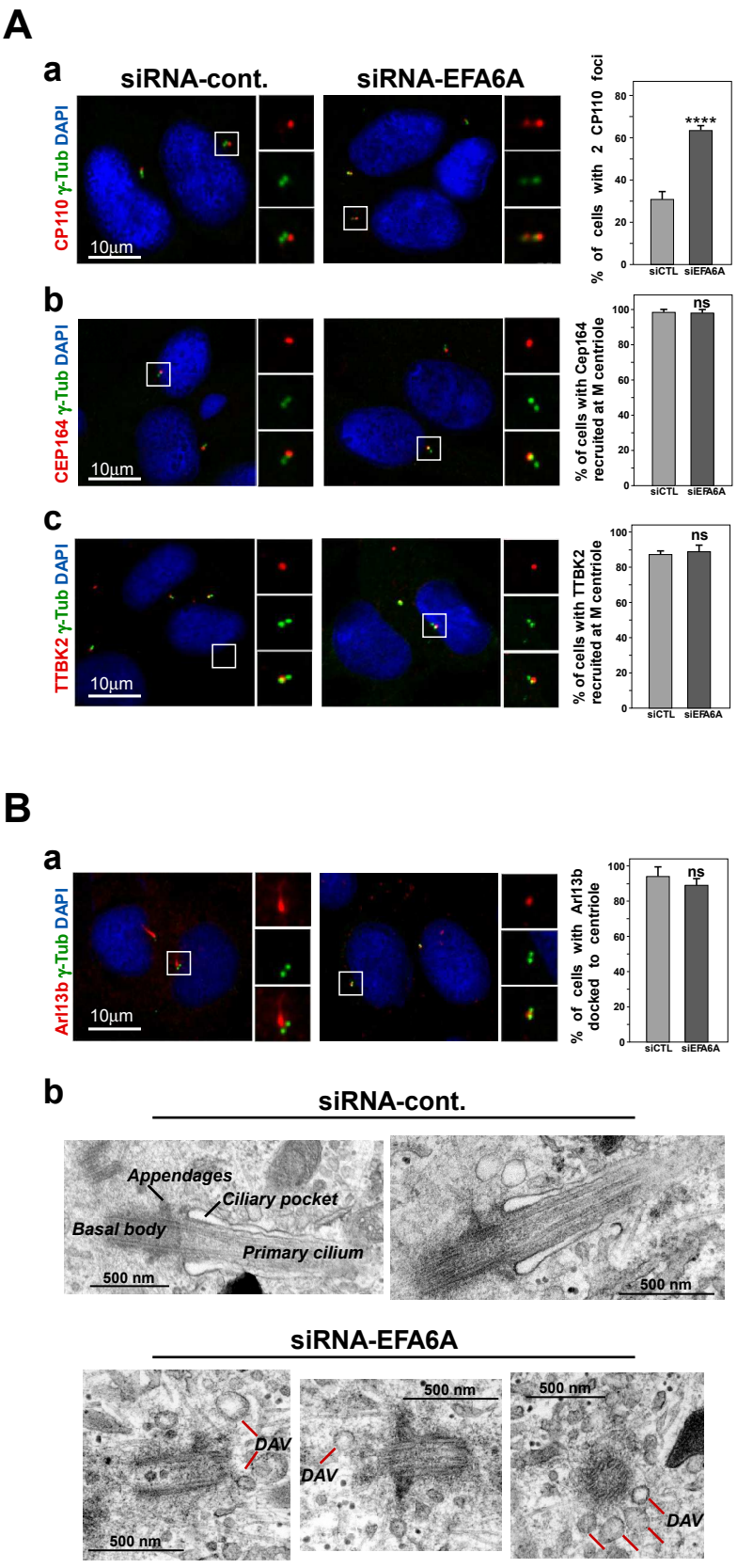
A
a
siRNA-cont.
siRNA-EFA6A
CP110 γ-Tub DAPI
10μm
% of cells with 2 CP110 foci
****
siCTL
siEFA6A
b
CEP164 γ-Tub DAPI
10μm
% of cells with Cep164 recruited at M centriole
ns
c
TTBK2 γ-Tub DAPI
10μm
% of cells with TTBK2 recruited at M centriole
ns
B
a
Arl13b γ-Tub DAPI
10μm
% of cells with Arl13b docked to centriole
ns
b
siRNA-cont.
Appendages
Ciliary pocket
Basal body
Primary cilium
500 nm
500 nm
siRNA-EFA6A
DAV
500 nm
500 nm
DAV
500 nm
DAV

Fig.4

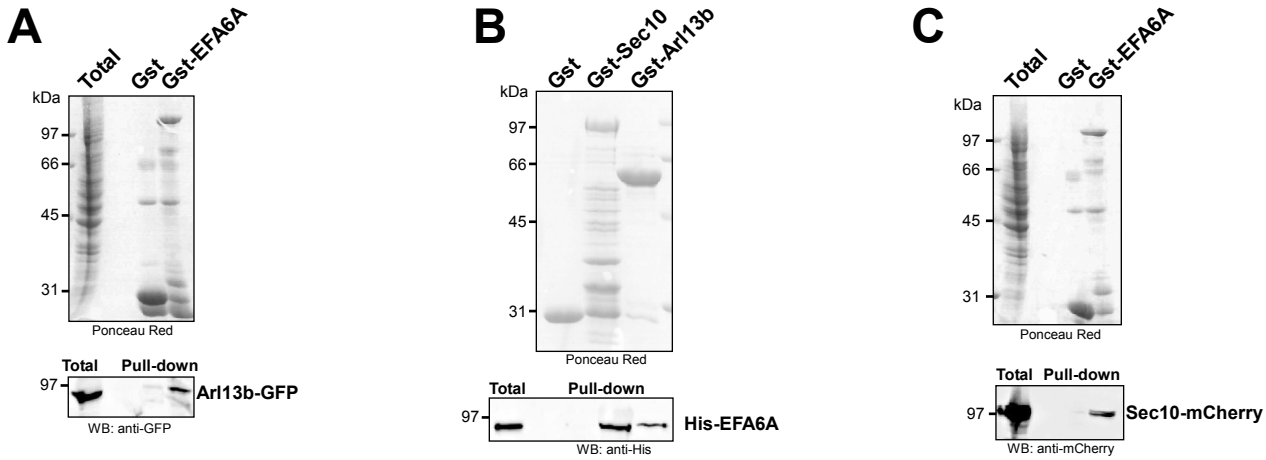

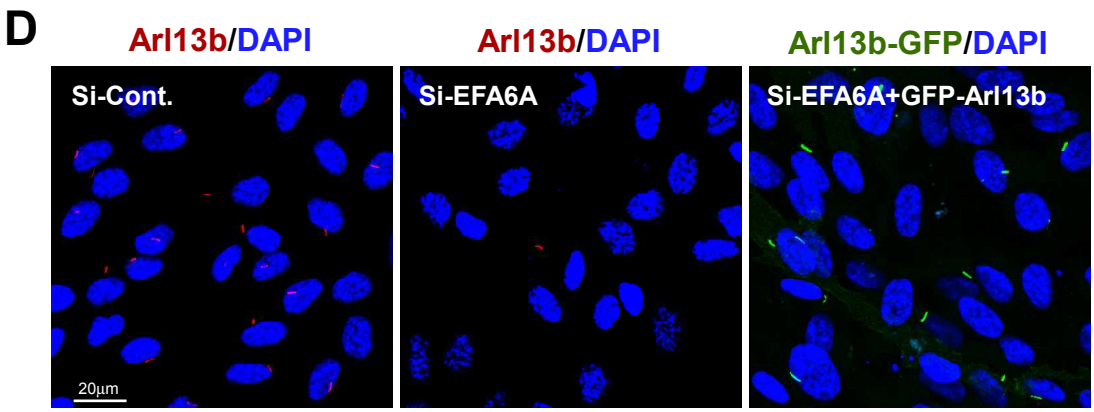

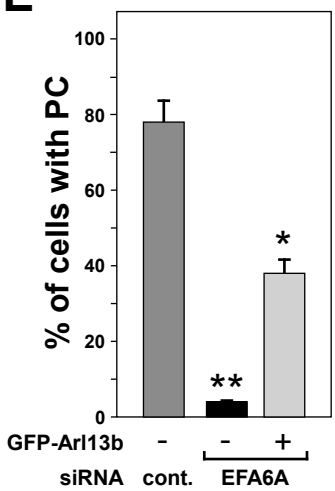

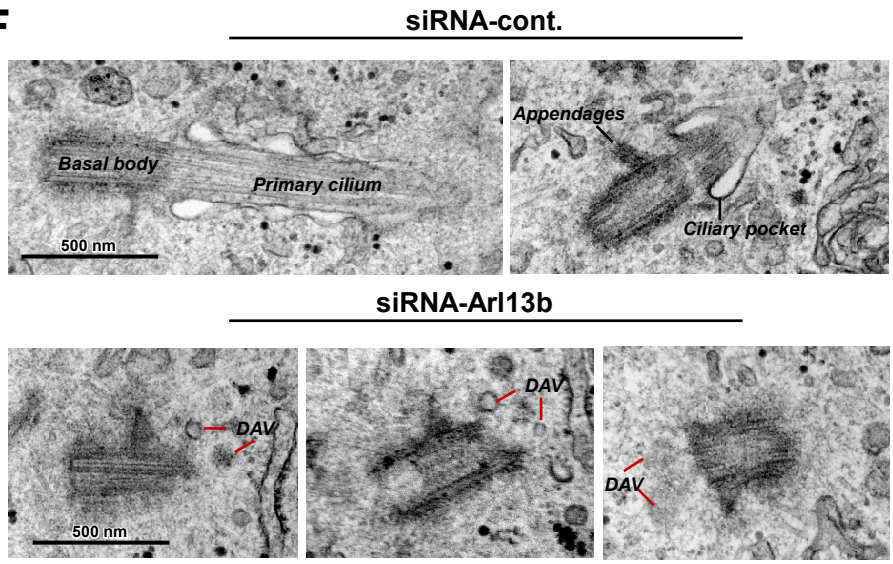

G

	DAV	No vesicle docked	CV	n
siControl	2 (14)	8 (58)	4 (28)	14 (100)
siEFA6A	31 (73)	7 (17)	4 (10)	42 (100)
siArl13b	23 (48)	13 (27)	12 (25)	48 (100)

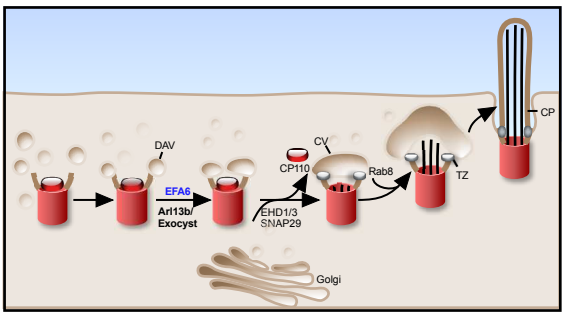

Fig.5

EFA6A plays a key role in retinal function by controlling ciliogenesis.

Partisani et al

Supplemental Information:

Figure S1. (**A)** Confocal immunofluorescence micrographs show, by colabeling with anti-rhodopsin (Rho, upper panels), that EFA6A is expressed in OS particularly in connecting cilium (red arrows), scale bar 25 µm. Colabeling with Peanut Agglutinin (middle panels) indicates that EFA6A is present in the IS and OS segments of cones (arrows). Scale bar, 50 µm. Finally, colabeling with anti-RPE65 (lower panels) shows the presence of EFA6A in the RPE (arrows). Scale bar, 25 µm. (**B**) *In situ* hybridization experiments on mouse retina using an EFA6A antisense or sense (as control) probe and diaminobenzidine detection. Antisense oligonucleotide probe revealed labeled cells in the ganglion cell layer, in the inner and outer nuclear layers and in the retinal pigment epithelium. (**C,D**) Control of EFA6A depletion in mouse retina after 7 days siRNA treatment (by intra-vitreal injection of siRNA) by Western blotting (**C**) or RT-PCR (**D**). (**E**) Electron micrographs of RPE cells (**a,b**), and of outer nuclear layer (**c,d**) of si-RNA control (**a,c**) or siRNA-EFA6A (**b,d**) treated retinas illustrating lack of well-organized OS at the RPE/OS interface and the presence of some degenerative cell bodies of rod (*) and cone photoreceptors (**) in siRNA-EFA6A retina. (**F**) Mislocalisation of rhodopsin in EFA6A depleted retinas. Immunohistochemical analysis of cryosections of si-control (**a**) or si-EFA6A (**b**) treated retina using rhodopsin (green) antibodies and Peanut Agglutunin (red). DAPI was used to stain the nuclei (blue). RPE, retinal pigment epithelium; OS, outer segment; IS, inner segment, ONL, outer nuclear layer; CC, connecting cilium. Scale bars: 20 µm. (**G**) Diagram summarizing the morphological alterations observed in siEFA6A-treated retinas.

Figure S2. (**A,B,C**) Effect of EFA6A depletion on scotopic luminance-response function: (**A**) ERG profiles obtained at flash intensities ranging from -4.72 to 1.87 log scot td/s in control, siRNA control, si-EFA6A#a and si-EFA6A#b groups respectively at day 7 post-injection. Each trace is the average of at least nine mice. (**B**) Intensity response curve of the dark adapted b-waves in retina of 3-month-old control mice (black square) or subjected to intravitreal injection of siRNA control (gray inverted triangle), siEFA6A#a (black circle) and si-EFA6A#b (gray triangle) respectively. Mean amplitude + SD are plotted. **(C**) The dark-adapted b/a-wave ratio obtained at flash intensities ranging from - 1.12 to 1.87 log scot td/s in retinas of control mice (black square) and in mice submitted to intravitreal injection of siRNA control (red inverted triangle) and si-EFA6A#a (red circle) and si-EFA6A#b (blue triangle) respectively at 7-days post-injection. Mean amplitude ± SD are plotted, n=3 and pvalues <0.001). (**D,E,F**) Effect of EFA6A depletion on light-adapted retinas. ERG waveform extracted at 2.2 Hz. (**D**) photopic ERG traces elicited at flash intensities ranging from - 2.32 to 1.87 log scot td/s in retinas of 3-month-old control mice or submitted to intravitreal injection of siRNA control, si-EFA6A#a and si-EFA6A#b groups respectively at day 7 post-injection. Each photopic ERG trace represents the average of at least nine mice. (**E)** intensity-response curve of the light-adapted ERG b-waves in retina of control (black square), siRNA control (gray inverted triangle), si-EFA6A#a (dark circle) and siEFA6A#b (gray triangle). Mean amplitudes ± SD are plotted, n=3 and pvalues <0.001). (**F**) The light adapted b/a-wave ratio obtained at day 7 post-injection and at flash intensities ranging from 0.47 to 1.87 log scot td/s in retinas of control mice (black square) and in mice subjected to intravitreal injection of siRNA control (red inverted triangle) and si-EFA6A#a (red circle) and si-EFA6A#2 (blue triangle) respectively at 7 day post-injection. Mean amplitude ± SD are plotted.

Figure S3. (**A, B**) Western blotting (**A**) or Q-PCR (**B**) analyses to control the efficiency of siRNA-mediated depletion of EFA6A, EFA6B and EFA6D in RPE-1 cells after 48h siRNA treatment. (**C**) EFA6A depletion inhibits ciliogenesis without affecting Golgi apparatus morphology. P23 (Golgi) and Arl13b (cilium) were detected in siRNA control or EFA6A siRNA pool treated RPE-1 cells for 48h with 24h serum starvation. (**D**) Western blot analysis of vsv-g-EFA6A overexpression in MDCK cells. (E) Q-PCR analysis of the effect of the siRNA anti-canine EFA6A in MDCK cells.

Figure S4. EFA6A interacts with Arl13b. (**A)** GST pull-down of Arl13b-GFP expressed in BHK cells with different constructs of EFA6A fused to GST. (**B**) GST pull-down of purified His-EFA6A by Arl13b fused to GST and bound to GDP or GTPγS. (**C**) Kinetics of [^{35}S]GTPγS binding to purified Arf6-His or GST-Arl13b in the presence or the absence of EFA6A. (**D**) Western blotting to control the efficiency of siRNA-mediated depletion of Arl13b in RPE-1 cells. (**E**) Overexpressed GFP-EFA6A did not rescue the si-Arl13b mediated inhibition of ciliogenesis in serum-starved RPE-1 cells. (**F,G**) GST pull-down of mCherry tagged Exo84 (E) or Exo70 (F) expressed in BHK cells with different constructs of EFA6A fused to GST. (**H**) GST-EFA6A but not GST-Arl13b pull-downed endogenous Sec10 from BHK cell lysate.

A

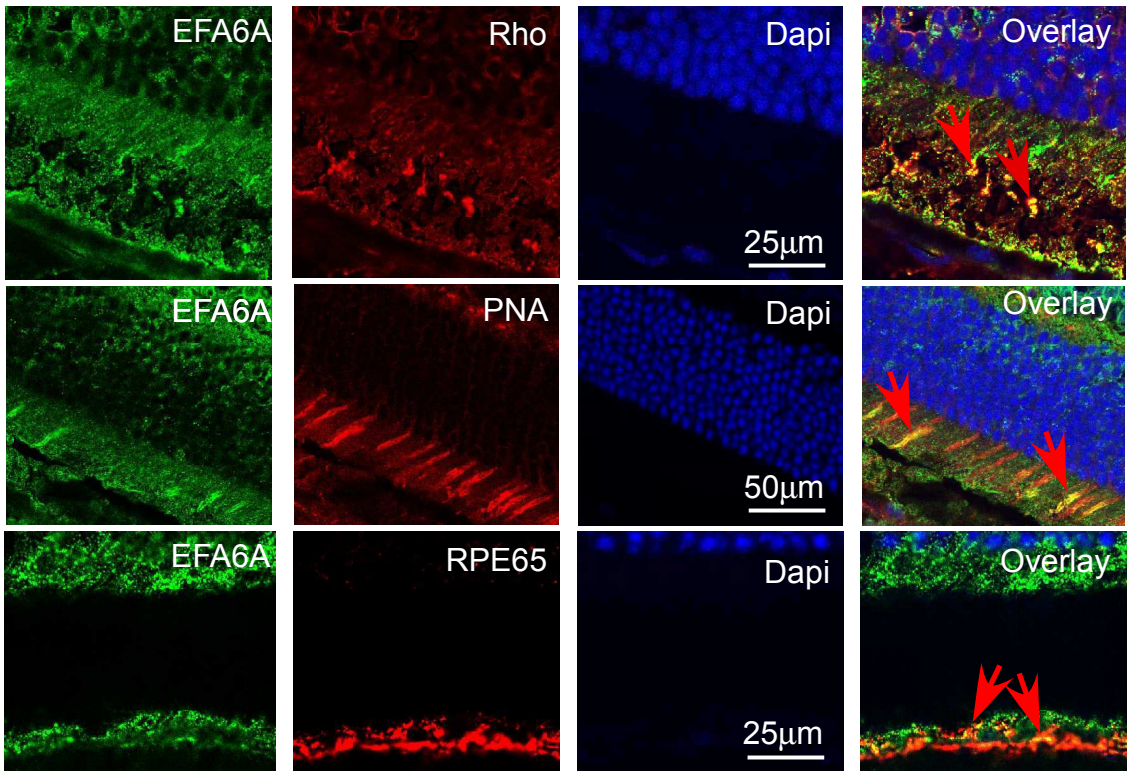

B

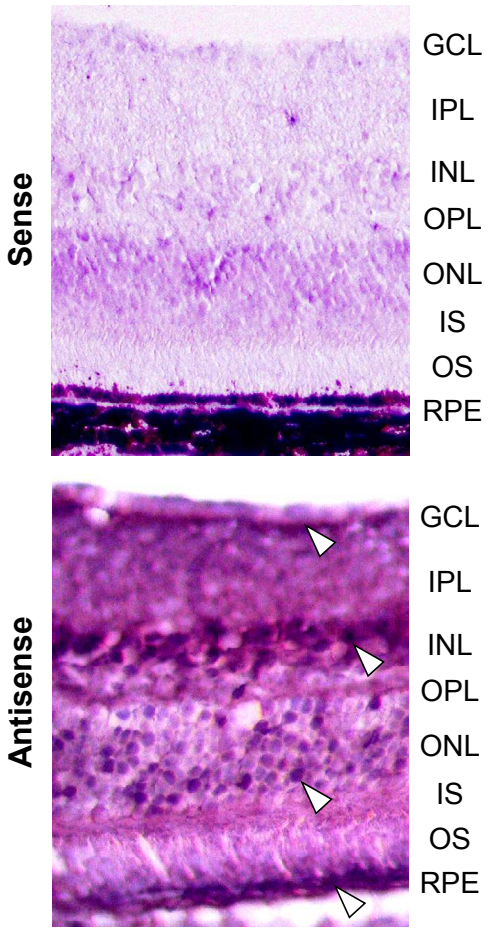

C

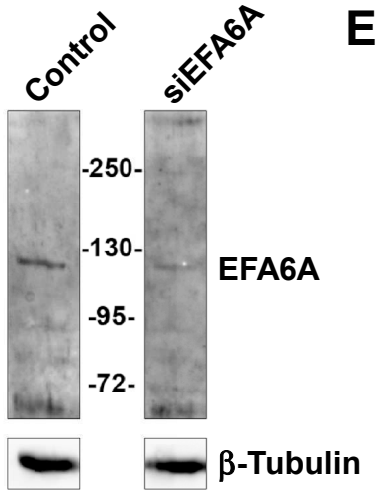

D

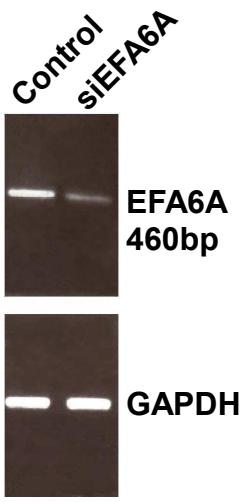

E

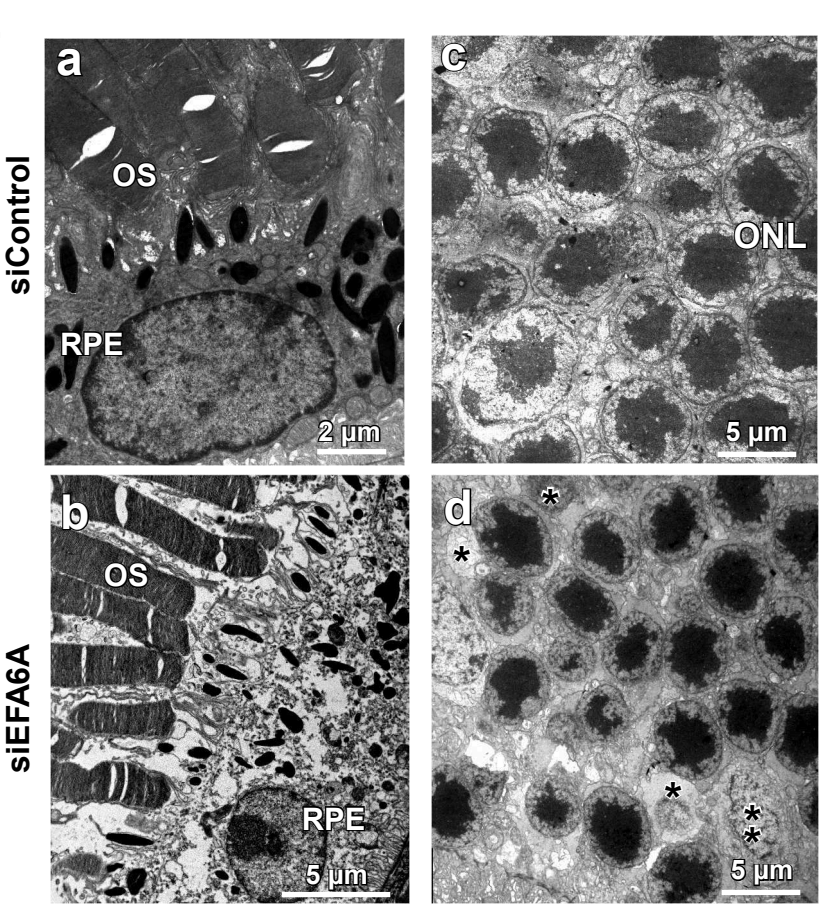

F

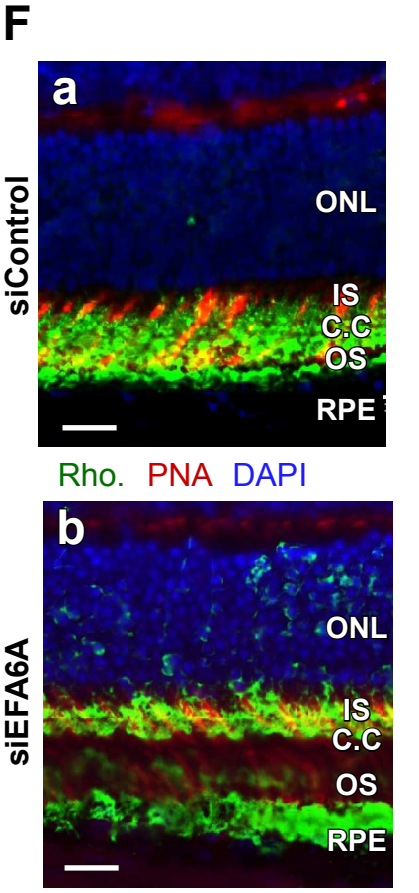

G

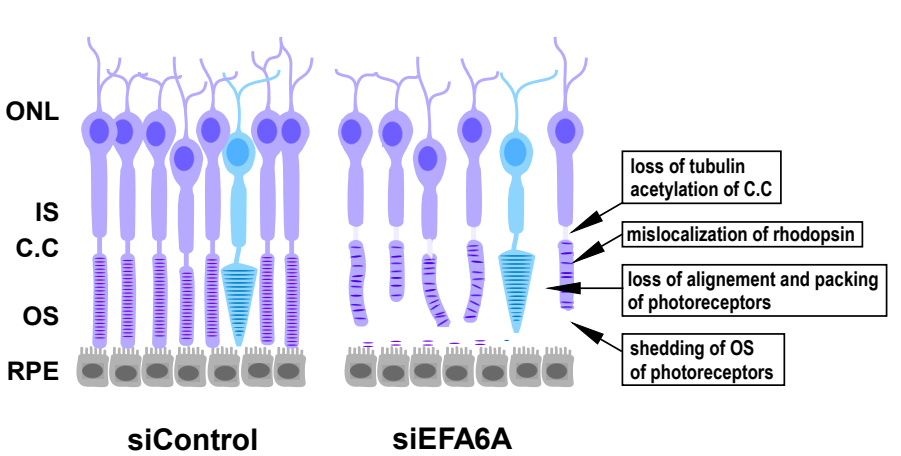

Supp. Fig.1

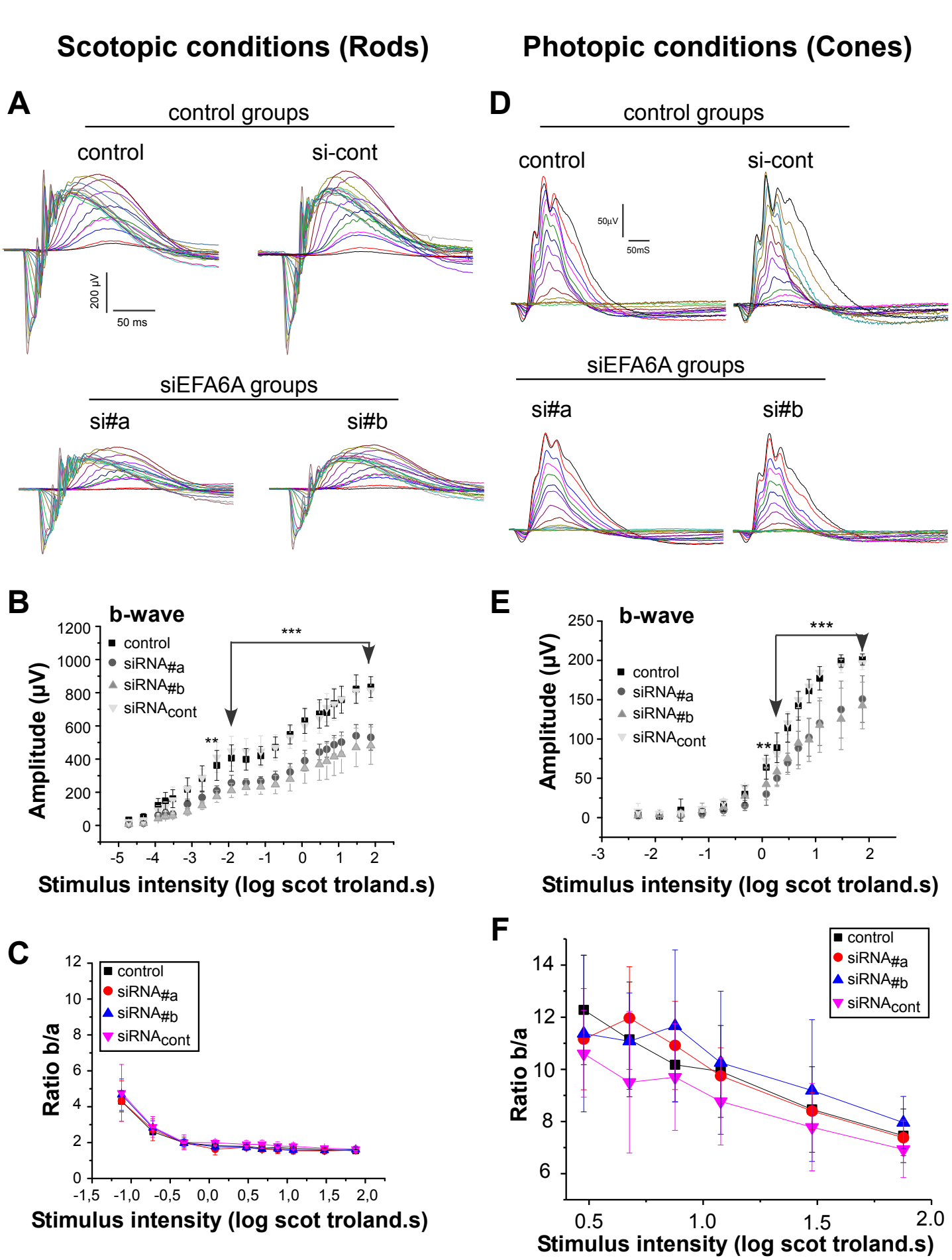
Scotopic conditions (Rods)
Photopic conditions (Cones)
A
control groups
control
si-cont
200 µV
50 ms
siEFA6A groups
si#a
si#b
D
control groups
control
si-cont
50µV
50mS
siEFA6A groups
si#a
si#b
B
b-wave
control
siRNA#a
siRNA#b
siRNAcont
Amplitude (µV)
Stimulus intensity (log scot troland.s)
E
b-wave
control
siRNA#a
siRNA#b
siRNAcont
Amplitude (µV)
Stimulus intensity (log scot troland.s)
C
control
siRNA#a
siRNA#b
siRNAcont
Ratio b/a
Stimulus intensity (log scot troland.s)
F
control
siRNA#a
siRNA#b
siRNAcont
Ratio b/a
Stimulus intensity (log scot troland.s)

Supp. Fig.2

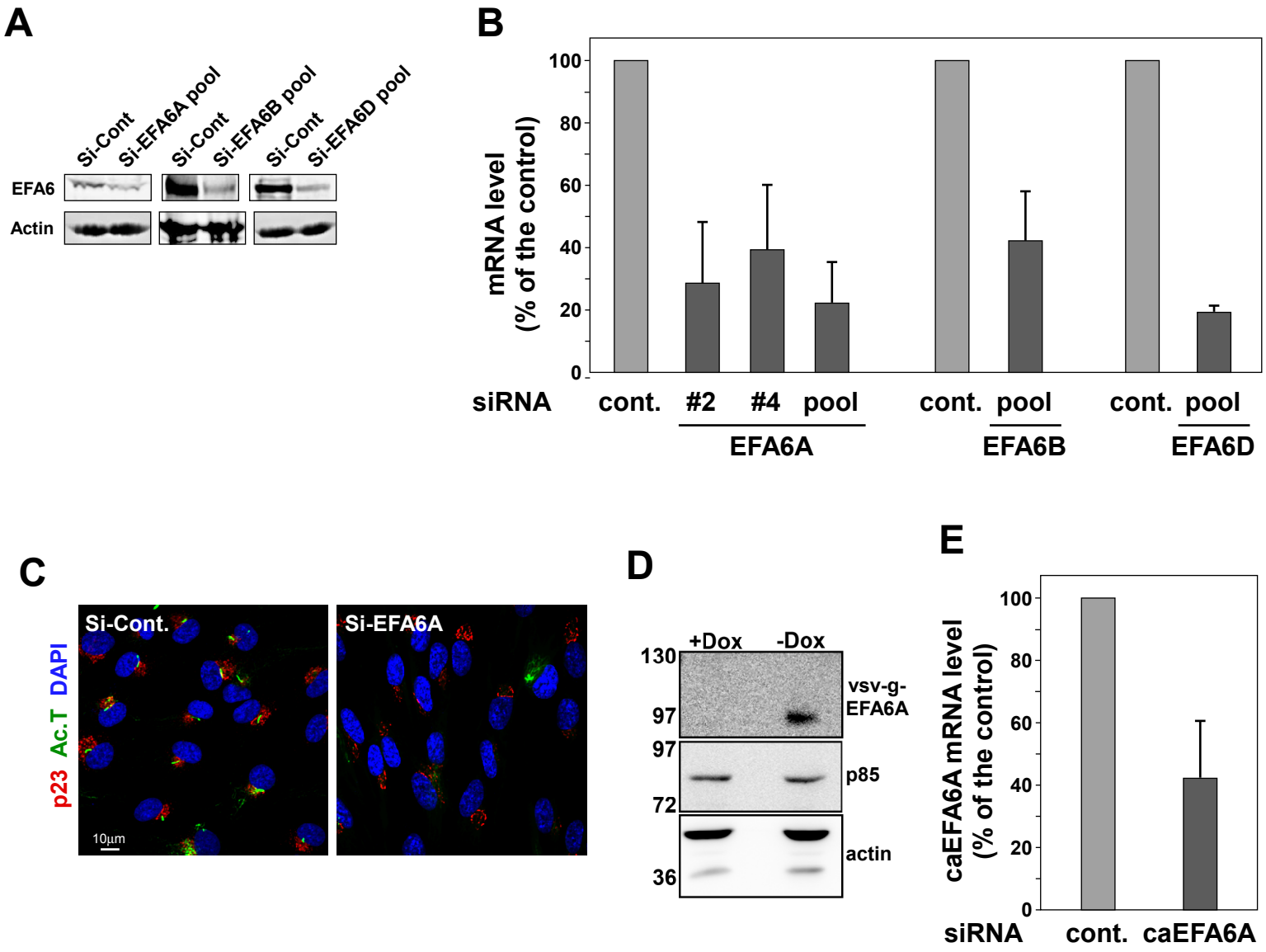
A
Si-Cont
Si-EFA6A pool
Si-Cont
Si-EFA6B pool
Si-Cont
Si-EFA6D pool
EFA6
Actin
B
mRNA level
(% of the control)
100
80
60
40
20
0
siRNA
cont.
#2
#4
pool
cont.
pool
cont.
pool
EFA6A
EFA6B
EFA6D
C
Si-Cont.
Si-EFA6A
p23 Ac.T DAPI
10μm
D
+Dox
-Dox
130
97
97
72
36
vsv-g-
EFA6A
p85
actin
E
caEFA6A mRNA level
(% of the control)
100
80
60
40
20
0
siRNA
cont.
caEFA6A

Supp. Fig.3

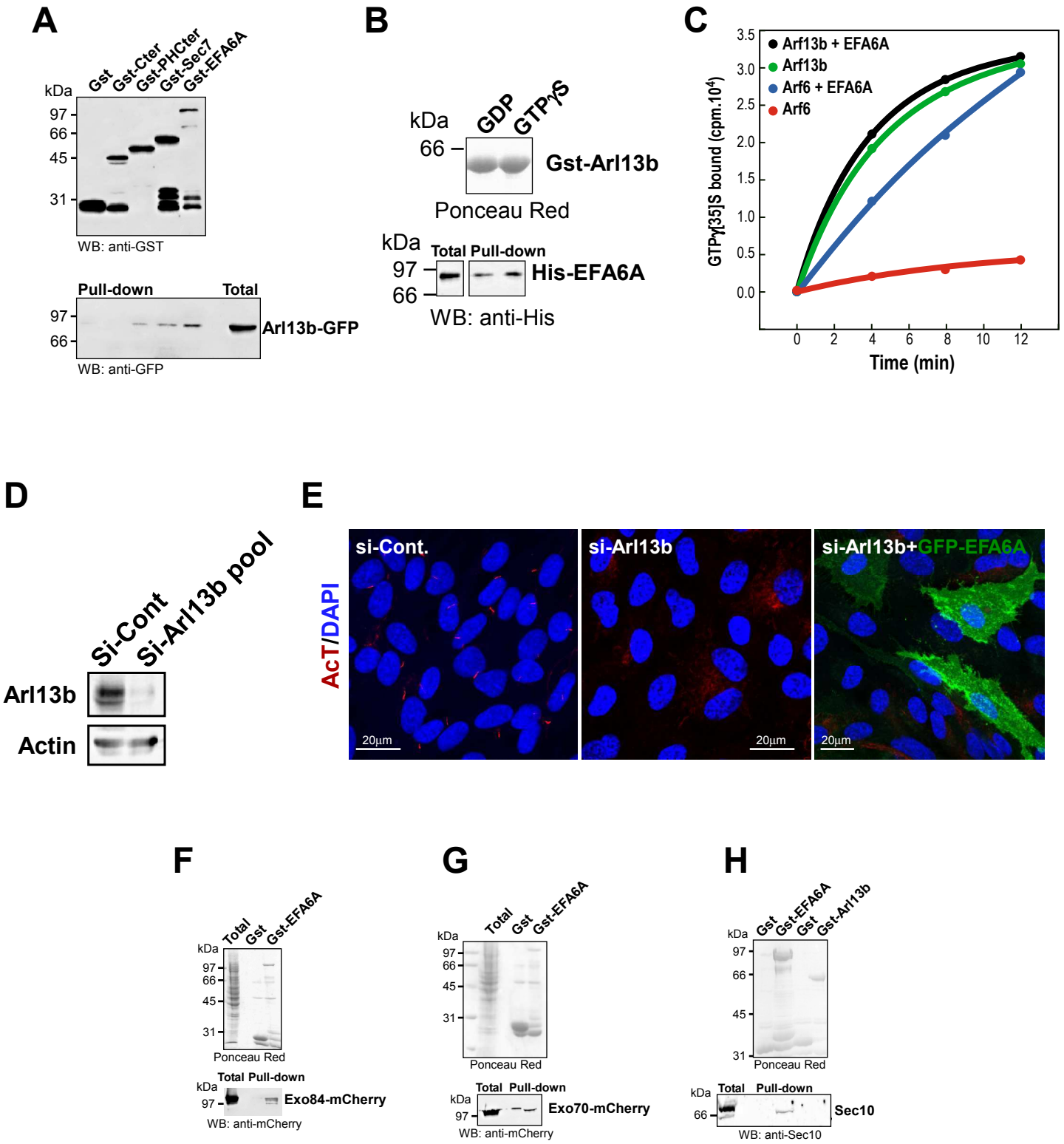
A
Gst
Gst-Cter
Gst-PHCter
Gst-Sec7
Gst-EFA6A
kDa
97
66
45
31
WB: anti-GST
Pull-down
Total
97
66
Arl13b-GFP
WB: anti-GFP
B
kDa
GDP
GTPγS
66
Gst-Arl13b
Ponceau Red
kDa
Total Pull-down
97
66
His-EFA6A
WB: anti-His
C
Arf13b + EFA6A
Arf13b
Arf6 + EFA6A
Arf6
GTPγ[35]S bound (cpm.10⁴)
3.5
3.0
2.5
2.0
1.5
1.0
0.5
0.0
0
2
4
6
8
10
12
Time (min)
D
Si-Cont
Si-Arl13b pool
Arl13b
Actin
E
AcT/DAPI
si-Cont.
si-Arl13b
si-Arl13b+GFP-EFA6A
20µm
20µm
20µm
F
Total
Gst
Gst-EFA6A
kDa
97
66
45
31
Ponceau Red
Total Pull-down
kDa
97
Exo84-mCherry
WB: anti-mCherry
G
Total
Gst
Gst-EFA6A
kDa
97
66
45
31
Ponceau Red
Total Pull-down
kDa
97
Exo70-mCherry
WB: anti-mCherry
H
Gst
Gst-EFA6A
Gst
Gst-Arl13b
kDa
97
66
45
31
Ponceau Red
Total Pull-down
kDa
66
Sec10
WB: anti-Sec10

Supp. Fig.4

References

References

Aceto, N., Bardia, A., Miyamoto, D.T., Donaldson, M.C., Wittner, B.S., Spencer, J.A., Yu, M., Pely, A., Engstrom, A., Zhu, H., et al. (2014). Circulating Tumor Cell Clusters Are Oligoclonal Precursors of Breast Cancer Metastasis. Cell *158*, 1110–1122.

Adams, A.E. (1990). CDC42 and CDC43, two additional genes involved in budding and the establishment of cell polarity in the yeast Saccharomyces cerevisiae. J. Cell Biol. *111*, 131–142.

Adriance, M.C., Inman, J.L., Petersen, O.W., and Bissell, M.J. (2005). Myoepithelial cells: good fences make good neighbors. Breast Cancer Res. *7*, 190.

Ahmadzadeh, H., Webster, M.R., Behera, R., Jimenez Valencia, A.M., Wirtz, D., Weeraratna, A.T., and Shenoy, V.B. (2017). Modeling the two-way feedback between contractility and matrix realignment reveals a nonlinear mode of cancer cell invasion. Proc. Natl. Acad. Sci. U. S. A. *114*, E1617–E1626.

Aigner, K., Dampier, B., Descovich, L., Mikula, M., Sultan, A., Schreiber, M., Mikulits, W., Brabletz, T., Strand, D., Obrist, P., et al. (2007). The transcription factor ZEB1 (δEF1) promotes tumour cell dedifferentiation by repressing master regulators of epithelial polarity. Oncogene *26*, 6979–6988.

Akhtar, N., and Hotchin, N.A. (2001). RAC1 Regulates Adherens Junctions through Endocytosis of E-Cadherin. Mol. Biol. Cell *12*, 847–862.

Alcaraz, J., Xu, R., Mori, H., Nelson, C.M., Mroue, R., Spencer, V.A., Brownfield, D., Radisky, D.C., Bustamante, C., and Bissell, M.J. (2008). Laminin and biomimetic extracellular elasticity enhance functional differentiation in mammary epithelia. EMBO J. *27*, 2829–2838.

Alexander, N.R., Tran, N.L., Rekapally, H., Summers, C.E., Glackin, C., and Heimark, R.L. (2006). N-cadherin Gene Expression in Prostate Carcinoma Is Modulated by Integrin-Dependent Nuclear Translocation of Twist1. Cancer Res. *66*, 3365–3369.

Al-Hajj, M., Wicha, M.S., Benito-Hernandez, A., Morrison, S.J., and Clarke, M.F. (2003). Prospective identification of tumorigenic breast cancer cells. Proc. Natl. Acad. Sci. U. S. A. *100*, 3983–3988.

Anbazhagan, R., Osin, P.P., Bartkova, J., Nathan, B., Lane, E.B., and Gusterson, B.A. (1998). The development of epithelial phenotypes in the human fetal and infant breast. J. Pathol. *184*, 197–206.

Andarawewa, K.L., Boulay, A., Masson, R., Mathelin, C., Stoll, I., Tomasetto, C., Chenard, M.-P., Gintz, M., Bellocq, J.-P., and Rio, M.-C. Dual Stromelysin-3 Function during Natural Mouse Mammary Tumor Virus-ras Tumor Progression. 7.

Andre, F., and Delaloge, S. (2009). Neoadjuvant chemotherapy for breast cancers: Current recommendations and future directions. Eur. J. Cancer *45*, 368–370.

Andres, A.-C., and Ziemiecki, A. (2003). Eph and Ephrin Signaling in Mammary Gland Morphogenesis and Cancer. J. Mammary Gland Biol. Neoplasia *8*, 475–485.

Ansieau, S., Bastid, J., Doreau, A., Morel, A.-P., Bouchet, B.P., Thomas, C., Fauvet, F., Puisieux, I., Doglioni, C., Piccinin, S., et al. (2008). Induction of EMT by twist proteins as a collateral effect of tumor-promoting inactivation of premature senescence. Cancer Cell *14*, 79–89.

Antonny, B., Beraud-Dufour, S., Chardin, P., and Chabre, M. (1997). N-Terminal Hydrophobic Residues of the G-Protein ADP-Ribosylation Factor-1 Insert into Membrane Phospholipids upon GDP to GTP Exchange. Biochemistry *36*, 4675–4684.

Arias-Romero, L.E., and Chernoff, J. (2013). Targeting Cdc42 in cancer. Expert Opin. Ther. Targets *17*, 1263–1273.

Aumailley, M., Brucknertuderman, L., Carter, W., Deutzmann, R., Edgar, D., Ekblom, P., Engel, J., Engvall, E., Hohenester, E., and Jones, J. (2005). A simplified laminin nomenclature. Matrix Biol. *24*, 326–332.

Avraham, H., and Weinberg, R.A. (1989). Characterization and expression of the human rhoH12 gene product. Mol. Cell. Biol. *9*, 2058–2066.

Balani, S., Nguyen, L.V., and Eaves, C.J. (2017). Modeling the process of human tumorigenesis. Nat. Commun. *8*, 15422.

Balda, M.S., Garrett, M.D., and Matter, K. (2003). The ZO-1–associated Y-box factor ZONAB regulates epithelial cell proliferation and cell density. J Cell Biol *160*, 423–432.

Barker, H.E., Cox, T.R., and Erler, J.T. (2012). The rationale for targeting the LOX family in cancer. Nat. Rev. Cancer *12*, 540–552.

Béglé, A., Tryoen-Tóth, P., Barry, J. de, Bader, M.-F., and Vitale, N. (2009). ARF6 Regulates the Synthesis of Fusogenic Lipids for Calcium-regulated Exocytosis in Neuroendocrine Cells. J. Biol. Chem. *284*, 4836–4845.

Bergamaschi, A., Tagliabue, E., Sørlie, T., Naume, B., Triulzi, T., Orlandi, R., Russnes, H.G., Nesland, J.M., Tammi, R., Auvinen, P., et al. (2008). Extracellular matrix signature identifies breast cancer subgroups with different clinical outcome. J. Pathol. *214*, 357–367.

Bertucci, F., Finetti, P., and Birnbaum, D. (2012). Basal Breast Cancer: A Complex and Deadly Molecular Subtype. Curr. Mol. Med. *12*, 96–110.

Birchmeier, W., and Behrens, J. (1994). Cadherin expression in carcinomas: role in the formation of cell junctions and the prevention of invasiveness. Biochim. Biophys. Acta BBA - Rev. Cancer *1198*, 11–26.

Bishop, A.L., and Hall, A. (2000). Rho GTPases and their effector proteins. 15.

Bissell, M.J., and Bilder, D. (2003). Polarity determination in breast tissue: desmosomal adhesion, myoepithelial cells, and laminin 1. Breast Cancer Res. *5*, 117–119.

Bissell, M.J., Hall, H.G., and Parry, G. (1982). How does the extracellular matrix direct gene expression? J. Theor. Biol. *99*, 31–68.

Bloushtain-Qimron, N., Yao, J., Snyder, E.L., Shipitsin, M., Campbell, L.L., Mani, S.A., Hu, M., Chen, H., Ustyansky, V., Antosiewicz, J.E., et al. (2008). Cell type-specific DNA methylation patterns in the human breast. Proc. Natl. Acad. Sci. U. S. A. *105*, 14076–14081.

Bondareva, A., Downey, C.M., Ayres, F., Liu, W., Boyd, S.K., Hallgrimsson, B., and Jirik, F.R. (2009). The Lysyl Oxidase Inhibitor, β-Aminopropionitrile, Diminishes the Metastatic Colonization Potential of Circulating Breast Cancer Cells. PLOS ONE *4*, e5620.

Bonnans, C., Chou, J., and Werb, Z. (2014). Remodelling the extracellular matrix in development and disease. Nat. Rev. Mol. Cell Biol. *15*, 786–801.

Borsig, L., Wolf, M.J., Roblek, M., Lorentzen, A., and Heikenwalder, M. (2014). Inflammatory chemokines and metastasis—tracing the accessory. Oncogene *33*, 3217–3224.

Bos, J.L., Rehmann, H., and Wittinghofer, A. (2007). GEFs and GAPs: Critical Elements in the Control of Small G Proteins. Cell *129*, 865–877.

Boulakirba, S., Macia, E., Partisani, M., Lacas-Gervais, S., Brau, F., Luton, F., and Franco, M. (2014a). Arf6 exchange factor EFA6 and endophilin directly interact at the plasma membrane to control clathrin-mediated endocytosis. Proc. Natl. Acad. Sci. *111*, 9473–9478.

Boulakirba, S., Macia, E., Partisani, M., Lacas-Gervais, S., Brau, F., Luton, F., and Franco, M. (2014b). Arf6 exchange factor EFA6 and endophilin directly interact at the plasma membrane to control clathrin-mediated endocytosis. Proc. Natl. Acad. Sci. U. S. A. *111*, 9473–9478.

Boulay, P.-L., Schlienger, S., Lewis-Saravalli, S., Vitale, N., Ferbeyre, G., and Claing, A. (2011). ARF1 controls proliferation of breast cancer cells by regulating the retinoblastoma protein. Oncogene *30*, 3846–3861.

Boussadia, O., Kutsch, S., Hierholzer, A., Delmas, V., and Kemler, R. (2002). E-cadherin is a survival factor for the lactating mouse mammary gland. Mech. Dev. *115*, 53–62.

Bovellan, M., Fritzsche, M., Stevens, C., and Charras, G. (2010). Death-associated protein kinase (DAPK) and signal transduction: blebbing in programmed cell death. FEBS J. *277*, 58–65.

Boyd, N.F., Dite, G.S., Stone, J., Gunasekara, A., English, D.R., McCredie, M.R.E., Giles, G.G., Tritchler, D., Chiarelli, A., Yaffe, M.J., et al. (2002). Heritability of Mammographic Density, a Risk Factor for Breast Cancer. N. Engl. J. Med. *347*, 886–894.

Brabletz, T., Kalluri, R., Nieto, M.A., and Weinberg, R.A. (2018). EMT in cancer. Nat. Rev. Cancer *18*, 128–134.

Bray, F., Ferlay, J., Soerjomataram, I., Siegel, R.L., Torre, L.A., and Jemal, A. (2018). Global cancer statistics 2018: GLOBOCAN estimates of incidence and mortality worldwide for 36 cancers in 185 countries. CA. Cancer J. Clin. *68*, 394–424.

Bray, K., Gillette, M., Young, J., Loughran, E., Hwang, M., Sears, J.C., and Vargo-Gogola, T. (2013). Cdc42 overexpression induces hyperbranching in the developing mammary gland by enhancing cell migration. Breast Cancer Res. *15*.

Britt, K., Ashworth, A., and Smalley, M. (2007). Pregnancy and the risk of breast cancer. Endocr. Relat. Cancer *14*, 907–933.

Bronsert, P., Enderle-Ammour, K., Bader, M., Timme, S., Kuehs, M., Csanadi, A., Kayser, G., Kohler, I., Bausch, D., Hoeppner, J., et al. (2014). Cancer cell invasion and EMT marker expression: a three-dimensional study of the human cancer-host interface. J. Pathol. *234*, 410–422.

Buccione, R., Caldieri, G., and Ayala, I. (2009). Invadopodia: specialized tumor cell structures for the focal degradation of the extracellular matrix. Cancer Metastasis Rev. *28*, 137–149.

Bustelo, X.R., Sauzeau, V., and Berenjeno, I.M. (2007). GTP-binding proteins of the Rho/Rac family: regulation, effectors and functions in vivo. BioEssays *29*, 356–370.

Butcher, D.T., Alliston, T., and Weaver, V.M. (2009). A tense situation: forcing tumour progression. Nat. Rev. Cancer *9*, 108–122.

Cardama, G.A., Gonzalez, N., Maggio, J., Menna, P.L., and Gomez, D.E. (2017). Rho GTPases as therapeutic targets in cancer (Review). Int. J. Oncol. *51*, 1025–1034.

Casalou, C., Faustino, A., and Barral, D.C. (2016). Arf proteins in cancer cell migration. Small GTPases *7*, 270–282.

Casanova, J.E. (2007). Regulation of Arf Activation: the Sec7 Family of Guanine Nucleotide Exchange Factors. Traffic *8*, 1476–1485.

Casu, B., Naggi, A., and Torri, G. (2010). Heparin-derived heparan sulfate mimics to modulate heparan sulfate-protein interaction in inflammation and cancer. Matrix Biol. *29*, 442–452.

Cathcart, J., Pulkoski-Gross, A., and Cao, J. (2015). Targeting matrix metalloproteinases in cancer: Bringing new life to old ideas. Genes Dis. *2*, 26–34.

Caumont, A.-S., Galas, M.-C., Vitale, N., Aunis, D., and Bader, M.-F. (1998). Regulated Exocytosis in Chromaffin Cells TRANSLOCATION OF ARF6 STIMULATES A PLASMA MEMBRANE-ASSOCIATED PHOSPHOLIPASE D. J. Biol. Chem. *273*, 1373–1379.

Cavallaro, U., and Christofori, G. (2004). Cell adhesion and signalling by cadherins and Ig-CAMs in cancer. Nat. Rev. Cancer *4*, 118–132.

Cavallaro, U., and Dejana, E. (2011). Adhesion molecule signalling: not always a sticky business. Nat. Rev. Mol. Cell Biol. *12*, 189–197.

Chaffer, C.L., Thompson, E.W., and Williams, E.D. (2007). Mesenchymal to epithelial transition in development and disease. Cells Tissues Organs *185*, 7–19.

Chaffer, C.L., Marjanovic, N.D., Lee, T., Bell, G., Kleer, C.G., Reinhardt, F., D'Alessio, A.C., Young, R.A., and Weinberg, R.A. (2013). Poised Chromatin at the ZEB1 Promoter Enables Breast Cancer Cell Plasticity and Enhances Tumorigenicity. Cell *154*, 61–74.

Chaffer, C.L., San Juan, B.P., Lim, E., and Weinberg, R.A. (2016). EMT, cell plasticity and metastasis. Cancer Metastasis Rev. *35*, 645–654.

Chang, C.-J., Chao, C.-H., Xia, W., Yang, J.-Y., Xiong, Y., Li, C.-W., Yu, W.-H., Rehman, S.K., Hsu, J.L., Lee, H.-H., et al. (2011). p53 regulates epithelial–mesenchymal transition and stem cell properties through modulating miRNAs. Nat. Cell Biol. *13*, 317–323.

Chardin, P., Paris, S., Antonny, B., Robineau, S., Béraud-Dufour, S., Jackson, C.L., and Chabre, M. (1996). A human exchange factor for ARF contains Sec7- and pleckstrin-homology domains. Nature *384*, 481.

Charras, G., and Paluch, E. (2008). Blebs lead the way: how to migrate without lamellipodia. Nat. Rev. Mol. Cell Biol. *9*, 730–736.

Cheah, M., and Andrews, M.R. (2018). Integrin Activation: Implications for Axon Regeneration. Cells *7*, 20.

Chen, J., Diacovo, T.G., Grenache, D.G., Santoro, S.A., and Zutter, M.M. (2002). The α2 Integrin Subunit-Deficient Mouse: A Multifaceted Phenotype Including Defects of Branching Morphogenesis and Hemostasis. Am. J. Pathol. *161*, 337–344.

Cheng, G.Z., Chan, J., Wang, Q., Zhang, W., Sun, C.D., and Wang, L.-H. (2007). Twist Transcriptionally Up-regulates AKT2 in Breast Cancer Cells Leading to Increased Migration, Invasion, and Resistance to Paclitaxel. Cancer Res. *67*, 1979–1987.

Cheung, K.J., Gabrielson, E., Werb, Z., and Ewald, A.J. (2013). Collective Invasion in Breast Cancer Requires a Conserved Basal Epithelial Program. Cell *155*, 1639–1651.

Choi, S., Ko, J., Lee, J.-R., Lee, H.W., Kim, K., Chung, H.S., Kim, H., and Kim, E. (2006). ARF6 and EFA6A Regulate the Development and Maintenance of Dendritic Spines. J. Neurosci. *26*, 4811–4819.

Chothia, C., and Jones, E.Y. (1997). The Molecular Structure of Cell Adhesion Molecules. Annu. Rev. Biochem. *66*, 823–862.

Clark, E.S., and Weaver, A.M. (2008). A new role for cortactin in invadopodia: Regulation of protease secretion. Eur. J. Cell Biol. *87*, 581–590.

Clark, E.A., Golub, T.R., Lander, E.S., and Hynes, R.O. (2000). Genomic analysis of metastasis reveals an essential role for RhoC. Nature *406*, 532–535.

Cohen, L.A., Honda, A., Varnai, P., Brown, F.D., Balla, T., Donaldson, J.G., and Schwartz, M.A. (2007). Active Arf6 Recruits ARNO/Cytohesin GEFs to the PM by Binding Their PH Domains. Mol. Biol. Cell *18*, 2244–2253.

Colombo, P.-E., Milanezi, F., Weigelt, B., and Reis-Filho, J.S. (2011). Microarrays in the 2010s: the contribution of microarray-based gene expression profiling to breast cancer classification, prognostication and prediction. Breast Cancer Res. *13*.

Comijn, J., Berx, G., Vermassen, P., Verschueren, K., van Grunsven, L., Bruyneel, E., Mareel, M., Huylebroeck, D., and van Roy, F. (2001). The Two-Handed E Box Binding Zinc Finger Protein SIP1 Downregulates E-Cadherin and Induces Invasion. Mol. Cell *7*, 1267–1278.

Conacci-Sorrell, M., Zhurinsky, J., and Ben-Ze'ev, A. (2002). The cadherin-catenin adhesion system in signaling and cancer. J. Clin. Invest. *109*, 987–991.

Condeelis, J., and Pollard, J.W. (2006). Macrophages: Obligate Partners for Tumor Cell Migration, Invasion, and Metastasis. Cell *124*, 263–266.

Cory, G.O.C., and Cullen, P.J. (2007). Membrane Curvature: The Power of Bananas, Zeppelins and Boomerangs. Curr. Biol. *17*, R455–R457.

Daniel, C.W. (1975). Regulation of cell division in aging mouse mammary epithelium. Adv. Exp. Med. Biol. *61*, 1–19.

Daniel, C.W., Strickland, P., and Friedmann, Y. (1995). Expression and functional role of E- and P-cadherins in mouse mammary ductal morphogenesis and growth. Dev. Biol. *169*, 511–519.

Das, M., Subbayya Ithychanda, S., Qin, J., and Plow, E.F. (2014). Mechanisms of talin-dependent integrin signaling and crosstalk. Biochim. Biophys. Acta BBA - Biomembr. *1838*, 579–588.

Davidson, L.A., and Keller, R.E. (1999). Neural tube closure in Xenopus laevis involves medial migration, directed protrusive activity, cell intercalation and convergent extension. Dev. Camb. Engl. *126*, 4547–4556.

DerMardirossian, C., and Bokoch, G.M. (2005). GDIs: central regulatory molecules in Rho GTPase activation. Trends Cell Biol. *15*, 356–363.

Derrien, V., Couillault, C., Franco, M., Martineau, S., Montcourrier, P., Houlgatte, R., and Chavrier, P. (2002). A conserved C-terminal domain of EFA6-family ARF6-guanine nucleotide exchange factors induces lengthening of microvilli-like membrane protrusions. J. Cell Sci. *115*, 2867–2879.

Desgrosellier, J.S., and Cheresh, D.A. (2010). Integrins in cancer: biological implications and therapeutic opportunities. Nat. Rev. Cancer *10*, 9–22.

Deugnier, M.-A., Teulière, J., Faraldo, M.M., Thiery, J.P., and Glukhova, M.A. (2002). The importance of being a myoepithelial cell. Breast Cancer Res. *4*.

Dias, K., Dvorkin-Gheva, A., Hallett, R.M., Wu, Y., Hassell, J., Pond, G.R., Levine, M., Whelan, T., and Bane, A.L. (2017). Claudin-Low Breast Cancer; Clinical & Pathological Characteristics. PLOS ONE *12*, e0168669.

Diaz, B., Shani, G., Pass, I., Anderson, D., Quintavalle, M., and Courtneidge, S.A. (2009). Tks5-Dependent, Nox-Mediated Generation of Reactive Oxygen Species Is Necessary for Invadopodia Formation. Sci Signal *2*, ra53–ra53.

Dickson, S.R., and Warburton, M.J. (1992). Enhanced synthesis of gelatinase and stromelysin by myoepithelial cells during involution of the rat mammary gland. J. Histochem. Cytochem. *40*, 697–703.

DiNitto, J.P., Delprato, A., Gabe Lee, M.-T., Cronin, T.C., Huang, S., Guilherme, A., Czech, M.P., and Lambright, D.G. (2007). Structural Basis and Mechanism of Autoregulation in 3-Phosphoinositide-Dependent Grp1 Family Arf GTPase Exchange Factors. Mol. Cell *28*, 569–583.

Dirat, B., Bochet, L., Dabek, M., Daviaud, D., Dauvillier, S., Majed, B., Wang, Y.Y., Meulle, A., Salles, B., Le Gonidec, S., et al. (2011). Cancer-Associated Adipocytes Exhibit an Activated Phenotype and Contribute to Breast Cancer Invasion. Cancer Res. *71*, 2455–2465.

Donaldson, J.G., and Jackson, C.L. (2011). ARF family G proteins and their regulators: roles in membrane transport, development and disease. Nat. Rev. Mol. Cell Biol. *12*, 362–375.

Dovas, A., and Cox, D. (2010). Regulation of WASp by phosphorylation: Activation or other functions? Commun. Integr. Biol. *3*, 101.

Drubin, D.G. (1991). Development of cell polarity in budding yeast. Cell *65*, 1093–1096.

Dubois, T., Paléotti, O., Mironov Jr, A.A., Fraisier, V., Stradal, T.E.B., De Matteis, M.A., Franco, M., and Chavrier, P. (2005). Golgi-localized GAP for Cdc42 functions downstream of ARF1 to control Arp2/3 complex and F-actin dynamics. Nat. Cell Biol. *7*, 353–364.

Duffy, M.J., Maguire, T.M., Hill, A., McDermott, E., and O'Higgins, N. (2000). Metalloproteinases: role in breast carcinogenesis, invasion and metastasis. Breast Cancer Res. BCR *2*, 252–257.

Dupont, S., Morsut, L., Aragona, M., Enzo, E., Giulitti, S., Cordenonsi, M., Zanconato, F., Le Digabel, J., Forcato, M., Bicciato, S., et al. (2011). Role of YAP/TAZ in mechanotransduction. Nature *474*, 179–183.

Eades, G., Wolfson, B., Zhang, Y., Li, Q., Yao, Y., and Zhou, Q. (2015). lincRNA-RoR and miR-145 Regulate Invasion in Triple-Negative Breast Cancer via Targeting ARF6. Mol. Cancer Res. *13*, 330–338.

Elenbaas, B., Spirio, L., Koerner, F., Fleming, M.D., Zimonjic, D.B., Donaher, J.L., Popescu, N.C., Hahn, W.C., and Weinberg, R.A. (2001). Human breast cancer cells generated by oncogenic transformation of primary mammary epithelial cells. Genes Dev. *15*, 50–65.

Ellenbroek, S.I.J., and Collard, J.G. (2007). Rho GTPases: functions and association with cancer. Clin. Exp. Metastasis *24*, 657–672.

ElMoneim, H.M.A., and Zaghloul, N.M. (2011). Expression of e-cadherin, n-cadherin and snail and their correlation with clinicopathological variants: an immunohistochemical study of 132 invasive ductal breast carcinomas in Egypt. Clinics *66*, 1765–1771.

Elston, C.W., and Ellis, I.O. (1991). pathological prognostic factors in breast cancer. I. The value of histological grade in breast cancer: experience from a large study with long-term follow-up. Histopathology *19*, 403–410.

Engler, A.J., Sen, S., Sweeney, H.L., and Discher, D.E. (2006). Matrix Elasticity Directs Stem Cell Lineage Specification. Cell *126*, 677–689.

Etienne-Manneville, S. (2004). Cdc42 - the centre of polarity. J. Cell Sci. *117*, 1291–1300.

Evers, E.E., Zondag, G.C.M., Malliri, A., Price, L.S., ten Klooster, J.-P., van der Kammen, R.A., and Collard, J.G. (2000). Rho family proteins in cell adhesion and cell migration. Eur. J. Cancer *36*, 1269–1274.

Ewald, A.J., Brenot, A., Duong, M., Chan, B.S., and Werb, Z. (2008). Collective Epithelial Migration and Cell Rearrangements Drive Mammary Branching Morphogenesis. Dev. Cell *14*, 570–581.

Ewald, A.J., Huebner, R.J., Palsdottir, H., Lee, J.K., Perez, M.J., Jorgens, D.M., Tauscher, A.N., Cheung, K.J., Werb, Z., and Auer, M. (2012). Mammary collective cell migration involves transient loss of epithelial features and individual cell migration within the epithelium. J. Cell Sci. *125*, 2638–2654.

Eyckmans, J., Boudou, T., Yu, X., and Chen, C.S. (2011). A Hitchhiker's Guide to Mechanobiology. Dev. Cell *21*, 35–47.

Faraldo, M.M., Teulière, J., Deugnier, M.-A., Taddei-De La Hosseraye, I., Thiery, J.P., and Glukhova, M.A. (2005). Myoepithelial Cells in the Control of Mammary Development and Tumorigenesis: Data From Genetically Modified Mice. J. Mammary Gland Biol. Neoplasia *10*, 211–219.

Farina, K.L., Wyckoff, J.B., Rivera, J., Lee, H., Segall, J.E., Condeelis, J.S., and Jones, J.G. (1998). Cell Motility of Tumor Cells Visualized in Living Intact Primary Tumors Using Green Fluorescent Protein. Cancer Res. *58*, 2528–2532.

Faroudi, M., Hons, M., Zachacz, A., Dumont, C., Lyck, R., Stein, J.V., and Tybulewicz, V.L.J. (2010). Critical roles for Rac GTPases in T-cell migration to and within lymph nodes. Blood *116*, 5536–5547.

Fässler, R., and Meyer, M. (1995). Consequences of lack of beta 1 integrin gene expression in mice. Genes Dev. *9*, 1896–1908.

Fata, J.E., Werb, Z., and Bissell, M.J. (2003). Regulation of mammary gland branching morphogenesis by the extracellular matrix and its remodeling enzymes. Breast Cancer Res. *6*.

Faulkin, L.J., and Deome, K.B. (1960). Regulation of growth and spacing of gland elements in the mammary fat pad of the C3H mouse. J. Natl. Cancer Inst. *24*, 953–969.

Feinberg, T.Y., Rowe, R.G., Saunders, T.L., and Weiss, S.J. (2016). Functional roles of MMP14 and MMP15 in early postnatal mammary gland development. Dev. Camb. Engl. *143*, 3956–3968.

Feinberg, T.Y., Zheng, H., Liu, R., Wicha, M.S., Yu, S.M., and Weiss, S.J. (2018). Divergent Matrix-Remodeling Strategies Distinguish Developmental from Neoplastic Mammary Epithelial Cell Invasion Programs. Dev. Cell *47*, 145-160.e6.

Feng, Y., Spezia, M., Huang, S., Yuan, C., Zeng, Z., Zhang, L., Ji, X., Liu, W., Huang, B., Luo, W., et al. (2018). Breast cancer development and progression: Risk factors, cancer stem cells, signaling pathways, genomics, and molecular pathogenesis. Genes Dis. *5*, 77–106.

Fidler, I.J. (2003). The pathogenesis of cancer metastasis: the "seed and soil" hypothesis revisited. Nat. Rev. Cancer *3*, 453–458.

Flavahan, W.A., Gaskell, E., and Bernstein, B.E. (2017). Epigenetic plasticity and the hallmarks of cancer. Science *357*, eaal2380.

Fraley, S.I., Wu, P.-H., He, L., Feng, Y., Krisnamurthy, R., Longmore, G.D., and Wirtz, D. (2015). Three-dimensional matrix fiber alignment modulates cell migration and MT1-MMP utility by spatially and temporally directing protrusions. Sci. Rep. *5*, 14580.

Franco, M., Chardin, P., Chabre, M., and Paris, S. (1993). Myristoylation is not required for GTP-dependent binding of ADP-ribosylation factor ARF1 to phospholipids. J. Biol. Chem. *268*, 24531–24534.

Franco, M., Chardin, P., Chabre, M., and Paris, S. (1995). Myristoylation of ADP-ribosylation Factor 1 Facilitates Nucleotide Exchange at Physiological Mg Levels. J. Biol. Chem. *270*, 1337–1341.

Franco, M., Chardin, P., Chabre, M., and Paris, S. (1996). Myristoylation-facilitated Binding of the G Protein ARF1 to Membrane Phospholipids Is Required for Its Activation by a Soluble Nucleotide Exchange Factor. J. Biol. Chem. *271*, 1573–1578.

Franco, M., Peters, P.J., Boretto, J., Donselaar, E. van, Neri, A., D'Souza-Schorey, C., and Chavrier, P. (1999). EFA6, a sec7 domain-containing exchange factor for ARF6, coordinates membrane recycling and actin cytoskeleton organization. EMBO J. *18*, 1480–1491.

Friedl, P., and Gilmour, D. (2009). Collective cell migration in morphogenesis, regeneration and cancer. Nat. Rev. Mol. Cell Biol. *10*, 445–457.

Friedl, P., and Wolf, K. (2003). Tumour-cell invasion and migration: diversity and escape mechanisms. Nat. Rev. Cancer *3*, 362–374.

Friedl, P., and Wolf, K. (2010). Plasticity of cell migration: a multiscale tuning model. J. Cell Biol. *188*, 11–19.

Friesland, A., Zhao, Y., Chen, Y.-H., Wang, L., Zhou, H., and Lu, Q. (2013). Small molecule targeting Cdc42–intersectin interaction disrupts Golgi organization and suppresses cell motility. Proc. Natl. Acad. Sci. *110*, 1261–1266.

Fritz, G., Just, I., and Kaina, B. (1999). Rho GTPases are over-expressed in human tumors. Int. J. Cancer *81*, 682–687.

Frixen, U.H., Behrens, J., Sachs, M., Eberle, G., Voss, B., Warda, A., Löchner, D., and Birchmeier, W. (1991). E-cadherin-mediated cell-cell adhesion prevents invasiveness of human carcinoma cells. J. Cell Biol. *113*, 173–185.

Fukuda, Y., Masuda, Y., Kishi, J., Hashimoto, Y., Hayakawa, T., Nogawa, H., and Nakanishi, Y. (1988). The role of interstitial collagens in cleft formation of mouse embryonic submandibular gland during initial branching. Development *103*, 259–267.

Gaggioli, C., Hooper, S., Hidalgo-Carcedo, C., Grosse, R., Marshall, J.F., Harrington, K., and Sahai, E. (2007). Fibroblast-led collective invasion of carcinoma cells with differing roles for RhoGTPases in leading and following cells. Nat. Cell Biol. *9*, 1392–1400.

Garber, K. (2008). Epithelial-to-Mesenchymal Transition Is Important to Metastasis, But Questions Remain. JNCI J. Natl. Cancer Inst. *100*, 232–239.

Gemmill, R.M., Roche, J., Potiron, V.A., Nasarre, P., Mitas, M., Coldren, C.D., Helfrich, B.A., Garrett-Mayer, E., Bunn, P.A., and Drabkin, H.A. (2011). ZEB1-responsive genes in non-small cell lung cancer. Cancer Lett. *300*, 66–78.

Ginestier, C., Hur, M.H., Charafe-Jauffret, E., Monville, F., Dutcher, J., Brown, M., Jacquemier, J., Viens, P., Kleer, C.G., Liu, S., et al. (2007). ALDH1 Is a Marker of Normal and Malignant Human Mammary Stem Cells and a Predictor of Poor Clinical Outcome. Cell Stem Cell *1*, 555–567.

Gjorevski, N., and Nelson, C.M. (2010). Endogenous patterns of mechanical stress are required for branching morphogenesis. Integr. Biol. *2*, 424.

Glukhova, M.A., and Streuli, C.H. (2013). How integrins control breast biology. Curr. Opin. Cell Biol. *25*, 633–641.

Golson, M.L., and Kaestner, K.H. (2016). Fox transcription factors: from development to disease. Development *143*, 4558–4570.

Gomes, A.M., Stelling, M.P., and Pavão, M.S.G. (2013). Heparan Sulfate and Heparanase as Modulators of Breast Cancer Progression.

Gomes, A.M., Bhat, R., Correia, A.L., Mott, J.D., Ilan, N., Vlodavsky, I., Pavão, M.S.G., and Bissell, M. (2015). Mammary Branching Morphogenesis Requires Reciprocal Signaling by Heparanase and MMP-14. J. Cell. Biochem. *116*, 1668–1679.

Gong, Y., Scott, E., Lu, R., Xu, Y., Oh, W.K., and Yu, Q. (2013). TIMP-1 Promotes Accumulation of Cancer Associated Fibroblasts and Cancer Progression. PLOS ONE *8*, e77366.

Goossens, S., Vandamme, N., Van Vlierberghe, P., and Berx, G. (2017). EMT transcription factors in cancer development re-evaluated: Beyond EMT and MET. Biochim. Biophys. Acta BBA - Rev. Cancer *1868*, 584–591.

Gouon-Evans, V., Rothenberg, M.E., and Pollard, J.W. (2000). Postnatal mammary gland development requires macrophages and eosinophils. Dev. Camb. Engl. *127*, 2269–2282.

Graham, T.R., Yacoub, R., Taliaferro-Smith, L., Osunkoya, A.O., Odero-Marah, V.A., Liu, T., Kimbro, K.S., Sharma, D., and O'Regan, R.M. (2010). Reciprocal regulation of ZEB1 and AR in triple negative breast cancer cells. Breast Cancer Res. Treat. *123*, 139–147.

Gregor, M.F., Misch, E.S., Yang, L., Hummasti, S., Inouye, K.E., Lee, A.-H., Bierie, B., and Hotamisligil, G.S. (2013). The Role of Adipocyte XBP1 in Metabolic Regulation during Lactation. Cell Rep. *3*, 1430–1439.

Grossmann, A.H., Yoo, J.H., Clancy, J., Sorensen, L.K., Sedgwick, A., Tong, Z., Ostanin, K., Rogers, A., Grossmann, K.F., Tripp, S.R., et al. (2013). The Small GTPase ARF6 Stimulates β-Catenin Transcriptional Activity During WNT5A-Mediated Melanoma Invasion and Metastasis. Sci Signal *6*, ra14–ra14.

Gudjonsson, T., Rønnov-Jessen, L., Villadsen, R., Rank, F., Bissell, M.J., and Petersen, O.W. (2002). Normal and tumor-derived myoepithelial cells differ in their ability to interact with luminal breast epithelial cells for polarity and basement membrane deposition. J. Cell Sci. *115*, 39–50.

Guo, W., and Giancotti, F.G. (2004). Integrin signalling during tumour progression. Nat. Rev. Mol. Cell Biol. *5*, 816–826.

Guo, W., Keckesova, Z., Donaher, J.L., Shibue, T., Tischler, V., Reinhardt, F., Itzkovitz, S., Noske, A., Zürrer-Härdi, U., Bell, G., et al. (2012). Slug and Sox9 Cooperatively Determine the Mammary Stem Cell State. Cell *148*, 1015–1028.

Haga, R.B., and Ridley, A.J. (2016). Rho GTPases: Regulation and roles in cancer cell biology. Small GTPases *7*, 207–221.

Hahn, W.C., Counter, C.M., Lundberg, A.S., Beijersbergen, R.L., Brooks, M.W., and Weinberg, R.A. (1999). Creation of human tumour cells with defined genetic elements. Nature *400*, 464–468.

Hall, A. (2005). Rho GTPases and the control of cell behaviour. Biochem. Soc. Trans. *33*, 891–895.

Hamidi, H., and Ivaska, J. (2018). Every step of the way: integrins in cancer progression and metastasis. Nat. Rev. Cancer *18*, 533–548.

Han, J., Hendzel, M.J., and Allalunis-Turner, J. (2011). Notch signaling as a therapeutic target for breast cancer treatment? Breast Cancer Res. *13*, 210.

Hanada, S., Harada, M., Kumemura, H., Omary, M.B., Kawaguchi, T., Taniguchi, E., Koga, H., Yoshida, T., Maeyama, M., Baba, S., et al. (2005). Keratin-containing inclusions affect cell morphology and distribution of cytosolic cellular components. Exp. Cell Res. *304*, 471–482.

Hanahan, D., and Coussens, L.M. (2012). Accessories to the Crime: Functions of Cells Recruited to the Tumor Microenvironment. Cancer Cell *21*, 309–322.

Hanahan, D., and Weinberg, R.A. (2000). The Hallmarks of Cancer. Cell *100*, 57–70.

Hanahan, D., and Weinberg, R.A. (2011). Hallmarks of Cancer: The Next Generation. Cell *144*, 646–674.

Hashimoto, A., Hashimoto, S., Ando, R., Noda, K., Ogawa, E., Kotani, H., Hirose, M., Menju, T., Morishige, M., Manabe, T., et al. (2011). GEP100-Arf6-AMAP1-Cortactin Pathway Frequently Used in Cancer Invasion Is Activated by VEGFR2 to Promote Angiogenesis. PLOS ONE *6*, e23359.

Hashimoto, S., Onodera, Y., Hashimoto, A., Tanaka, M., Hamaguchi, M., Yamada, A., and Sabe, H. (2004). Requirement for Arf6 in breast cancer invasive activities. Proc. Natl. Acad. Sci. *101*, 6647–6652.

Hashimoto, S., Hashimoto, A., Yamada, A., Onodera, Y., and Sabe, H. (2005). Assays and Properties of the ArfGAPs, AMAP1 and AMAP2, in Arf6 Function. In Methods in Enzymology, (Academic Press), pp. 216–231.

Hay, E.D. (1995). An overview of epithelio-mesenchymal transformation. Acta Anat. (Basel) *154*, 8–20.

Heerboth, S., Housman, G., Leary, M., Longacre, M., Byler, S., Lapinska, K., Willbanks, A., and Sarkar, S. (2015). EMT and tumor metastasis. Clin. Transl. Med. *4*, 6.

Hegerfeldt, Y., Tusch, M., Bröcker, E.-B., and Friedl, P. (2002). Collective cell movement in primary melanoma explants: plasticity of cell-cell interaction, beta1-integrin function, and migration strategies. Cancer Res. *62*, 2125–2130.

Helena, J.M., Joubert, A.M., Grobbelaar, S., Nolte, E.M., Nel, M., Pepper, M.S., Coetzee, M., and Mercier, A.E. (2018). Deoxyribonucleic Acid Damage and Repair: Capitalizing on Our Understanding of the Mechanisms of Maintaining Genomic Integrity for Therapeutic Purposes. Int. J. Mol. Sci. *19*, 1148.

Hennessy, B.T., Gonzalez-Angulo, A.-M., Stemke-Hale, K., Gilcrease, M.Z., Krishnamurthy, S., Lee, J.-S., Fridlyand, J., Sahin, A., Agarwal, R., Joy, C., et al. (2009). Characterization of a Naturally Occurring Breast Cancer Subset Enriched in Epithelial-to-Mesenchymal Transition and Stem Cell Characteristics. Cancer Res. *69*, 4116–4124.

Herschkowitz, J.I., Simin, K., Weigman, V.J., Mikaelian, I., Usary, J., Hu, Z., Rasmussen, K.E., Jones, L.P., Assefnia, S., Chandrasekharan, S., et al. (2007). Identification of conserved gene expression features between murine mammary carcinoma models and human breast tumors. Genome Biol. *8*, R76.

Heuvingh, J., Franco, M., Chavrier, P., and Sykes, C. (2007). ARF1-mediated actin polymerization produces movement of artificial vesicles. Proc. Natl. Acad. Sci. *104*, 16928–16933.

Hollstein, M., Sidransky, D., Vogelstein, B., and Harris, C.C. (1991). p53 mutations in human cancers. Science *253*, 49–53.

Hongu, T., Funakoshi, Y., Fukuhara, S., Suzuki, T., Sakimoto, S., Takakura, N., Ema, M., Takahashi, S., Itoh, S., Kato, M., et al. (2015). Arf6 regulates tumour angiogenesis and growth through HGF-induced endothelial β1 integrin recycling. Nat. Commun. *6*, 7925.

Hoshino, A., Costa-Silva, B., Shen, T.-L., Rodrigues, G., Hashimoto, A., Tesic Mark, M., Molina, H., Kohsaka, S., Di Giannatale, A., Ceder, S., et al. (2015). Tumour exosome integrins determine organotropic metastasis. Nature *527*, 329–335.

Hosseini, H., Obradović, M.M.S., Hoffmann, M., Harper, K.L., Sosa, M.S., Werner-Klein, M., Nanduri, L.K., Werno, C., Ehrl, C., Maneck, M., et al. (2016). Early dissemination seeds metastasis in breast cancer. Nature *540*, 552–558.

Houndolo, T., Boulay, P.-L., and Claing, A. (2005). G Protein-coupled Receptor Endocytosis in ADP-ribosylation Factor 6-depleted Cells. J. Biol. Chem. *280*, 5598–5604.

Hovey, R.C., and Aimo, L. (2010). Diverse and Active Roles for Adipocytes During Mammary Gland Growth and Function. J. Mammary Gland Biol. Neoplasia *15*, 279–290.

Howard, B.A., and Lu, P. (2014). Stromal regulation of embryonic and postnatal mammary epithelial development and differentiation. Semin. Cell Dev. Biol. *25–26*, 43–51.

Hu, M., Yao, J., Carroll, D.K., Weremowicz, S., Chen, H., Carrasco, D., Richardson, A., Violette, S., Nikolskaya, T., Nikolsky, Y., et al. (2008). Regulation of In Situ to Invasive Breast Carcinoma Transition. Cancer Cell *13*, 394–406.

Hu, N., Wang, C., Hu, Y., Yang, H.H., Giffen, C., Tang, Z.-Z., Han, X.-Y., Goldstein, A.M., Emmert-Buck, M.R., Buetow, K.H., et al. (2005). Genome-Wide Association Study in Esophageal Cancer Using GeneChip Mapping 10K Array. Cancer Res. *65*, 2542–2546.

Huck, L., Pontier, S.M., Zuo, D.M., and Muller, W.J. (2010). β1-integrin is dispensable for the induction of ErbB2 mammary tumors but plays a critical role in the metastatic phase of tumor progression. Proc. Natl. Acad. Sci. *107*, 15559–15564.

Huebner, R.J., and Ewald, A.J. (2014). Cellular foundations of mammary tubulogenesis. Semin. Cell Dev. Biol. *31*, 124–131.

Huebner, R.J., Neumann, N.M., and Ewald, A.J. (2016). Mammary epithelial tubes elongate through MAPK-dependent coordination of cell migration. Development *143*, 983–993.

Hunzicker-Dunn, M., Gurevich, V.V., Casanova, J.E., and Mukherjee, S. (2002). ARF6: a newly appreciated player in G protein-coupled receptor desensitization. FEBS Lett. *521*, 3–8.

Hüsemann, Y., Geigl, J.B., Schubert, F., Musiani, P., Meyer, M., Burghart, E., Forni, G., Eils, R., Fehm, T., Riethmüller, G., et al. (2008). Systemic Spread Is an Early Step in Breast Cancer. Cancer Cell *13*, 58–68.

Hynes, R.O. (2002). Integrins: Bidirectional, Allosteric Signaling Machines. Cell *110*, 673–687.

Inman, J.L., Robertson, C., Mott, J.D., and Bissell, M.J. (2015). Mammary gland development: cell fate specification, stem cells and the microenvironment. Development *142*, 1028–1042.

Insua-Rodríguez, J., and Oskarsson, T. (2016). The extracellular matrix in breast cancer. Adv. Drug Deliv. Rev. *97*, 41–55.

Iozzo, R.V. (1998). Matrix proteoglycans: from molecular design to cellular function. Annu. Rev. Biochem. *67*, 609–652.

Iozzo, R.V. (2005). Basement membrane proteoglycans: from cellar to ceiling. Nat. Rev. Mol. Cell Biol. *6*, 646–656.

Itoh, K., Yoshioka, K., Akedo, H., Uehata, M., Ishizaki, T., and Narumiya, S. (1999). An essential part for Rho–associated kinase in the transcellular invasion of tumor cells. Nat. Med. *5*, 221–225.

Jackson, C.L., and Casanova, J.E. (2000). Turning on ARF: the Sec7 family of guanine-nucleotide-exchange factors. Trends Cell Biol. *10*, 60–67.

Johnson, D.I. (1990). Molecular characterization of CDC42, a Saccharomyces cerevisiae gene involved in the development of cell polarity. J. Cell Biol. *111*, 143–152.

Johnson, E., Seachrist, D.D., DeLeon-Rodriguez, C.M., Lozada, K.L., Miedler, J., Abdul-Karim, F.W., and Keri, R.A. (2010). HER2/ErbB2-induced Breast Cancer Cell Migration and Invasion Require p120 Catenin Activation of Rac1 and Cdc42. J. Biol. Chem. *285*, 29491–29501.

Johnston, K.A., and Lopez, K.M. (2018). Lysyl oxidase in cancer inhibition and metastasis. Cancer Lett. *417*, 174–181.

Jovanovic, O.A., Brown, F.D., and Donaldson, J.G. (2005). An Effector Domain Mutant of Arf6 Implicates Phospholipase D in Endosomal Membrane Recycling. Mol. Biol. Cell *17*, 327–335.

Kahlert, U.D., Joseph, J.V., and Kruyt, F.A.E. (2017). EMT- and MET-related processes in nonepithelial tumors: importance for disease progression, prognosis, and therapeutic opportunities. Mol. Oncol. *11*, 860–877.

Kalluri, R., and Weinberg, R.A. (2009). The basics of epithelial-mesenchymal transition. J. Clin. Invest. *119*, 1420–1428.

Kalluri, R., and Zeisberg, M. (2006). Fibroblasts in cancer. Nat. Rev. Cancer *6*, 392–401.

Karlsson, R., Pedersen, E.D., Wang, Z., and Brakebusch, C. (2009). Rho GTPase function in tumorigenesis. Biochim. Biophys. Acta BBA - Rev. Cancer *1796*, 91–98.

Kass, L., Erler, J.T., Dembo, M., and Weaver, V.M. (2007). Mammary epithelial cell: Influence of extracellular matrix composition and organization during development and tumorigenesis. Int. J. Biochem. Cell Biol. *39*, 1987–1994.

Katz, E., and Streuli, C.H. (2007). The extracellular matrix as an adhesion checkpoint for mammary epithelial function. Int. J. Biochem. Cell Biol. *39*, 715–726.

Keely, P.J., Westwick, J.K., Whitehead, I.P., Der, C.J., and Parise, L.V. (1997). Cdc42 and Rac1 induce integrin-mediated cell motility and invasiveness through PI(3)K. Nature *390*, 632–636.

Kendrick, H., Regan, J.L., Magnay, F.-A., Grigoriadis, A., Mitsopoulos, C., Zvelebil, M., and Smalley, M.J. (2008). Transcriptome analysis of mammary epithelial subpopulations identifies novel determinants of lineage commitment and cell fate. BMC Genomics *9*, 591.

Keyomarsi, K., Ding, Y., and Toyofuku, W. (2002). Cyclin E and Survival in Patients with Breast Cancer. N. Engl. J. Med. 10.

Khosravi-Far, R., Solski, P.A., Clark, G.J., Kinch, M.S., and Der, C.J. (1995). Activation of Rac1, RhoA, and mitogen-activated protein kinases is required for Ras transformation. Mol. Cell. Biol. *15*, 6443–6453.

Kielty, C.M., Sherratt, M.J., and Shuttleworth, C.A. (2002). Elastic fibres. J. Cell Sci. *115*, 2817–2828.

Kim, T., Veronese, A., Pichiorri, F., Lee, T.J., Jeon, Y.-J., Volinia, S., Pineau, P., Marchio, A., Palatini, J., Suh, S.-S., et al. (2011). p53 regulates epithelial–mesenchymal transition through microRNAs targeting ZEB1 and ZEB2. J. Exp. Med. *208*, 875–883.

Kirschmann, D.A., Seftor, E.A., Fong, S.F.T., Nieva, D.R.C., Sullivan, C.M., Edwards, E.M., Sommer, P., Csiszar, K., and Hendrix, M.J.C. (2002). A Molecular Role for Lysyl Oxidase in Breast Cancer Invasion. Cancer Res. *62*, 4478–4483.

Klein, S., Franco, M., Chardin, P., and Luton, F. (2006). Role of the Arf6 GDP/GTP Cycle and Arf6 GTPase-activating Proteins in Actin Remodeling and Intracellular Transport. J. Biol. Chem. *281*, 12352–12361.

Klein, S., Partisani, M., Franco, M., and Luton, F. (2008a). EFA6 Facilitates the Assembly of the Tight Junction by Coordinating an Arf6-dependent and -independent Pathway. J. Biol. Chem. *283*, 30129–30138.

Klein, S., Partisani, M., Franco, M., and Luton, F. (2008b). EFA6 Facilitates the Assembly of the Tight Junction by Coordinating an Arf6-dependent and -independent Pathway. J. Biol. Chem. *283*, 30129–30138.

Klinowska, T.C.M., Alexander, C.M., Georges-Labouesse, E., Van der Neut, R., Kreidberg, J.A., Jones, C.J.P., Sonnenberg, A., and Streuli, C.H. (2001). Epithelial Development and Differentiation in the Mammary Gland Is Not Dependent on α3 or α6 Integrin Subunits. Dev. Biol. *233*, 449–467.

Kordon, E.C., and Smith, G.H. (1998). An entire functional mammary gland may comprise the progeny from a single cell. Dev. Camb. Engl. *125*, 1921–1930.

Kowalski, P.J., Rubin, M.A., and Kleer, C.G. (2003). E-cadherin expression in primary carcinomas of the breast and its distant metastases. Breast Cancer Res. *5*.

Kratochwil, K. (1969). Organ specificity in mesenchymal induction demonstrated in the embryonic development of the mammary gland of the mouse. Dev. Biol. *20*, 46–71.

Krebs, A.M., Mitschke, J., Losada, M.L., Schmalhofer, O., Boerries, M., Busch, H., Boettcher, M., Mougiakakos, D., Reichardt, W., Bronsert, P., et al. (2017). The EMT-activator Zeb1 is a key factor for cell plasticity and promotes metastasis in pancreatic cancer. Nat. Cell Biol. *19*, 518–529.

Kumar, S., and Weaver, V.M. (2009). Mechanics, malignancy, and metastasis: The force journey of a tumor cell. Cancer Metastasis Rev. *28*, 113–127.

Kumar, R., Gururaj, A.E., and Barnes, C.J. (2006). p21-activated kinases in cancer. Nat. Rev. Cancer *6*, 459–471.

Kumari, S., and Mayor, S. (2008). ARF1 is directly involved in dynamin-independent endocytosis. Nat. Cell Biol. *10*, 30–41.

Kurahara, H., Takao, S., Maemura, K., Mataki, Y., Kuwahata, T., Maeda, K., Ding, Q., Sakoda, M., Iino, S., Ishigami, S., et al. (2012). Epithelial–mesenchymal transition and mesenchymal–epithelial transition via regulation of ZEB-1 and ZEB-2 expression in pancreatic cancer. J. Surg. Oncol. *105*, 655–661.

Lahlou, H., and Muller, W.J. (2011). β1-integrins signaling and mammary tumor progression in transgenic mouse models: implications for human breast cancer. Breast Cancer Res. *13*, 229.

Lahlou, H., Sanguin-Gendreau, V., Frame, M.C., and Muller, W.J. (2012). Focal adhesion kinase contributes to proliferative potential of ErbB2 mammary tumour cells but is dispensable for ErbB2 mammary tumour induction in vivo. Breast Cancer Res. *14*, R36.

Lamouille, S., Xu, J., and Derynck, R. (2014). Molecular mechanisms of epithelial-mesenchymal transition. Nat. Rev. Mol. Cell Biol. *15*, 178–196.

Lawson, C.D., and Burridge, K. (2014). The on-off relationship of Rho and Rac during integrin-mediated adhesion and cell migration. Small GTPases *5*, e27958.

Lawson, C.D., and Ridley, A.J. (2018). Rho GTPase signaling complexes in cell migration and invasion. J Cell Biol *217*, 447–457.

Lawson, D.A., Kessenbrock, K., Davis, R.T., Pervolarakis, N., and Werb, Z. (2018). Tumour heterogeneity and metastasis at single-cell resolution. Nat. Cell Biol. *20*, 1349.

LeBleu, V.S., and Kalluri, R. (2018). A peek into cancer-associated fibroblasts: origins, functions and translational impact. Dis. Model. Mech. *11*, dmm029447.

Levental, K.R., Yu, H., Kass, L., Lakins, J.N., Egeblad, M., Erler, J.T., Fong, S.F.T., Csiszar, K., Giaccia, A., Weninger, W., et al. (2009). Matrix Crosslinking Forces Tumor Progression by Enhancing Integrin Signaling. Cell *139*, 891–906.

Lewis-Saravalli, S., Campbell, S., and Claing, A. (2013). ARF1 controls Rac1 signaling to regulate migration of MDA-MB-231 invasive breast cancer cells. Cell. Signal. *25*, 1813–1819.

Li, A., Ma, Y., Yu, X., Mort, R.L., Lindsay, C.R., Stevenson, D., Strathdee, D., Insall, R.H., Chernoff, J., Snapper, S.B., et al. (2011). Rac1 Drives Melanoblast Organization during Mouse Development by Orchestrating Pseudopod- Driven Motility and Cell-Cycle Progression. Dev. Cell *21*, 722–734.

Li, M., Ng, S.S., Wang, J., Lai, L., Leung, S.Y., Franco, M., Peng, Y., He, M., Kung, H., and Lin, M.C. (2006). EFA6A Enhances Glioma Cell Invasion through ADP Ribosylation Factor 6/Extracellular Signal–Regulated Kinase Signaling. Cancer Res. *66*, 1583–1590.

Li, N., Zhang, Y., Naylor, M.J., Schatzmann, F., Maurer, F., Wintermantel, T., Schuetz, G., Mueller, U., Streuli, C.H., and Hynes, N.E. (2005). β1 integrins regulate mammary gland proliferation and maintain the integrity of mammary alveoli. EMBO J. *24*, 1942–1953.

Lim, K.B., Bu, W., Goh, W.I., Koh, E., Ong, S.H., Pawson, T., Sudhaharan, T., and Ahmed, S. (2008). The Cdc42 Effector IRSp53 Generates Filopodia by Coupling Membrane Protrusion with Actin Dynamics. J. Biol. Chem. *283*, 20454–20472.

Liu, J.C., Voisin, V., Wang, S., Wang, D.-Y., Jones, R.A., Datti, A., Uehling, D., Al-awar, R., Egan, S.E., Bader, G.D., et al. (2014). Combined deletion of Pten and p53 in mammary epithelium accelerates triple-negative breast cancer with dependency on eEF2K. EMBO Mol. Med. *6*, 1542–1560.

Liu, K., Cheng, L., Flesken-Nikitin, A., Huang, L., Nikitin, A.Y., and Pauli, B.U. (2010). Conditional knockout of fibronectin abrogates mouse mammary gland lobuloalveolar differentiation. Dev. Biol. *346*, 11–24.

Loskutov, Y.V., Kozyulina, P.Y., Kozyreva, V.K., Ice, R.J., Jones, B.C., Roston, T.J., Smolkin, M.B., Ivanov, A.V., Wysolmerski, R.B., and Pugacheva, E.N. (2015). NEDD9/Arf6-dependent endocytic trafficking of matrix metalloproteinase 14: a novel mechanism for blocking mesenchymal cell invasion and metastasis of breast cancer. Oncogene *34*, 3662–3675.

Lozano, E., Betson, M., and Braga, V.M.M. (2003). Tumor progression: Small GTPases and loss of cell–cell adhesion. BioEssays *25*, 452–463.

Lu, P., Ewald, A.J., Martin, G.R., and Werb, Z. (2008). Genetic mosaic analysis reveals FGF receptor 2 function in terminal end buds during mammary gland branching morphogenesis. Dev. Biol. *321*, 77–87.

Lu, P., Takai, K., Weaver, V.M., and Werb, Z. (2011). Extracellular Matrix Degradation and Remodeling in Development and Disease. Cold Spring Harb. Perspect. Biol. *3*, a005058–a005058.

Lu, P., Weaver, V.M., and Werb, Z. (2012). The extracellular matrix: A dynamic niche in cancer progression. J Cell Biol *196*, 395–406.

Luton, F. (2005). The Role of EFA6, Exchange Factor for Arf6, for Tight Junction Assembly, Functions, and Interaction with the Actin Cytoskeleton. In Methods in Enzymology, (Academic Press), pp. 332–345.

Luton, F., Klein, S., Chauvin, J.-P., Le Bivic, A., Bourgoin, S., Franco, M., and Chardin, P. (2003). EFA6, Exchange Factor for ARF6, Regulates the Actin Cytoskeleton and Associated Tight Junction in Response to E-Cadherin Engagement. Mol. Biol. Cell *15*, 1134–1145.

Macara, I.G., Guyer, R., Richardson, G., Huo, Y., and Ahmed, S.M. (2014). Epithelial homeostasis. Curr. Biol. CB *24*, R815-825.

Machacek, M., Hodgson, L., Welch, C., Elliott, H., Pertz, O., Nalbant, P., Abell, A., Johnson, G.L., Hahn, K.M., and Danuser, G. (2009). Coordination of Rho GTPase activities during cell protrusion. Nature *461*, 99–103.

Macia, E., Partisani, M., Favard, C., Mortier, E., Zimmermann, P., Carlier, M.-F., Gounon, P., Luton, F., and Franco, M. (2008). The Pleckstrin Homology Domain of the Arf6-specific Exchange Factor EFA6 Localizes to the Plasma Membrane by Interacting with Phosphatidylinositol 4,5-Bisphosphate and F-actin. J. Biol. Chem. *283*, 19836–19844.

Macia, E., Partisani, M., Paleotti, O., Luton, F., and Franco, M. (2012). Arf6 negatively controls the rapid recycling of the β2 adrenergic receptor. J Cell Sci *125*, 4026–4035.

Macias, H., and Hinck, L. (2012). Mammary gland development: Mammary gland development. Wiley Interdiscip. Rev. Dev. Biol. *1*, 533–557.

Madaule, P., and Axel, R. (1985). A novel ras-related gene family. Cell *41*, 31–40.

Maller, O., Martinson, H., and Schedin, P. (2010). Extracellular Matrix Composition Reveals Complex and Dynamic Stromal-Epithelial Interactions in the Mammary Gland. J. Mammary Gland Biol. Neoplasia *15*, 301–318.

Malliri, A., and Collard, J.G. (2003). Role of Rho-family proteins in cell adhesion and cancer. Curr. Opin. Cell Biol. *15*, 583–589.

Man, Y.-G., and Sang, Q.-X.A. (2004). The significance of focal myoepithelial cell layer disruptions in human breast tumor invasion: a paradigm shift from the "protease-centered" hypothesis. Exp. Cell Res. *301*, 103–118.

Man, Y., Tai, L., Barner, R., Vang, R., Saenger, J.S., Shekitka, K.M., Bratthauer, G.L., Wheeler, D.T., Liang, C.Y., Vinh, T.N., et al. (2003). Cell clusters overlying focally disrupted mammary myoepithelial cell layers and adjacent cells within the same duct display different immunohistochemical and genetic features: implications for tumor progression and invasion. Breast Cancer Res. *5*.

Marchesin, V., Castro-Castro, A., Lodillinsky, C., Castagnino, A., Cyrta, J., Bonsang-Kitzis, H., Fuhrmann, L., Irondelle, M., Infante, E., Montagnac, G., et al. (2015a). ARF6–JIP3/4 regulate endosomal tubules for MT1-MMP exocytosis in cancer invasion. J Cell Biol *211*, 339–358.

Marchesin, V., Montagnac, G., and Chavrier, P. (2015b). ARF6 Promotes the Formation of Rac1 and WAVE-Dependent Ventral F-Actin Rosettes in Breast Cancer Cells in Response to Epidermal Growth Factor. PLOS ONE *10*, e0121747.

Martin, K., Reimann, A., Fritz, R.D., Ryu, H., Jeon, N.L., and Pertz, O. (2016). Spatio-temporal co-ordination of RhoA, Rac1 and Cdc42 activation during prototypical edge protrusion and retraction dynamics. Sci. Rep. *6*.

Masson, R., Lefebvre, O., Noël, A., Fahime, M.E., Chenard, M.-P., Wendling, C., Kebers, F., LeMeur, M., Dierich, A., Foidart, J.-M., et al. (1998). In Vivo Evidence That the Stromelysin-3 Metalloproteinase Contributes in a Paracrine Manner to Epithelial Cell Malignancy. J. Cell Biol. *140*, 1535–1541.

McDaniel, S.M., Rumer, K.K., Biroc, S.L., Metz, R.P., Singh, M., Porter, W., and Schedin, P. (2006). Remodeling of the Mammary Microenvironment after Lactation Promotes Breast Tumor Cell Metastasis. Am. J. Pathol. *168*, 608–620.

Melendez, J., Grogg, M., and Zheng, Y. (2011). Signaling Role of Cdc42 in Regulating Mammalian Physiology. J. Biol. Chem. *286*, 2375–2381.

Mendez, M.G., Kojima, S.-I., and Goldman, R.D. (2010). Vimentin induces changes in cell shape, motility, and adhesion during the epithelial to mesenchymal transition. FASEB J. *24*, 1838–1851.

Menon, S., and Beningo, K.A. (2011). Cancer Cell Invasion Is Enhanced by Applied Mechanical Stimulation. PLOS ONE *6*, e17277.

Merlo, L.M.F., Pepper, J.W., Reid, B.J., and Maley, C.C. (2006). Cancer as an evolutionary and ecological process. Nat. Rev. Cancer *6*, 924–935.

Micalizzi, D.S., Farabaugh, S.M., and Ford, H.L. (2010). Epithelial-Mesenchymal Transition in Cancer: Parallels Between Normal Development and Tumor Progression. J. Mammary Gland Biol. Neoplasia *15*, 117–134.

Mierke, C.T., Frey, B., Fellner, M., Herrmann, M., and Fabry, B. (2011). Integrin α5β1 facilitates cancer cell invasion through enhanced contractile forces. J Cell Sci *124*, 369–383.

Milanini, J., Fayad, R., Partisani, M., Lecine, P., Borg, J.-P., Franco, M., and Luton, F. (2018). EFA6 proteins regulate lumen formation through α-actinin 1. J Cell Sci *131*, jcs209361.

Milella, M., Falcone, I., Conciatori, F., Cesta Incani, U., Del Curatolo, A., Inzerilli, N., Nuzzo, C.M.A., Vaccaro, V., Vari, S., Cognetti, F., et al. (2015). PTEN: Multiple Functions in Human Malignant Tumors. Front. Oncol. *5*, 24.

Mohammadi, H., and Sahai, E. (2018). Mechanisms and impact of altered tumour mechanics. Nat. Cell Biol. *20*, 766.

Montagnac, G., de Forges, H., Smythe, E., Gueudry, C., Romao, M., Salamero, J., and Chavrier, P. (2011). Decoupling of Activation and Effector Binding Underlies ARF6 Priming of Fast Endocytic Recycling. Curr. Biol. *21*, 574–579.

Montell, D.J., Yoon, W.H., and Starz-Gaiano, M. (2012). Group choreography: mechanisms orchestrating the collective movement of border cells. Nat. Rev. Mol. Cell Biol. *13*, 631–645.

Moody, S.E., Perez, D., Pan, T., Sarkisian, C.J., Portocarrero, C.P., Sterner, C.J., Notorfrancesco, K.L., Cardiff, R.D., and Chodosh, L.A. (2005). The transcriptional repressor Snail promotes mammary tumor recurrence. Cancer Cell *8*, 197–209.

Moon, S. (2003). Rho GTPase-activating proteins in cell regulation. Trends Cell Biol. *13*, 13–22.

Morel, A.-P., Lièvre, M., Thomas, C., Hinkal, G., Ansieau, S., and Puisieux, A. (2008). Generation of Breast Cancer Stem Cells through Epithelial-Mesenchymal Transition. PLOS ONE *3*, e2888.

Morel, A.-P., Ginestier, C., Pommier, R.M., Cabaud, O., Ruiz, E., Wicinski, J., Devouassoux-Shisheboran, M., Combaret, V., Finetti, P., Chassot, C., et al. (2017). A stemness-related ZEB1–MSRB3 axis governs cellular pliancy and breast cancer genome stability. Nat. Med. *23*, 568–578.

Moreno-Bueno, G., Portillo, F., and Cano, A. (2008). Transcriptional regulation of cell polarity in EMT and cancer. Oncogene *27*, 6958–6969.

Mori, H., Lo, A.T., Inman, J.L., Alcaraz, J., Ghajar, C.M., Mott, J.D., Nelson, C.M., Chen, C.S., Zhang, H., Bascom, J.L., et al. (2013). Transmembrane/cytoplasmic, rather than catalytic, domains of Mmp14 signal to MAPK activation and mammary branching morphogenesis via binding to integrin 1. Development *140*, 343–352.

Morishige, M., Hashimoto, S., Ogawa, E., Toda, Y., Kotani, H., Hirose, M., Wei, S., Hashimoto, A., Yamada, A., Yano, H., et al. (2008). GEP100 links epidermal growth factor receptor signalling to Arf6 activation to induce breast cancer invasion. Nat. Cell Biol. *10*, 85–92.

Morse, E.M., Sun, X., Olberding, J.R., Ha, B.H., Boggon, T.J., and Calderwood, D.A. (2016). PAK6 targets to cell–cell adhesions through its N-terminus in a Cdc42-dependent manner to drive epithelial colony escape. J. Cell Sci. *129*, 380–393.

Moss, J., and Vaughan, M. (1995). Structure and Function of ARF Proteins: Activators of Cholera Toxin and Critical Components of Intracellular Vesicular Transport Processes. J. Biol. Chem. *270*, 12327–12330.

Moumen, M., Chiche, A., Cagnet, S., Petit, V., Raymond, K., Faraldo, M.M., Deugnier, M.-A., and Glukhova, M.A. (2011). The mammary myoepithelial cell. Int. J. Dev. Biol. *55*, 763–771.

Murata, T., Arii, S., Nakamura, T., Mori, A., Kaido, T., Furuyama, H., Furumoto, K., Nakao, T., Isobe, N., and Imamura, M. (2001). Inhibitory effect of Y-27632, a ROCK inhibitor, on progression of rat liver fibrosis in association with inactivation of hepatic stellate cells. J. Hepatol. *35*, 474–481.

Murdoch, C., Muthana, M., Coffelt, S.B., and Lewis, C.E. (2008). The role of myeloid cells in the promotion of tumour angiogenesis. Nat. Rev. Cancer *8*, 618–631.

Murphy, A.M., and Montell, D.J. (1996). Cell type-specific roles for Cdc42, Rac, and RhoL in Drosophila oogenesis. J. Cell Biol. *133*, 617–630.

Muschler, J., and Streuli, C.H. (2010). Cell-Matrix Interactions in Mammary Gland Development and Breast Cancer. Cold Spring Harb. Perspect. Biol. *2*, a003202–a003202.

Myllyharju, J., and Kivirikko, K.I. (2004). Collagens, modifying enzymes and their mutations in humans, flies and worms. Trends Genet. *20*, 33–43.

Naba, A., Clauser, K.R., Lamar, J.M., Carr, S.A., and Hynes, R.O. (2014). Extracellular matrix signatures of human mammary carcinoma identify novel metastasis promoters. ELife *3*, e01308.

Naccarato, A.G., Viacava, P., Vignati, S., Fanelli, G., Bonadio, A.G., Montruccoli, G., and Bevilacqua, G. (2000). Bio-morphological events in the development of the human female mammary gland from fetal age to puberty. Virchows Arch. Int. J. Pathol. *436*, 431–438.

Nakajima, S. (2004). N-Cadherin Expression and Epithelial-Mesenchymal Transition in Pancreatic Carcinoma. Clin. Cancer Res. *10*, 4125–4133.

Nakopoulou, L., Giannopoulou, I., Stefanaki, K., Panayotopoulou, E., Tsirmpa, I., Alexandrou, P., Mavrommatis, J., Katsarou, S., and Davaris, P. (2002). Enhanced mRNA expression of tissue inhibitor of metalloproteinase-1 (TIMP-1) in breast carcinomas is correlated with adverse prognosis. J. Pathol. *197*, 307–313.

Nalbant, P. (2004). Activation of Endogenous Cdc42 Visualized in Living Cells. Science *305*, 1615–1619.

Naslavsky, N., Weigert, R., and Donaldson, J.G. (2004). Characterization of a Nonclathrin Endocytic Pathway: Membrane Cargo and Lipid Requirements. Mol. Biol. Cell *15*, 3542–3552.

Navarro, C., Nola, S., Audebert, S., Santoni, M.-J., Arsanto, J.-P., Ginestier, C., Marchetto, S., Jacquemier, J., Isnardon, D., Le Bivic, A., et al. (2005). Junctional recruitment of mammalian Scribble relies on E-cadherin engagement. Oncogene *24*, 4330–4339.

Naylor, M.J., Li, N., Cheung, J., Lowe, E.T., Lambert, E., Marlow, R., Wang, P., Schatzmann, F., Wintermantel, T., Schüetz, G., et al. (2005). Ablation of β1 integrin in mammary epithelium reveals a key role for integrin in glandular morphogenesis and differentiation. J. Cell Biol. *171*, 717–728.

Nerger, B.A., and Nelson, C.M. (2018). 3D culture models for studying branching morphogenesis in the mammary gland and mammalian lung. Biomaterials.

Neumann, N.M., Perrone, M.C., Veldhuis, J.H., Huebner, R.J., Zhan, H., Devreotes, P.N., Brodland, G.W., and Ewald, A.J. (2018). Coordination of Receptor Tyrosine Kinase Signaling and Interfacial Tension Dynamics Drives Radial Intercalation and Tube Elongation. Dev. Cell *45*, 67-82.e6.

Nguyen-Ngoc, K.-V., Cheung, K.J., Brenot, A., Shamir, E.R., Gray, R.S., Hines, W.C., Yaswen, P., Werb, Z., and Ewald, A.J. (2012). ECM microenvironment regulates collective migration and local dissemination in normal and malignant mammary epithelium. Proc. Natl. Acad. Sci. *109*, E2595–E2604.

Nikolaev, A., and Yang, E.S. (2017). The Impact of DNA Repair Pathways in Cancer Biology and Therapy. Cancers *9*, 126.

Nik-Zainal, S., and Morganella, S. (2017). Mutational Signatures in Breast Cancer: The Problem at the DNA Level. Clin. Cancer Res. Off. J. Am. Assoc. Cancer Res. *23*, 2617–2629.

Nishida, N., Yano, H., Nishida, T., Kamura, T., and Kojiro, M. (2006). Angiogenesis in Cancer. Vasc. Health Risk Manag. *2*, 213–219.

Olmeda, D., Moreno-Bueno, G., Flores, J.M., Fabra, A., Portillo, F., and Cano, A. (2007). SNAI1 Is Required for Tumor Growth and Lymph Node Metastasis of Human Breast Carcinoma MDA-MB-231 Cells. Cancer Res. *67*, 11721–11731.

Olmeda, D., Montes, A., Moreno-Bueno, G., Flores, J.M., Portillo, F., and Cano, A. (2008). Snai1 and Snai2 collaborate on tumor growth and metastasis properties of mouse skin carcinoma cell lines. Oncogene *27*, 4690–4701.

Olofsson, B. Rho Guanine Dissociation Inhibitors: Pivotal Molecules in Cellular Signalling. 10.

Olson, M.F. (2004). Contraction reaction: mechanical regulation of Rho GTPase. Trends Cell Biol. *14*, 111–114.

Olson, M.F., Ashworth, A., and Hall, A. (1995). An essential role for Rho, Rac, and Cdc42 GTPases in cell cycle progression through G1. Science *269*, 1270–1272.

Onder, T.T., Gupta, P.B., Mani, S.A., Yang, J., Lander, E.S., and Weinberg, R.A. (2008). Loss of E-Cadherin Promotes Metastasis via Multiple Downstream Transcriptional Pathways. Cancer Res. *68*, 3645–3654.

Onodera, Y., Hashimoto, S., Hashimoto, A., Morishige, M., Mazaki, Y., Yamada, A., Ogawa, E., Adachi, M., Sakurai, T., Manabe, T., et al. (2005). Expression of AMAP1, an ArfGAP, provides novel targets to inhibit breast cancer invasive activities. EMBO J. *24*, 963–973.

O'Rourke, S.M., Christensen, S.N., and Bowerman, B. (2010). *Caenorhabditis elegans* EFA-6 limits microtubule growth at the cell cortex. Nat. Cell Biol. *12*, 1235–1241.

Osborne, C., Wilson, P., and Tripathy, D. (2004). Oncogenes and Tumor Suppressor Genes in Breast Cancer: Potential Diagnostic and Therapeutic Applications. The Oncologist *9*, 361–377.

Oskarsson, T. (2013). Extracellular matrix components in breast cancer progression and metastasis. The Breast *22*, S66–S72.

Ozdamar, B., Bose, R., Barrios-Rodiles, M., Wang, H.-R., Zhang, Y., and Wrana, J.L. (2005). Regulation of the polarity protein Par6 by TGFbeta receptors controls epithelial cell plasticity. Science *307*, 1603–1609.

Padovani, D., Folly-Klan, M., Labarde, A., Boulakirba, S., Campanacci, V., Franco, M., Zeghouf, M., and Cherfils, J. (2014). EFA6 controls Arf1 and Arf6 activation through a negative feedback loop. Proc. Natl. Acad. Sci. *111*, 12378–12383.

Palacios, F., Price, L., Schweitzer, J., Collard, J.G., and D'Souza-Schorey, C. (2001). An essential role for ARF6-regulated membrane traffic in adherens junction turnover and epithelial cell migration. EMBO J. *20*, 4973–4986.

Palacios, F., Schweitzer, J.K., Boshans, R.L., and D'Souza-Schorey, C. (2002). ARF6-GTP recruits Nm23-H1 to facilitate dynamin-mediated endocytosis during adherens junctions disassembly. Nat. Cell Biol. *4*, 929–936.

Palacios, F., Tushir, J.S., Fujita, Y., and D'Souza-Schorey, C. (2005). Lysosomal Targeting of E-Cadherin: a Unique Mechanism for the Down-Regulation of Cell-Cell Adhesion during Epithelial to Mesenchymal Transitions. Mol. Cell. Biol. *25*, 389–402.

Paňková, K., Rösel, D., Novotný, M., and Brábek, J. (2010). The molecular mechanisms of transition between mesenchymal and amoeboid invasiveness in tumor cells. Cell. Mol. Life Sci. *67*, 63–71.

Paolillo, M., and Schinelli, S. (2017). Integrins and Exosomes, a Dangerous Liaison in Cancer Progression. Cancers *9*, 95.

Parri, M., and Chiarugi, P. (2010). Rac and Rho GTPases in cancer cell motility control. Cell Commun. Signal. *8*, 23.

Paszek, M.J., and Weaver, V.M. (2004). The tension mounts: mechanics meets morphogenesis and malignancy. J. Mammary Gland Biol. Neoplasia *9*, 325–342.

Paszek, M.J., Zahir, N., Johnson, K.R., Lakins, J.N., Rozenberg, G.I., Gefen, A., Reinhart-King, C.A., Margulies, S.S., Dembo, M., Boettiger, D., et al. (2005a). Tensional homeostasis and the malignant phenotype. Cancer Cell *8*, 241–254.

Paszek, M.J., Zahir, N., Johnson, K.R., Lakins, J.N., Rozenberg, G.I., Gefen, A., Reinhart-King, C.A., Margulies, S.S., Dembo, M., Boettiger, D., et al. (2005b). Tensional homeostasis and the malignant phenotype. Cancer Cell *8*, 241–254.

Peinado, H., Portillo, F., and Cano, A. (2005). Switching On-Off Snail: LOXL2 Versus GSK3? Cell Cycle *4*, 1749–1752.

Peng, J., Wallar, B.J., Flanders, A., Swiatek, P.J., and Alberts, A.S. (2003). Disruption of the Diaphanous-Related Formin Drf1 Gene Encoding mDia1 Reveals a Role for Drf3 as an Effector for Cdc42. Curr. Biol. *13*, 534–545.

Perou, C.M., Sørlie, T., Eisen, M.B., van de Rijn, M., Jeffrey, S.S., Rees, C.A., Pollack, J.R., Ross, D.T., Johnsen, H., Akslen, L.A., et al. (2000). Molecular portraits of human breast tumours. Nature *406*, 747–752.

Perrais, M., Chen, X., Perez-Moreno, M., and Gumbiner, B.M. (2007). E-Cadherin Homophilic Ligation Inhibits Cell Growth and Epidermal Growth Factor Receptor Signaling Independently of Other Cell Interactions. Mol. Biol. Cell *18*, 2013–2025.

Pichot, C.S., Arvanitis, C., Hartig, S.M., Jensen, S.A., Bechill, J., Marzouk, S., Yu, J., Frost, J.A., and Corey, S.J. (2010). Cdc42-Interacting Protein 4 Promotes Breast Cancer Cell Invasion and Formation of Invadopodia through Activation of N-WASp. Cancer Res. *70*, 8347–8356.

Pickup, M.W., Mouw, J.K., and Weaver, V.M. (2014). The extracellular matrix modulates the hallmarks of cancer. EMBO Rep. *15*, 1243–1253.

Pils, D., Horak, P., Gleiss, A., Sax, C., Fabjani, G., Moebus, V.J., Zielinski, C., Reinthaller, A., Zeillinger, R., and Krainer, M. (2005). Five genes from chromosomal band 8p22 are significantly down-regulated in ovarian carcinoma. Cancer *104*, 2417–2429.

Piotrowski-Daspit, A.S., Nerger, B.A., Wolf, A.E., Sundaresan, S., and Nelson, C.M. (2017). Dynamics of Tissue-Induced Alignment of Fibrous Extracellular Matrix. Biophys. J. *113*, 702–713.

Pitelka, D.R., Hamamoto, S.T., Duafala, J.G., and Nemanic, M.K. (2009). Cell contacts in the mouse mammary gland: I. Normal Gland in Postnatal Development and the Secretory Cycle. J. Mammary Gland Biol. Neoplasia *14*, 295–316.

Place, A.E., Jin Huh, S., and Polyak, K. (2011). The microenvironment in breast cancer progression: biology and implications for treatment. Breast Cancer Res. *13*.

Plaks, V., Brenot, A., Lawson, D.A., Linnemann, J.R., Van Kappel, E.C., Wong, K.C., de Sauvage, F., Klein, O.D., and Werb, Z. (2013). Lgr5-expressing cells are sufficient and necessary for postnatal mammary gland organogenesis. Cell Rep. *3*, 70–78.

Poincloux, R., Lizárraga, F., and Chavrier, P. (2009). Matrix invasion by tumour cells: a focus on MT1-MMP trafficking to invadopodia. J Cell Sci *122*, 3015–3024.

Poincloux, R., Collin, O., Lizárraga, F., Romao, M., Debray, M., Piel, M., and Chavrier, P. (2011). Contractility of the cell rear drives invasion of breast tumor cells in 3D Matrigel. Proc. Natl. Acad. Sci. *108*, 1943–1948.

Polyak, K., and Weinberg, R.A. (2009). Transitions between epithelial and mesenchymal states: acquisition of malignant and stem cell traits. Nat. Rev. Cancer *9*, 265–273.

Powelka, A.M., Sun, J., Li, J., Gao, M., Shaw, L.M., Sonnenberg, A., and Hsu, V.W. (2003). Stimulation-Dependent Recycling of Integrin β1 Regulated by ARF6 and Rab11. Traffic *5*, 20–36.

Prat, A., and Perou, C.M. (2009). Mammary development meets cancer genomics. Nat. Med. *15*, 842–844.

Prat, A., and Perou, C.M. (2011a). Deconstructing the molecular portraits of breast cancer. Mol. Oncol. *5*, 5–23.

Prat, A., and Perou, C.M. (2011b). Deconstructing the molecular portraits of breast cancer. Mol. Oncol. *5*, 5–23.

Prat, A., Adamo, B., Cheang, M.C.U., Anders, C.K., Carey, L.A., and Perou, C.M. (2013). Molecular Characterization of Basal-Like and Non-Basal-Like Triple-Negative Breast Cancer. The Oncologist *18*, 123–133.

Prince, J.M., Klinowska, T.C.M., Marshman, E., Lowe, E.T., Mayer, U., Miner, J., Aberdam, D., Vestweber, D., Gusterson, B., and Streuli, C.H. (2002). Cell–matrix interactions during development and apoptosis of the mouse mammary gland in vivo. Dev. Dyn. *223*, 497–516.

Provenzano, P.P., Eliceiri, K.W., Campbell, J.M., Inman, D.R., White, J.G., and Keely, P.J. (2006). Collagen reorganization at the tumor-stromal interface facilitates local invasion. BMC Med. *4*, 38.

Provenzano, P.P., Inman, D.R., Eliceiri, K.W., Knittel, J.G., Yan, L., Rueden, C.T., White, J.G., and Keely, P.J. (2008). Collagen density promotes mammary tumor initiation and progression. BMC Med. *6*, 11.

Provenzano, P.P., Inman, D.R., Eliceiri, K.W., and Keely, P.J. (2009). Matrix density-induced mechanoregulation of breast cell phenotype, signaling and gene expression through a FAK–ERK linkage. Oncogene *28*, 4326–4343.

Puisieux, A., Valsesia-Wittmann, S., and Ansieau, S. (2006). A twist for survival and cancer progression. Br. J. Cancer *94*, 13–17.

Puisieux, A., Brabletz, T., and Caramel, J. (2014a). Oncogenic roles of EMT-inducing transcription factors. Nat. Cell Biol. *16*, 488–494.

Puisieux, A., Brabletz, T., and Caramel, J. (2014b). Oncogenic roles of EMT-inducing transcription factors. Nat. Cell Biol. *16*, 488–494.

Pulgar, T.G. del, Benitah, S.A., Valerón, P.F., Espina, C., and Lacal, J.C. (2005). Rho GTPase expression in tumourigenesis: Evidence for a significant link. BioEssays *27*, 602–613.

Qiu, R.G., Chen, J., McCormick, F., and Symons, M. (1995a). A role for Rho in Ras transformation. Proc. Natl. Acad. Sci. *92*, 11781–11785.

Qiu, R.-G., Chen, J., Kirn, D., McCormick, F., and Symons, M. (1995b). An essential role for Rac in Ras transformation. Nature *374*, 457–459.

Qiu, R.G., Abo, A., McCormick, F., and Symons, M. (1997). Cdc42 regulates anchorage-independent growth and is necessary for Ras transformation. Mol. Cell. Biol. *17*, 3449–3458.

Radice, G.L., Ferreira-Cornwell, M.C., Robinson, S.D., Rayburn, H., Chodosh, L.A., Takeichi, M., and Hynes, R.O. (1997). Precocious Mammary Gland Development in P-Cadherin–deficient Mice. J. Cell Biol. *139*, 1025–1032.

Radice, G.L., Sauer, C.L., Kostetskii, I., Peralta Soler, A., and Knudsen, K.A. (2003). Inappropriate P-cadherin expression in the mouse mammary epithelium is compatible with normal mammary gland function. Differ. Res. Biol. Divers. *71*, 361–373.

Radisky, E.S., and Radisky, D.C. (2010). Matrix Metalloproteinase-Induced Epithelial-Mesenchymal Transition in Breast Cancer. J. Mammary Gland Biol. Neoplasia *15*, 201–212.

Ramirez, N.E., Zhang, Z., Madamanchi, A., Boyd, K.L., O'Rear, L.D., Nashabi, A., Li, Z., Dupont, W.D., Zijlstra, A., and Zutter, M.M. (2011). The α2β1 integrin is a metastasis suppressor in mouse models and human cancer.

Ramovs, V., te Molder, L., and Sonnenberg, A. (2017). The opposing roles of laminin-binding integrins in cancer. Matrix Biol. *57–58*, 213–243.

Randazzo, P.A., and Hirsch, D.S. (2004). Arf GAPs: multifunctional proteins that regulate membrane traffic and actin remodelling. Cell. Signal. *16*, 401–413.

Raymond, K., Cagnet, S., Kreft, M., Janssen, H., Sonnenberg, A., and Glukhova, M.A. (2011). Control of mammary myoepithelial cell contractile function by α3β1 integrin signalling: Integrin signalling in the myoepithelium. EMBO J. *30*, 1896–1906.

Raymond, K., Faraldo, M.M., Deugnier, M.-A., and Glukhova, M.A. (2012). Integrins in mammary development. Semin. Cell Dev. Biol. *23*, 599–605.

Rebustini, I.T., Patel, V.N., Stewart, J.S., Layvey, A., Georges-Labouesse, E., Miner, J.H., and Hoffman, M.P. (2007). Laminin α5 is necessary for submandibular gland epithelial morphogenesis and influences FGFR expression through β1 integrin signaling. Dev. Biol. *308*, 15–29.

Ree, A.H., Florenes, V.A., Berg, J.P., Maelandsmo, G.M., Nesland, J.M., and Fodstad, O. (1997). High levels of messenger RNAs for tissue inhibitors of metalloproteinases (TIMP-1 and TIMP-2) in primary breast carcinomas are associated with development of distant metastases. Clin. Cancer Res. Off. J. Am. Assoc. Cancer Res. *3*, 1623–1628.

Reversi, A., Cassoni, P., and Chini, B. (2005). Oxytocin Receptor Signaling in Myoepithelial and Cancer Cells. J. Mammary Gland Biol. Neoplasia *10*, 221–229.

Ribelles, N., Santonja, A., Pajares, B., Llácer, C., and Alba, E. (2014). The seed and soil hypothesis revisited: Current state of knowledge of inherited genes on prognosis in breast cancer. Cancer Treat. Rev. *40*, 293–299.

Ridley, A.J. (2001a). Rho family proteins: coordinating cell responses. Trends Cell Biol. *11*, 471–477.

Ridley, A.J. (2001b). Rho GTPases and cell migration. J. Cell Sci. *114*, 2713–2722.

Ridley, A.J. (2004). Rho proteins and cancer. Breast Cancer Res. Treat. *84*, 13–19.

Ridley, A.J. (2011). Life at the Leading Edge. Cell *145*, 1012–1022.

Ridley, A.J. (2015). Rho GTPase signalling in cell migration. Curr. Opin. Cell Biol. *36*, 103–112.

Ridley, A.J., and Hall, A. (1992). The small GTP-binding protein rho regulates the assembly of focal adhesions and actin stress fibers in response to growth factors. Cell *70*, 389–399.

Ridley, A.J., Paterson, H.F., Johnston, C.L., Diekmann, D., and Hall, A. (1992). The small GTP-binding protein rac regulates growth factor-induced membrane ruffling. Cell *70*, 401–410.

Riento, K., and Ridley, A.J. (2003). ROCKs: multifunctional kinases in cell behaviour. Nat. Rev. Mol. Cell Biol. *4*, 446–456.

Rihet, S., Vielh, P., Camonis, J., Goud, B., Chevillard, S., and Gunzburg, J. (2001). Mutation status of genes encoding RhoA, Rac1, and Cdc42 GTPases in a panel of invasive human colorectal and breast tumors. J. Cancer Res. Clin. Oncol. *127*, 733–738.

Rios, A.C., Fu, N.Y., Lindeman, G.J., and Visvader, J.E. (2014). In situ identification of bipotent stem cells in the mammary gland. Nature *506*, 322–327.

Runswick, S.K., O'Hare, M.J., Jones, L., Streuli, C.H., and Garrod, D.R. (2001). Desmosomal adhesion regulates epithelial morphogenesis and cell positioning. Nat. Cell Biol. *3*, 823–830.

Sabe, H. (2003). Requirement for Arf6 in Cell Adhesion, Migration, and Cancer Cell Invasion. J. Biochem. (Tokyo) *134*, 485–489.

Sabe, H., Onodera, Y., Mazaki, Y., and Hashimoto, S. (2006). ArfGAP family proteins in cell adhesion, migration and tumor invasion. Curr. Opin. Cell Biol. *18*, 558–564.

Sahai, E. (2005). Mechanisms of cancer cell invasion. Curr. Opin. Genet. Dev. *15*, 87–96.

Sahai, E., and Marshall, C.J. (2002). RHO–GTPases and cancer. Nat. Rev. Cancer *2*, 133–142.

Sakagami, H. (2008). The EFA6 Family: Guanine Nucleotide Exchange Factors for ADP Ribosylation Factor 6 at Neuronal Synapses. Tohoku J. Exp. Med. *214*, 191–198.

Sakagami, H., Matsuya, S., Nishimura, H., Suzuki, R., and Kondo, H. (2004). Somatodendritic localization of the mRNA for EFA6A, a guanine nucleotide exchange protein for ARF6, in rat hippocampus and its involvement in dendritic formation. Eur. J. Neurosci. *19*, 863–870.

Sakagami, H., Suzuki, H., Kamata, A., Owada, Y., Fukunaga, K., Mayanagi, H., and Kondo, H. (2006). Distinct spatiotemporal expression of EFA6D, a guanine nucleotide exchange factor for ARF6, among the EFA6 family in mouse brain. Brain Res. *1093*, 1–11.

Sakagami, H., Honma, T., Sukegawa, J., Owada, Y., Yanagisawa, T., and Kondo, H. (2007). Somatodendritic localization of EFA6A, a guanine nucleotide exchange factor for ADP-ribosylation factor 6, and its possible interaction with α-actinin in dendritic spines. Eur. J. Neurosci. *25*, 618–628.

Sakakura, T., Nishizuka, Y., and Dawe, C. (1976). Mesenchyme-dependent morphogenesis and epithelium-specific cytodifferentiation in mouse mammary gland. Science *194*, 1439–1441.

Satija, R., Farrell, J.A., Gennert, D., Schier, A.F., and Regev, A. (2015). Spatial reconstruction of single-cell gene expression data. Nat. Biotechnol. *33*, 495–502.

Schedin, P., and Keely, P.J. (2011). Mammary Gland ECM Remodeling, Stiffness, and Mechanosignaling in Normal Development and Tumor Progression. Cold Spring Harb. Perspect. Biol. *3*, a003228.

Schedin, P., O'Brien, J., Rudolph, M., Stein, T., and Borges, V. (2007). Microenvironment of the Involuting Mammary Gland Mediates Mammary Cancer Progression. J. Mammary Gland Biol. Neoplasia *12*, 71–82.

Scheel, C., and Weinberg, R.A. (2012). Cancer stem cells and epithelial–mesenchymal transition: Concepts and molecular links. Semin. Cancer Biol. *22*, 396–403.

Schlienger, S., Campbell, S., Claing, A., and Gutkind, J.S. (2013). ARF1 regulates the Rho/MLC pathway to control EGF-dependent breast cancer cell invasion. Mol. Biol. Cell *25*, 17–29.

Schlienger, S., Ramirez, R.A.M., and Claing, A. (2015). ARF1 regulates adhesion of MDA-MB-231 invasive breast cancer cells through formation of focal adhesions. Cell. Signal. *27*, 403–415.

Schmidt, A. (2002). Guanine nucleotide exchange factors for Rho GTPases: turning on the switch. Genes Dev. *16*, 1587–1609.

Schmidt, M., Victor, A., Bratzel, D., Boehm, D., Cotarelo, C., Lebrecht, A., Siggelkow, W., Hengstler, J.G., Elsässer, A., Gehrmann, M., et al. (2009). Long-term outcome prediction by clinicopathological risk classification algorithms in node-negative breast cancer--comparison between Adjuvant!, St Gallen, and a novel risk algorithm used in the prospective randomized Node-Negative-Breast Cancer-3 (NNBC-3) trial. Ann. Oncol. Off. J. Eur. Soc. Med. Oncol. *20*, 258–264.

Schnelzer, A., Prechtel, D., Knaus, U., Dehne, K., Gerhard, M., Graeff, H., Harbeck, N., Schmitt, M., and Lengyel, E. (2000). Rac1 in human breast cancer: overexpression, mutation analysis and characterization of a new isoform, Rac1b. Oncogene *19*, 3013–3020.

Schoumacher, M., Goldman, R.D., Louvard, D., and Vignjevic, D.M. (2010). Actin, microtubules, and vimentin intermediate filaments cooperate for elongation of invadopodia. J. Cell Biol. *189*, 541–556.

Schweitzer, J.K., Sedgwick, A.E., and D'Souza-Schorey, C. (2011a). ARF6-mediated endocytic recycling impacts cell movement, cell division and lipid homeostasis. Semin. Cell Dev. Biol. *22*, 39–47.

Schweitzer, J.K., Sedgwick, A.E., and D'Souza-Schorey, C. (2011b). ARF6-mediated endocytic recycling impacts cell movement, cell division and lipid homeostasis. Semin. Cell Dev. Biol. *22*, 39–47.

Seguin, L., Desgrosellier, J.S., Weis, S.M., and Cheresh, D.A. (2015). Integrins and cancer: regulators of cancer stemness, metastasis, and drug resistance. Trends Cell Biol. *25*, 234–240.

Selamat, W., Tay, P.-L.F., Baskaran, Y., and Manser, E. (2015). The Cdc42 Effector Kinase PAK4 Localizes to Cell-Cell Junctions and Contributes to Establishing Cell Polarity. PLOS ONE *10*, e0129634.

Seldin, L., Le Guelte, A., and Macara, I.G. (2017). Epithelial plasticity in the mammary gland. Curr. Opin. Cell Biol. *49*, 59–63.

Shackleton, M., Vaillant, F., Simpson, K.J., Stingl, J., Smyth, G.K., Asselin-Labat, M.-L., Wu, L., Lindeman, G.J., and Visvader, J.E. (2006). Generation of a functional mammary gland from a single stem cell. Nature *439*, 84–88.

Shamir, E.R., and Ewald, A.J. (2015). Adhesion in Mammary Development. In Current Topics in Developmental Biology, (Elsevier), pp. 353–382.

Shamir, E.R., Pappalardo, E., Jorgens, D.M., Coutinho, K., Tsai, W.-T., Aziz, K., Auer, M., Tran, P.T., Bader, J.S., and Ewald, A.J. (2014). Twist1-induced dissemination preserves epithelial identity and requires E-cadherin. J. Cell Biol. *204*, 839–856.

Shamir, E.R., Coutinho, K., Georgess, D., Auer, M., and Ewald, A.J. (2016). Twist1-positive epithelial cells retain adhesive and proliferative capacity throughout dissemination. Biol. Open *5*, 1216–1228.

Shapiro, E., Biezuner, T., and Linnarsson, S. (2013). Single-cell sequencing-based technologies will revolutionize whole-organism science. Nat. Rev. Genet. *14*, 618–630.

Shirakihara, T., Kawasaki, T., Fukagawa, A., Semba, K., Sakai, R., Miyazono, K., Miyazawa, K., and Saitoh, M. (2013). Identification of integrin α3 as a molecular marker of cells undergoing epithelial–mesenchymal transition and of cancer cells with aggressive phenotypes. Cancer Sci. *104*, 1189–1197.

Simi, A.K., Pang, M.-F., and Nelson, C.M. (2018). Extracellular Matrix Stiffness Exists in a Feedback Loop that Drives Tumor Progression. In Biomechanics in Oncology, C. Dong, N. Zahir, and K. Konstantopoulos, eds. (Cham: Springer International Publishing), pp. 57–67.

Sirka, O.K., Shamir, E.R., and Ewald, A.J. (2018). Myoepithelial cells are a dynamic barrier to epithelial dissemination. J. Cell Biol. *217*, 3368–3381.

Sironi, C., Teesalu, T., Muggia, A., Fontana, G., Marino, F., Savaresi, S., and Talarico, D. (2009). EFA6A encodes two isoforms with distinct biological activities in neuronal cells. J Cell Sci *122*, 2108–2118.

Snapper, S.B., Takeshima, F., Antón, I., Liu, C.-H., Thomas, S.M., Nguyen, D., Dudley, D., Fraser, H., Purich, D., Lopez-Ilasaca, M., et al. (2001). N-WASP deficiency reveals distinct pathways for cell surface projections and microbial actin-based motility. Nat. Cell Biol. *3*, 897–904.

Soini, Y., Tuhkanen, H., Sironen, R., Virtanen, I., Kataja, V., Auvinen, P., Mannermaa, A., and Kosma, V.-M. (2011). Transcription factors zeb1, twist and snai1 in breast carcinoma. BMC Cancer *11*, 73.

Somlyo, A.V., Bradshaw, D., Ramos, S., Murphy, C., Myers, C.E., and Somlyo, A.P. (2000). Rho-Kinase Inhibitor Retards Migration and in Vivo Dissemination of Human Prostate Cancer Cells. Biochem. Biophys. Res. Commun. *269*, 652–659.

Sorlie, T., Perou, C.M., Tibshirani, R., Aas, T., Geisler, S., Johnsen, H., Hastie, T., Eisen, M.B., van de Rijn, M., Jeffrey, S.S., et al. (2001). Gene expression patterns of breast carcinomas distinguish tumor subclasses with clinical implications. Proc. Natl. Acad. Sci. *98*, 10869–10874.

Spaderna, S., Schmalhofer, O., Wahlbuhl, M., Dimmler, A., Bauer, K., Sultan, A., Hlubek, F., Jung, A., Strand, D., Eger, A., et al. (2008). The Transcriptional Repressor ZEB1 Promotes Metastasis and Loss of Cell Polarity in Cancer. Cancer Res. *68*, 537–544.

Spike, B.T., Engle, D.D., Lin, J.C., Cheung, S.K., La, J., and Wahl, G.M. (2012). A mammary stem cell population identified and characterized in late embryogenesis reveals similarities to human breast cancer. Cell Stem Cell *10*, 183–197.

Spurlin, J.W., and Nelson, C.M. (2017). Building branched tissue structures: from single cell guidance to coordinated construction. Philos. Trans. R. Soc. B Biol. Sci. *372*, 20150527.

Spuul, P., Ciufici, P., Veillat, V., Leclercq, A., Daubon, T., Kramer, Ij., and Génot, E. (2014). Importance of RhoGTPases in formation, characteristics, and functions of invadosomes. Small GTPases *5*, e28195.

Stalder, D., Barelli, H., Gautier, R., Macia, E., Jackson, C.L., and Antonny, B. (2011). Kinetic Studies of the Arf Activator Arno on Model Membranes in the Presence of Arf Effectors Suggest Control by a Positive Feedback Loop. J. Biol. Chem. *286*, 3873–3883.

Stamnes, M. (2002). Regulating the actin cytoskeleton during vesicular transport. Curr. Opin. Cell Biol. *14*, 428–433.

Stengel, K., and Zheng, Y. (2011). Cdc42 in oncogenic transformation, invasion, and tumorigenesis. Cell. Signal. *23*, 1415–1423.

Sternlicht, M.D., and Barsky, S.H. (1997). The myoepithelial defense: a host defense against cancer. Med. Hypotheses *48*, 37–46.

Stingl, J., Eirew, P., Ricketson, I., Shackleton, M., Vaillant, F., Choi, D., Li, H.I., and Eaves, C.J. (2006). Purification and unique properties of mammary epithelial stem cells. Nature *439*, 993–997.

Suzuki, T., Kanai, Y., Hara, T., Sasaki, J., Sasaki, T., Kohara, M., Maehama, T., Taya, C., Shitara, H., Yonekawa, H., et al. (2006). Crucial Role of the Small GTPase ARF6 in Hepatic Cord Formation during Liver Development. Mol. Cell. Biol. *26*, 6149–6156.

Takai, Y., Sasaki, T., and Matozaki, T. (2001). Small GTP-Binding Proteins. Physiol. Rev. *81*, 153–208.

Tang, N.H., and Chisholm, A.D. (2016). Regulation of Microtubule Dynamics in Axon Regeneration: Insights from C. elegans. F1000Research *5*, 764.

Tao, L., Huang, G., Song, H., Chen, Y., and Chen, L. (2017). Cancer associated fibroblasts: An essential role in the tumor microenvironment. Oncol. Lett. *14*, 2611–2620.

Tapon, N., and Hall, A. (1997). Rho, Rac and Cdc42 GTPases regulate the organization of the actin cytoskeleton. Curr. Opin. Cell Biol. *9*, 86–92.

Tarin, D. (2005). The Fallacy of Epithelial Mesenchymal Transition in Neoplasia. Cancer Res. *65*, 5996–6001.

Tcherkezian, J., and Lamarche-Vane, N. (2007). Current knowledge of the large RhoGAP family of proteins. Biol. Cell *99*, 67–86.

Tevaarwerk, A.J., Gray, R.J., Schneider, B.P., Smith, M.L., Wagner, L.I., Fetting, J.H., Davidson, N., Goldstein, L.J., Miller, K.D., and Sparano, J.A. (2013). Survival in patients with metastatic recurrent breast cancer after adjuvant chemotherapy: Little evidence of improvement over the past 30 years. Cancer *119*, 1140–1148.

Théard, D., Labarrade, F., Partisani, M., Milanini, J., Sakagami, H., Fon, E.A., Wood, S.A., Franco, M., and Luton, F. (2010). USP9x-mediated deubiquitination of EFA6 regulates de novo tight junction assembly. EMBO J. *29*, 1499–1509.

Thiery, J.P., Acloque, H., Huang, R.Y.J., and Nieto, M.A. (2009). Epithelial-Mesenchymal Transitions in Development and Disease. Cell *139*, 871–890.

Thomassen, M., Tan, Q., and Kruse, T.A. (2009). Gene expression meta-analysis identifies chromosomal regions and candidate genes involved in breast cancer metastasis. Breast Cancer Res. Treat. *113*, 239–249.

Thompson, W.D. (1994). Genetic epidemiology of breast cancer. Cancer *74*, 279–287.

Tinevez, J.-Y., Schulze, U., Salbreux, G., Roensch, J., Joanny, J.-F., and Paluch, E. (2009). Role of cortical tension in bleb growth. Proc. Natl. Acad. Sci. *106*, 18581–18586.

Toivola, D.M., Tao, G.-Z., Habtezion, A., Liao, J., and Omary, M.B. (2005). Cellular integrity plus: organelle-related and protein-targeting functions of intermediate filaments. Trends Cell Biol. *15*, 608–617.

Torregrosa, D., Bolufer, P., Lluch, A., López, J.A., Barragán, E., Ruiz, A., Guillem, V., Munárriz, B., and García Conde, J. (1997). Prognostic significance of c-erbB-2/neu amplification and epidermal growth factor receptor (EGFR) in primary breast cancer and their relation to estradiol receptor (ER) status. Clin. Chim. Acta Int. J. Clin. Chem. *262*, 99–119.

Tran, H.D., Luitel, K., Kim, M., Zhang, K., Longmore, G.D., and Tran, D.D. (2014). Transient SNAIL1 Expression Is Necessary for Metastatic Competence in Breast Cancer. Cancer Res. *74*, 6330–6340.

Tremblay, M., Sanchez-Ferras, O., and Bouchard, M. (2018). GATA transcription factors in development and disease. Development *145*, dev164384.

Tsuchiya, M., Price, S.R., Tsai, S.C., Moss, J., and Vaughan, M. (1991). Molecular identification of ADP-ribosylation factor mRNAs and their expression in mammalian cells. J. Biol. Chem. *266*, 2772–2777.

Tushir, J.S., and D'Souza-Schorey, C. (2007). ARF6-dependent activation of ERK and Rac1 modulates epithelial tubule development. EMBO J. *26*, 1806–1819.

Tushir, J.S., Clancy, J., Warren, A., Wrobel, C., Brugge, J.S., D'Souza-Schorey, C., and Schwarzbauer, J. (2010). Unregulated ARF6 Activation in Epithelial Cysts Generates Hyperactive Signaling Endosomes and Disrupts Morphogenesis. Mol. Biol. Cell *21*, 2355–2366.

Vadlamudi, R.K., and Kumar, R. (2003). P21-activated kinases in human cancer. Cancer Metastasis Rev. *22*, 385–393.

Varner, V.D., and Nelson, C.M. (2014). Cellular and physical mechanisms of branching morphogenesis. Dev. Camb. Engl. *141*, 2750–2759.

Viloria-Petit, A.M., and Wrana, J.L. (2010). The TGFβ-Par6 polarity pathway: Linking the Par complex to EMT and breast cancer progression. Cell Cycle *9*, 623–624.

Visvader, J.E. (2009). Keeping abreast of the mammary epithelial hierarchy and breast tumorigenesis. Genes Dev. *23*, 2563–2577.

Visvader, J.E., and Stingl, J. (2014). Mammary stem cells and the differentiation hierarchy: current status and perspectives. Genes Dev. *28*, 1143–1158.

Vleminckx, K., Vakaet, L., Mareel, M., Fiers, W., and Van Roy, F. (1991). Genetic manipulation of E-cadherin expression by epithelial tumor cells reveals an invasion suppressor role. Cell *66*, 107–119.

Vogelstein, B., Papadopoulos, N., Velculescu, V.E., Zhou, S., Diaz, L.A., and Kinzler, K.W. (2013). Cancer Genome Landscapes. Science *339*, 1546–1558.

Vollenweider-Zerargui, L., Barrelet, L., Wong, Y., Lemarchand-Béraud, T., and Gómez, F. (1986). The predictive value of estrogen and progesterone receptors' concentrations on the clinical behavior of breast cancer in women. Clinical correlation on 547 patients. Cancer *57*, 1171–1180.

Vos, C.B., Cleton-Jansen, A.M., Berx, G., de Leeuw, W.J., ter Haar, N.T., van Roy, F., Cornelisse, C.J., Peterse, J.L., and van de Vijver, M.J. (1997). E-cadherin inactivation in lobular carcinoma in situ of the breast: an early event in tumorigenesis. Br. J. Cancer *76*, 1131–1133.

Wallace, S.W., Durgan, J., Jin, D., and Hall, A. (2010). Cdc42 Regulates Apical Junction Formation in Human Bronchial Epithelial Cells through PAK4 and Par6B. Mol. Biol. Cell *21*, 2996–3006.

Wan, L., Pantel, K., and Kang, Y. (2013). Tumor metastasis: moving new biological insights into the clinic. Nat. Med. *19*, 1450–1464.

Wang, D., Cai, C., Dong, X., Yu, Q.C., Zhang, X.-O., Yang, L., and Zeng, Y.A. (2015). Identification of multipotent mammary stem cells by protein C receptor expression. Nature *517*, 81–84.

Wang, X., Allen, W.E., Wright, M.A., Sylwestrak, E.L., Samusik, N., Vesuna, S., Evans, K., Liu, C., Ramakrishnan, C., Liu, J., et al. (2018). Three-dimensional intact-tissue sequencing of single-cell transcriptional states. Science *361*, eaat5691.

Wang, Y., Han, K.-J., Pang, X.-W., Vaughan, H.A., Qu, W., Dong, X.-Y., Peng, J.-R., Zhao, H.-T., Rui, J.-A., Leng, X.-S., et al. (2002). Large Scale Identification of Human Hepatocellular Carcinoma-Associated Antigens by Autoantibodies. J. Immunol. *169*, 1102–1109.

Warburton, M.J., Mitchell, D., Ormerod, E.J., and Rudland, P. (1982). Distribution of myoepithelial cells and basement membrane proteins in the resting, pregnant, lactating, and involuting rat mammary gland. J. Histochem. Cytochem. *30*, 667–676.

Weaver, A.M. (2009). Regulation of Cancer Invasion by Reactive Oxygen Species and Tks Family Scaffold Proteins. Sci. Signal. *2*, pe56–pe56.

Wehrle-Haller, B. (2012). Structure and function of focal adhesions. Curr. Opin. Cell Biol. *24*, 116–124.

Weigelt, B., and Reis-Filho, J.S. (2010). Molecular profiling currently offers no more than tumour morphology and basic immunohistochemistry. Breast Cancer Res. *12*, S5.

Weigelt, B., Peterse, J.L., and van't Veer, L.J. (2005). Breast cancer metastasis: markers and models. Nat. Rev. Cancer *5*, 591–602.

Weigelt, B., Geyer, F.C., and Reis-Filho, J.S. (2010). Histological types of breast cancer: How special are they? Mol. Oncol. *4*, 192–208.

Wennerberg, K., and Der, C.J. (2004). Rho-family GTPases: it's not only Rac and Rho (and I like it). J. Cell Sci. *117*, 1301–1312.

Wennerberg, K., Rossman, K.L., and Der, C.J. (2005). The Ras superfamily at a glance. J Cell Sci *118*, 843–846.

White, D.E., Kurpios, N.A., Zuo, D., Hassell, J.A., Blaess, S., Mueller, U., and Muller, W.J. (2004). Targeted disruption of β1-integrin in a transgenic mouse model of human breast cancer reveals an essential role in mammary tumor induction. Cancer Cell *6*, 159–170.

Whiteside, T.L. (2008). The tumor microenvironment and its role in promoting tumor growth. Oncogene *27*, 5904–5912.

Wilkinson, S., Paterson, H.F., and Marshall, C.J. (2005). Cdc42–MRCK and Rho–ROCK signalling cooperate in myosin phosphorylation and cell invasion. Nat. Cell Biol. *7*, 255–261.

Willenborg, C., and Prekeris, R. (2011). Apical protein transport and lumen morphogenesis in polarized epithelial cells. Biosci. Rep. *31*, 245–256.

Williams, J.M., and Daniel, C.W. (1983). Mammary ductal elongation: Differentiation of myoepithelium and basal lamina during branching morphogenesis. Dev. Biol. *97*, 274–290.

Wiseman, B.S., Sternlicht, M.D., Lund, L.R., Alexander, C.M., Mott, J., Bissell, M.J., Soloway, P., Itohara, S., and Werb, Z. (2003). Site-specific inductive and inhibitory activities of MMP-2 and MMP-3 orchestrate mammary gland branching morphogenesis. J. Cell Biol. *162*, 1123–1133.

Wolf, K., Mazo, I., Leung, H., Engelke, K., Andrian, U.H. von, Deryugina, E.I., Strongin, A.Y., Bröcker, E.-B., and Friedl, P. (2003). Compensation mechanism in tumor cell migration: mesenchymal–amoeboid transition after blocking of pericellular proteolysis. J. Cell Biol. *160*, 267–277.

Wolf, K., Wu, Y.I., Liu, Y., Geiger, J., Tam, E., Overall, C., Stack, M.S., and Friedl, P. (2007). Multi-step pericellular proteolysis controls the transition from individual to collective cancer cell invasion. Nat. Cell Biol. *9*, 893–904.

Wood, R.D. (2018). Fifty years since DNA repair was linked to cancer. Nature *557*, 648.

Wozniak, M.A., Desai, R., Solski, P.A., Der, C.J., and Keely, P.J. (2003). ROCK-generated contractility regulates breast epithelial cell differentiation in response to the physical properties of a three-dimensional collagen matrix. J Cell Biol *163*, 583–595.

Wu, C. (2007). Focal adhesion: a focal point in current cell biology and molecular medicine. Cell Adhes. Migr. *1*, 13–18.

Wu, C., Asokan, S.B., Berginski, M.E., Haynes, E.M., Sharpless, N.E., Griffith, J.D., Gomez, S.M., and Bear, J.E. (2012). Arp2/3 Is Critical for Lamellipodia and Response to Extracellular Matrix Cues but Is Dispensable for Chemotaxis. Cell *148*, 973–987.

Wu, Y., Sarkissyan, M., and Vadgama, J.V. (2016). Epithelial-Mesenchymal Transition and Breast Cancer. J. Clin. Med. *5*, 13.

Wuidart, A., Sifrim, A., Fioramonti, M., Matsumura, S., Brisebarre, A., Brown, D., Centonze, A., Dannau, A., Dubois, C., Van Keymeulen, A., et al. (2018). Early lineage segregation of multipotent embryonic mammary gland progenitors. Nat. Cell Biol. *20*, 666–676.

Würtz, S.Ø., Schrohl, A.-S., Sørensen, N.M., Lademann, U., Christensen, I.J., Mouridsen, H., and Brünner, N. (2005). Tissue inhibitor of metalloproteinases-1 in breast cancer. Endocr. Relat. Cancer *12*, 215–227.

Xu, R., Boudreau, A., and Bissell, M.J. (2009). Tissue architecture and function: dynamic reciprocity via extra- and intra-cellular matrices. Cancer Metastasis Rev. *28*, 167–176.

Xu, R., Zhang, Y., Gu, L., Zheng, J., Cui, J., Dong, J., and Du, J. (2015). Arf6 regulates EGF-induced internalization of E -cadherin in breast cancer cells. Cancer Cell Int. *15*, 11.

Yamaguchi, H., Lorenz, M., Kempiak, S., Sarmiento, C., Coniglio, S., Symons, M., Segall, J., Eddy, R., Miki, H., Takenawa, T., et al. (2005). Molecular mechanisms of invadopodium formation: the role of the N-WASP-Arp2/3 complex pathway and cofilin. J. Cell Biol. *168*, 441–452.

Yamashita, N., Tokunaga, E., Iimori, M., Inoue, Y., Tanaka, K., Kitao, H., Saeki, H., Oki, E., and Maehara, Y. (2018). Epithelial Paradox: Clinical Significance of Coexpression of E-cadherin and Vimentin With Regard to Invasion and Metastasis of Breast Cancer. Clin. Breast Cancer *18*, e1003–e1009.

Yang, J., and Weinberg, R.A. (2008). Epithelial-Mesenchymal Transition: At the Crossroads of Development and Tumor Metastasis. Dev. Cell *14*, 818–829.

Yang, J., Mani, S.A., Donaher, J.L., Ramaswamy, S., Itzykson, R.A., Come, C., Savagner, P., Gitelman, I., Richardson, A., and Weinberg, R.A. (2004). Twist, a master regulator of morphogenesis, plays an essential role in tumor metastasis. Cell *117*, 927–939.

Yang, L., Wang, L., and Zheng, Y. (2006). Gene Targeting of Cdc42 and Cdc42GAP Affirms the Critical Involvement of Cdc42 in Filopodia Induction, Directed Migration, and Proliferation in Primary Mouse Embryonic Fibroblasts□D. Mol. Biol. Cell *17*, 11.

Yap, A.S. (2015). Preface. Cellular adhesion in development and disease. Curr. Top. Dev. Biol. *112*, xv–xvii.

Yap, A.S., and Kovacs, E.M. (2003). Direct cadherin-activated cell signaling: a view from the plasma membrane. J. Cell Biol. *160*, 11–16.

Yates, L.R., Knappskog, S., Wedge, D., Farmery, J.H.R., Gonzalez, S., Martincorena, I., Alexandrov, L.B., Van Loo, P., Haugland, H.K., Lilleng, P.K., et al. (2017). Genomic Evolution of Breast Cancer Metastasis and Relapse. Cancer Cell *32*, 169-184.e7.

Ye, X., Tam, W.L., Shibue, T., Kaygusuz, Y., Reinhardt, F., Ng Eaton, E., and Weinberg, R.A. (2015). Distinct EMT programs control normal mammary stem cells and tumour-initiating cells. Nature *525*, 256–260.

Yu, M., Stott, S., Toner, M., Maheswaran, S., and Haber, D.A. (2011). Circulating tumor cells: approaches to isolation and characterization. J. Cell Biol. *192*, 373–382.

Zangari, J., Partisani, M., Bertucci, F., Milanini, J., Bidaut, G., Berruyer-Pouyet, C., Finetti, P., Long, E., Brau, F., Cabaud, O., et al. (2014). EFA6B Antagonizes Breast Cancer. Cancer Res. *74*, 5493–5506.

Zegers, M.M., and Friedl, P. (2014). Rho GTPases in collective cell migration. Small GTPases *5*, e983869.

Zeng, Y.A., and Nusse, R. (2010). Wnt proteins are self-renewal factors for mammary stem cells and promote their long-term expansion in culture. Cell Stem Cell *6*, 568–577.

Zhang, M., Behbod, F., Atkinson, R.L., Landis, M.D., Kittrell, F., Edwards, D., Medina, D., Tsimelzon, A., Hilsenbeck, S., Green, J.E., et al. (2008). Identification of Tumor-Initiating Cells in a p53-Null Mouse Model of Breast Cancer. Cancer Res. *68*, 4674–4682.

Zhou, Y.-M., Cao, L., Li, B., Zhang, R.-X., Sui, C.-J., Yin, Z.-F., and Yang, J.-M. (2012). Clinicopathological Significance of ZEB1 Protein in Patients with Hepatocellular Carcinoma. Ann. Surg. Oncol. *19*, 1700–1706.

Zins, K., Lucas, T., Reichl, P., Abraham, D., and Aharinejad, S. (2013). A Rac1/Cdc42 GTPase-Specific Small Molecule Inhibitor Suppresses Growth of Primary Human Prostate Cancer Xenografts and Prolongs Survival in Mice. PLoS ONE *8*, e74924.

Zobel, M., Disanza, A., Senic-Matuglia, F., Franco, M., Colaluca, I.N., Confalonieri, S., Bisi, S., Barbieri, E., Caldieri, G., Sigismund, S., et al. (2018). A NUMB–EFA6B–ARF6 recycling route controls apically restricted cell protrusions and mesenchymal motility. J Cell Biol *217*, 3161–3182.